SYNTHESIS OF GLYCOPOLYPEPTIDES, THEIR SELF-ASSEMBLY AND IT'S INTERACTIONS WITH LECTINS

THESIS SUBMITTED TO THE
UNIVERSITY OF PUNE

FOR THE DEGREE OF
DOCTOR OF PHILOSOPHY
(IN CHEMISTRY)

By
DEBASIS PATI

Research Supervisor
DR. SAYAM SEN GUPTA

CHEMICAL ENGINEERING DIVISION
NATIONAL CHEMICAL LABORATORY
PUNE-411008
INDIA

AUGUST 2013

DECLARATION

I hereby declare that the research work embodied in this thesis has been carried out by me at National Chemical Laboratory, Pune, under the supervision of Dr. Sayam Sen Gupta, scientist, National Chemical Laboratory, Pune. I also affirm that this work is original and has not been submitted in part or full, for any other degree or diploma to this or any other University or Institution.

Date: **Debasis Pati**

.....DEDICATED

TO MY PARENTS

Research is a never ending process involving a team of persons striving to attain newer horizons in the field of sciences. This thesis would not have been completed without the encouragement and co-operation of my teachers, parents, friends, well-wishers and relatives. I take this opportunity to express my deep gratitude to one and all.

It gives me immense pleasure to express my deep sense of gratitude to my supervisor and mentor ***Dr. Saym Sen Gupta*** *for his excellent guidance, continuous encouragement, and generous support in achieving this entire endeavor. Wholeheartedly, I am very much grateful to him for motivating me in the field of Glycopolypeptides. Without his encouragement and constant guidance, I could not have finished my doctoral degree. I do sincerely acknowledge the freedom rendered by him in the laboratory for the independent thinking, planning and execution of research. Working with him was really a great pleasure and fetched me a lot of learning experience.*

It gives me immense pleasure to thank Dr. Ashootosh V. Ambade, who was and is always ready for help, guidance, in writing manuscript, thesis, or proposal or any discussion about any arising problem on going project and moral support. I also thank Prof. Srinivas Hotha and Dr. Kumar Vanka for their helpful discussions and suggestions and initial teaching on Chemistry.

I wholeheartedly thank and give acknowledgements to entire NMR and Elemental analysis group especially Dr. Rajmohan, from NMR facility.

I am thankful to my mentors from School and College for their inspirational teaching, ethics and discipline. I sincerely thank Gouri Sankar Maity for his continuous encouragement, Dr. Avinash Kumbhar and other professors from department of chemistry, University of Pune, for their encouragement. I am also thankful to my lecturers and professors from Midnapore College, Midnapore.

During the course of this work in NCL, I learnt that a journey is easier when we travel together. I would like to express special thanks to my labmates Malvi, Mrituynjoy, Anal, Chaka, Soumen, Munmun, Ashif, Sushma, Neha, Vinita, Kundan, Santanu and Basabda and all my lamemates for their kind help and support, invaluable discussions which we shared and maintaining a lively environment in the laboratory during every

walk of life in the laboratory to achieve this goal. Specially I want to thank Asif, Soumen, Nagendra and Nagnath for helping me to make the starting materials which help a lot to do more reactions in the forward steps.

During this work in NCL, I have collaborated with many colleagues for whom I have great regard, and I would like to express my warmest thanks to all colleagues from Dr. S.Hotha's lab., Dr. Ashootosh V. Ambade's lab., Dr. Musti J. Sawamy's lab (specially want to thank his student Pravin) in Hyyderabad Central Universityan and Dr. K. Guruswamy… for their timely help. I wish to extend my sincere thanks to the friends from Dr Sudip Roy's group and Dr. Rahul Banerjee's group, Dr. B. L. V. Prasad's lab and Dr. Tulshiram's lab in NCL. I would like to thank all other friends for their cheerful support, co-operation and making my stay at NCL very comfortable and memorable one.

My stay here was made livelier by GJ hostel, a hostel unique in ways more than one. It provided the perfect atmosphere to spend leisure time and I thoroughly enjoyed all the sports & cultural activities that abounded in the hostel.

Friends make things go easy and life beautiful. Indeed I am blessed to have friends like Debasis (my host in pune and also guided me throughout my master study in University of Pune and also not possible to forget his help and support during carrying out research in NCL for PhD), Sujitda,Pradipda, Anal, Anupam, Deepa (Anupam's wife), Prithvi, Roopadi, Bibhashada, Prabashda, Sankho, Soumitrada, Sumantra, Debabrata Bhatasalli, Kaushi Ghosh and Debdut Roy, Partho, Binoy, Sumantra, Sumanta where I don't have words to describe them as individuals and it should suffice to say that I am simply blessed to have them ever by my side; I've spent the best of times with them and all they have been great in putting up with a lot of my gibberish and form an indispensable part of my life. The care and emotional support of these people has been no less than that of my family and for all that they have done for me I don't want to thank them simply because I don't need to.

Lastly, I also spent some goodtime with the juniors; Kanok, Mrinmoy, Anup, Saibal, Sanjib, Saikat, Pravat, Arya, Achinta, Arijit, Chandan, Krisanu, Shyam and Tamos, Jagadish, Arpan, Sanjib and others from IISER like Biplob, Anupam etc. I am really grateful to them for spending some good time with me.

I am thankful to my graduation and post-graduation friends Dr. Debabrata Patra (college friend), Dhiraj Bhatia (M.Sc. friend), Dhimoy Roy (M.Sc. friend), and others for their support and co-operation.

I am grateful to Council of Scientific and Industrial Research, Government of India, for awarding the junior and senior research fellowships and Dr. S. Pal, Director, National Chemical Laboratory, Pune to carry out my research works, extending all infrastructure facilities.

No word would suffice to express my gratitude and love to my mother and my elder brother for their continuous showering of boundless affection on me and supporting me in whatever I choose or did. It is my mother and father's prayer, constant struggle and relentless hard work to overcome the odds of life, which has inspired me to pursue life with a greater optimism. The warmth and moral value of my parents have stood me in good stead throughout my life and I would always look up to them for strength no matter what I have to go through. This Ph. D. thesis is a result of the extraordinary will, efforts and sacrifices of my family. I would like to dedicate this moment of joy to my family members especially my mother, my father, my elder brother (Animesh), sister in law (Sampa), Sister (Sipra), brother in law (Anup), Cousins (Chanchal, Vambal and Chottu), my nephew (Sayan) and my cute niece (Riya).....

I wish to express my gratitude towards "God-almighty", who gave me the strength and courage to fulfil my dreams and has showered upon me his choicest blessings. As I believe on faith, therefore it is very appropriate to conclude with the famous quotation of Mr. Paulo Coelho from his critically acclaimed Novel Alchemist "When you want something, all the universe conspires in helping you to achieve it."

……Debasis

Ac	Acetyl
Ac_2O	Acetic anhydride
AcOH	Acetic acid
AIBN	2,2-Azobisisobutyronitrile
Aq	Aqueous
$BF_3.Et_2O$	Boron trifluoride diethyl etherate
Bn	Benzyl
Bz	Benzoyl
BnCl	Benzyl chloride
BzCl	Benzoyl chloride
BnBr	Benzyl bromide
Cat	Catalytic
Conc	Concentrated
DBU	1,8-Diazabicycloundec-7-ene
DMAP	N,N-Dimethylaminopyridine
DMTST	Dimethyl sulphonium triflate
DMF	N,N-Dimethylformamide
DMSO	Dimethyl sulfoxide
DEPT	Distortionless Enhancement by Polarization Transfer
Ech-OH	1-Ethynylcyclohexanol
EtOAc	Ethyl Acetate
eq	Equivalents
g	Gram
h	Hour
Hz	Hertz
IDCP	Iodonium dicollidine perchlorate
J	Coupling constant
NIS	*N*-Iodosuccinimide
mL	Millilitre
mol	Mole
mmol	Millimole
Me	Methyl
MeOH	Methanol
4ÅMS	4Å Molecualar sieves
mg	Milligram
min	Minutes
NMR	Nuclear Magnetic Resonance
PMB	*para*- methoxy benzyl

PTSA, TsOH	*para*-Tolune sulphonic acid
PMDETA	Penta-Methyl-Diethylene-Tri-Amine
rt	Room temperature
SBox	*S*-benzoxazolyl
SEC	Size exclusion chromatography
TBAI	Tetra-*n*-butylammonium iodide
TESOTf	Triethylsilyl trifluoromethanesulfonate
tert-BuCl	*tert*-Butyl Chloride
TFA	Trifluoroacetic acid
THF	Tetrahydrofuran
TfOH	Trifluoromethane sulphonic acid
TCA	Trichloroacetamidate
TLC	Thin Layer Chromatography
TMSOTf	Trimethylsilyl trifluoromethanesulfonate
Tr	Trityl

- ^{1}H NMR spectra were recorded on AV-200 MHz, AV-400 MHz, DRX-500 MHz, or JEOL ECX 400 MHz and Bruker Advance 500 MHz spectrometer using tetramethylsilane (TMS) as an internal standard. Chemical shifts have been expressed in ppm units downfield from TMS.
- ^{13}C NMR spectra were recorded on AV-50 MHz, AV-100 MHz, DRX-125 or JEOL ECX 100 MHz and Bruker Advance 125 MHz spectrometer.
- Low resolution mass spectroscopy (LRMS) was performed on Waters Acquity UPLC-MS (H Class). High resolution mass spectroscopy (HRMS) was performed on ABI-MALDI-TOF mass spectrometer using TiO_2 as the solid matrix.
- Infrared spectra were scanned on Shimadzu IR 470 and Perkin-Elmer 683 or 1310 spectrometers with sodium chloride optics and are measured in cm^{-1}.
- Optical rotations were measured with a JASCO P-1020 or Rudolph polarimeter.
- GC Analyses were carried out on an Agilent 7890 instrument equipped with a hydrogen flame ionization detector and HP-5 capillary column (30m x 0.32mm x 0.25 μm, J & W Scientific). Nitrogen was used as the carrier gas at a flow rate of 1mL/min.
- All reactions are monitored by Thin Layer Chromatography (TLC) carried out on 0.25 mm E-Merck silica gel plates (60F-254) with UV light, I_2, and anisaldehyde in ethanol as developing agents.
- All reactions were carried out under nitrogen or argon atmosphere with dry, freshly distilled solvents under anhydrous conditions unless otherwise specified. Yields refer to chromatographically and spectroscopically homogeneous materials unless otherwise stated.
- All evaporations were carried out under reduced pressure on Büchi rotary evaporator below 45 °C unless otherwise specified.
- Silica gel (60–120), (100-200), and (230-400) mesh were used for column chromatography.
- α-β ratio of anomeric position was determined by relative peak intensities of resonances from the most characteristic protons in the ^{1}H NMR spectrum of the partially purified product
- Scheme, Figure and Compound numbers in abstract and individual chapters are different.

CONTENTS

Synthesis of glycopolypeptides, their self-assembly and it's interactions with lectins

ABSTRACT

Introduction

Most abundant in nature, carbohydrates play a key role in a myriad of biological processes including inflammation, cell–cell contacts, signal transmission, fertilization and protein folding. In particular the saccharides that are conjugated to proteins, known as glycoproteins, are functionally very important in biology and there have been a lot of efforts directed for their efficient synthesis.[1] Since biological synthesis of such glycoproteins is still very complex, artificial glycoconjugates provide an interesting bio mimetic analogue. In this regard glycopolymers, featuring synthetic macromolecules with pendant carbohydrate moieties, have found widespread applications in various fields such as macromolecular drugs and drug delivery systems, hydrogels, matrices for controlled cell culture and as models of biological systems. [2] Majority of these glycopolymers are acrylate based and controlled radical polymerization is used to synthesize polymers with controlled molecular weight, glycosylation density and position – attributes that are necessary for biological recognition processes. However, these polymers do not have well-defined higher order structures and often adopt a random-coil conformation which inevitably renders some of the side-chain bioactive moieties inaccessible toward biological active sites. On the other hand glycopolypeptides (glycopolymers with pendant carbohydrates on a polypeptide backbone) not only has the ability to fold into well-defined secondary structures[3] (e.g., helix) but mimic the molecular composition of proteoglycans. Therefore it is desirable to develop methodologies that afford easy and well defined synthetic polypeptides.

The key to the recognition process is their interactions with carbohydrate-binding protein receptors known as lectins.[4-5] The interaction between lectins and carbohydrates is weak; dissociation constants; K_d are typically 10^{-3}–10^{-6} M, but may be greatly enhanced through polyvalency. Since glycopolymers are typically polyvalent as they have several pendant carbohydrate groups; they present a platform for which multiple copies of a carbohydrate can be presented simultaneously, thus enhancing their affinity and selectivity for lectins many folds. Carbohydrate recognising receptors are found on many cell surfaces. An excellent example is the asialoglycoprotein receptor (ASGP-R) displayed on the hepatocyte cell surface that interacts uniquely with galactose/N-acetyl-β-galactosamine containing carbohydrate ligands.[6-9] Galactose containing synthetic linear glycopolymers can therefore be used to guide hepatocyte adhesion through this unique ASGP-R–carbohydrate interaction. This strategy has been used to design extra cellular matrices using galactose containing synthetic polymers for liver tissue engineering.[10] Similarly, the use of glycopolymers as vehicles for therapeutics has also shown a lot of promise.[11-12]

For glycopolymers to be used as delivery vehicles and as biomaterials, it would be advantageous if these could be assembled into supramolecular nanostructures that can be tuned to appropriately display their carbohydrate moieties. Thus, amphiphilic block copolymers containing glycopolymers as one of their blocks represent an interesting motif to build self-assembled nanostructures.[13-14] For example, glucose-grafted polybutadiene-block-polystyrene was shown to self-assemble into vesicles in organic as well as aqueous media. However, synthetic glycopolymers typically do not form well-defined secondary structures and, that may render them less effective for biological recognition processes. On the other hand, glycopolypeptides (GP), wherein

sugar units are attached to a polypeptide backbone, mimic the molecular composition of proteoglycans and have been demonstrated to fold into well-defined secondary structures (e.g. α-helix), that allows ordered display of the carbohydrate moieties. Hence, they represent suitable candidates for biological applications. This has led to a surge in reports on their synthesis.

By keeping the above objectives in mind, the following specific work was selected for the present thesis:

1. Introduction and literature survey.

2. Synthesis of glycopolypeptides by ring opening polymerization of α-amino acid N- carboxyanhydrides (NCA).

3. Controlled Synthesis of *O*-Glycopolypeptide Polymers and their Molecular Recognition by Lectins.

4. Multiple Topologies from Glycopolypeptide-Dendron Conjugate self-assembly: Nanorods, Micelles and Organogels.

5. Bioactive Polymersomes 'assemblies' derived from Glycopolypeptide-b-Polycaprolactone conjugate and the study of their preferential cellular uptake.

6. Future aspects of the thesis work.

The thesis has been divided into following six chapters.

Chapter 1: Introduction and literature survey

A comprehensive review of literature on synthesis and characterization of novel glycopolypeptides. Their details biological responses towards lectins and toxins. The carbohydrates based self-assembled nanostructures for the uses of drug delivery and tissue engineering fields.

Chapter 2: Synthesis of glycopolypeptides by ring opening polymerization of α-amino acid N-carboxyanhydrides (NCA).

The novel synthesis of *O*-glycosylated lysine-NCA from a stable glycosyl donor and a commercially available protected amino acid in very high yield is reported. These *O*-glycosylated lysine-NCA monomers underwent ring opening polymerization using simple primary amine initiators to form well defined, high molecular weight homoglycopolypeptides and diblock co-glycopolypeptides. The synthesis of azide labelled end functionalized glycopolypeptides and amphiphilic diblock copolypeptides is also reported. This methodology represents an easy and practical route to the synthesis of *O*-glycosylated polypeptides with 100% glycosylation.

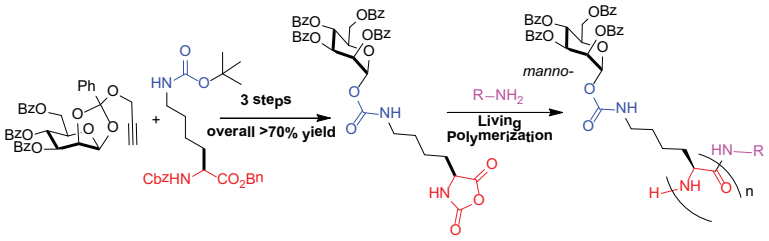

Scheme 1: Synthesis of "*Glycopolypeptides*"

Pati, D. *et al Polym. Chem. 2011*, **2**, 805-811.

Chapter 3: **Controlled Synthesis of *O*-Glycopolypeptide Polymers and their Molecular Recognition by Lectins.**

The facile synthesis of high molecular weight water-soluble *O*-glycopolypeptide polymers by the ring-opening polymerization of their corresponding N-

carboxyanhydride (NCA) in very high yield (overall yield > 70%) is reported. The *per*-acetylated-*O*-glycosylated lysine-NCA monomers, synthesized using stable glycosyl donors and a commercially available protected amino acid in very high yield, was polymerized using commercially available amine initiators. The synthesized water soluble glycopolypeptides were found to be α-helical in aqueous solution. However, we were able to control the secondary conformation of the glycopolypeptides (α-helix vs nonhelical structures) by polymerizing racemic amino acid glyco NCAs. We have also investigated the binding of the glycopolypeptide poly(α-manno-*O*-lys) with the lectin Con-A using precipitation and hemagglutination assays as well as by isothermal titration calorimetry (ITC). The ITC results clearly show that the binding process is enthalpy driven for both α-helical and nonhelical structures, with negative entropic contribution. Binding stoichiometry for the glycopolypeptide poly(α-manno-*O*-lys) having a nonhelical structure was slightly higher as compared to the corresponding polypeptide which adopted an α-helical structure.

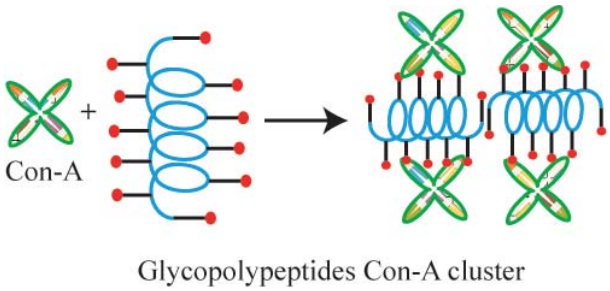

Fig 2: Graphical representation of helical Vs. Coil glycopolypeptides Con-A clustering

Pati, D. *et al Biomacromolecules* **2012**, *13*, 1287-1295.

Chapter 4: Multiple Topologies from Glycopolypeptide-Dendron Conjugate self-assembly: Nanorods, Micelles and Organogels.

Glycopolypeptides (GPs) were synthesized by ring-opening polymerization of glycosylated N-carboxyanhydride monomer and attached to hydrophobic dendrons at one chain end by "click" reaction to obtain amphiphilic anisotropic macromolecules. We show that by varying polypeptide chain length and dendron generation, an organogel was obtained in dimethylsulfoxide, while nanorods and micellar aggregates were observed in aqueous solutions. Assemblies in water were characterized by electron microscopy and dye encapsulation. Secondary structure of the GP chain was shown to affect the morphology, where as the chain length of the poly(ethylene glycol) linker between the GP and dendron did not alter rod-like assemblies. Bioactive surface chemistry of these assemblies displaying carbohydrate groups was demonstrated by interaction of mannose-functionalized nanorods with *Con-A*.

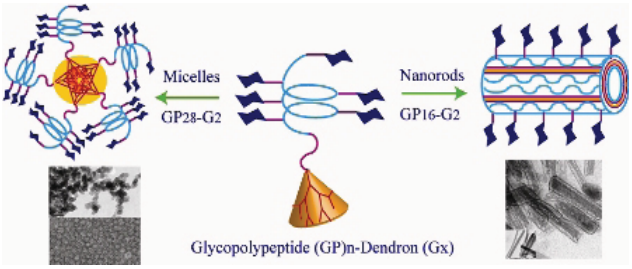

Fig 3: Graphical representation of Nanorods and Micelles

Pati, D. *et al Journal of American Chemical Society* **2012**, *134*, 7796-7802.

Chapter 5: Bioactive Polymersomes 'assemblies' derived from Glycopolypeptide-b-Polycaprolactone conjugate and the study of their preferential cellular uptake.

Well characterized biocompatible glycopolypeptides conjugated branched polycaprolactones were synthesised by "click" reaction. The hydrophilic

glycopolypeptides conjugated hydrophobic polycaprolactones block copolymers self-assembled micelle, vesicles and nanorods in aqueous solution of different anisotropic block polymers derivatives. We also shown the difference in assembly derived from linear polycaprolactone conjugated glycopolypeptides. The preferential cellular uptakes of all the galactosylated micro-assemblies to the HEPG2 cell line were preferentially uptaken.

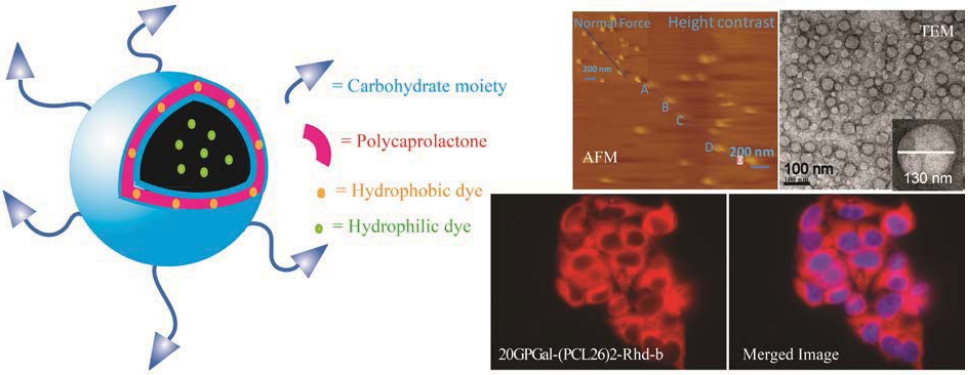

(Pati, D. *et al Manuscript under preparation*)

Fig 4: Graphical representation of nano-assemblies and their cellular uptake.

Chapter 6: Future aspects of the thesis work

This chapter includes three proposals based on the thesis work.

References:

1. Gamblin, D. P.; Scanlan, E. M.; Davis, B. G. *Chemical Reviews* **2008,** *109* (1), 131-163.
2. (a) Albertin, L.; Cameron, N. R. *Macromolecules* **2007,** *40* (17), 6082-6093; (b) Chen, G.; Tao, L.; Mantovani, G.; Geng, J.; Nyström, D.; Haddleton, D. M. *Macromolecules* **2007,** *40* (21), 7513-7520; (c) Ladmiral, V.; Mantovani, G.;

Clarkson, G. J.; Cauet, S.; Irwin, J. L.; Haddleton, D. M., *Journal of the American Chemical Society* **2006,** *128* (14), 4823-4830; (d) Ladmiral, V.; Melia, E.; Haddleton, D. M.,*European Polymer Journal* **2004,** *40* (3), 431-449;

3. Deming, T. J. *Soft Matter* **2005,** *1* (1), 28-35.
4. Ambrosi, M.; Cameron, N. R.; Davis, B. G. *Org. Biomol. Chem.* **2005**, *3*, 1593-1608.
5. Ting, S. R. S.; Chen, G.; Stenzel, M. H. *Polym. Chem.* **2010**, *1*, 1392-1412.
6. Mammen, M.; Choi, S.-K.; Whitesides, G. M. *Angew. Chem. In. Ed.* **1998**, *37*, 2754-2794.
7. Connolly, D. T.; Townsend, R. R.; Kawaguchi, K.; Bell, W. R.; Lee, Y. C. *J. Biol. Chem.* **1982**, *257*, 939-945.
8. Weigel, P. H.; Oka, J. A. *J. Biol. Chem.* **1983**, *258*, 5095-5102.
9. Weigel, P. H.; Yik, J. H. N. *Biochim. Biophys. Acta.* **2002**, *1572*, 341-363.
10. Cho, C. S.; Seo, S. J.; Park, I. K.; Kim, S. H.; Kim, T. H.; Hoshiba, T.; Harada, I.; Akaike, T. *Biomaterials* **2006**, *27*, 576-585.
11. Pati, D.; Shaikh, A. Y.; Hotha, S.; Sen Gupta, S. *Polym. Chem.* **2011**, *2*, 805-811.
12. Pati, D.; Shaikh, A.; Das. S.; Nareddy, P. K.; Swamy, M. J.; Hotha, S.; Sen Gupta, S. *Biomacromolecules* **2012** DOI:10.1021/bm201813s.
13. You, L.; Schlaad, H. *J. Am. Chem. Soc.*, **2006**, *128*, 13336–13337.
14. Schatz, C.; Louguet, S.; Le Meins, J.-F.; Lecommandoux, S. *Angew. Chem. Int. Ed.* **2009**, *48*, 2572 –2575.

Chapter I
Introduction and literature survey

1.1 Carbohydrates in nature and biology

Carbohydrates represent the most abundant biomolecule among the four major biomolecules in nature that also include proteins, nucleotides, and lipids. Carbohydrates, also commonly known as saccharides, have several roles in living organisms, including energy transportation, as well as being structural components of plants and arthropods. Carbohydrate derivates are actively involved in several biochemical processes including blood clotting, immune systems and the development of diseases. The carbohydrates (saccharides) are divided into four chemical groupings: monosaccharide, disaccharides, oligosaccharides, and polysaccharides. In general, the monosaccharide and disaccharides, which are smaller (lower molecular weight) carbohydrates, are commonly referred to as sugars.

In cells, the cell membrane displays a complex glycocalyx (extracellular polymeric material) that includes oligosaccharides and membrane proteins like the carbohydrate containing proteins and lipids that are known as glycoproteins and glycolipids. These carbohydrate containing biomolecules regulate a wide range of cellular processes such as cell migration, proliferation, transcriptional regulation and differentiation among others[1, 2]. They also modulate cellular growth, motility and are involved in cellular communications. Glycoproteins serve an essential role in many biological processes, including, but not limited to: binding, signalling, protein folding and metabolism. Mutation of the gene which leads to deletion of the glycosylation machinery often has lethal effects in both test animals and humans. Glycosylation is one of the most ubiquitous cellular processes in post-translational modifications since more than 50% of the human proteins are expected to be glycosylated. It adds another dimension to the complexity of proteoglycans which allow them to encode the specific molecular recognition for regulation of protein folding, defolding and pharmacokinetics.

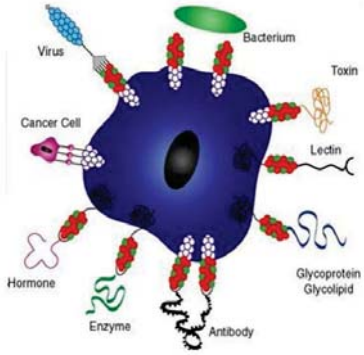

Fig. 1.1.1: Schematic represents the presence of multi-complex glycocalyx on the cell membrane and their interaction with various pathogens.

Glycoconjugates biosynthesis is neither template driven nor translational control. Oligosaccharides are self-assembled in the endoplasmic reticulum (ER) and golgi apparatus by stepwise conjugation of monosaccharide to form a complex glycocalyx which then is finally conjugated to the proteins by glycosyltransferase in post-translational step[3-7].

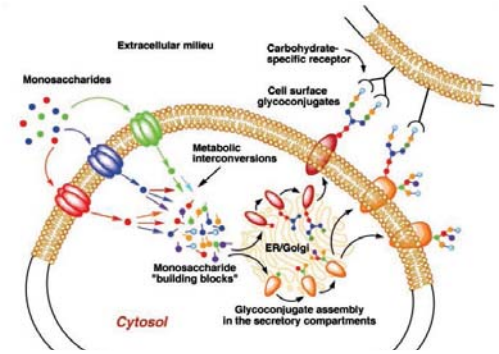

Fig. 1.1.2: Schematic representation of the formation of glycocalyx by glycosidase and post-translational modifications by glycotranferase in ER/Golgi. Adapted from reference [3].

The chemical diversity in the structurally complex glycan modifications containing multiple monosaccharide or complex glycans in linear or branched fashion enables multiple cellular functions. This encompasses structural stability and proteolytic protection of proteins to recognition and regulation of cell signalling networks, such as the regulation of nervous system development and its functions. Glycosylation influences neuronal processes such as neurite outgrowth and morphology. This might modulate physiological events like learning, memory storage and transfer. On the other hand glycosylation in enzymes often leads to developmental defects and can control the physiological behaviour like stress and cognition. The complexity of glycans plays the directorial role in neuronal development during embryogenesis. They also influence behaviour in adult organisms[8-13]. The importance of glycosylation further attracts attention because defects in the structures of the carbohydrates often create human diseases that are known as congenital disorders of glycosylations (CDG). These are all inherited diseases/disorders resulting from glycan biosynthesis, and cause severe abnormalities such as mental disorders and difficulties in motor coordination. Such disorders highlight the importance of glycan biosynthesis in human health development[14-18].

Glyco-proteins are also found in a wide range of organisms that includes plants, bacteria, insects and fish. They possess a diverse range of chemical structures and have some unique properties. For example, in certain mammals they are known to function

as "anti-freeze" protein due to their unique ability to non-colligatively decrease the freezing point of aqueous solutions. This inhibits ice recrystallisation to induce dynamic ice and hence may find many applications in cell/tissue/organ cryostorage, as frozen food preservatives, texture enhancers or even as cryosurgery adjuvant among others.

The key to regulating such cellular processes lie in the variety of carbohydrate units present on the cell surface together with the number of copies of such units present. These concepts will be discussed using two terminologies: 1) The concept of sugar code and 2) Poly-valency of Glycoconjugates.

1.1.1 The concept of the sugar code

The specific recognition of carbohydrates with its corresponding receptors is absolutely essential for carrying out cellular functions. Nature has evolved a large number of carbohydrate binding proteins by taking advantage of the combinatorial potential of carbohydrates, which far outweighs that of DNA and proteins. For example, three different nucleotides or amino acids can be used to create just six distinguishable molecules (3!), while over 1000 polysaccharides may be synthesized from three monosaccharides.

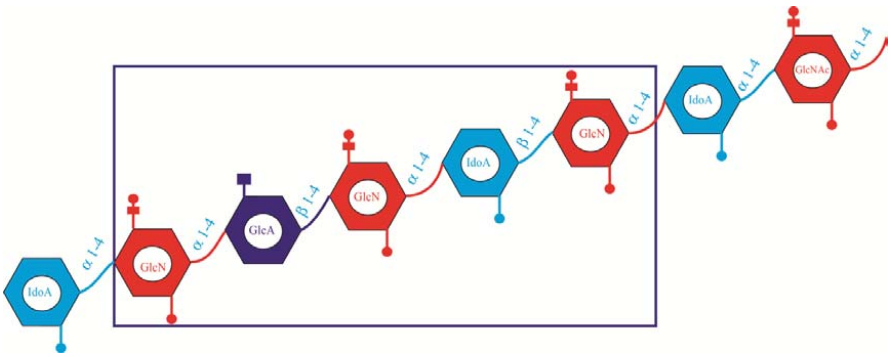

Fig. 1.1.3: Structural representation of the antithrombin III binding pentasaccharides of heparin constituted by a distinct set of C-2, C-3 and C-6 sulfation and N-2-sulfation on D-glucosamine (GlcN) and L-Iduronic acid (IdoA) residues. Adapted from reference [4].

Therefore carbohydrates can rival the information storage and transfer chip in biological system (called the genetic code), which are typically the hallmark of nucleic

acids and proteins. Important cellular binding events utilizing carbohydrates are found in many mammalian systems and are especially prevalent in the immune system. For instance, during an inflammatory response, endothelial cells lining the lumen of blood vessels upregulate expression of carbohydrate binding proteins known as selectins. Transient binding of leukocyte glycoproteins to selectins initiate leukocyte "rolling" and, eventually cause binding and extravasation. For example, the anticoagulant activity of the glycoprotein heparin originates from the binding of the carbohydrate units of heparin to the protein antithrombin III. The specificity of this binding event is dependent on the nature of the carbohydrate unit present in heparin. The full potential of the "sugar code" is revealed when we consider the arrangements of hydroxyls groups (1.2, 1.3 and 1.4) and the linkage in between the two carbohydrates moieties (the anomeric position α/β). Accounting for all combinations, 20 amino acids will yield 6.4 x 10^7 hexapeptide isomers. On the other hand, under same conditions sugars will facilitate formation of 1.44 x 10^{15} different oligosaccharides. The occurrence of glycoprotein or glycolipids in the mammalian glycocalyx decorated with sugars in all the organisms of the evolutionary tree is not a surprising existence. Its function to preserve the actual feasibility of generating "compact units with explicit information properties" has led to the assumption that "the significance of the residue is to impart a discrete recognition role on the protein"[19-28].

1.2 Poly-valency of Glycopolymers

The valency of a substrate (a small molecule, oligosaccharide, protein, nucleic acid, lipid or aggregates of these molecules, organelle, virus, bacterium or cells) is the ratio of the binding affinity of each ligand in the multimer to the monomer.

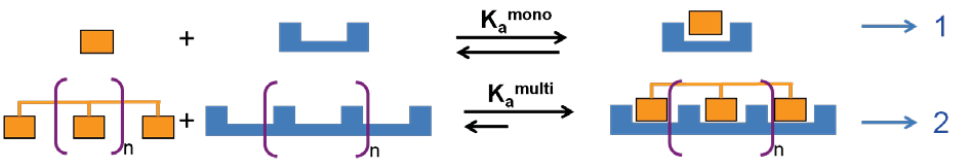

Fig. 1.2.1: Monovalent versus polyvalent binding of ligand to receptor.

The possibility of multiple interactions with unique summation properties opens up new therapeutic strategy for the development of drug and research reagents in biology.

Several examples of polyvalent interactions are observed in biology. One classical example is the adhesion of a virus onto the cell surface; for example the infection of bronchial epithelial cells by influenza virus particles[29] (Figure 1.2.2).

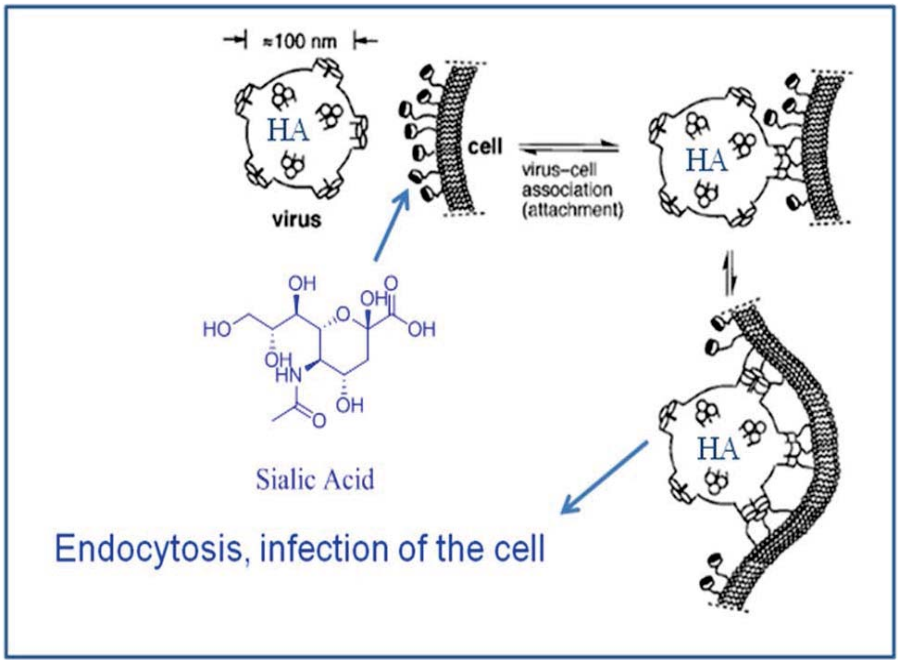

Fig. 1.2.2: Schematic representation for the binding of influenza virus to the epithelial cells [29].

In first step of the infection, the influenza virus attaches to the bronchial epithelial cells, followed by the multiple interactions between trimeric hemagglutinin (HA, a lectin that is very densely arrayed on the surface of the virus particles; 2-4 units/100 nm^2 or 600-1200 per virus particles) and multiple moieties of the carbohydrate N-acetylneuraminic acid (SA= sialic acid) that are densely arranged on the cells surface (50-200/ 100 nm^2)[30-37]. The interaction of N-acetylneuraminic acid and the HA displayed on the virus particle is weak (mM) but they are enhanced by several orders due to the polyvalent interaction as shown in figure 1.2.2.

1.2.1 Polyvalency of carbohydrate in biology

The early steps in cell-surface carbohydrate-mediated cellular processes that involve binding events between carbohydrates and receptors in surface of other cells are expected to be highly specific. However, studies in solution have shown that carbohydrate–protein binding interactions have dissociation constants that are typically in the mM range and that different carbohydrate ligands have similar affinities for the same protein receptor. Hence the origin of the specificity of carbohydrate-protein interaction that mediates specific cellular processes in spite of very weak affinity was paradoxical. However this has been partially explained by the phenomenon of polyvalency. Carbohydrate–protein binding events usually involve several simultaneous contacts between carbohydrates that are clustered on cell surfaces and protein receptors that contain multiple carbohydrate-binding sites. Although the binding of one ligand to one receptor is very weak, multiple binding events among receptors and ligands enhances the binding affinity many folds. This is called "Glyco cluster effect" where the binding epitopes displayed on a large platform can saturate the multiple receptors hanging on the receptor and enhance their binding avidities (the synergistic bond strength between multiple ligands and multiple receptors) many folds through what is called the "Poly-valency" [38-43].

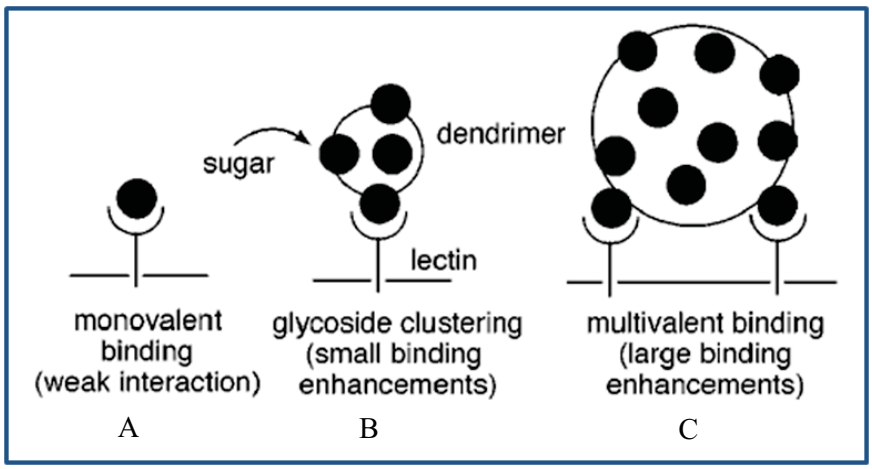

Fig. 1.2.3: Schematic representation of A) mono-valency, B) glyco-cluster effect and C) the poly-valency [44].

1.2.2 Lectins

Lectins are sugar binding proteins that bind to carbohydrates very specifically. This class of proteins are present in all types of organisms and play key role in cellular process such as cell adhesion. Emil Fischer first introduced the concept of cellular recognition as lock-and-key complementarily. The "gluco-cluster-effect" was explained by the concept of "bind and slide" mechanism, which increases the multivalent interactions many fold than their monomeric binding. The lectin proteins are sub-divided into two major classes according to the nature of binding with their corresponding carbohydrates, (1) one binds the carbohydrate moieties in its deep pockets and (2) binds the carbohydrates on the shallow pockets or the surface of the proteins. All of these interactions are also applicable in other organisms'. The class of lectins are subdivided according to their source (A) Plant Lectins, and (B) Animal Lectins. Plant lectins belong to the legume family of proteins/ lectins. They are isolated mainly from plant seeds (M_w~ 40 KD) and consist of 2-4 subunits. Two such lectins (a) Concanavalin A (*Con-A*) and (b) Peanut Agglutinin (*PNA*) are discussed below. *Con-A* is the most abundant protein isolated from jack beans. Mannose and glucose moieties bind to *Con-A* in its deep pockets although the binding affinity towards mannose is four times greater than that for glucose. The binding is mediated by divalent cations such as Ca^{2+} and Mn^{2+} [44-50]. Peanut Agglutinin (*PNA* specifically binds to galactosyl moiety and do not require any divalent metal ions to enhance their binding affinity. These two lectins are mostly abundant in nature are also easy to isolate. There are several other plant lectins in nature such as wheat germ agglutinin (WGA), immunoglobulin (IgA) and Ricinus communis agglutinin (RCA).[51, 52]. Animal lectins are originally divided into two categories: C-type (Ca^{2+} ion dependent) and S-type (sulfydryl dependent). According to their structural diversities several lectins have been classified as C-type, S-type (galactins), I-type, P-type (Phosphomannosyl receptor) etc[51-53]. Animal lectins play a pivotal role in a variety of functions that includes self / non-self recognition, intracellular routing of glycoconjugates, as molecular chaperones during glycoprotein synthesis, mediation of endocytosis, cellular growth regulation, extracellular molecular binding, cell-cell interactions for homing

Fig. 1.2.4: Con-A,tetrameric

and trafficking, scavenging of cellular debris, anti-inflammatory and urate transport actions among others. Lectins regulate molecules within the immune systems for recognition and trafficking within the immune systems, immune regulations (suppressions or enhancements) and prevention of auto-immunity.

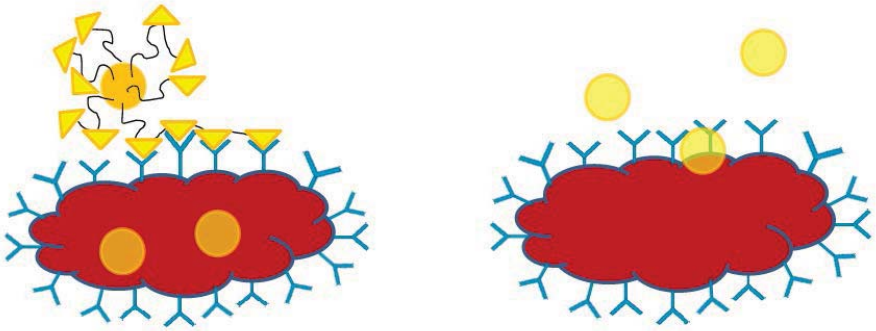

Fig. 1.2.5: Ligand decorated drug cellular uptake by receptor mediated endocytosis (left) by pinocytosis (right) [37].

1.2.3 Evaluation of lectin/carbohydrate interaction

Several methods have been used to qualitatively and quantitatively estimate carbohydrate-lectin interaction. Some of them are summarized below.

1.2.3.1 HIA Assay

Out of the several techniques used to assay carbohydrate-lectin interaction, Hemaagglutinin Inhibition Assay (HIA), is one of the oldest and widely used method. Although it does not give absolute binding constants, it gives the relative binding affinities between two carbohydrate epitopes. Ligand solutions are initially placed at different concentrations into the microwells, and this is followed by the addition of soluble lectin to allow precipitation of aggregates. Upon completion of the precipitation, the minimum concentration of carbohydrate that inhibits the hemagglutinination reaction is reported[54].

1.2.3.2 Isothermal Titration Calorimetry (ITC)

Isothermal Titration Calorimetry (ITC) allows determination of physical parameters such as the binding constant, the enthalpy and the entropy of binding. In ITC measurements, the enthalpy change occurs upon binding of carbohydrates with their corresponding lectins due to the change in the geometry of the water clusters that surround the binding sites [55, 56].

1.2.3.3 Surface Plasmon Resonance (SPR)

SPR evaluates the binding constant of ligand receptor interactions and also allows measurement of kinetic parameters such as the "on" and "off" rates. These parameters are measured by observing the refractive index change on the surface upon binding of lectin to carbohydrates that are immobilized on a gold [57].

Other than these sophisticated techniques, other techniques based on the UV-Visible spectrometer such as turbidimetry assay, quantitative precipitation assay are performed to get rough idea about the binding affinity among lectins/carbohydrates. Other than these, there are some complementary techniques like ELISA or ELLA Assay, Turbidity Assay, Quartz Crystal Microbalance (QCM) and electrophoresis to determine the molecular size of the proteins adhered [58-60].

1.2.4 Synthetic glycopolymers

Glycopolymers, synthetic macromolecules featuring pendant carbohydrate moieties, have been investigated in diverse biomedical applications including, but not limited to, macromolecular drugs and drug delivery systems, biocatalytic and biosensitive hydrogels and matrices for controlled cell culture. Many of these require synthesis of glycopolymers of controlled structure with respect to attributes such as molecular weight, glycosylation density, and position. These polymers have been typically synthesized by a) polymerization of glycans containing monomer (radical polymerization) and b) or the post-polymerization modification with glycans on the polymeric backbone. Several polymerization techniques (FRP, ATRP, ROP, ROMP etc.) have been used to synthesize well defined glycopolymers by polymerization of glycan containing monomers. The chemical structures of some of these polymers that

have been obtained are shown below [61-71] (Figure 1.2.7). The interaction of these glycopolymers with their corresponding lectins (*RCA/Con-A*) have been studied in detail.

The interaction between glycopolymers and lectins are modulated by several parameters. These include 1) flexibility of glycopolymers or ligand, 2) number of sugar moieties present on the backbone and available for binding, 3) molecular weight and length of the glycopolymers chain [61]. Considering all these factors, it has been suggested that the polymer architecture has great influence on the binding interactions.

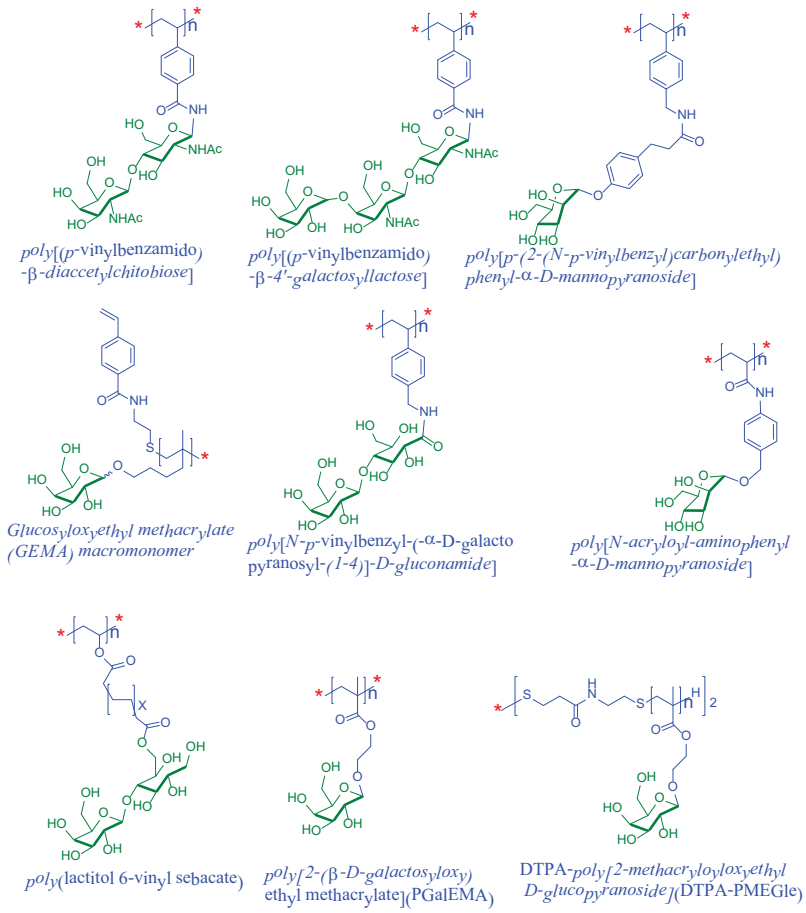

Fig. 1.2.6: Structures of glycopolymers obtained by polymerization (ATRP or RAFT) of glycan containing monomers[61-69].

1.2.4.1 Synthesis of glycopolymers by ring opening metathesis polymerization (ROMP)

Kiessling and co-workers have synthesized glycopolymers by ruthenium catalyst initiated ROMP via controlled/living polymerization method. The glycan content of the highly glycosylated norbornene copolymers containing mono/disaccharides were varied by mixing mannosyl/galactosyl containing monomers in various ratios. The interaction of the synthesized polymers with the model lectin concanavalin-A (mannose specific) was studied in detail by various techniques such as quantitative precipitation assay, ELISA and ELLA[72-74].

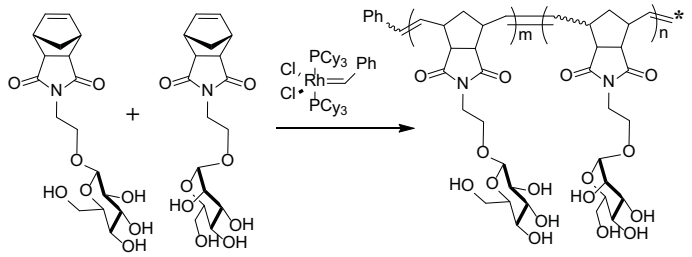

Fig. 1.2.7A: Monosaccharide containing monomer [83].

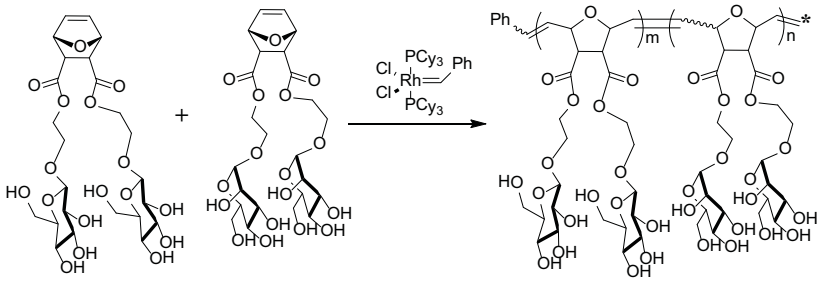

Fig. 1.2.7B: Disaccharides containing monomer [83, 84].

1.2.4.2 Post-polymerization modification on polymer backbone

Strong and Kiessling synthesized a series of N-hydoxy succinimide (NHS) functionalized polymers via ATRP and ROMP which were subsequently treated with amine containing mannose derivatives to obtain desired glycopolymers as shown below[75-85] (Figure 1.2.9).

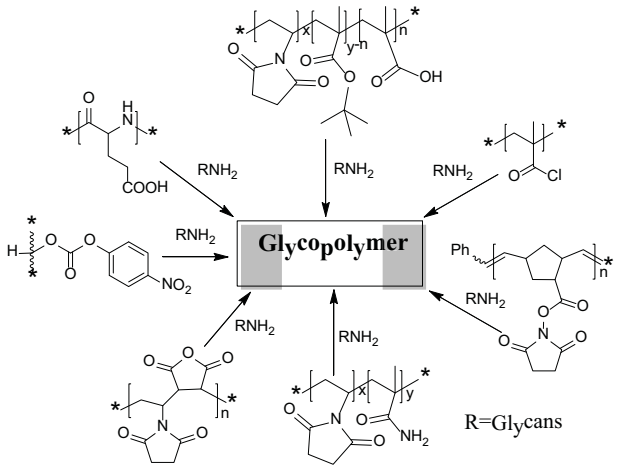

Fig. 1.2.8: Represented the glycosylated amide bond formation

Glycopolymers have also been synthesized by post-polymerization modifications using Cu catalyzed azide-alkyne reaction (CuAAC) and by thiol-ene click reaction. Haddleton and co-workers have investigated the synthesis of glycopolymers by click reactions from well defined polymer back-bone having an alkyne side-chain [76-79].

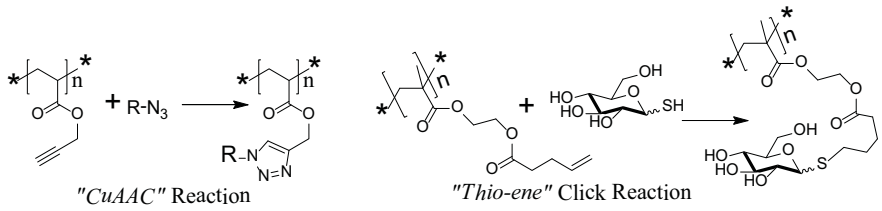

Fig. 1.2.9: Representation of post-polymerization modification by "click" reactions.

1.2.4.3 Glycosylated Dendrimer

Another approach was taken by Collinger and co-workers wherein PAMAM dendrimers were synthesized and then subsequently glycosylated using mannose and galactose derivatives. The details of binding with their corresponding lectins were studied and these materials were found to be poly-valent [45].

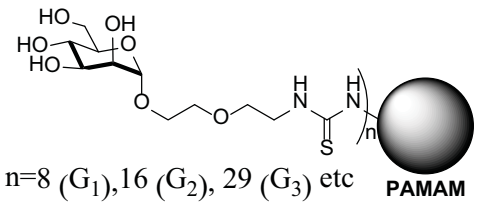

Fig. 1.2.10: Representation of the glycosylated dendrimers.

1.2.4.4 Glycosylated Nano Objects: from micelle to nano-fibres

Synthetic glycopolymers can be classified into glycodendrimers, linear glycopolymers, branched/brush-like glycopolymers and spherical glycopolymers in the form of the micelle, vesicles and micro/nano-particles. These advanced materials are capable of showing multiple interactions via the so called "cluster glycoside effect". This section is completely focused on glycopolymers with different architectures and understanding of their interaction with lectins (*Con-A*). These glycopolymers are classified into four categories, (A) linear glycopolymers, (B) spherical or surface assemblies of glycopolymers, (C) glycopolymers adhered on the materials surfaces and (D) glycosylated dendrimers[43-47]. The syntheses of glycopolymers are carried out by a) polymerization of sugar containing monomer and b) post-polymerization modification of the polymer. However, there are many issues in the synthesis of these polymers as well as their biocompatibility for use *in vivo* application. On the other hand, polypeptides are constituents of the proteins and can be promising materials in tissue engineering and biomedical applications. When these polypeptides are glycosylated they are called the glycoproteins or glycopolypeptides. They have well defined secondary structures, are expected to be biocompatible and are functionally close to naturally occurring proteoglycans.

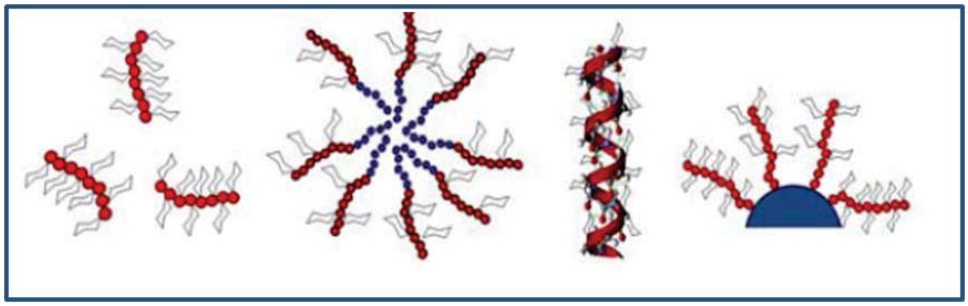

Fig. 1.2.11: Represents linear (A), spherical assemblies (B), helical (C) and Surface functionalized (D) glycopolymers [37].

Amphiphilic block copolymers containing hydrophilic glycopolymers conjugated to hydrophobic block self-assemble into micelles, vesicles, worm-like aggregates or nano-fibers. Such assemblies have a large surface area and effectively bind with lectin proteins. Haddleton and co-workers modified Wang resin with mannose to get active surface and used these as column materials for protein purification chromatography[80-88].

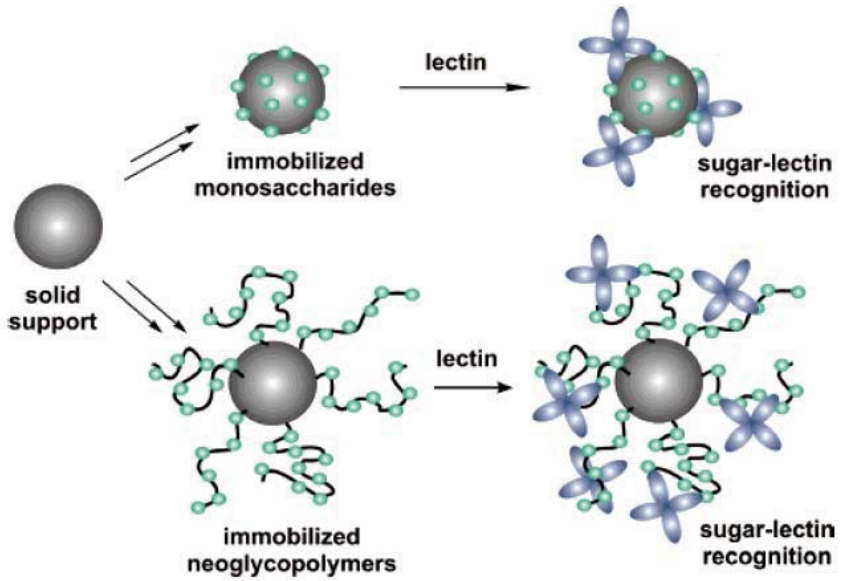

Fig. 1.2.12: Representation of the surface functionalization of Wang resin[37].

Glycopolymer architectures	**Synthesis method**	**Carbohydrate epitope**	**Lectin**	**Assay**
Linear polymer	FRP	α-D-Glc(1/4)D-Glc,-β-D-Gal(1/4)D-Glc, α-D-Glc(1/4)DGlc(1/4)D-Glc	Con-A	Turbidity
Linear polymer	ROMP	α-D-GlcNAc	Con-A	HIA
Linear polymer	FRP	β-D-Gal(1/4)D-GlcNAc	EC or L	Fluorescence
Linear polymer	ROMP	α-Glc, α-man	Con-A	HIA
Linear polymer	ROMP	α-GluNAc, α-manNAc	Con-A	HIA
Linear polymer	FRP	β-Lac, β-chitobiose	WGA, PNA, RCA120, ECA, DSA	DDA, HIA
Linear polymer	ROMP, PF	α-man	Con-A	HIA
Linear polymer	ROMP	SO_3 -β-Gal(1/4)-α-Fuc(1/3)SO_3_β-Glc	L-selectin	ELISA
Linear polymer	FRP, PF	α-Glc, β-Glc, β-Gal, β-Lac	ConA, RCA_{120}	HIA
Grafting onto gold surface via thiol	FRP	α-Man	Con-A	QCM

functionality				
Grafting onto gold surface via thiol functionality	ATRP	Lactoselactone	RCA_{120}	SPR
Grafting from gold surfaces	ATRP	β-Gal(1/4)Glc	RCA_{120}	SPR
Grafted from honeycomb structured films	RAFT	Glc	Con-A	Fluorescence
Linear polymer	ATRP, PF (Click)	α-D-Man, β-D-Gal	Con-A	SPR, ELISA
Linear polymer	FRP	α-D-Gal(1/1)α-D-Glc, α-D-Gal(1 /1)β-D-Glc	BSI–B4, Shiga toxin-1	Turbidity
Linear polymer	Suzuki P., PF (Click)	Glc	Con-A, PNA	Turbidity
Liposome	Chemical enzymatic	α*l*Fuc	E-selectin	ELISA
Core-shell, nano spheres	FRP	Glc	Con-A	ELLA
Micelles and other self-assembled structures	ATRP	β-D-Gal(1/4)β-D-Glc	RCA_{120}	Turbidity

Table 1.2.1: Represents different synthetic route of the glycopolymers and their molecular recognition towards lectins determination by different techniques [80-88].

1.3 Synthetic Development of Well Defined Glycopolypeptides

1.3.1 Importance of polypeptides in biological system

Synthetic polypeptides, which are poly-(amino acid)s linked by peptide bonds, are unique biodegradable and biocompatible synthetic polymers having structures that

mimic natural proteins. In comparison with conventional biodegradable polymers, synthetic polypeptides may form stable secondary structures, such as α-helix and β-sheet, leading to unique self-assembly behaviours. In addition, the self-assembly structures of some polypeptides exhibit physical changes in response to external stimuli, such as pH, salt, and temperature. Especially, some polypeptides with charged side groups can form electrostatic interactions with oppositely charged drugs and bioactive macromolecules, such as DNAs, RNAs, and proteins. Therefore, polypeptide-based materials have attracted increasing attention for their great potential in biomedical and pharmaceutical applications. Synthesis of polypeptides by conventional solid phase synthesis is very laborious and purification steps are very tedious. This methodology does not allow higher chain length polypeptides (> 100 repeating units). The practical route to synthesise high molecular weight polypeptides is by the ring-opening polymerization of their corresponding amino acid N-carboxyanhydride's. This allows one to obtain very high molecular weight polypeptides in very good yields having extremely low polydispersities[89-93].

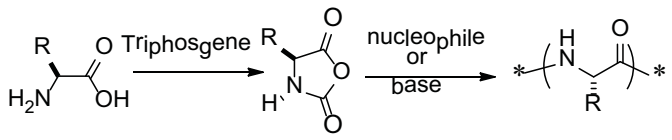

Scheme 1.3.1: Schematic representation of NCA polymerization.

Glycopolypeptides (glycopolymers with pendant carbohydrates on a polypeptide backbone) mimic the molecular composition of proteoglycans and are expected to mimic glycoproteins that control several cellular processes. Hence the glycopolypeptides can show promises are materials for tissue engineering scaffolds and as drug delivery vehicles. Unfortunately, there are very few literature reports for the synthesis of glycopolypeptides. The synthetic approaches reported in the literature can be subdivided into three classes[94-96]; A) Solid phase synthesis of glycopolypeptides from glycosylated amino acid constituents, B) Post-polymerization modification of the functional polypeptides backbone, C) Polymerization of glycosylated N-carboxyanhydrides of amino acids.

1.3.2.1 Solid phase synthesis of glycopolypeptides from glycosylated amino acid constituents

I*. N-glycosylated glycopolypeptides:* N-glycosylation is the most common post-translational modification of proteins wherein carbohydrates are transferred to the asparagines residue in the common sequence Asn-X-Ser/Thr in the proteins. The importance of the N-glycosylated glycopolypeptides in biological system has resulted in development of two methodologies[97].

1) In the sequential glycosylations of glycosylated amino acids, cassettes are used to elongate the peptide chain. By incorporation of the side chain oligosaccharides, the polarity and solubility as well as reactivity changes due to the presence of free –OH groups.

2) Another approach is the convergent synthetic method, where aspartate in the protein is glycosylated. However, there are also lots of drawbacks due to the formation of undesired side products and overall yield is very low.

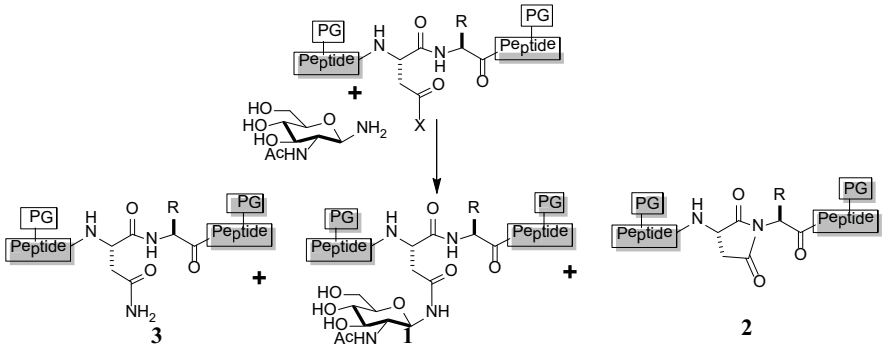

Lansbury aspartylation leads to glycopolypeptides 1, Asn peptide 3 and aspartimide side product 2, PG= Protecting Group

Scheme 1.3.2: Schematic representation of the solid phase synthesis of N-glycosylated polypeptides [97].

II. *O-glycosylated polypeptides by solid-phase synthesis*

In most glycopolypeptides, the carbohydrate groups are structurally connected to the serine/threonine residue of the polypeptide backbone. For example, anti-cancer vaccine candidates Tn and STn antigens contain the carbohydrates GalNAcα and NeuAcα2-6 GalNAcα that are linked to the serine/threonine residue of the polypeptide. Hence development of O-linked glycopolypeptides is of great interest for the development of drugs and vaccines. Synthetic developments have basically involved solid phase synthesis by taking glycans (sugar containing amino acids) as building blocks. This approach can be used for the synthesis of glycopeptides and glycoprotein libraries if standard building blocks (glycosylated amino acids) that are compatible with automated peptide synthesizer is readily available. This is very important to achieve synthetic control over these glycopeptides which is extremely critical for the study of structure-activity relationship (SAR) in biology[98-105]. However this is a very big challenge since the coupling reaction of the linker conjugated resins to glycans (sugar conjugated amino acids) is not very efficient and leads to incomplete functionalization making final purification of the glycopolypeptide extremely difficult.

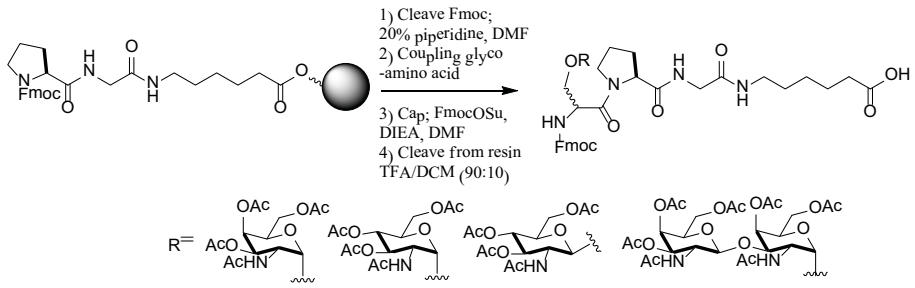

Scheme 1.3.3: Representation of solid phase synthesis of the *O*-glycosylated glycopolypeptides[98].

III. *Solid phase synthesis of glycosylated polyproline*

Conformational differences in the secondary structures in polyprolines (PP II) has unique significance in protein folding and defolding with characteristically left handed helix (ϕ = -78° and Ψ = 146°) with three amino acids residues per turn and all-trans amide bonds (ω = 180°). It has implications in protein-protein recognition which

regulates biological functions like signal transduction, cell motility and immune response[106]. Among naturally occurring amino acids, proline and hydroxy-prolines (HYP), dominate the polyproline II conformation. They have excellent biological functions like crossing cell membranes, molecular spacer, molecular rulers, cell wall penetrating and antibiotic activities. The hydroxy-proline rich glycoproteins (HRGPs) are abundant in plant kingdom and they can form very stable poly-proline II conformation (PP II). They are mostly linked by β-glycosidic bonds with either monosaccharides or oligosaccharides depending on the post-translational modification of hydroxy-proline residue part of the proteins[107-109].

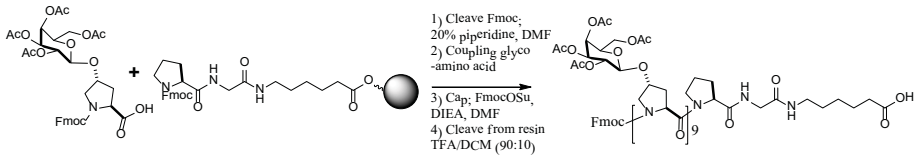

Scheme 1.3.4: Representation of the solid phase synthesis of poly-(glycosylated proline)$_9$-NH_2[106].

This synthetic methodology also suffers from common limitation of solid-phase synthesis which makes synthesis and purification of glycosylated polyproline with high molecular weights very difficult.

1.3.2.2 Post-polymerization modification of the functionalized polypeptide backbone

Glycopolypeptides synthesized by post-polymerization methods have typically used "click chemistry" strategies in which carbohydrates are attached to a side chain of a pre-made polypeptide using either the azide-alkyne cycloaddition reaction (CuAAC) or the "thiol-ene" reaction[109, 110].

1) Glycopolypeptides have been synthesized by attaching azide functionalized glycans to alkynylated polypeptide backbone using CuAAC. Zhong *et al.* were the first to report the synthesis of glycopolypeptides by this methodology in which azide containing carbohydrates were conjugated to alkyne side-chain of poly-γ-propyl-glutamate using CuAAC. Around the same time, Heise and co-workers synthesized a copolymer of poly-propargyl-glycine and poly-γ-benzyl glutamate in which the alkyne side chain in the co-polypeptide was subsequently

functionalized with azido-sugars by using CuAAC. Deprotection of the benzyl ester as well as acetyl groups of the sugars led to the synthesis of completely water soluble glycopolypeptides.

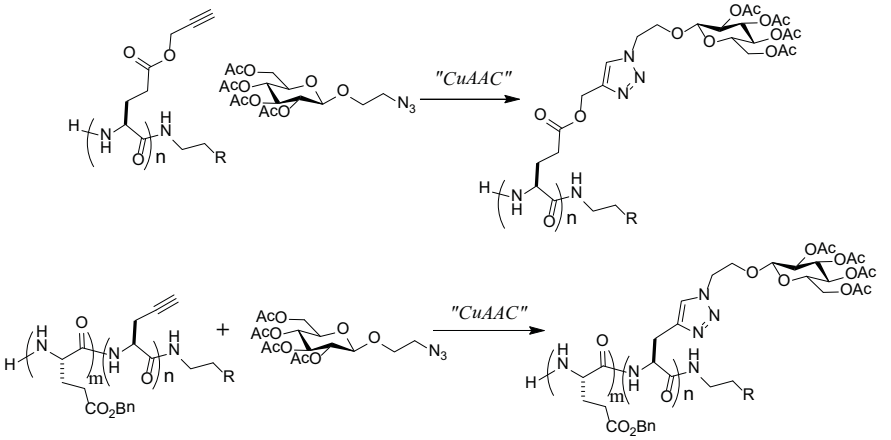

Scheme 1.3.5: Representation of the "*CuAAC*" reaction for post-polymerization modification of polymer backbone[109, 110].

2) Glyopolypeptides have also been synthesized by reaction of thiolated glycans onto the alkene functionalized polypeptides using the "thiol-ene" click reaction. Schlaad and co-workers first reported this methodology for synthesis of glycopolypeptides as has been shown below [111].

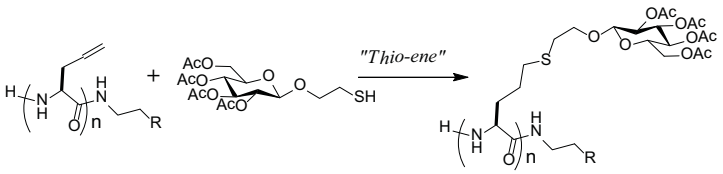

Scheme 1.3.6: Representation of the "*Thiol-ene*" reaction for post-polymerization modification of polymer backbone[111].

Although the post-polymerizations have been carried out by the very-efficient CuAAC or the thiol-ene click reaction, it is statistically nearly impossible to synthesize well-defined stable and water soluble glycopolypeptides with 100% functionalization. Further, the glycans are conjugated to the polypeptide backbone by triazole linkage or sulphide linkage and these are typically not bio-mimetic and their cytotoxicity is

unknown. Hence synthesis of bio-mimetic glycopolypeptides with 100% glycosylation is necessary for biomedical applications. One strategy to obtain this would be by polymerization of glycosylated N-carboxy-anhydride of amino acid (Glyco-NCA's) monomers as shown below.

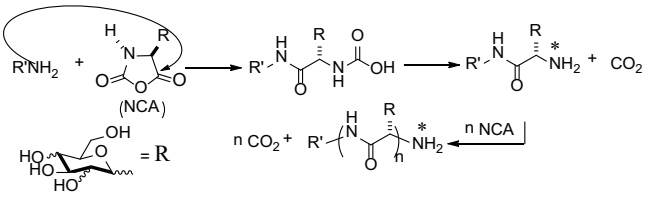

Scheme 1.3.8: Representation the Ring Opening Polymerization (ROP) of the "Glyco-NCA's".

1.3.2.3 Polymerization of glycosylated amino acid N-carboxy-anhydrides (NCA's) by Ring Opening Polymerization

In 1994, Okada and co-workers reported the first synthesis of well defined 100% glycosylated glycopolypeptides by ring-opening polymerization of their corresponding glycosylated amino acid N-carboxy-anhydrides (NCA's). It should be also mentioned that in 1966, Rude *et al*. had successfully synthesized saccharide conjugated amino acid N-carboxy-anhydrides (NCA's) [112] but they were unable to polymerize them to obtain well-defined glycopolypeptides. Okada and co-workers prepared well-defined and fully characterized water soluble glycopolypeptides with controlled molecular weight and low polydispersities by modifying the methodology published by Rude and co-workers [112-116]. However, this methodology has several limitations and hence was not used by any other group subsequently. These limitations are discussed below.

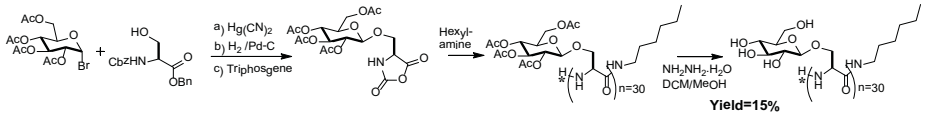

Scheme 1.3.9: Representation of Ring Opening Polymerization (ROP) of "Glyco-NCA's" (glycosylated serine NCA)[115].

1.3.3.1 Limitations of this methodology

1) The glycoconjugate of amino-acid (serine) was prepared by the "Koenings-Knorr" reaction using the environmentally toxic mercuric cyanide $Hg(CN)_2$. This glycosidation reaction is not very efficient (overall yield < 40%) and several side products such as lactol are formed during the course of the reaction. The overall yield for the synthesis was extremely low (<15%).

2) The kinetics of polymerization was extremely slow and it took 4 days to synthesize a glycopolypeptide with 30 repeating units. The authors have proposed that the sluggishness of the polymerization reaction is due to the stability of the monomers due the H-bonding in between C-2 acetyl of the sugar and NH of the cyclic N-carboxy-anhydride in the monomer. This inhibits the nucleophilic attack of the initiator onto the carbonyl nucleophilic centre of the cyclic N-carboxy-anhydrides [116](Fig. 1.3.1).

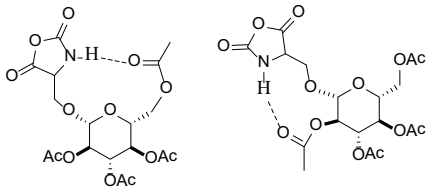

Fig. 1.3.1: Representation of the H-bonding in between C-2, C-6 acetyl of sugar and the NH in the cyclic anhydride ring[116].

3) The secondary structures of this synthesized glycopolypeptides were not reported

1.3.3.2 Towards more efficient synthesis of glycopolypeptides

Efficient synthesis of glycopolypeptides requires development of new synthetic methodology that allows the glycosylation step to be carried out quantitatively under environmentally friendly conditions. The cyclic N-carboxy-anhydride ring should be sufficiently away from the glycosylated moiety so that there is no H bonding interaction or steric crowding to inhibit

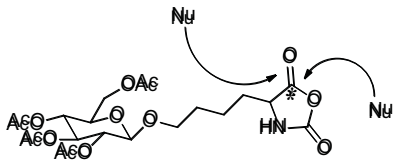

Fig. 1.3.2: Representation of hypothesized structure of the glycoconjugated amino acid and nucleophilic attack on the carbonyl nucleophilic centre of the cyclic anhydrides.

nucleophilic attack on the carbonyl nucleophilic centre of the cyclic ring.

1.3.4.1 Deming's glycosylated lysine NCA Polymerization approach

In 2011, Deming and co-workers reported a new synthetic methodology for the development of 100% glycosylated glycopolypeptides with controlled molecular weights and well-defined secondary structures [117].

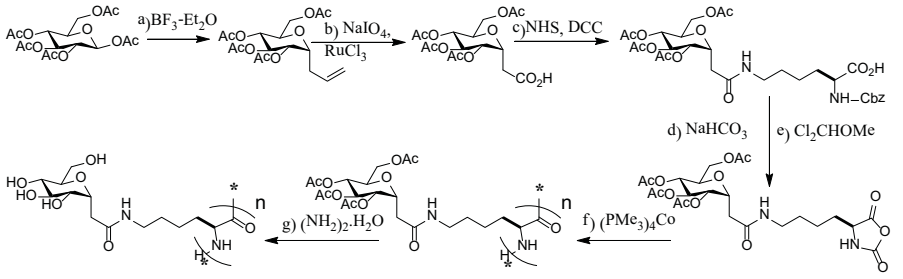

Scheme 1.3.10: Schematic representation of the approach by Deming and co-workers[117].

The key step of glycoconjugation in this synthetic scheme followed previous reports by Dondoni and co-workers. However, this methodology has several limitations. These include (i) poor over all yield of <25% since the long six-step synthetic scheme involves some low-yielding reactions (ii) $RuCl_3$ catalyzed alkene oxidation step renders this scheme unsuitable for synthesis of disaccharide or oligosaccharide conjugated amino acids. (iii) use of metal initiator for polymerization renders generation of end group functionalized polypeptides difficult.

From all the approaches discussed above it is clear that there is still scope for development of a new synthetic methodology to fulfil the demand of glycopolypeptides that are functionally and structurally similar to naturally occurring glycoproteins. I am going to discuss a completely new synthetic methodology developed by us which involved well characterized, controlled, living and high molecular weight polymerization technique of "Glyco-NCA's" in the Chapter II of my thesis.

1.3.4.2 Investigation of secondary structures of the glycopolypeptides

Several proteins posses' secondary structures, those are critical for their function in biological systems. Synthetic polypeptides that are analogues of constituents of proteins may also have secondary structures either in solution or in the solid state. Poly-lysine or poly-glutamic acid are normally α-helical in nature when their side chains are uncharged but at neutral pH when their side-chains are charged they adopt a random coil conformation. Recently Cheng and co-workers have beautifully demonstrated that if the charged side chain is sufficiently elongated, the α-helical conformations of those polypeptides are not disrupted. Deming and co-workers have showed that glycosylated ε-NH (amine) of lysine linked glycopolypeptides have a stable α-helical conformation. Circular dichroism analysis of these glycopolypeptide solutions in water showed sharp signal at 208 nm and 222 nm, indicating that they are fully α-helical in nature. Simultaneously, increasing the temperature of solution showed decrease in helicity while upon cooling was regained. Hence the changes are reversible in nature and the helicity decrease with increasing the temperature can be explained by the disruption of H-bonding in amide backbone of i and (i+4) residue[117, 118]. Deming and co-workers have recently reported the transition of an α-helical glycopolypeptide to one having a random coil conformation upon oxidation of sulphur atom to sulphoxide at the junction between glycans and cysteine.(Scheme 1.3.11) The change in conformation occurs since the disulphoxide breaks the intramolecular H-bonding between amide and carbonyl in the peptide backbone. This results in a transition from α-helical to random coil conformation[119].

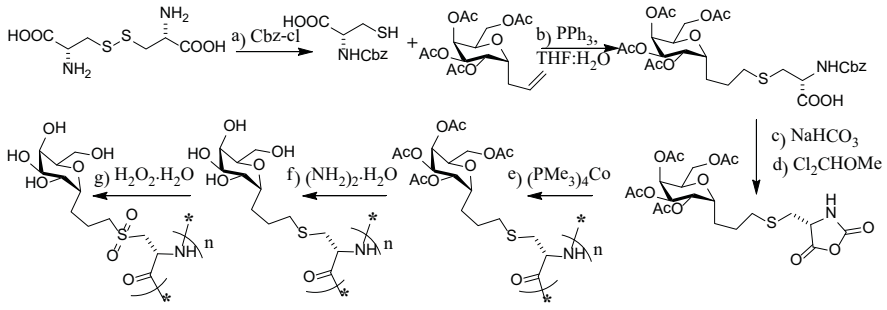

Scheme 1.3.11: Represented the schematic of chemical structures from α-helical to random coil conformation by Deming and co-workers[119].

Co-polymerizations of racemic amino-acid N-carboxyanhydrides typically incorporates both the enantiomers randomly and this disrupts the α-helical structure to form the extended coil conformation[120-122]. This concept helps us to make glycopolypeptides wherein the glycosylated recimic amino acids N-carboxy-anhydrides were copolymerized to achieve extended coil structures. The details on synthetic and structural analyses as well as their effect on binding properties are discussed in the Chapter III of my thesis.

1.4 Polypeptides self-assemblies

1.4.1 Importance of block-copolypeptides self-assembly

Due to their excellent biocompatibility and biodegradability, polypeptide copolymers and their self-assembly into various supramolecular aggregates may find important applications in bio-related fields, such as drug delivery and tissue engineering. Like natural proteins, polypeptide segments can adopt various conformations, such as a random coil, α-helix and β-strand which under certain conditions, can transform from one to another. For block co-polypeptides, the conformation is related to the solubility and rigidity of the polypeptide blocks. Both of these have a significant influence on the self-assembly behaviour of copolymers in solution. Understanding supramolecular assembly of simple block copolypeptides could be helpful for knowing the aggregation behaviour of complex polypeptides and, by extension, protein systems. This would also allow the creation of hierarchically self-assembled structures since they are of great interest in applications such as photonic crystals, biosensors and fuel cells among others.

In nature, the self-assembled compartmentalization is a powerful tool for efficient functioning of metabolic and signalling pathways in cells. For example, many serial catalytic reactions take place in cells in a consecutive manner such that the ultimate final products are formed via series of enzymatic activities in a predominant order[123]. They also protect the cells from its contents in the lysosomes or proteosomes. The compartmentalisations in the cell membranes create the protein channels, which function to rearrange the membrane proteins and cytosolic proteins in cells during cellular migration and endocytosis processes. Deep understanding of the process of self-assembly of block co-polypeptides would allow the fabrication of hierarchical

structures by a polymer self-assembly process. Polypeptide-based block copolymers can serve as promising building blocks in fabricating hierarchical assemblies with sophisticated structures[124, 125].

1.4.2 Energetic of block-copolymer self-assembly

Amphiphilic block copolymers are able to self-assemble into well-defined nanostructures in aqueous solution. The equilibrium morphology and aggregation number of diblock copolymer assemblies is primarily determined by the balance of three energetic factors: (1) interfacial tension, (2) corona chain crowding, and (3) core chain stretching[126-130]. The balance of these three factors dictates an equilibrium curvature for the aggregate. Typically, solution morphologies formed by amphiphilic block copolymers follow a trend of increasing interfacial curvature. As the hydrophilic fraction is increased in the copolymer, vesicles, cylindrical micelles, and spherical micelles (in the order of increasing interfacial curvature) are the most common morphologies[131-134]. Physically, this is explained as a balance between entropic freedom of the hydrophilic coronal chains and shielding of the hydrophobic blocks from the aqueous solution. As the hydrophilic fraction increases, the chains are more able to effectively stabilize these assemblies without close-packing, and the free energy of the system is lowered when the coronal chains are provided more entropic freedom/mobility through increased curvature. For diblock copolymers, the size of spherical micelles can be predicted based on the aggregation number and degree of polymerization of the coronal chains[133]. Eisenberg and co-workers at first reported the aggregation behaviour of the block copolymers. The self-assemblies of those block copolymers manifested into micro to nano structures[134]. They showed that different morphologies can be achieved by employing block copolymers with varying amphiphilicity that can be tuned by synthesizing polymers with different chain lengths. The amphiphilic block copolymers assemble in solution (hydrophilic/hydrophobic solvent to minimize the total energy of the system) in such a way that they form commonly bilayer or multilayers that result into multi-compartment or mono-compartment geometries based on cylindrical or conical shapes of the amphiphiles. The theoretical sizes of vesicles and worm-like micelles are difficult to predict, yet the thickness of these types of assemblies is often dictated by the chain length of the

hydrophobic blocks. Other non-typical morphologies such as multi-compartment micelles, disk micelles, nano-tubes, toroidal micelles, bicontinuous micelles, and corkscrew micelles have been observed, often arising through structural complexity, solvent composition, or specific interactions. The intrinsic shape of the polymer amphiphile, in between cylindrical and conical shape, depends on the ratio of the hydrophilic and hydrophobic volume fractions of the block copolymer amphiphiles[135, 136].

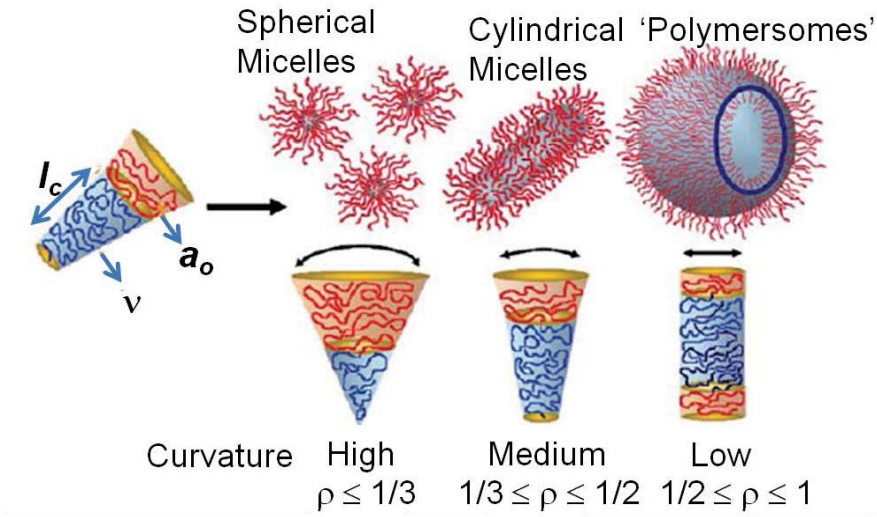

Fig. 1.4.1: Representation of different shapes of the amphiphiles[137, 138].

For small molecules these geometries can be explained by the dimensionless term "packing parameter" (p) and can be applied to some extent to the polymeric amphiphiles. More intuitively, the hydrophilic fraction (f) is better suited to predict geometry of the block copolymer.

Shape (Morphology)	Packing Parameter (v/al)	Hydrophilic Fraction (f)
Sphere (Micelle)	1/3	> (50)%
Cylinder (Worm like micelle)	1/2	≈ 50%
Bilayer (Polymersomes)	1	≤ 50%

Table 1.4.1: Represents the co-relations of amphiphiles shape to morphology with respect to their "packing parameter" and "hydrophilic fraction".

For block copolymers, with a hydrophilic fraction (f) > 40-50 % mostly micelles are formed while for (f) ≈ (35 ± 10)% mostly vesicles or "polymersomes" and for (f) < 25% inverse structures are obtained, whereas (f) ≈ 50% wormlike micelle structures are obtained. The dependence on the other thermodynamic and kinetic parameters and the chemical nature of block copolymer yields different structures, which might be perfectly fitted with the hydrophilic fraction (f) [137, 138].

1.4.3 Preparation of "Polymer self-assemblies"

Polymer self-assemblies are obtained classically by two major methodologies although there are several other methods reported for their preparation.

1.4.3.1 "Solvent Switch" method

The block copolymers are dissolved in a suitable organic solvent where both of the blocks are soluble. Subsequent addition of a second solvent, which solubilises only one block (mostly water) leads to the formation of aggregates. Finally on removal of the organic solvent by dialysis self-assembled structures are obtained. The main drawback of this process is that for biological applications the complete removal of organic solvent is necessary to avoid toxicity issues. Nevertheless this technique is the most convenient one and is broadly used to encapsulate desired molecules inside the polymersomes.

1.4.3.2 Rehydration method

Electroformation or rehydration to the bulk procedure involves coating polymer film on the surface followed by rehydration in which with the film is put in water or the water is injected into the film[139].

1.4.4 Mechanism for the self-assembly into polymersomes

Among most of the morphologies that are obtained upon self-assembly of block-copolymers, the mechanism for assembly into functionally active polymersomes (*vesicles*) is best understood. Two major pathways have been proposed in literature. These include transition of bilayer to polymersomes (pathway I) and dynamic transition of micelle to polymersomes (pathway II).

1.4.4.1 Assembly via pathway I

In this mechanism, amphiphilic polymers at first form a bilayer from a miceller or polymeric cluster which subsequently closes to form polymersomes. This leads to high encapsulation or loading of molecules inside polymerosomes. Upon studying the assembly of poly(ethylene oxide)-*block*-poly[3-(trimethoxysilyl)propyl methacrylate] (PEO_x-*b*-$PTMSPMA_y$), Du and Chen experimentally observed first the formation of miceller aggregates which then transformed into lamellar or bilayer structures and finally lead to the formation of polymersomes. They were able to adjust the solvent polarity and were also able to trap the intermediates by using microscopic techniques (TEM) [140].

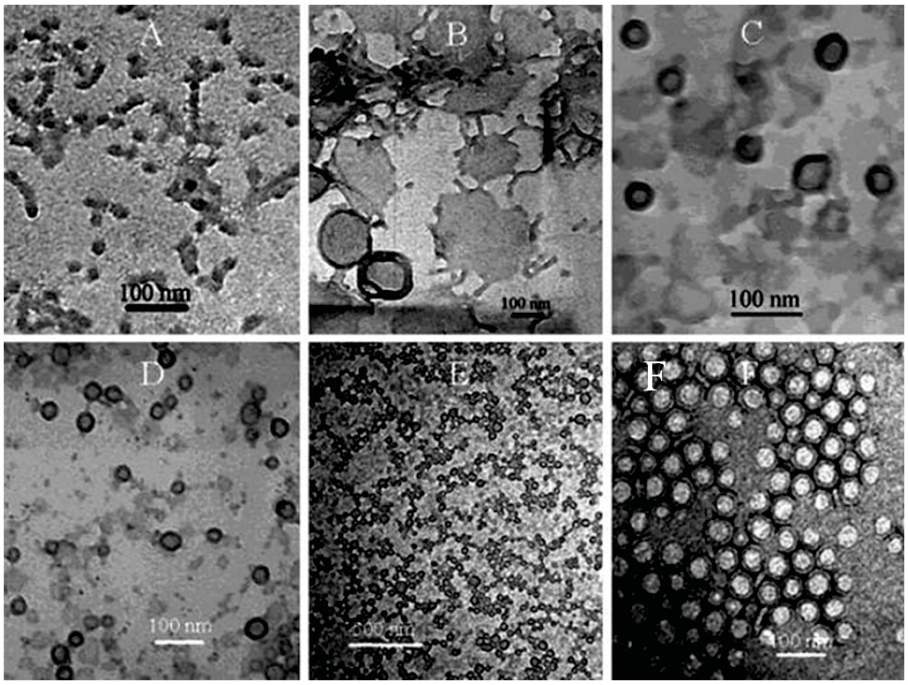

Fig. 1.4.2: Represented (Path I mechanism) several stages of polymersome formation, captured in TEM by Du and co-workers. First spheres and rods are formed that transform into lamella which close to form polymersomes due to an increase in water content[140].

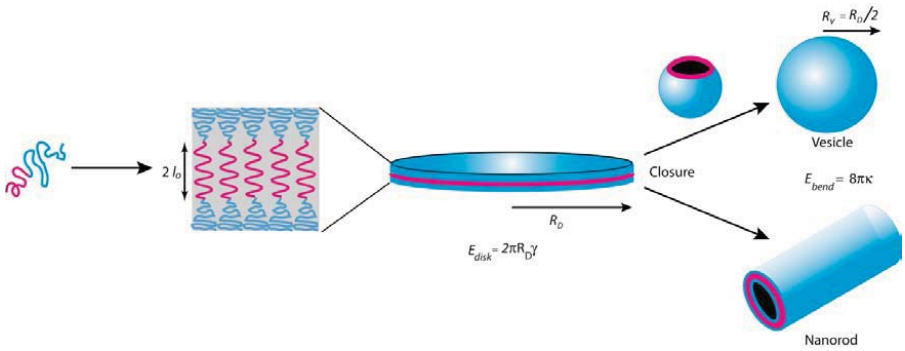

Fig. 1.4.3: Represented the closing of bilayer into "polymersomes".

1.4.4.1 Path II

Recent simulation studies of amphiphiles have shown that the miceller morphology directly changes into vesicular structure without the intermediate step of bilayer closing. Experimental evidence were established by Adams *et al*. to show that the encapsulation efficiency is very low than the former mechanism described in Path I, if there is no step to form bilayer or closing of the bilayer[141].

Although only two mechanisms are represented here, there might be more mechanisms to form vesicular structures, depending upon the condition that has been applied for the formation of micro/nano structures.

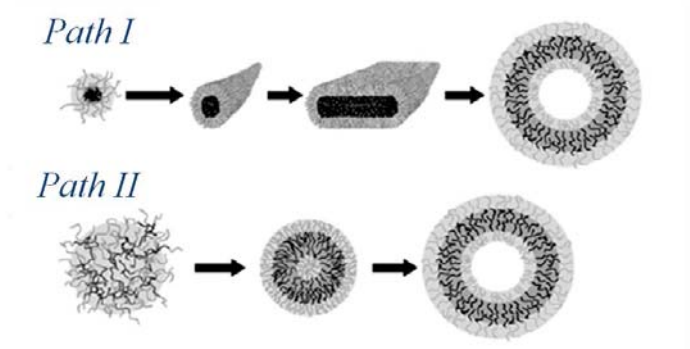

Fig. 1.4.4: Represented the two different path ways to form "polymersomes", *Path I*) step-wise aggregation of polymer amphiphiles, followed by bilayer formation and the closing of the bilayer into vesicles, *Path II*) polymer amphiphiles aggregate into micelle and dynamic self-organization into vesicles [141].

1.4.5 Block copolymers as amphiphilic polymeric materials

In biological systems, lipids self-assemble to form spherical vesicular structures that are called lipid bilayer. Proteins in virus capsids self-assemble into regular vesicle-like structures upon folding and defolding of the individual protein subunits. Some examples for self-assembly involving three classes of amphiphiles are described below. A) amphiphiles with completely amphiphilic peptide back-bone, B) amphiphiles having a conjugated non-peptide segment onto the peptide backbone and C) completely non peptide amphiphiles.

1.4.5.1 Design of polypeptides based block copolymer backbone

Deming and co-workers first reported the synthetic methodology to develop polypeptide-based amphiphilic block copolypeptides in controlled manner [142]. The self-assembly of these amphiphiles can be easily controlled by varying size and structures which can be dictated by block copolypeptide segments. The self-assemblies can be made stimuli-sensitive and can be controlled by change in stimuli such as pH. Such stimuli-sensitive assemblies can function as a very attractive trigger release for drug delivery applications. Several tunable parameters can be used to design stimuli sensitive polypeptide assemblies. These parameters include 1) secondary structures (α-helix, β-sheet and random coil etc.), 2) hydrophobic and hydrophilic segments in these block copolypeptides, 3) pH responsiveness by incorporation of pH active functionalities and 4) redox active moieties. Fabrication of these materials which typically mimic the functionalities and structures of proteins can be very promising for applications in biotechnology, drug delivery and tissue engineering.

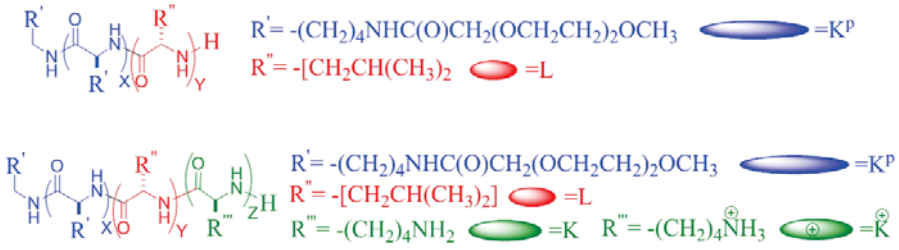

Fig. 1.4.5: Represented the chemical structures of the block copolymers by Deming and co-workers[142].

These materials typically contain both hydrophilic as well as hydrophobic segments in a coil-coil or rod-coil conformation. The secondary conformations of the "super amphiphilic" block copolypeptides are important for them to assemble into ordered structures[143-148]. The polypeptides amphiphiles were chosen based on three building blocks. A) ethylene glycol modified amino acid building blocks to afford stable α-helical conformation in water[149-151], B) polylysine or polyarginine as one block for pH responsive hydrophilic electrolytes (these segments also mimic highly charged such as DNA and C) hydrophobic segments having poly-leucine which forms a stable helical secondary structure. The bilayer assembly for uncharged block copolymers containing varying hydrophobic volume fraction reflects the influence of the secondary structural parameters in the assemblies. For example, side by side ordered packing of the α-helical block copolymer segments results into vesicular structures. In contrast, the presence of racemic amino acids (*rec*K^P*L*/K^P*recL*) does not lead to formation of vesicular structure due to disruption of the helical conformations. Copolymer $K^P_{160}(L_{0.3}/K_{0.7})_{40}$ was prepared such that 70% of the L-leucine residues of the hydrophobic domain of a $K^P_{160}L_{40}$ block copolymer were replaced in a statistical sequence with L-lysine (K). At high pH, uncharged poly(L-lysine) is not water soluble, and preferentially adopts the α-helical conformation. Under these conditions, incorporation of lysine residues into this copolymer should neither disrupt the hydrophobicity or helicity of the leucine-rich domain, nor should they greatly disturb the higher-order assembly of the chains. Accordingly, aqueous suspensions of $K^P_{160}(L_{0.3}/K_{0.7})_{40}$ at pH > 9 were found to form vesicles similar to those formed by $K^P_{100}L_{20}$. Protonation of the amino side-chains on the lysine residues in $K^P_{160}(L_{0.3}/K_{0.7})_{40}$ considerably enhances their hydrophilicity and also destabilizes the α-helical structure of the leucine-rich domain due to electrostatic repulsion of the like charges. The result should be a helix-to-coil conformation transition in this domain that is pH responsive (Fig. 1.4.6). We reasoned that such a change would also destabilize the vesicular assembly, leading to porous membranes or even complete dissociation of the structures. Such properties were demonstrated by formation of vesicles of $K^P_{160}(L_{0.3}/K_{0.7})_{40}$ in the presence of Fura-2 dye at pH 10.6. Under these conditions, the excitation maximum of vesicle-encapsulated dye in the presence of external calcium solution was found to be constant for several days, indicating no dye

or calcium transport across the membrane barrier had occurred. When the pH was lowered by addition of HCl, the excitation maximum of the dye was shifted within seconds, indicating near-instantaneous disruption of the vesicle membranes and complexation of the calcium by Fura-2 (Fig. 1.4.6).

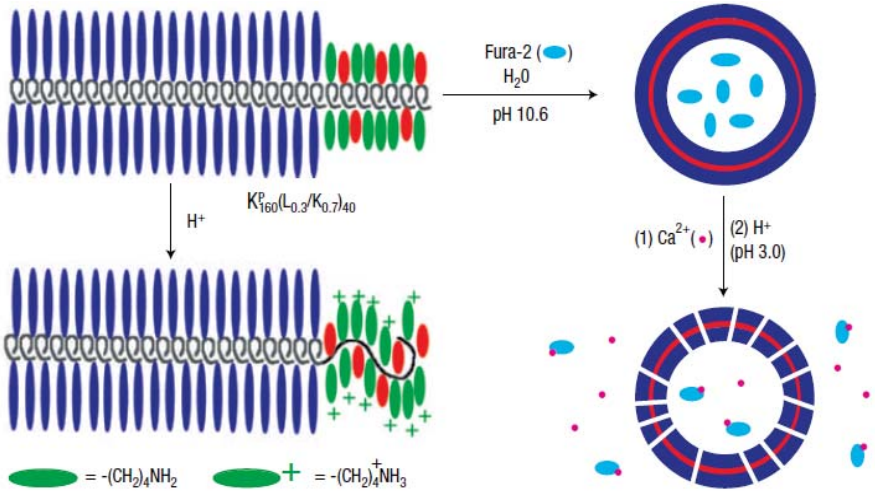

Fig. 1.4.6: Represented the pH responsive vesicular rupture to release the encapsulated molecules[142].

1.4.5.2 Poly-prolines II (PP II)-Cell Penetrating Protein (Tat-CPP) conjugated rod coil amphiphiles

Among 20 naturally occurring amino acids, proline forms pyrrolidine ring in the poly-proline backbone unlike other natural amino acid containing polypeptides. The cyclic structures of pyrrolidine ring forces the polypeptide to adopt rigid rod like structures called polyprolines II (PPII). PPII is sufficiently hydrophobic due to the alignment of three methylene groups outside of the PPII and exists in the helical conformation. The PPII helix is relatively open and has no internal hydrogen bonding as opposed to the more common helical secondary structures, the alpha helix and its relatives the 3_{10} helix, the π helix and the β-helix. The amide nitrogen and oxygen atoms are too far apart (approximately 3.8 Å) and oriented incorrectly for hydrogen bonding. Moreover, these atoms are both H-bond acceptors in proline; there is no H-bond donor due to the cyclic side chain. Recently, Lee and co-workers reported the

microphase segregation behaviour when the hydrophobic polyproline was conjugated to the hydrophilic Tat CPP coil segment leading to the anisotropic orientational ordering of the rod structured PPII resulting in the vesicular morphology[152].

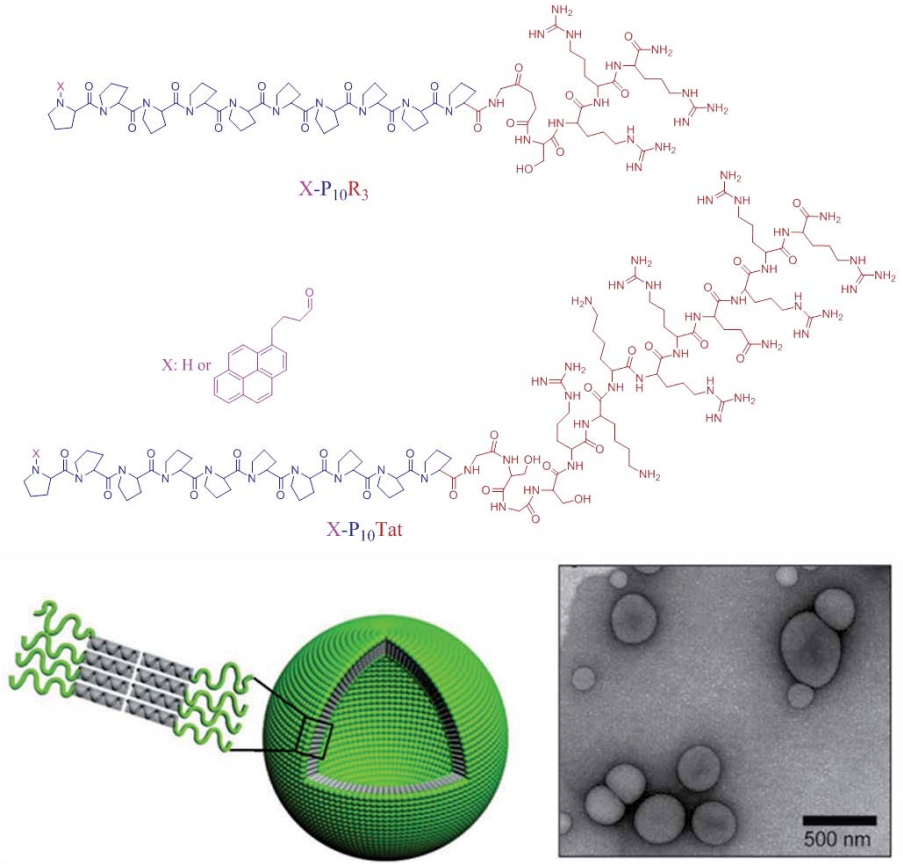

Fig. 1.4.7: Represented the chemical structure, the cartoon and the microscopic image of the block copolymers self-assembly (vesicles) of the polyproline conjugated Tat CPP[152].

1.4.5.3 Hydrophilic polyethylene glycol conjugated poly-aromatic segment as amphiphiles

In all eukaryotic cells microtubules are filamentous intracellular structures are involved in nucleic and cell division, organization of intracellular structure, and intracellular transport, as well as capillary and flagellar motility. Because the functions of microtubules are so critical to the existence of eukaryotic cells (including our own),

understanding their assembly and disassembly process is critical functions. A host of effort has been directed towards development of synthetic mimics of these microtubules. One such effort involves the use aromatic amphiphiles of oligo or polypeptides conjugated carbohydrate segments to produce morphologies that mimic microtubules. Lee and co-workers have demonstrated the formation of pulsating microtubules by controlling non-covalent aromatic stacking interaction in the oligo-ethylene glycol conjugated aromatic amphiphile. The synthetic methodology allowed the researchers to evaluate the effect of the amphiphile architecture and chirality on it self-assembly process.

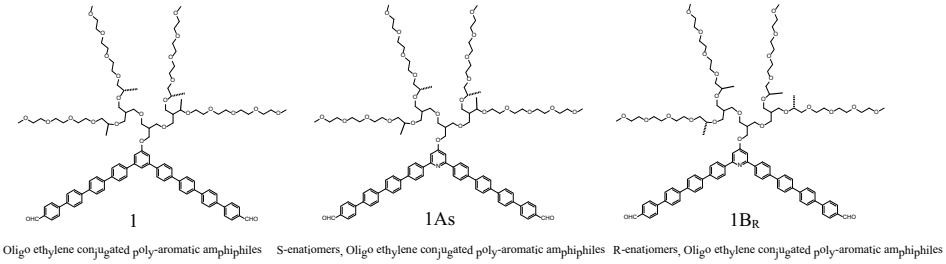

Fig. 1.4.8: Represented the chemical structures of the oligo-ethylene conjugated poly-aromatic systems by Lee and co-workers [153].

The lipid bilayer is stable in physiological conditions due to strong H bonding interaction, but lipid layer structures disrupt upon heating as an external trigger. To solve this problem, Lee and co-workers incorporated another interaction, the π-π aromatic stacking interaction. Amphiphile **1** forms microtubules by hexameric H-type aggregation of the amphiphiles with external diameter of 7 nm with hollow internal diameter of 3 nm. The microstructures are quite stable upon heating as proved by microscopic analysis. In the amphiphiles **1As**, pyridine unit was incorporated on the concave side of the apex of the bent aromatic segment to induce the adjacent molecule to slightly slide off, because pyridine is well known to form water cluster through H-bonding interactions. Transmission electron microscopy data did not show any structural difference between **1** and **1As** amphiphiles under identical conditions [153].

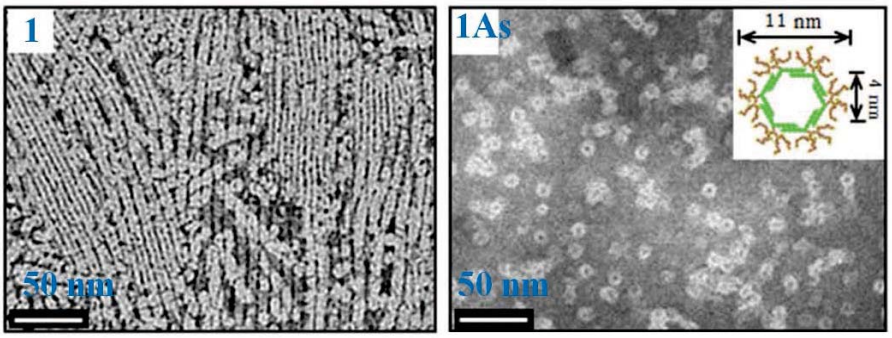

Fig. 1.4.9: Represented the TEM of the self-assemblies generated from amphiphiles 1 (0.01 wt%) and 1As (0.002 wt%) [153] in the self-assemblies[153].

2) The incorporation of the chirality in the oligo-ethylene moieties preserved the aromatic H-stacking but with increasing concentration CD signal increases due the helical aromatic stacking by the preferred handedness.

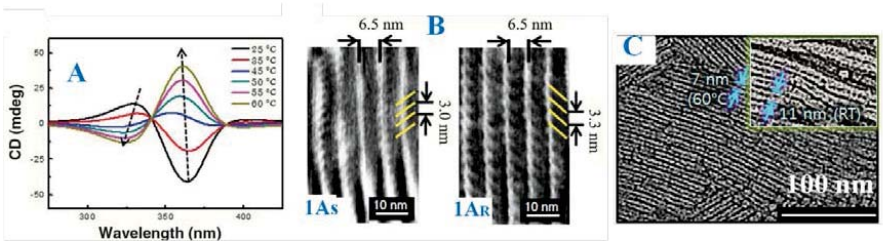

Fig. 1.4.10: Represented the CD Spectra (A), AFM of the chiral amphiphiles (B) and the AFM of the 1As at room temperature and at 60°C (C) [153].

Assemblies obtained from **1As** give the opposite signal with respect to **1AR** in circular dichroism spectra and also the mirror image in AFM, which clearly indicates that

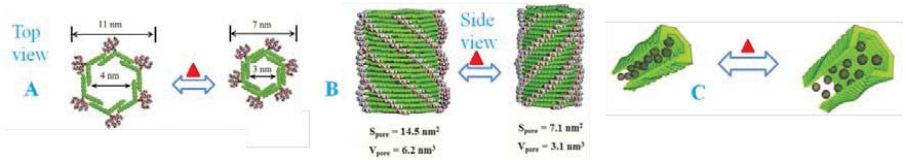

Fig. 1.4.11: Represented the top view (A), side view (B) and the cartoon of release of fullerenes during heating those assemblies (C) [153].

molecular chirality, was transferred to the assemblies. AFM image (Fig. 1.4.10) shows that upon heating to 60°C the cavity decreases to 7nm due to the removal of water molecules from the core of the assembly.

3) They were able to encapsulate fullerene C_{60} molecules inside the tubular cavity. During heating the tubular structures opens up and some of the encapsulated fullerenes come out from the tubular cavity.

Block co-polypeptide self-assemblies provide significant advantages in terms of control over biologically inspired structures and functions. Incorporation of the conformational effects show additional control over the assemblies and can be better tuned under physiological triggers like pH, temperature and redox. So, these materials can be very promising materials for drug delivery and tissue engineering purposes. Tat CPP conjugated polyproline (PP II) has significant promising activities for intercellular delivery of hydrophilic as well as hydrophobic cargos. The pulsating tubules are very promising materials that are able to encapsulate the hydrophobic fullerene C_{60} molecules inside the cavity of microtubules and also can release upon heating them (60°C temperature). These might be applicable as nano-wires or memory device chips for data storage [153, 154].

Based on the results discussed above we hypothesized that hydrophilic glycopolypeptides that were conjugated to the hydrophobic gallate dendrons would self-assemble in aqueous solution to achieve nano or micro scale assemblies all of which are discussed in detail in Chapter IV of my thesis.

1.5 Glycopolymer based self-assemblies as nanocarriers

Nano-carriers resulting from the biocompatible amphiphilic block copolymers are very promising biomaterials. Different morphologies obtained from the self-assembly of block copolymers completely depend on the ratio of the hydrophilic and hydrophobic unit in the amphiphiles. Syntheses of miceller assemblies of block copolymers are important since they can function as carriers for drug delivery. However they are limited because only hydrophobic drug molecules can be encapsulated inside the core. On the other hand, polymersomes (vesicles) are effective for encapsulation of both hydrophilic as well as hydrophobic drug molecules inside

their hydrophilic cavity and hydrophobic membrane respectively. For the targeted delivery, polymersomes should be decorated with biological recognition units on their surface to interact with the receptors of cells. In this respect, glycans (carbohydrates) are ideal candidates due to their importance in cellular process such as cellular adhesion, proliferation and cell-cell signalling among others. However understanding of the specific recognition route and control of cell physiology by carbohydrates is extremely important for designing such polymeric carriers for targeted drug delivery[155-157].This requires synthesis of macromolecules which poyvalently display carbohydrates on their surface such that they can mimic the natural glyco-conjugates such as glyco-proteins and glyco-lipids[29, 158-160]. However, syntheses of carbohydrate containing macromolecules such as glycodendrimers or complex glycoconjugates is time consuming and involve multi-step synthesis. On the other hand amphiphilic glycopolymers are advantageous since can be synthesized from their corresponding monomers by a one-step polymerization. They can also be assembled into precise structure by simple hydration of film formed by amphiphile in an organic solvent. Since this hydration can be carried out in presence of small molecules, these get entrapped inside and the assemblies which are very important for drug delivery applications. The self-assembly of two classes of carbohydrate containing macromolecules will be discussed. These include (i) amphiphilic glycodendrimers and (ii) amphiphilic glycopolypeptides.

1.5.1 Amphiphilic glyco-dendrimers

Percec and coworkers recently reported the new class of amphiphiles called janus dendrimers, which self-assembled by simple solvent injection method[160-163]. The amphiphilic glyco-dendrimers contain two identical carbohydrate moieties as hydrophilic segments that are conjugated to the hydrophobic segment by triethylene glycol by the very facile CuAAC reaction. Several glyco-dendrimers with different hydrophilic glycans, hydrophobic weight fraction as well as the arrangement of the hydrophobic aliphatic segment were synthesized and their self-assembly in water was studied. Multiple morphologies that ranged from rigid sphere to polydispersed nano-sized vesicles were observed. The nano-structures were generated by simple water injection into the tetrahydrofuran/ethanol solution of the amphiphiles. Subsequent

dialysis of the organic solvent resulted in unilameller hard/soft spheres, polygonal vesicles and tubular vesicles which has been named as dendrimersomes. These assemblied might find application in lectin mediated drug/gene delivery, as imaging agents and as vaccines towards dendritic cells. The cavity of the dendrimersomes can be loaded with drugs for drug delivery appliation[162].

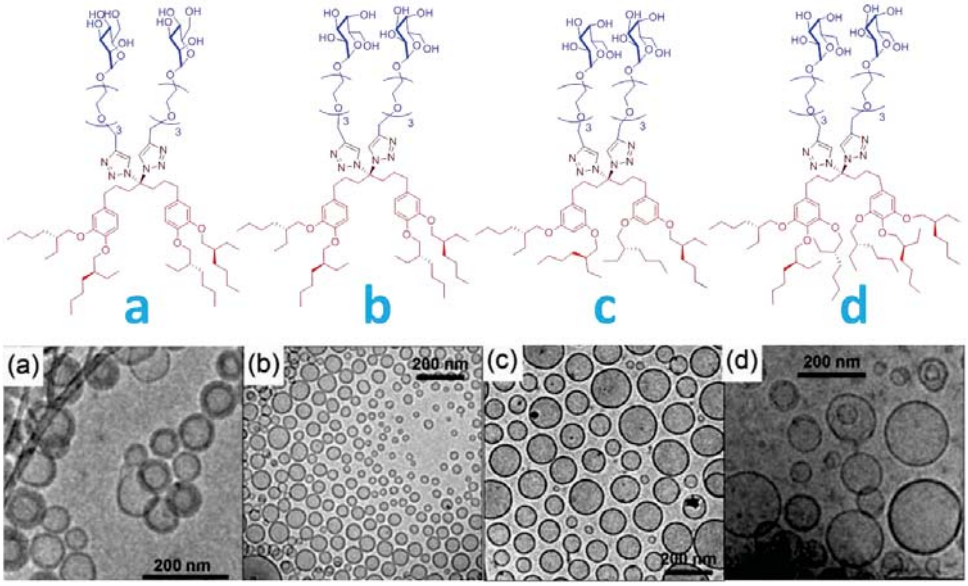

Fig. 1.5.1: Represented chemical structures and the corresponding nano-structures imaged by TEM[162].

1.5.2 Post-polymerization modification of the polypeptide backbone

Synthetic polymers, polypeptides and block-copolypeptides are very promising materials for fabrication of polymersomes. Due to their biocompatibility and biodegradability as well as their propensity to self-organize, they offer unique advantage for generation of hierarchal structures. For example, hydrophilic oligosaccharides such as dextrans and hyaluranic acids that are conjugated to helical hydrophobic polypeptides are known to generate polymersomes by efficient packing between the helices of neighbouring amphiphiles. This promising approach allows for generation of self-assembled nanostructures in aqueous solution by chemical conjugation of oligosaccharides and polypeptides. The polymersomes generated are

structurally and functionally very close to the virus capsids. However, this synthetic methodology is not very efficient and purification of non-functionalized starting materials is very laborious[164, 165].

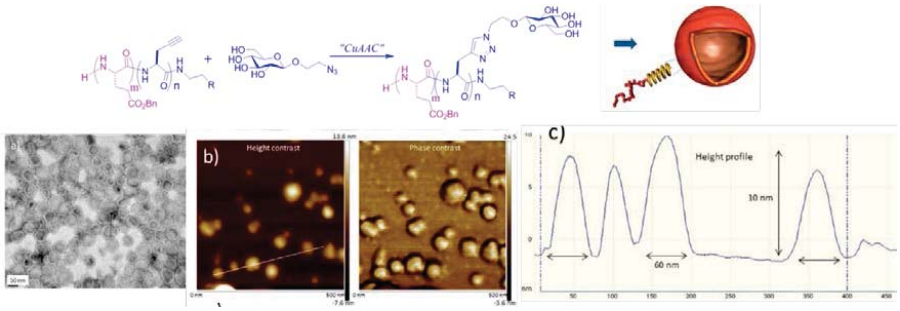

Fig. 1.5.2: Represented chemical structure produce the corresponding nano-structures imaged by TEM and AFM[166].

Recently, Heise and co-workers demonstrated an interesting post-polymerization modification of the well characterised monodisperse poly(γ-benzyl-*l*-glutamate)-*block*-poly(propargyl-*l*-glysine) ($PBLG_x$-*b*-PGG_y) polypeptides by functionalization of azido glycans using the "click" reaction (CuAAC). They were able to tune the morphologies by changing the hydrophilic weight fraction from 25% to 68% that were controlled during polymerization of PBLG*x*-*b*-PGG*y* (Keeping $x = 20$ fixed and varying $y = 5$, 9, 18, 25 and 32 etc.). The amphiphiles $PBLG_{20}$-*b*-PGG_{25} synthesized after glycosylation by CuAAC genetated polymersomes when the hydrophilic weight fraction was 63%. The polymersome formation is copletely driven by thermodynamics. The following parameters were found to contribute strongly towards polymerosome formation (i) hydrophobic weight fraction (around 47%), 2) helix-helix packing of the polypeptides and 3) aromatic π-π stacking of the benzyl groups. The assemblies were throughly charecterised by TEM and AFM. The glycans on the surface of the polymersomes were found to bind the model lectin $RCA_{120,}$ that specifically recognised the galactosyl moieties on the surface of those vesicles[166].

However it should be noted that there are several limitations involved with post-polymerization modification. This includes: 1) an extra step has to be added to the synthetic methodology, 2) acheiving 100% functionalization is extremely difficult and 3) the secondary structure of postpolymerized glycosylated polypeptides is undefined

compared to naturally occuring glycoproteins due to the presence of extra triazole ring in between the peptide backbone and glycosyl moiety[169,170].

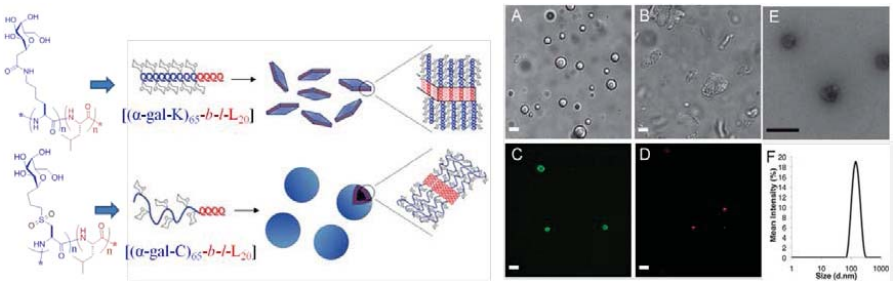

Fig. 1.5.3: Represented chemical structures of [(α-gal-K)$_{65}$-*b*-*l*-L$_{20}$] and [(α-gal-C)$_{65}$-*b*-*l*-L$_{20}$] that produce the corresponding nano-structures; A) DIC, B) DICO$_{18}$, C) dye loaded, D) Dextran red loaded image and E) TEM image and F) the DLS of [(α-gal-K)$_{65}$-*b*-*l*-L$_{20}$] [171].

Recently, Deming and coworkers developed materials possessing the ordered, controllable chain conformation and secondary structures that are very close to the protein structures. The chain conformation affects the nanostructured morphologies thus providing them with an external additional parameter to control the nanostructures. They described the preperation and assembly of the glycosylated block copolypeptides where the hydrophilic glycosylated segments adopt either α-helix [(α-gal-K)$_{65}$-*b*-*l*-L$_{20}$] or coil conformation [(α-gal-C)$_{65}$-*b*-*l*-L$_{20}$] and hydrophobic segments from poly-leusine are in completely α-helix conformation. The amphiphile *poly*-α-D-galactose-*l*-lys-*block*-*poly*-*l*-Leucine [(α-gal-K)$_{65}$-*b*-*l*-L$_{20}$] adopts helix-helix conformation where as *poly*-α-D-galactose-*l*-cys-*block*-*poly*-*l*-Leucine [(α-gal-C)$_{65}$-*b*-*l*-L$_{20}$] adopts coil-helix conformation. The amphiphile *poly*-α-D-galactose-*l*-lys-*block*-*poly*-*l*-Leucine [(α-gal-K)$_{65}$-*b*-*l*-L$_{20}$] self-assembles into lameller structure by helix-helix interaction that ultimately aggregates into disk or plate morphology. On ther hand, the amphiphiles *poly*-α-D-galactose-*l*-cys-*block*-*poly*-*l*-Leucine [(α-gal-C)$_{65}$-*b*-*l*-L$_{20}$] packs into bilayer assembly by helix-coil interaction and closes the bilayer into spherical vesicular morphology. The vesicles were well charecterised by TEM, DLS and cryo-DIC (differential interference contrast) imaging. They were able to encapsulate hydrophilic as well as hydrophobic dyes inside their cavity. These

materials are biocompatible and MTT assay shows that those are not toxic at all and hence probably applicable to biomedical purposes.

In chapter V of my thesis I will discuss the effects of glycopolypeptide secondary conformation on the formation of self-assembled nanostructures from aphphiphilic polymers made of biocompatible polycaprolactone and glycopolypeptide[171].

1.6 Nano-carriers for drug delivery vehicles

1.6.1 The basic concepts of nano-carriers for drug delivery vehicles

Cancer, known as the "Emperor of All Maladies", is the key cause of 10 million new cases every year worldwide. There is no clear improvement in therapeutics although the mortality rate has come down due to better understanding of tumour biology and development of diagnostic devices. The greatest challenge in cancer treatment is the metastasis - the spread of cancer from primary tumour to seed secondary tumours at distant sites before the detection[172]. Current cancer treatments include surgical intervention, radiation and chemotherapeutic drugs. Since most of the drugs are extremely cytotoxic, they often kill healthy cells and cause toxicity to the patient. Across all the cancer types only one out of five patients survives with metastasis for more than five years after detection[173]. It would therefore be desirable to develop chemotherapeutics that can either passively or actively target cancerous cells without affecting the healthy cells for successful treatment of cancer.

In cancerous tumours, the endothelial lining of the blood vessel wall becomes more permeable than in the normal state. As a result, in such areas, large molecules and even relatively certain particles ranging from 10 to 500 nm in size, can leave the vascular bed and accumulate inside the interstitial space. This was clearly demonstrated in many tumours. Hence drug loaded nanoparticles (~100 nm diameter) have been shown to enter areas with increased vascular permeability, where the active drug can be eventually released from a carrier. Such spontaneous accumulation or "passive" targeting is currently known as enhanced permeability and retention (EPR) effect. In other words, high permeability of the tumour vasculature allows macromolecules and nanoparticles to enter the tumour interstitial space, while the compromised lymphatic filtration allows them to stay there. Unlike nanoparticles,

"small" low-molecular weight pharmaceutical agents are not retained in tumours because of their ability to return to the circulation by diffusion. Nano-carriers offer many advantages over free drug for drug-delivery into cancer cells. They (a) protect the drug from premature degradation (b) prevent the drug molecules from permanently interacting with the biological system (c) enhance absorption of the drugs into the selected tissue (for example solid tumour) and d) control the pharmacokinetics or drug tissue distribution profile [172-174]. EPR-mediated drug delivery using drug-loaded nanocarriers is currently seen as an effective way to bring drugs to and into tumours.

1.6.1.1 Passive targeting of tumour cells

General features of the tumour cells such as leaky blood vessels and poor lymphatic drainage enhance the passive targeting pathway to the tumour cells. Whereas free drug can diffuse non-specifically, nano-carriers can extravasate into the tumour tissues via leaky vessels by enhanced permeation and retention (EPR) effect[175]. The increased permeability of the blood vessels in tumour is characteristic of rapid and defective angiogenesis (formation of new blood vessels from existing one). The dysfunctional lymphatic drainage in tumours retains the accumulated nano-carriers and allows them to release drugs into the vicinity of the tumour cells[176]. Experiments using liposomes of different mean size suggest that the threshold vesicle size for extravasations into the tumour is ~400 nm (diameter) but other studies have shown that particles with diameter < 200 nm are more effective[177, 178]. Passive targeting of nano-carriers first reached into clinical trials in the mid 1980s, and the first product based on liposome-protein-polymer conjugation was marketed in the 1990s[174].

1.6.1.2 Limitations for passive targeting

Although passive targeting approaches from the basis of the chemical therapy, they suffer from several limitations. Ubiquitously targeting cells within a tumour is not always feasible because some drugs cannot diffuse effectively and the random nature of this approach makes it difficult to control. This lack of control may induce multiple drug resistance (MDR), a situation where chemotherapy treatments fail patients owing to resistance of cancer cells towards one or multiple drugs[179, 180]. MDR causes expulsion of the drugs from cells due to over expressed membrane transporter proteins

on the surface of the tumour cells. Expelling drugs inevitably lowers down the therapeutic effect and tumour cells soon develop resistance to a variety of drugs. Passive targeting furthermore suffers due to some tumour cells not exhibiting EPR effect and permeability of the vessels may not be same throughout a single tumour[181].

1.6.1.3 Active targeting of tumour cells

One way to overcome these limitations is to programme the nano-carriers so they actively bind to the specific cell surface after extravasations. The binding may be achieved by attaching targeting agents (ligands) that bind to the specific receptors on the cell surface. By ligand-receptor interaction, nano-carriers recognize the specific cells and get internalized before delivery of the drug inside the cells[182].

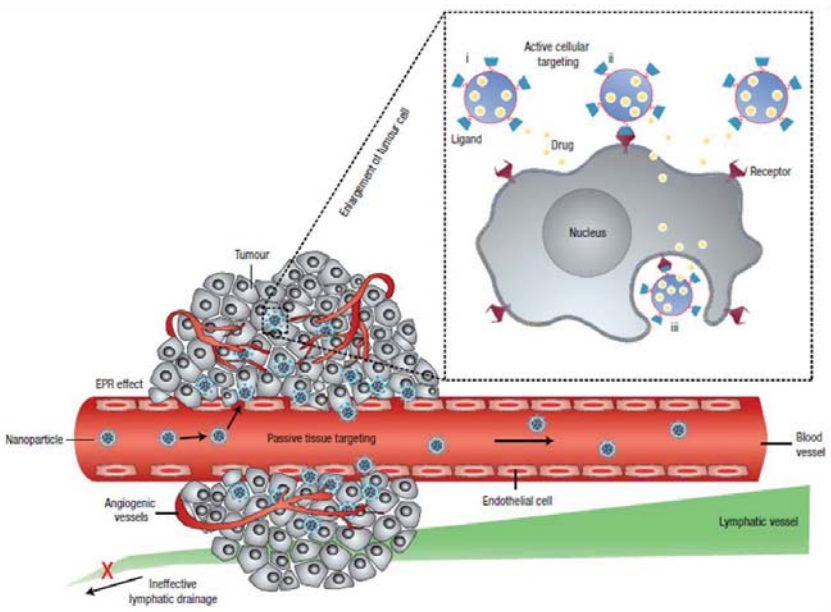

Fig. 1.6.1: Represents the Passive tissue targeting is achieved by extravasation of nanoparticles through increased permeability of the tumour vasculature and ineffective lymphatic drainage (EPR effect). Active cellular targeting can be achieved by functionalizing the surface of nanoparticles with ligands that promote cell-specific receptor recognition and binding[174].

There are multiple factors that are desirable in order to achieve good/effective drug delivery nano-carriers. Among them, the interactions between the targeting ligand

and receptor should be very specific with high binding affinities and avidities. High binding avidity can be achieved through polyvalency as has been discussed in section **1.2**. For example, efficient liposomal delivery to B-cell receptors using the anti CD19 monoclonal antibody (mAb), the density of the receptors on the cell surfaces is ~10^4-10^5 copies per cell. In a breast cancer model, receptor density of 10^5 ErbB2 receptors per cell was necessary to improve the therapeutic efficiency[183]. There are multiple such active targeting drug conjugated nano-carriers in the market (Table 1.6.1).

Compound	Commercial name	Nano-carrier	Indications
Styrene-maleic anhydride neocarzinostatin(SMANCS)	Zinostatin/Stimalmer	Polymer–protein conjugate	Hepatocellular carcinoma
PEG -l-asparaginase	Oncaspar	Polymer–protein conjugate	Acute lymphoblastic leukemia
PEG-granulocyte colony-stimulating factor (G-CSF)	Neulasta/PEG filgrastim	Polymer–protein conjugate	Prevention of chemotherapy-associated neutropenia
IL 2 fused to diphtheria toxin	Ontak (Denilelukin diftitox)	Immunotoxin (fusion protein)	Cutaneous T-cell lymphoma
Anti-CD20 conjugated to yttrium-90 or indium-111	Zevalin	Radio-immunoconjugate	Relapsed or refractory, low-grade, follicular, or transformed non-Hodgkin's lymphoma
Doxorubicin	Myocet	Liposomes	Combinational

			therapy of recurrent breast cancer, ovarian cancer, Kaposi's sarcoma
Doxorubicin	Doxil/Caelyx	PEG -liposomes	Refractory Kaposi's sarcoma, recurrent breast cancer, ovarian cancer
Vincristine	Onco TCS	Liposomes	Relapsed aggressive non-Hodgkin's lymphoma (NHL)
Paclitaxel	Abraxane	Albumin-bound paclitaxel nanoparticles	Metastatic breast cancer

Table 1.6.1: Represents the marketed nano-particles based therapeutics agents used for cancer treatmenyts[174].

1.6.3 The nanoparticles for cargo delivery

Nanocarriers are nanosized materials (diameter 1~100 nm) that can carry multiple drugs and imaging agents among other things. Due to their high specific area over volume ratio, it is possible to achieve high ligand density on the surface for targeting purposes. Nanocarriers can be used to increase local drug concentration by

carrying the drugs and releasing it in controlled manner when bound to the targets. Nowadays the synthetic and naturally occurring block polymers are used as drug delivery vectors. Nano-material composed of polymeric self-assemblies, polymer conjugates, lipid based nano-carriers such as liposomes, micelles, dendrimers, carbon nano-tubes, and gold nanoparticles including nano shell and cages are used in a variety of applications in drug delivery, imaging, photothermal ablation of tumours, radiation sensitizers, detection of apoptosis and sentinel lymph node mapping[183-193].

1.6.4 Effect of nano-particle size and shape on cellular delivery

The most significant recent advances in nanoparticle engineering have come in the area of particle shape and its effects on the cellular internalization and circulation time. Recent studies show the effect of nanoparticles during their internalization and circulation times. To observe the effect of size and geometry, spherical and non-spherical polystyrene micro-particles encapsulation during phagocytosis in macrophages was studied[194, 195]. When macrophages interact with elliptical disk-shaped nanoparticle along the major axis it is internalized very quickly (< 6 minutes), but when it interacted with the minor axis, no internalization was observed even after 12 hours. Spherically shaped nanoparticles are internalized very rapidly and uniformly due to their symmetry. This effect of the shape was studied in the range of 0.1-100% volume with respect to the macrophage. The only difference was observed when the volume of the nano-particle was more than the volume of the macrophage[195].

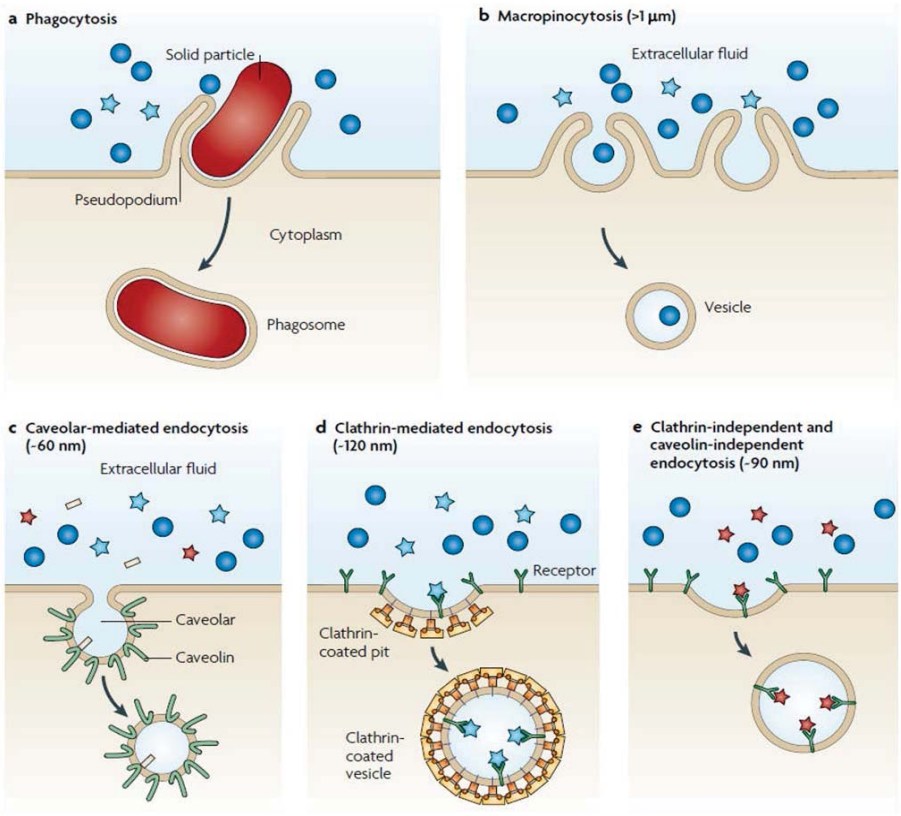

Fig. 1.6.2: Represents models of cellular internalization of nanoparticles and respective size limitations. Internalization of a) large particles is facilitated by phagocytosis, b) nonspecific internalization of smaller particles (>1 µm) can occur through macropinocytosis, c) smaller nanoparticles can be internalized through several pathways, including caveolar-mediated endocytosis, d) clathrin-mediated endocytosis and clathrin-independent and caveolin-independent endocytosis, e) with each being subject to slightly different size constraints. Nanoparticles are represented by blue circles (> 1 µm), blue stars (about 120 nm), red stars (about 90 nm) and yellow rods (about 60 nm). Adapted from the paper [195].

Another classical example of the filamentous fibril micelles (filomicelles) of about 18µm in length with circulation half-life of more than 5 days, that is more than that of sleath liposomes, remarkably highlighted the fact that micrometer sized spheroids are cleared from circulation instantly. The unique characteristic of the filomicelles contain two aspects as carriers[196].

1) They have two dimensions on the length scale (diameter 20-60 nm) that allow them to traverse extremely small openings, such as those found in spleen.

2) Their shape helps reduce the rate of phagocytosis by cells of the mononuclear phagocyte system. Shear forces of the blood flow do not allow their cellular internalization and exerts enough forces to pull them through circulation system.

Geng *et al*. reported the filomicelles, assembled from polyethylene glycol-*b*-polycaprolactone (PEG-*b*-PCL) that encapsulated paclitaxol in the hydrophobic core of the assemblies and were able to deliver the cargo to the tumour sites, which showed significant reduction of tumour size in vivo[195].

1.6.5 Aspect ratio

New tools are emerging that allow a systematic study of the internalization kinetics and mechanism of a series of nanoparticles or microparticles in which a single parameter (shape or size) can be altered independently of other parameter attributes. Grotton *et al*. reported the rate of cellular internalization of two particles with same volume but completely different three dimensional structures. The particles with an aspect ratio of 3 internalized at least four times faster than those with the aspect ratio of 1. For example, in case of particles with cylindrical shape, one particle with high aspect ratio of 2.66 (diameter 150 nm and height 400 nm) internalized faster than that with low aspect ratio of 1 (diameter and height 200 nm). However, it was observed that a particle of diameter 100 nm with aspect ratio of 3 internalized at the same rate as a particle with aspect ratio of 1 with diameter and height equal to 200 nm. So, apparently the size and shape of particles has some influence on cellular uptake but it is not clearly understood[196, 197].

1.6.7 Carbohydrate based nanoparticles for drug delivery

The design of new nano-carriers is important because it is difficult to interpret their efficacy on the basis of few existing comparative studies. Simultaneously, several factors might affect biodistribution and targeting. In addition suitable screening methodologies for determination of optimal characteristics of nanocarriers remain elusive. Developing targeted delivery to avoid non-specific uptake by mononuclear

phagocytes and by non-targeted cells, it is very challenging to maintain the balance between the synthetic complexity of the nano-carriers as well as their commercial scale-up. Design and development of efficacious targeted drug delivery methods is an inspiring goal to study intra and intercellular interaction processes. In this context, replacement of the body's replication strategy for postal-code-like determinants demands the chemical design of targeted binding epitope. When represented without any pay-loaded carrier, they just diffuse to saturate the receptors by anti-adhesion strategy and block the cellular routing process. But on the contrary, carrier immobilization aided poly-valency leads to the favourable increment of the chosen determinants. Important cellular binding events utilizing carbohydrates are found in many mammalian systems and are especially prevalent in the immune system. For instance, during an inflammatory response, endothelial cells lining the lumen of blood vessels upregulate expression of carbohydrate binding proteins known as selectins. Carbohydrate binding to glycan receptors is essential, but binding constants for these events are relatively weak (saccharide-protein binding events $\leq 10^6$ M^{-1}). The binding increases both in affinities as well as selectivity by multiple bindings events among ligands and receptors. The entropic advantage gained from arraying binding carbohydrates on a surface, allowing multiple copies to bind multiple receptors at once, increases the avidity (the synergistic bond strength between multiple ligands and multiple receptors) of the overall display platform and effectively increases binding efficiency. Furthermore, the attachment of the therapeutic drug molecules to the carbohydrate based polymeric backbone affords hybrid materials with multiple characteristics: a) target specific (such as ASGP receptor in the liver cells) and b) therapeutic pay-loaded, which ensure the cellular uptake and also decrease the undesired side effects. Thus, development of proper nano-carrier requires exact understanding of the structure-activity relationship responsible for physiological mail-order business like mechanism. Since all the work is at the interface of chemistry and biology as well as medical fields, there should be accurate communication to understand the mechanism and effectiveness to avoid the undesired results. The emerging field should be nurtured carefully to avoid development of delivery vehicles with less-than-desired properties after westing a huge amount of effort. Finally, the goal of developing a "Magic Bullet" - a term coined by German bacteriologist Paul

Ehrlich, meaning a chemical that could travel through the body and selectively kill the tumour cells without affecting the healthy normal cells, is yet to be reached.

1.7 Outline of thesis work

We have developed a facile synthesis of high molecular weight water-soluble *O*-glycopolypeptide polymers by the ring-opening polymerization of their corresponding N-carboxyanhydride (NCA) in very high yield (overall yield > 70%) in three very high yielding steps[198]. The synthesized water-soluble glycopolypeptides were found to be α-helical in aqueous solution. We were also able to control the secondary conformation of the glycopolypeptides by polymerizing racemic amino acid glyco NCAs. The synthesized glycopoplypeptides were found to be polyvalent as was observed during binding studies with its corresponding lectin Con-A. We have also been able to investigate for the first time the effect of secondary structure of the glycopolypeptides on binding to the lectin *Con-A*[199]. The details are discussed in the Chapter **II** and Chapter **III**.

We then proceeded to develop these glycopolypeptides as vehicles for drug delivery in cancer cells. For glycopolypeptides to be used as delivery vehicles and as biomaterials, it would be advantageous if these could be assembled into supramolecular nanostructures that can be tuned to appropriately display their carbohydrate moieties. Thus, amphiphilic block copolymers containing glycopolypeptides as one of their blocks was synthesized as they could self-assemble into various nanostructures. We were the first to report synthetic glycopolypeptide-dendron conjugates that self-assembled into various nanostructures such as nanorods and micelles that displayed carbohydrates on their surface[200]. Our design of the highly anisotropic amphiphilic block copolymer architecture was based on a perfectly branched wedge-shaped hydrophobic dendron attached to a hydrophilic polypeptide chain with significant α-helical character displaying an ordered array of sugar residues. We further demonstrated that these nanoscale structures were indeed bioactive by studying their interaction with lectins. The details work is demonstrated in the Chapter **IV**.

Finally, we have been able to synthesize amphiphilic glycopolypeptides from glycopolypeptides-polycaprolactone conjugates. The uniqueness of this amphiphilic polymer is that both the glycopolypeptide and caprolactone is expected to be biocompatible. We have shown that these nanostructures with multiple topologies such as vesicles, micelles and nanorods can be obtained upon self-assembly of these polymers with varying hydrophobicity/hydrophilicity. We have shown that vesicles made from glycopolypeptides having β-galactose in the side chain can enter specifically the liver cancer cell HepG2 by receptor mediated endocytosis using the over-expressed asialo-glycoprotein receptor. We are currently evaluating these vesicles to deliver anti-cancer drugs into liver cancer cell[201]. The details work is discussed in the Chapter **V**.

1.8 References

1) Yamazaki, N.; Kojima, S.; Bovin, N.V.; Andre, S.; Gabius, S.; Gabius, H.-J. *Advanced Drug Delivery Reviews* **2000**, *43*, 225–244.
2) Murrey, H. E.; Hsieh-Wilson, L.C.; *Chem. Rev.* **2008**, *108*, 1708–1731.
3) Carolyn R. Bertozzi1, C. R.; Kiessling, L. L. *Science* **2001**, *291*, 2357-2364.
4) Becker, D. J.; Lowe, J. B. *Glycobiology* **2003**, *13*, 41–53.
5) Gama, C. I.; Hsieh-Wilson, L. C. *Curr. Opin. Chem. Biol.* **2005**, *9*, 609–619.
6) Rampal, R.; Luther, K. B.; Haltiwanger, R. S. *Curr. Mol. Med.* **2007**, *7*, 427–445.
7) Gabius, H. J.; Andre, S.; Kaltner, H.; Siebert, H. C. *Biochim. Biophys. Acta* **2002**, *1572*, 165–177.
8) Rudd, P. M.; Merry, A. H.; Wormald, M. R.; Dwek, R. A. *Curr. Opin. Struct. Biol.* **2002**, *12*, 578–586.
9) Yamaguchi, H. *Trends Glycosci. Glycotechnol.* **2002**, *14*, 139–151.
10) Wells, L.; Vosseller, K.; Hart, G. W. *Science* **2001**, *291*, 2376–2378.
11) Murrey, H. E.; Gama, C. I.; Kalovidouris, S. A.; Luo, W. I.; Driggers, E. M.; Porton, B.; Hsieh-Wilson, L. C. *Proc. Natl. Acad. Sci. U.S.A.* **2006**, *103*, 21–26.
12) Kalovidouris, S. A.; Gama, C. I.; Lee, L. W.; Hsieh-Wilson, L. C. *J. Am. Chem. Soc.* **2005**, *127*, 1340–1341.
13) Sandi, C.; Rose, S. P. R.; Mileusnic, R.; Lancashire, C. *Neuroscience* **1995**, *69*, 1087–1093.
14) Nishihira, J. *Int. J. Mol. Med.* **1998**, *2*, 17–28.
15) Apweiler, R.; Hermjakob, H.; Sharon, N. *Biochim. Biophys. Acta* **1999**, *1473*, 4–8.
16) Kleene, R.; Schachner, M. *Nat. Rev. Neurosci.* **2004**, *5*, 195–208.
17) Rexach, J. E.; Clark, P. M.; Hsieh-Wilson, L. C. *Nat. Chem. Biol.* **2008**, *4*, 97–106.
18) Wujek, P.; Kida, E.; Walus, M.; Wisniewski, K. E.; Golabek, A. A. *J. Biol. Chem.* **2004**, *279*, 12827–12839.
19) Salinska, E.; Bourne, R. C.; Rose, S. P. R. *Eur. J. Neurosci.* **2004**, *19*, 3042–3047.
20) Welzl, H.; Stork, O. *News Physio. Sci.* **2003**, *18*, 147–150.
21) Murphy, K. J.; Regan, C. M. *Neuobiol. Leran. Mem.* **1998**, *70*, 73–81.

22) Jaeken, J.; Matthijs, G. *Annu. Rev. Genomics Hum. Genet.* **2007**, *8*, 261–278.

23) Ohtsubo, K.; Marth, J. D. *Cell* **2006**, *126*, 855–867.

24) Best, T.; Kemps, E.; Bryan, *J. Nutr. Rev.* **2005**, *63*, 409–418.

25) Kudo, T.; Fujii, T.; Ikegami, S.; Inokuchi, K.; Takayama, Y.; Ikehara, Y.; Nishihara, S.; Togayachi, A.; Takahashi, S.; Tachibana, K.; Yuasa, S.; Narimatsu, H. *Glycobiology* **2007**, *17*, 1–9.

26) Muramatsu, T. *J. Biochem.* **2000**, *127*, 171–176.

27) Stickens, D.; Zak, B. M.; Rougier, N.; Esko, J. D.; Werb, Z. *Development* **2005**, *132*, 5055–5068.

28) Di Rocco, M.; Hennet, T.; Grubenmann, C. E.; Pagliardini, S.; Allegri, A. E. M.; Frank, C. G.; Aebi, M.; Vignola, S.; Jaeken, J. *J. Inherited. Metab. Dis.* **2005**, *28*, 1162–1164.

29) Mammen, M.; Chio, S.-K. and Whitesides, G. M. *Angew. Chem. Int. Ed.* **1998**, *37*, 2754–2794.

30) Lees, W. J.; Spaltenstein, A.; Kingery, W. J. E. and Whitesides, G. M. *J. Med. Chem.* **1994**, *37*, 3419 - 3433.

31) Mammen, M.; Dahmann, G.; Whitesides, G. M. *J. Med. Chem*. **1995**, *38*, 4179 - 4190.

32) Norkin, L. C. *Clin. Microbiol. Rev.* **1995**, *8*, 293 - 315.

33) Miller, A. D. *Proc. Natl. Acad. Sci. USA* **1996**, *93*, 11407 - 11413.

34) Bergelson, J. M. and Finberg, R. W. *Trends Microbiol*. **1993**, *1*, 287 - 288.

35) Stehle, T. and Harrison, S. C. *Structure* **1996**, *4*, 183 - 194.

36) Fried, H.; Cahan, L. D. and Paulson, J. C. *Virology* **1981**, *109*, 188 - 192.

37) Ting, S. R. S.; Chen, G. and Stenzel, M. H. *Polym. Chem.* **2010**, *1*, 1392–1412.

38) David, A.; Kopeckova, P.; Kopecek, J. and Rubinstein, A. *Pharm. Res*. **2002**, *19*, 1114–1122.

39) David, A.; Kopeckova, P.; Rubinstein, A. and J. Kopecek, *Bioconjugate Chem.* **2001**, *12*, 890–899.

40) Montet, X.; Funovics, M.; Montet-Abou, K.; Weissleder, R.; Josephson, L. *J. Med. Chem.* **2006**, *49*, 6087–6093.

41) Shamay, Y.; Paulin, D.; Ashkenasy, G. and David, A. *J. Med. Chem.* **2009**, *52*, 5906–5915.

42) Sliedregt, L. A. J. M. *et al. J. Med. Chem*. **1999**, *42*, 609–618.

43) Lee, R. T. and Lee, Y. C. *Glycoconjugate J.* **2000**, *17*, 543–551.

44) Woller, Eric K. and Cloninger, Mary *J. Org. Lett*. **2002**, *4*, 7-10.

45) Pieters, R. J. *Org. Biomol. Chem*. **2009**, *7*, 2013–2025.

46) Chabre, Y. M. and Roy, R. *Curr. Top. Med. Chem*. **2008**, *8*,1237–1285.

47) Sharon, N. and Lis, H. *Science,* **1989**, *246*, 227–234.

48) Pieters, R. J. *Org. Biomol. Chem*. **2009**, *7*, 2013–2025.

49) Ambrosi, M.; Cameron, N. R. and B. G. Davis, *Org. Biomol. Chem*. **2005**, *3*, 1593–1608.

50) Wright, C. S. *J. Mol. Biol.* **1987**, *194*, 501–529.

51) The Lectins. Properties, Functions, and Applications in Biology and Medicine, ed. I. E. Liener, N. Sharon and I. J. Goldstein, *Academic Press Inc.,* **1986**.

52) Kilpatrick, D. C. *Biochim. Biophys. Acta, Gen. Subj*. **2002**, *1572*,187–197.

53) Lundquist, J. J. and Toone, E. J. *Chem. Rev*. **2002**, *102*, 555–578.

54) McCoy, J. P.; Varani, J. and Goldstein, I. J. *Exp. Cell Res.* **1984**,*151*, 96–103.

55) Freire, E.; Mayorga, O. L. and Straume, M. *Anal. Chem*. **1990**, *62*, 950–959.

56) Jager, W. *Carbohydr. Chem. Biol*. **2000**, 1045–1057.

57) Cairo, C. W.; Gestwicki, J. E.; Kanai, M. and Kiessling, L. L. *J. Am. Chem. Soc*. **2002**, *124*, 1615–1619.

58) Deng, Z.; Li, S.; Jiang, X. and Narain, R. *Macromolecules* **2009**, *42*, 6393–6405.

59) Yang, Q.; Hu, M.-X.; Dai, Z.-W.; Tian, J. and Xu, Z.-K. *Langmuir* **2006**, *22*, 9345–9349.

60) Spain, S. G.; Gibson, M. I. and Cameron, N. R. *J. Polym. Sci., Part A: Polym. Chem.* **2007**, *45*, 2059–2072.

61) Kobayashi, K.; Tsuchida, A.; Usui, T. and Akaike, T. *Macromolecules* **1997**, *30*, 2016–2020.

62) Akai, S.; Kajihara, Y.; Nagashima, Y.; Kamei, M.; Arai, J.; Bito M. and Sato, K.-I. *J. Carbohydr. Chem.* **2001**, *20*,121–143.

63) Ambrosi, M.; Batsanov, A. S.; Cameron, N. R.; Davis, B. G.; Howard, J. A. K. and Hunter, R. *J. Chem. Soc. Perkin Trans.* **2002**, *1*, 45–52.

64) Ambrosi, M.; Cameron, N. R.; Davis, B. G. and Stolnik, S. *Org. Biomol. Chem.* **2005**, *3*, 1476–1480.

65) Cuervo-Rodriguez, R.; Bordege, V. and Fernandez-Garcia, M. *Carbohydr. Polym.* **2007**, *68*, 89–94.

66) Furuike, T.; Nishi, N.; Tokura, S. and Nishimura, S.-I. *Macromolecules* **1995**, *28*, 7241–7247.

67) Kim, S.-H.; Goto, M.; Cho, C.-S. and Akaike, T. *Biotechnol. Lett*. **2000**, *22*, 1049–1057.

68) Miyachi, A.; Dohi, H.; Neri, P.; Mori, H.; Uzawa, H.; Seto, Y. and Nishida, Y. *Biomacromolecules* **2009**, *10*, 1846–1853.

69) Nagahori, N. and Nishimura, S.-I. *Biomacromolecules* **2001**, *2*, 22–24.

70) Serizawa, T.; Yasunaga, S. and Akashi, M. *Biomacromolecules* **2001**, *2*, 469–475.

71) Tsuchida, A.; Akimoto, S.; Usui, T. and Kobayashi, K. *J. Biochem*. **1998**, *123*, 715–721.

72) Yang, Q.; Wu, J.; Li, J.-J.; Hu, M.-X. and Xu, Z.-K. *Macromol. Rapid Commun.* **2006**, *27*, 1942–1948.

73) Yoshizumi, A.; Kanayama, N.; Maehara, Y.; Ide, M. and Kitano, H. *Langmuir* **1999**, *15*, 482–488.

74) Meng, J. Q.; Du, F. S.; Liu, Y. S. and Li, Z. C. *J. Polym. Sci., Part A: Polym. Chem.* **2005**, *43*, 752.

75) Muthukrishnan, S.; Erhard, D. P.; Mori, H. and Muller, A. H. E. *Macromolecules* **2006**, *39*, 2743.

76) Muthukrishnan, S.; Jutz, G.; Andre, A.; Mori, H. and Muller, A. H. E. *Macromolecules* **2005**, *38*, 9.

77) Ohno, K.; Tsujii, Y. and Fukuda, T. *J. Polym. Sci., Part A: Polym. Chem*. **1998**, *36*, 2473–2481.

78) Vazquez-Dorbatt, V. and Maynard, H. D. *Biomacromolecules* **2006***, 7*, 2297.

79) Dai, X.-H. and Dong, C.-M. *J. Polym. Sci., Part A: Polym. Chem.* **2008**, *46*, 817–829.

80) Dai, X.-H.; Dong, C.-M. and Yan, D. *J. Phys. Chem. B* **2008**, *112*, 3644–3652.

81) Mateescu, A.; Ye, J.; Narain, R. and Vamvakaki, M. *Soft Matter* **2009**, *5*, 1621–1629.

82) Mizukami, K.; Takakura, H.; Matsunaga, T. and Kitano, H. *Colloids Surf. B* **2008**, *66*, 110–118.

83) Ladmiral, V.; Mantovani, G.; Clarkson, G. J.; Cauet, S.; Irwin, J. L. and Haddleton, D. M. *J. Am. Chem. Soc*. **2006**, *128*, 4823–4830.

84) Strong, L. E. and Kiessling, L. L. *J. Am. Chem. Soc.* **1999**, *121*, 6193–6196.

85) Chen, G.; Tao, L.; Mantovani, G.; Geng, J.; Nyströem, D. and Haddleton, D. M. *Macromolecules* **2007**, *40*, 7513–7520.

86) Geng, J.; Lindqvist, J.; Mantovani, G.; Chen, G.; Sayers, C. T.; Clarkson, G. J. and Haddleton, D. M. *QSAR Comb. Sci.* **2007**, *26*, 1220–1228.

87) Nurmi, L.; Lindqvist, J.; Randev, R.; Syrett, J. and Haddleton, D. M. *Chem. Commun*. **2009**, 2727–2729.

88) Hoyle, C. E. and Bowman, C. N. *Angew. Chem. Int. Ed.* **2010**, *49*, 1540–1573.

89) Deming, T. J.; *J. Polym. Sc.; Part A: Polym. Chem.* **2000**, *38*, 3011-3018.

90) a) Kwon, G. S.; Naito, M.; Kataoka, K.; Yokoyama, M.; Sakurai, Y.; Okano, T. *Colloids Surf. B* **1994**, *2*, 429–434; b) Welsh, E. R.; Tirrell, D. A. *Biomacromolecules* **2000**, *1*, 23–30.

91) a) Kröger, N.; Deutzmann, R.; Sumper, M. *Science* **1999**, *286*, 1129–1132; b) Cha, J. N.; Stucky, G. D.; Morse, D. E.; Deming, T. J. *Nature* **2000**, *403*, 289–292.

92) a) Maeda, M.; Tsuzaki, Y.; Nakano, K.; Tagaki, M. *J. Chem. Soc., Chem. Commun.* **1990**, 1529–1530; b) Ito, Y.; Ochiai, Y.; Park, Y.; Imanishi, Y. *J. Am. Chem. Soc.* **1997**, *119*, 1619–1623.

93) a) Kricheldorf, H. R. *α-Aminoacid-N-Carboxyanhydrides and Related Materials; Springer-Verlag: New York*, **1987**; pp 1–280; b) Kricheldorf, H. R. In Models of Biopolymers by Ring-Opening Polymerization; Penczek, S., Ed.; CRC: Boca Raton, FL, **1990**; pp 160–225.

94) a) Dwek, R. A. *Chem. Rev.* **1996**, *96*, 683–720. b) Carlstedt, I.; Davies, J. R. *Biochem. Soc. Trans.* **1997**, *25*, 214–219. c) Wu, A. M.; Csako, G.; Herp, A. *Mol. Cell. Biochem.* **1994**, *137*, 39–55. d) Jentoft, N. *Trends Biochem. Sci.* **1990**, *15*, 291–296.

95) Gestwicki, J. E.; Cairo, C. W.; Strong, L. E.; Oetjen, K. A.; Kiessling, L. L. *J. Am. Chem. Soc.* **2002**, *124*, 14922–14933.

96) Cairo, C. W.; Gestwicki, J. E.; Kanai, M.; Kiessling, L. L. *J. Am. Chem. Soc.* **2002**, *124*, 1615–1619.

97) Ullmann, V.; Rädisch, M.; Boos I.; Freund, J.; Pçhner, C.; Schwarzinger, S.; Unverzagt, C. *Angew. Chem. Int. Ed.* **2012**, *51*, 1 – 6.

98) Zhang, Y.; Muthana, S. M.; Farnsworth, D.; Ludek, O.; Adams, K.; Barchi, Jr., J. J.; Gildersleeve, J. C.; *J. Am. Chem. Soc.* **2012**, *134*, 6316−6325.

99) a) Herzner, H.; Reipen, T.; Schultz, M.; Kunz, H. *Chem. Rev.* **2000**, *100*, 4495; b) Seitz, O. *Chem. Bio. Chem* **2000**, *1*, 214; c) Buskas, T.; Ingale, S.; Boons, G. J. *Glycobiology* **2006**, *16*, 113; d) Meldal, M.; Bock, K.; *Glycoconjugate J.* **1994**, *11*, 59.

100) a) Yamamoto, N.; Tanabe, Y.; Okamoto, R.; Dawson, P. E.; Kajihara, Y. *J. Am. Chem. Soc*. **2008**, *130*, 501; b) Heinlein, C.; Varon Silva, D.; Trçster, A.; Schmidt, J.; Gross, A. and Unverzagt, C. *Angew. Chem. Int. Ed.* **2011**, *50*, 6406.

101) Subirös-Funosas, R.; El-Faham, A.; Albericio, F. *Tetrahedron* **2011**, *67*, 8595.

102) Bodanszky, M.; Kwei, J. Z. *Int. J. Pept. Protein. Res.* **1978**, *12*, 69.

103) Grogan, M. J.; Pratt, M. R.; Marcaurelle, L. A.; Bertozzi, C. R. *Annu. Rev. Biochem.* **2002**, *71*, 593−634.

104) Springer, G. F. *Science* **1984**, *224*, 1198−1206.

105) Holmberg, L. A.; Sandmaier, B. M. *Expert Rev*. *Vaccines* **2004**, 3, 655−663.

106) Owens, N. W.; Stetefeld, J.; Lattovà, E.; Frank Schweizer, F. *J. Am. Chem. Soc.* **2010**, *132*, 5036–5042.

107) Mayer, B. J. *J. Cell Sci.* **2001**, *114*, 1253–1263.

108) Pawson, T. *Nature* **1995**, *373*, 573–580.

109) Tang, H.; Zhang, D. *Biomacromolecules* **2010**, *11*, 1585–1592.

110) Sun, J.; Schlaad, H. *Macromolecules* **2010**, *43*, 4445−4448.

111) Huang, J.; Habraken, G.; Audouin, F.; Heise, A. *Macromolecules* **2010**, *43*, 6050−6057.

112) Rüde, E.; Westphal, O.; Hurwitz, E.; Fuchs, S.; Sela, M. *Immunochemistry* **1966**, 3, 137−151.

113) Aoi, K.; Tsutsumiuchi, K. and Okada, M. *Macromolecules* **1994**, *27*, 875–877.

114) Aoi, K.; Itoh, K. and Okada, M. *Macromolecules* **1995**, *28*, 5391–5393.

115) Aoi, K.; Tsutsumiuchi, K.; Aoki, E. and Okada, M. *Macromolecules* **1996**, *29*, 4456–4458.

116) Tsutsumiuchi, K.; Aoi, K. and Okada, M. *Macromolecules*, **1997**, *30*, 4013–4017.

117) Kramer, J. R.; Deming, T. J. *J. Am. Chem. Soc*. **2010**, *132*, 15068−15071.

118) Lu, H.; Wang, J.; Bai, Y. G.; Lang, J. W.; Liu, S. Y.; Lin, Y.; Cheng, J. J. *Nat. Commun*. **2011**, 2, 206.

119) Kramer, J. R.; Deming, T. J. *J. Am. Chem. Soc.* **2012**, *134*, 4112−4115.

120) Hanson, J. A.; Li, Z.; Deming, T. J. *Macromolecules* **2010**, *43*, 6268−6269.

121) Chen, C.; Wang, Z.; Li, Z. *Biomacromolecules* **2011**, *12*, 2859−2863.

122) Gabrielson, N. P.; Lu, H.; Yin, L.; Li, D.; Wang, F.; Cheng, J. *Angew. Chem., Int. Ed.* **2009**, *48*, 2572−2575.

123) Alberts, B. *Cell* **1998**, *92*, 291.

124) Vriezema, D. M.; Aragones, M. C.; Elemans, J. A. A. W.; Cornelissen, J. J. L. M.; Rowan, A. E.; Nolte, R. J. M. *Chem. Rev.* **2005**, *105*, 1445.

125) Baumeister, W.; Walz, J.; Zühl, F.; Seemüller, E. *Cell* **1998**, *92*, 367.

126) Antonietti, M.; Forster, S. *Adv. Mater.* **2003**, *15*, 1323–1333.

127) Bates, F. S.; Fredrickson, G. H. *Phys. Today* **1999**, *52*, 32–38.

128) Cölfen, H. *Macromol. Rapid Commun.* **2001**, *22*, 219–252.

129) Forster, S.; Antonietti, M. *Adv. Mater*. **1998**, *10*, 195–217.

130) Forster, S.; Konrad, M. *J. Mater. Chem*. **2003**, *13*, 2671–2688.

131) Evans, D. F.; Wennerstrom, H. *The Colloidal Domain*, *Second Ed.*; *Wiley-VCH*: *New York* **1999**.

132) Hadjichristidis, N.; Pispas, S.; Floudas, G. *Block Copolymers*: *Wiley*: *Hoboken NJ* **2003**.

133) Zhulina, E. B.; Adam, M.; LaRue, I.; Sheiko, S. S.; Rubinstein, M. *Macromolecules* **2005**, *38*, 5330–5351.

134) D. E. Discher and A. Eisenberg, *Science* **2002**, *297*, 967–973.

135) Lensen, D.; Vriezema, D. M.; van Hest, J. C. M. *Macromol. Biosci.* **2008**, *8*, 991.

136) Brinkhuis, R. P.; Rutjes, F. P. J. T.; Hest, Van Jan C. M. *Polym. Chem.* **2011**, *2*, 1449-1462.

137) Du, J. Z. and O'Reilly, R. K. *Soft Matter* **2009**, *5*, 3544–3561.

138) Blanazs, A.; Armes, S. P. and Ryan, A. J. *Macromol. Rapid Commun*. **2009**, *30*, 267–277.

139) Soo, P. L. and Eisenberg, A. *J. Polym. Sci., Part B: Polym. Phys.* **2004**, *42*, 923–938.

140) Du, J. Z.; and Chen, Y. M. *Macromolecules* **2004**, *37*, 5710–5716.

141) Adams, D. J.; Adams, S.; Atkins, D.; Butler, M. F. and Furzeland, S. *J. Controlled Release* **2008**, *128*, 165–170.

142) Bellomo, E. G.; Wyrsta, M. D.; Pakstis, L.; Pochan, D. J.; Deming, T. J. *Nat. Mater*. **2004**, *3*, 244–248. 143) Caspar, D. L. D. & Klug, A. Physical principles in construction of regular viruses. *Cold Spring Harbor. Symp. Quant. Biol.* **1962,** *27***,** 1–24.

144) Deming, T. J. *Nature* **1992**, *390***,** 386–389.

145) Deming, T. J. *Macromolecules* **1999**, *32,* 4500–4502.

146) Deming, T. J. and Curtin, S. A. *J. Am. Chem. Soc*. **2000**, *122,* 5710–5717.

147) Chécot, F., Lecommandoux, S., Klok, H.-A.; Gnanou,Y. *Eur. Phys. J. E.* **2003,** *10,* 25–35.

148) Schlaad, H.; Antonetti, M. *Eur. Phys. J. E.* **2003***, 10,* 17–23.

149) Nagasawa, M. and Holtzer, A. *J. Am. Chem. Soc.* **1964***, 86,* 538–543.

150) Epand, R. F.; Scheraga, H. A. *Biopolymers* **1968,** *6,* 1383–1386.

151) Katchalski, E.; Sela, M. *Adv. Protein Chem.* **1958***, 13,* 243–492.

152) Yoon, Y.-R.; Lim, Y.-b.; Lee, E.; Lee, M. *Chem*. *Commun*. **2008**, *1892*.

153) Huang, Z.; Kang, S.-K.; Banno, M.; Yamaguchi, T.; Lee, D.; Seok, C.; Yashima, E.; Lee, M. *Science* **2012**, *337,* 1521-1526.

154) Qi, S.; Iida, H.; Liu, L.; Irle, S.; Hu, W.; Yashima, E. *Angew. Chem. Int. Ed.* **2013** (DOI; 10.1002/anie.201208481).

155) Bertozzi, C. R.; Kiessling, L. L. *Science* **2001**, *291,* 2357−2364.

156) Kiessling, L. L.; Gestwicki, J. E.; Strong, L. E. *Curr. Opin. Chem. Biol*. **2000**, *4,* 696−703.

157) Roy, R. *Curr. Opin. Struct. Biol*. **1996**, *6,* 692−702.

158) Lees, W. J.; Spaltenstein, A.; Kingery, W. J. E.; Whitesides, G. M. *J. Med. Chem*. **1994**, *37,* 3419-3433.

159) Gabius, H.-J., Ed. *The Sugar Code. Fundamentals of Glycosciences, Wiley-VCH: Weinheim*, **2009**.

160) Kramer, J. R.; Deming, T. J. *J. Am. Chem. Soc.* **2012**, *134,* 4112−4115.

161) Wagner, A.; Vorauer-Uhl, K.; Katinger, H. *Eur. J. Pharm. Biopharm*. **2002**, *54,* 213−219.

162) Percec *et al. J. Am. Chem. Soc*. **2013** DOI; org/10.1021/ja403323y.

163) Percec *et al*. *Science* **2010**, *328*, 1009−1014.

164) Carlsen, A.; Lecommandoux, S. *Curr. Opin. Colloid Interface Sci*. **2009**, *14,* 329.

165) Holowka, E. P.; Pochan, D. J.; Deming, T. J. *J. Am. Chem. Soc.* **2005**, *127,* 12423.

166) Huang, J.; Bonduelle, C.; Thévenot, J.; Lecommandoux, S.; Heise, A. *J. Am. Chem. Soc*. **2012**, *134,* 119−122.

167) Torchilin, V. P. *Adv. Drug Delivery Rev.* **2006**, *58*, 1532–1555.

168) Bae, Y.; Fukushima, S.; Harada, A.; Kataoka, K. *Angew. Chem., Int. Ed.* **2003**, *42*, 4640–4643.

169) Bae, Y.; Jang, W.-D.; Nishiyama, N.; Fukushima S.; Kataoka, K. *Mol. Bio Syst*. **2005**, *1*, 242–250.

170) Li, Z.; Hillmyer, M. A.; Lodge, T. P. *Nano Lett*. **2006**, *6*, 1245–1249.

171) Kramer, J. R.; Rodriguez, A. R.; Kameib, U.-J.C.; D. T.; Deming, T. J. *Soft Matter* **2013**, *9*, 3389–3395.

172) Stewart, B. W.; Kleihues, P. *World Cancer Report* (*World Health Organization Press, Geneva*, **2003**).

173) Steeg, P. S. *Nature Med*. **2006**, *12*, 895–904.

174) Peer, D.; Karp, J. M.; Hong, S.;Farokhzad, O.C.; Margalit, R.; Robert Langer, R. *Nature Nanotechnology* **2007**, *2*, 751-760.

175) Matsumura, Y.; Maeda, H. *Cancer Res.* **1986**, *46*, 6387–6392.

176) Yuan, F. *et al. Cancer Res.* **1995**, *55*, 3752–3756.

177) Torchilin, V. P. *Nat. Rev. Drug Discov*. **2005**, *4*, 145–160.

178) Hobbs, S. K. *et al. Proc. Natl. Acad. Sci. USA* **1998**, *95*, 4607–4612.

179) Gottesman, M. M.; Fojo, T.; Bates, S. E. *Nat. Rev. Cancer* **2002**, *2*, 48–58.

180) Peer, D.; Margalit, R. *Cancer Lett*. **2006**, *237*, 180–187.

181) Jain, R. K. *Sci. Am*. **1994**, *271*, 58–65.

182) Torchilin, V. P. *Nat. Rev. Drug Discov*. **2005**, *4*, 145–160.

183) Menezes, D. E. L.; Pilarski, L. M.; Allen, T. M. *Cancer Res.* **1998**, *58*, 3320–3330.

184) Warenius, H. M.; Galfre, G.; Bleehen, N. M.; Milstein, C. *Eur. J. Cancer Clin. Oncology* **1981**, *17*, 1009–1015.

185) Gabizon, A. A. *Cancer Invest*. **2001**, *19*, 424–436.

186) James, J. S.; Dubs, G. *AIDS Treat. News* **1997**, *284*, 2–3.

187) Ferrara, N. *Oncology* **2005**, *69*, 11–16.

188) Peer, D., Zhu, P.; Carman, C. V.; Lieberman, J.; Shimaoka, M. *Proc. Natl. Acad. Sci. USA* **2007**, *104*, 4095–4100.

189) Farokhzad, O. C. *et al. Proc. Natl. Acad. Sci. USA* **2006**, *103*, 6315–6320.

190) Sanfilippo, J. S. *et al. Cancer* **1996**, *77*, 710–716.

191) Ishida, O. *et al. Pharm. Res*. **2001**, *18*, 1042–1048.

192) Li, J. *et al. Cancer Gene Ther.* **2004**, *11*, 363–370.

193) Ruoslahti, E.; Takamatsu, P.; *Symp*. **1994**, *24*, 99–105.

194) Champion, J. A.; Mitragotri, S. *Proc. Natl. Acad. Sci. USA* **2006**, *103*, 4930–4934.

195) Geng, Y.*et al. Nature Nanotech*. **2007**, *2*, 249–255.

196) Gratton, S. E. *et al. Proc. Natl. Acad. Sci. USA* **2008**, *105*, 11613–11618.

197) Gottesman, M. M.; Fojo, T.; Bates, S. E. *Nat. Rev. Cancer* **2002**, *2*, 48–58.

198) Pati, D. *et al. Polym. Chem.* **2011**, *2*, 805-811.

199) Pati D. *et al. Biomacromolecules* **2012**, *13*, 1287-1295.

200) Pati, D. *et al. J. Am. Chem. Soc.* **2012**, *134*, 7796-7802.

201) Pati, D. *et al.* Manuscript under preparation.

Chapter 2

Synthesis of Glycopeptides by the ring opening polymerization of *O*-glycosylated-α-Amino Acid N-Carboxyanhydride (NCA)

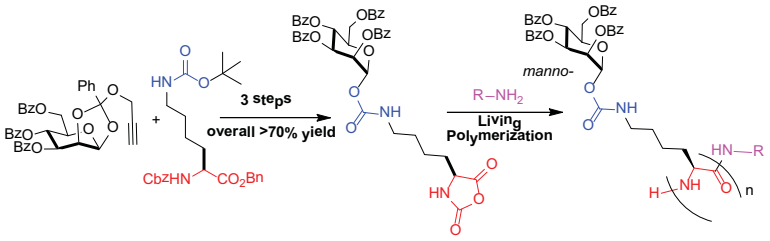

Abstract: The novel synthesis of *O*-glycosylated Lysine-NCA from a stable glycosyl donor and a commercially available protected amino acid in very high yield is reported. These *O*-glycosylated Lysine-NCA monomers underwent ring opening polymerization using simple primary amine initiators to form well defined, high molecular weight homo glycopolypeptides and diblock co-glycopolypeptides. The synthesis of azide labelled end functionalized glycopolypeptides and amphiphilic diblock copolypeptides is also reported. This methodology represents an easy and practical route to the synthesis *O*-glycosylated polypeptides with 100% glycosylation.

This chapter has been adapted from the corresponding paper;

"Synthesis of glycopolypeptides by ring opening polymerization of α-amino acid N-carboxyanhydrides (NCA)" **Debasis Pati**, Asif Y. Shaikh, Srinivas Hotha, Sayam Sen Gupta, *Polym. Chem*. *2011*, **2**, 805-811.

2.1 Introduction

Although well defined polypeptides based on natural and unnatural amino acids have been very successfully synthesized by the ring opening polymerization of their corresponding *N*-carboxyanhydrides (NCA),[1] the synthesis of glycopolypeptide still remains a major challenge. Glycopolypeptides can be synthesized by (1) ring opening polymerizations of glycosylated *N*-carboxyanhydride (NCA) monomers or (2) post polymerization modification of polypeptide side chains.[2] The first synthesis of glycopolypeptides using the ring opening polymerization of *O*-linked glycoserine NCA was reported quite some time back by Okada *et al.* [3-6] However, the synthesis of the NCA monomer was very inefficient and required the usage of toxic Hg salts for the key glycosylation step.[7] Further, the polymerization was extremely slow and limited to low degrees of polymerization. This was attributed to the steric effects and H-bonding between the sugar residue and NCA ring.[4-6] The synthesis of the monomer has been improved upon by Cameron *et al.* but no polymerization of the synthesized *O*-linked glyco-serine NCA was reported subsequently.[8] Very recently, Deming *et al.* has elegantly synthesized *C*-linked glycosylated-*l*-lysine NCA monomers and have successfully polymerized it using transition metal initiators.[9] Synthesis of glycopolypeptides by post polymerization modification of synthetic polypeptides on the contrary has been more successful and several methods have been reported recently. These methods include coupling of β-D-galactosylamine to carboxylic acid group of poly-*l*-glutamic acid[10] to more recent reports of azide-alkyne cyclo-addition reaction[11] and thiol-ene click reactions[12] for synthesis of glycopolypeptides. Although glycopeptides have been successfully synthesized by these methodologies, their main drawback is the incomplete sugar fictionalization which is more predominant for high molecular weight polypeptides. Hence there is a need to develop simple and efficient methodologies to synthesize glycosylated amino acid NCA's which can be then polymerized to afford high molecular weight glycopolypeptides.

In this chapter, I report a novel and simple methodology for the synthesis of *O*-glycosylated-*l*-lysine NCA and their subsequent polymerization to afford glycopolypeptides. The *O*-glycosylated-*l*-lysine NCA that was synthesized has several attributes. First, the presence of the lysine side chain would put the sugar residue much

farther away from the NCA ring. This would in turn reduce the sterics that was responsible for the inefficient polymerization of *O*-linked glyco-serine NCA. Further, ROP of lysine NCA bearing various protecting groups have been extensively investigated and shown to undergo very efficient ROP to yield very high molecular weight polypeptides. Finally, the *O*-glycoside linkage between the sugar and the lysine side chain resemble more closely to the native linkages. The *O*-glycosylated-*l*-lysine NCA synthesized by our methodology underwent ring opening polymerization into well defined high molecular weight glycopolypeptide and diblock glycopolypeptide copolymers using simple amine initiators.

O-Linked glycopolypeptides synthesized by the NCA polymerization have not received the same attention as glycopolymers synthesized from acrylates and methacrylates[13-20] since the critical glycosidation step for the synthesis of amino acid carbohydrate conjugate is very inefficient. The key to the successful synthesis of glycopolypeptides lies in development of a methodology that allows synthesis of glycosylated amino acids in very high yield. We used the methodology developed by Hotha *et al.* [21-23] for the synthesis of 1,2-*trans* glycosides only by the use of propargyl-1,2-orthoesters in the presence of $AuBr_3$/4 Å molecular sieves powder at room temperature .

By following methodology developed by Shaikh *et al.* [24-25], we envisioned that ε-Boc protected CbzLysOBn would be ideal to prepare amino acid glycoconjugate which can subsequently be converted to the corresponding glycosyl carbamate using gold catalyzed glycosylation procedure. Accordingly, glycosylation reaction between ε-Boc protected CbzLysOBn and propargyl-1,2-orthoester of glucose and mannose was conducted in the presence of $HAuCl_4$ and 4 Å molecular sieves powder in CH_2Cl_2 at room temperature to afford the glycosylated carbamates (Scheme 2.1) in almost quantitative yield. Furthermore, we continued our journey towards the glyco-NCA in two steps: first, we subjected the glycoconjugates **2a** and **2b** to hydrogenation using 10% Pd/C at 400 psi to obtain *per*-*O*-benzoylated-D-glucose-*l*-lysine carbamate or *per*-*O*-benzoylated-D-mannose-*l*-lysine carbamate. They were then subsequently converted to their corresponding NCA's **3a** (β-gluco-*O*-lys) and **3b** (α-manno-*O*-lys) using triphosgene and α-pinene[8] in 80% yield after three crystallizations (Scheme 2.1). The

purified NCAs **3a** and **3b** were thoroughly characterized by NMR spectroscopic studies. As delineated above, the major hurdle for the synthesis of biomimetic glycopolypeptides has been the limited access to this important class of glyco amino acid NCA's. Literature methods suffer from one or more of (i) toxic metals for the activation, (ii) long reaction times, (iii) laborious purification procedures and (iv) poor yields. A recent report revealed glycopolypeptides with lysine backbone from a known C-glycosyl precursor in a multistep manner with a poor overall yield. On the other hand, our current endeavour for the synthesis of glyco amino acid NCA is novel, has near quantitative yield, uses catalytic quantity of $HAuCl_4$ and involves a very simple purification procedure.

2.2 Experimental Section

2.2.1 Materials and Methods

Propargyl-1,2-orthoesters **1a** and **1b** were prepared according to literature procedure.[22] CbzLys(Boc)OH was obtained from Aldrich and converted to CbzLys(Boc)OBn using standard literature procedure[23]. $HAuCl_4$, *p*-methoxy benzyl alcohol, hexyl amine, triphosgene and azido-PEG-amine(n=11) were obtained from Aldrich. All other chemicals used were obtained from Merck, India. Diethyl ether, petroleum ether (60-80^oC), ethylacetate, dichloromethane, tetrahydrofuran, dioxane were brought from Merck and dried by conventional methods and stored in the glove box. DMF (99.99% dry) obtained from Sigma Aldrich was used for polymerization inside the glove box. FT-IR spectra were recorded on Perkin Elmer FT-IR spectrum GX instrument by making KBr pellets. Pellets were prepared by mixing 3mg of sample with 97mg of KBr. ^1H NMR spectra were recorded on Bruker Spectrometers (200 MHz, 400 MHz or 500 MHz). ^{13}C NMR and DEPT spectra were recorded on Bruker Spectrometer (50 MHz, 100MHz or 125MHz) and reported relative signals according to deuterated solvent used. Size-exclusion chromatography of the glycopolypeptides was performed using an instrument equipped with Waters 590 pump with an Spectra System RI-150 RI detector. Separations were effected by 10^5 and 10^3 Å Phenomenex 5μ columns using 0.1M LiBr in DMF eluent at 60 °C at the samples concentrations of 5mg/ml. A constant flow rate of 1 mL/min was maintained, and the instrument was calibrated using polystyrene standards.

*2.2.2 General procedure for the synthesis of amino acid glycosyl carbamates (**2a** and **2b**)*

To a solution of propargyl-1,2-orthoester[12b] (**1a** or **1b**; 0.1 mmol), CbzLys(Boc)OBn (0.11 mmol) and activated 4Å molecular sieves powder (50 mg) in anhydrous CH_2Cl_2 (5 mL) was added $HAuCl_4$ (7 mol%) under argon atmosphere at room temperature. The reaction mixture was stirred at room temperature for the specified time and the reaction mixture was filtered and the filtrate was concentrated *in vacuo*. The resulting residue was purified by silica gel column chromatography using ethyl acetate-petroleum ether as the mobile phase to afford the compounds **2a** and **2b**.

Compound **2a**: $[\alpha]^{D}_{25}$ = +52.7 (*c* = 1.0 in $CHCl_3$); ^{1}H NMR (200.13 MHz, $CDCl_3$): δ = 1.03-1.78(m, 6H), 3.02(q, 2H, *J* = 6.2, 12.5 Hz), 4.10-4.36(m, 2H), 4.45(dd, 1H, *J* = 4.4, 12.5 Hz), 4.62(dd, 1H, *J* = 2.5, 12.1 Hz), 4.93(t, 1H, *J* = 5.7 Hz), 5.11(m, 2H), 5.12(s, 2H), 5.37(d, 1H, *J* = 8.0 Hz), 5.64(dd, 1H, *J* = 8.3, 9.5 Hz), 5.74(t, 1H, *J* = 9.7 Hz), 5.93(t, 1H, *J* = 9.6 Hz), 6.03(d, 1H, *J* = 8.2 Hz), 7.21-7.59(m, 22H), 7.80-8.06(m, 8H); ^{13}C NMR (50.32 MHz, $CDCl_3$): δ = 21.9, 28.9, 31.8, 40.4, 53.6, 62.6, 66.9, 67.1, 69.0, 70.9, 72.7, 72.8, 93.1, 128.0-129.9, 133.0, 133.2, 133.4, 133.4, 135.2, 136.2, 153.8, 155.9, 165.0, 165.2, 165.6, 166.0, 172.1; HRMS (MALDI-TOF): *m/z*: calcd for $[C_{56}H_{52}N_2O_{15}Na]^+$: 1015.3265; found: 1015.3254.

Compound **2b**: $[\alpha]^{D}_{25}$ = -29.2(*c* = 1.0 in $CHCl_3$); ^{1}H NMR (200.13 MHz, $CDCl_3$): δ = 1.25-1.95(m, 6H), 3.19(q, 2H, *J* = 6.3, 12.1 Hz), 4.38-4.56(m, 3H), 4.71(dd, 1H, *J* = 3.6, 13.2 Hz), 5.13(s, 2H), 5.19(m, 3H), 5.47(d, 1H, *J* = 8.1 Hz), 5.74(dd, 1H, *J* = 2.4, 3.1 Hz),5.90(dd, 1H, *J* = 3.3, 10.2 Hz), 6.19(t, 1H, *J* = 10.0 Hz), 6.31(d, 1H, *J* = 1.9 Hz), 7.21-7.66(m, 22H), 7.78-8.15(m, 8H); ^{13}C NMR (50.32 MHz, $CDCl_3$): δ = 22.3, 29.0, 32.2, 40.8, 53.6, 62.4, 66.2, 67.0, 67.1, 69.4, 69.9, 70.4, 91.3, 128.0-129.9, 133.0, 133.3, 133.4, 133.5, 135.2, 136.1, 153.1, 156.0, 165.1, 165.2, 165.6, 166.0, 172.2; HRMS (MALDI-TOF): *m/z*: calcd for $[C_{56}H_{52}N_2O_{15}Na]^+$: 1015.3265; found: 1015.3254.

2.2.3 General procedure for the N-carboxyanhydrides synthesis

*2.2.3.1 Synthesis of glyco N-carboxyanhydrides (**3a** and **3b**)*

Hydrogenolysis of compounds **2a** and **2b** was carried out using 10% Pd/C in MeOH/EtOAc (9:1) at 400 psi for 12 h. After completion of the reaction, the reaction mixture was filtered and concentrated under reduced pressure to afford *per*-*O*-benzoylated-D-glucose-*l*-lysine carbamate or *per*-*O*-benzoylated-D-mannose-*l*-lysine carbamate in almost quantitative yield. The resulting compounds were directly used for NCA synthesis without any further purification.

To a solution of *per*-*O*-benzoylated-D-Glucose-*l*-lysine carbamate or *per*-*O*-benzoylated-D-mannose-*l*-lysine carbamate (654 mg, 0.85 mmol) in freshly distilled out tetrahydrofuran (10 ml) was added a solution of triphosgene (126 mg, 0.425 mmol) in anhydrous tetrahydrofuran (2ml) under argon and the reaction mixture was heated to 50-55°C. α-pinene (0.202 ml, 1.28 mmol) was then added and the reaction mixture was allowed to stir for an additional 2 h. The reaction mixture was then cooled to room temperature and then poured into dry hexane (300 ml) to afford a white precipitate; which was filtered off quickly and crystallized two more times using a mixture of ethyl acetate and petroleum ether. Finally, the white precipitate of glyco *N*-carboxyanhydride (**3a** or **3b**) was dried under vacuum and transferred into the glove box. Final yield 544 mg (80%).

Compound **3a**: ^{1}H NMR (400.13 MHz, CD_3CN): δ = 1.15-1.80(m, 6H), 3.03(q, 2H, *J* = 6.3, 12.0 Hz), 4.30(dd, 1H, *J* = 5.5, 6.7 Hz), 4.48(td, 1H, *J* = 3.0, 6.4, 9.8 Hz), 4.54(dd, 1H, *J* = 4.0, 12.5 Hz), 4.58(dd, 1H, *J* = 2.8, 12.5 Hz), 5.67(t, 1H, *J* = 8.8 Hz), 5.83(t, 1H, *J* = 9.6 Hz), 5.94(t, 1H, *J* = 5.9 Hz), 6.06(t, 1H, *J* = 9.5 Hz), 6.17(d, 1H, *J* = 8.2 Hz), 6.86(s, 1H), 7.32-7.68(m, 12H), 7.81(d, 2H, *J* = 7.5 Hz), 7.90(d, 2H, *J* = 7.5 Hz), 7.93(d, 2H, *J* = 7.2 Hz), 8.05(d, 2H, *J* = 7.7 Hz); ^{13}C NMR (100.61MHz, CD_3CN): δ = 22.5, 29.4, 31.6, 41.0, 58.2, 63.3, 70.0, 71.1, 73.2, 74.3, 93.7, 129.4-132.7, 134.2, 134.5, 134.6, 134.7, 152.8, 154.8, 165.9, 166.0, 166.3, 166.7, 171.9; HRMS (MALDI-TOF): *m/z*: calcd for $[C_{42}H_{38}N_2O_{14}Na]^+$: 817.2221; found: 817.2237.
Compound **3b**: ^{1}H NMR (400.13 MHz, CD_3CN): δ = 1.38-1.94(m, 6H), 3.20(q, 2H, *J* = 6.6, 12.7 Hz), 4.38(t, 1H, *J* = 6.2 Hz), 4.58(ABq, 1H, *J* = 3.0 Hz), 4.59(s, 1H), 4.68(t, 1H, *J* = 11.5 Hz), 5.73(s, 1H), 5.89(dd, 1H, *J* = 2.8, 10.2 Hz), 6.12(t, 1H, *J* =

10.2 Hz), 6.18(t, 1H, *J* = 5.6 Hz), 6.23(s, 1H), 6.90(s, 1H), 7.31-7.73(m, 12H), 7.77(d, 2H, *J* = 7.5 Hz), 7.95(d, 2H, *J* = 7.5 Hz), 8.01(d, 2H, *J* = 7.6 Hz), 8.10(d, 2H, *J* = 7.2 Hz); ^{13}C NMR (100.61MHz, CD_3CN): δ = 22.6, 29.6, 31.7, 41.2, 58.4, 63.0, 67.0, 70.5, 71.2, 71.3, 91.9, 129.5-131.0, 134.3, 134.5, 134.6, 134.7, 152.9, 154.4, 166.0, 166.2, 166.2, 166.6, 172.1; HRMS (MALDI-TOF): *m/z*: calcd for $[C_{42}H_{38}N_2O_{14}Na]^+$: 817.2221; found: 817.2217.

2.2.3.2 Synthesis of γ-Benzyl-l-glutamate- N-carboxyanhydride (***3c***)

To a solution of γ-Benzyl-*l*-glutamate amino acid (1 g, 4.21 mmol) in freshly distilled out tetrahydrofuran (10 ml) was added a solution of triphosgene (625mg, 2.11 mmol) in anhydrous tetrahydrofuran (4 ml) under argon and the reaction mixture was heated to 50-55° C. Then α-pienene (1.0 ml, 6.32 mmol) was added and the reaction mixture was allowed to stir for 2 hrs. The reaction mixture was then cooled to room temperature and thereafter poured into dry hexane (400 ml) to afford a white precipitate. The white precipitate of N-carboxyanhydrides was filtered off by vacuum quickly and crystallized two more times by using ethyl acetate/petroleum ether mixtures. Finally the precipitate of γ-Benzyl-*l*-glutamate- N-carboxyanhydride was dried under vacuum and transferred into glove box. Final yield 900 mg (81%).

Compound **3c**: ^{1}H NMR (400.13 MHz, $CDCl_3$): δ = 2.33-2.58(m, 2H), 2.85(t, 2H, *J* = 7.0 Hz), 4.66(t, 1H, *J* = 6.0 Hz), 5.40(s, 2H), 7.25(bs, 1H), 7.61-7.65(m, 5H); ^{13}C NMR (100.61MHz, $CDCl_3$): δ = 26.7, 29.5, 56.7, 67.0, 128.2-128.7, 135.2, 152.2, 169.9, 172.3.

*2.2.3.3 Synthesis of ε-N-carbobenzoxy-l-lysine-N-carboxyanhydride (**3d**)*

To a solution of ε,α-di-N-carbobenzoxy-*l*-lysine (1 g, 2.41 mmol) in freshly distilled out diethyl ether (10 ml) was added phosphorous pentachloride (603 mg, 2.90mmol) under argon at 0°-5° C and the reaction mixture was allowed to stir for 30 min. As soon as the reaction mixture turned homogeneous, the solvent was removed slowly under reduced pressure and the residue redissolved in dry ethyl acetate. The mixture was filtered to remove undissolved solid particles and the filtrate was poured into dry hexane (400 ml) to afford white precipitate. The white precipitate of N-carboxyanhydride was filtered off by vacuum quickly and crystallized two more times by using ethyl acetate/petroleum ether mixtures. Finally precipitate of ε-N-

carbobenzoxy-*l*-lysine-carboxyanhydride was dried under vacuum and transferred into glove box. Final yield 500 mg (67%).

Compound **3d**: ^{1}H NMR (400.13 MHz, $CDCl_3$): δ = 1.32-1.56(m, 4H), 1.70-1.91(m, 2H), 3.12(dd, 2H, *J* = 6.5, 12.8 Hz), 4.33(t, 1H, *J* = 6.0 Hz), 5.07(s, 2H), 5.70(bs, 1H), 6.96(bs, 1H), 7.31-7.42(m, 5H); ^{13}C NMR (100.61MHz, $CDCl_3$): δ = 22.6, 29.9, 31.7, 41.0, 58.3, 66.7, 128.5-129.4, 138.4, 152.9, 157.4, 172.1.

*2.2.3.4 Synthesis of γ-p-OMe-benzyl-l-glutamate-N-carboxyanhydride (**3e**)*

To a solution of γ-p-OMe-benzyl-*l*-glutamate amino acid (1 g, 3.74 mmol) in freshly distilled out tetrahydrofuran (10 ml) was added a solution of triphosgene (555 mg, 1.87 mmol) in anhydrous tetrahydrofuran (4 ml) under argon and the reaction mixture was heated to 50-55° C. Then α-pienene (0.89 ml, 5.6 mmol) was added and the reaction mixture was allowed to stir for 2 h. The reaction mixture was then cooled to room temperature, there after poured into dry hexane (400 ml) and then kept in the refrigerator for 4-5 h at -20° C under argon to afford a white precipitate. The white precipitate of N-carboxyanhydride was filtered off by vacuum quickly and crystallized two more times by using ethyl acetate/petroleum ether mixture. Finally the white precipitate of γ-p-OMe-benzyl-*l*-glutamate-N-carboxyanhydride was dried under vacuum and transferred into the glove box. Final yield 800 mg (80%).

Compound **3e**: ^{1}H NMR (400.13 MHz, CD_3CN): δ = 1.98-2.23(m, 2H), 2.49(dt, 2H, *J* = 3.3, 7.4 Hz), 3.80(s, 3H), 4.41(t, 1H, *J* = 6.6 Hz), 5.05(s, 2H), 6.86(bs, 1H), 6.93(m, 2H), 7.32(m, 2H); ^{13}C NMR (100.61MHz, CD_3CN): δ = 27.4, 30.1, 55.8, 57.4, 66.9, 114.8(2C), 129.1, 130.9(2C), 152.7, 166.6, 171.7, 172.2.

2.2.4 General procedure for the synthesis of glycopolypeptides

To a solution of glyco-*l*-lysine NCA **3a** or **3b** (100mg/ml) in dry dioxane, acetonitrile or DMF was added with "proton sponge" 1,8-bis(dimethylamino)naphthalene (0.25 equivalent to monomer; 1 M) as an additive and hexylamine or Azido-PEG-amine (0.5 M) as the initiator inside the glove box. The progress of the polymerization were monitored by FT-IR spectroscopy by comparing with the intensity of the initial NCA's anhydride stretching at 1789 cm^{-1} and 1852 cm^{-1}. The reactions generally completed within 24 to 30 h. Aliquotes were removed after completion of polymerization for GPC analysis. Finally the solvent was removed under reduced pressure from the reaction mixture. The

resulting residue was redissolved in DCM and then the polymer precipitated out by addition of methanol. The precipitated polymer was collected by centrifugation and dried to afford white glycopolypeptides **4a**, **4b**, **4c**, **5a**, **5b** and **5c** in almost 85-90% yield.

Polymer **4a**. ^{1}H NMR (400.13 MHz, $CDCl_3$): δ = 1.15-1.19(br, m, 6H), 2.25-3.30(br, m, 2H,), 3.48-4.00(br, m, 1H), 4.25-4.80(br, m, 3H), 5.50-6.7(br, m, 5H), 6.86-7.50(br, m, 12H), 7.65-8.50(br, m, 8H)

Polymer **5a**: ^{1}H NMR (200. MHz, $CDCl_3$): δ = 1.15-2.29(br, m, 6H), 2.89-3.87(br, m, 2H,), 4.08-5.00(br, m, 4H), 5.5-6.45(br, m, 5H), 6.86-7.50(br, m, 12H), 7.65-8.50(br, m, 8H)

2.2.4.1 General procedure for the synthesis of diblock coglycopolypeptides

To a solution of the first NCA monomer (15 eq, 100 mg/mL) in DMF was added hexylamine (1 eq) at rt inside the glove box. The progress of the reaction was monitored by FT-IR. Upon near comsumption of the first monomer (>95%), the second glyco amino acid NCA (25 eq of **3a** or 15 eq of **3b**) together with proton sponge (0.25 eq of the second NCA monomer) in DMF (100 mg/mL) was added and the progress of the reaction was monitored by FT-IR. The reactions generally completed within 30 hrs. Aliquotes were removed after completion of polymerization for GPC analysis. Finally the solvent was removed under reduced pressure from the reaction mixture. The resulting residue was redissolved in DCM and then the polymer precipitated out by addition of methanol. The precipitated polymer was collected by centrifugation and dried to afford white diblock coglycopolypeptides **6a**, **7a**, **7b** and **8** in almost 85-90% yield.

Compound **6a**: ^{1}H NMR (400.13 MHz, $CDCl_3$): δ = 1.15-1.18(br, m, 6H), 1.9-3.4(br, m, 6H,), 3.48-4.00(br, m, 4H), 4.25-4.80(br, m, 4H), 4.7-5.2(bs, 2H), 5.50-6.5(br, m, 5H), 6.6-7.80(br, m, 16H), 7.85-8.50(br, m, 8H)

Compound **7b**: ^{1}H NMR (400.13 MHz, $CDCl_3$): δ = 1.25-2.78(br, m, 8H), 2.98-3.45(br, m, 2H,), 3.50-4.12(br, m, 2H),3.66(bs, for CH_2CH_2O unit in initiator) 4.22-4.90(br, m, 5H), 4.92-5.23(br, m, 2H), 5.45-6.45(br, m, 5H), 7.1-7.70(br, m, 17H), 7.71-8.24(br, m, 8H).

*2.2.4.2 Synthesis of poly-l-glutamate-b-poly-per-O-benzoylated-D-glucose-l-Lysine (**9**)*

To a solution of Poly-PMBnLG-*b*-poly-*per*-*O*-benzoylated-D-glucose-*l*-lysine (**6a**) polymer in dichloromethane was added 10% TFA in dichloromethane (2.5 equivalent) and the reaction mixture was stirred for 30 min at room temperature. The reaction was then quenched by the addition of triethylamine (3 equivalent) and the volume of the reaction mixture was reduced to half. The polymer was precipitated out by addition of diethyl ether and resultant white precipitate (**9**) was collected by centrifugation. The complete deprotection of the p-methoxybenzylester was confirmed by ^{1}H and ^{13}C NMR. Yield 90%.

*2.2.4.3 Synthesis of fluorescein labelled block polypeptide (7**c**)*

The alkyne labelled fluorescein was synthesized according to published procedures.[27] To a solution of 22 mg azide functionalized blockcopolymer (**7b**) in DMF was added alkyne labeled fluorecein (1mg, 3 eq), Cu(I)Br (0.1 mg, 0.50 eq) and PMDETA (0.5 eq) under nitrogen and the reaction mixture was stirred for 24 hrs. The completion of the reaction was observed by the near dissaperance (more than 90-95%) of the azide stretching by FT-IR. Then, the solvent was removed under reduced pressure and the reaction mixture was dissolved in dichloromethane. It was then washed multiple times using dilute aqueous ammonia solution to remove copper(I) salt and excess fluorecein alkyne. Finally the dichloromethane was removed and the resultant polymer **7c** reprecipitated three times by addition of methanol to the solution of **7c** in dichloromethane. Polymer **7c** was thoroughly dried and its absorption spectra taken in UV-VIS spectrophotometer. Yield: 8 mg

2.3 Results and Discussion

Glycosylation reaction between ε-Boc protected CbzLysOBn and propargyl-1,2-orthoester of glucose (**1a**) and mannose (**1b**) was conducted in the presence of $HAuCl_4$ and 4 Å molecular sieves powder in CH_2Cl_2 at room temperature to afford the carbamates **2a** and **2b** in 95% and 92% yield respectively (Scheme 2.1). Furthermore, we continued our journey towards the glyco-NCA in two steps: first, we subjected the glycoconjugates **2a** and **2b** to hydrogenation using 10% Pd/C at 400psi to obtain *per*-*O*-benzoylated-D-glucose-*l*-lysine carbamate or *per*-*O*-benzoylated-D-mannose-*l*-

lysine carbamate. They were then subsequently converted to their corresponding NCA's **3a** (β-gluco-*O*-lys) and **3b** (α-manno-*O*-lys) using triphosgene and α-pinene[7] in 80% yield after three crystallizations (Scheme 2.1). The purified NCAs **3a** and **3b** were thoroughly characterized by NMR spectroscopic studies. As delineated above, the major hurdle for the synthesis of biomimetic glycopolypeptides has been the limited access to this important class of glyco amino acid NCA's. Literature methods suffer from one or more of (i) toxic metals for the activation, (ii) long reaction times, (iii) laborious purification procedures and (iv) poor yields. A recent report revealed glycopolypeptides with lysine backbone from a known C-glycosyl precursor in a multistep manner with a poor overall yield. On the other hand, our current endeavour for the synthesis of glyco amino acid NCA is novel, has near quantitative yield, uses catalytic quantity of $HAuCl_4$ and involves a very simple purification procedure.

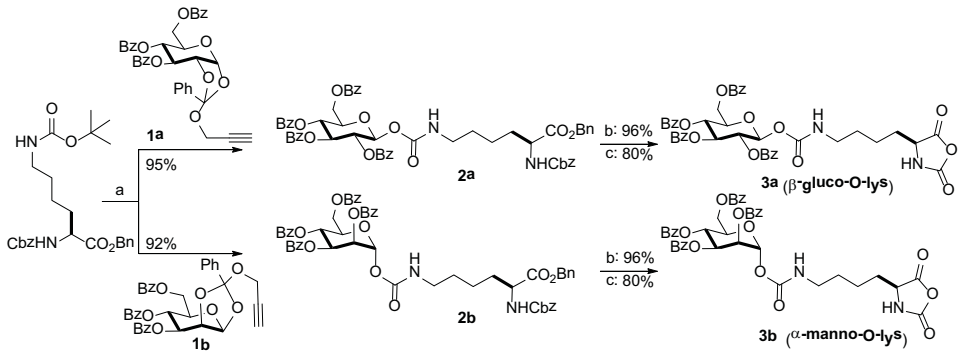

a) $HAuCl_4$, CH_2Cl_2, rt, 0.5h, 4A° MS Powder, Yield (90-95%); b) Pd/C, H_2, 400psi, CH_3OH, 12h, Yield (> 95%); c) Triphosgene, THF, α-pinene, 70°C, Yield (85%)

Scheme 2.1: Synthesis of glyco amino acid NCA's.

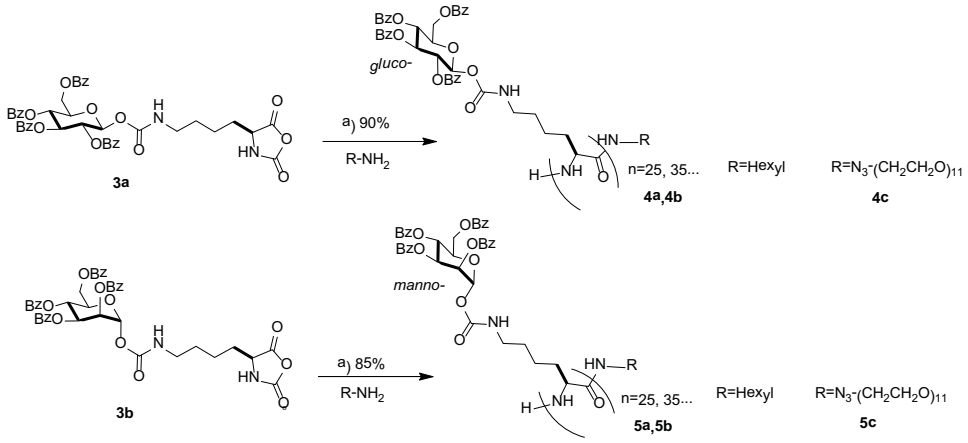

a) Dioxane/Acetonitrile/DMF, Proton Sponge (0.25 equiv), 24 hrs, RT

Scheme 2.2: Synthesis of glycopolypeptides by ROP of glycol amino acid NCA's.

Polymerization of **3a** (β-gluco-*O*-lys NCA) was first attempted using hexyl amine as the initiator (M/I = 25) in dry acetonitrile (Scheme 2.2). The progress of the polymerization was followed by monitoring the disappearance of the anhydride stretch of the NCA ring at 1787 and 1852 cm^{-1} by FT-IR spectroscopy. However, no decrease in the anhydride stretch was observed even after 48 h of initiation. Similar observation was noted even when the solvent was changed to dry dioxane or DMF. We reasoned that there might be very small amounts of residual acid left which protonated the primary amine initiator to inhibit the initiation of the polymerization reaction. To remove the residual acid, we proceeded with the polymerization again in the presence of a small amount of non-nucleophilic base 1,8-bis(dimethylamino)naphthalene "proton sponge" (0.25 eq with respect to monomer; run 1).

		Initiator				**Product Polymer**			
Run no	Monomer (M)	Initiator (I)	M/I[a]	Solvent	Polymer	M_n[b] $*10^3$	Mw/Mn[b]	DP[c]	Yield[d]
1	β-gluco-*O*-lys	Hexylamine	25	CH_3CN	**4a**	73	1.50	97	90%
2	β-gluco-*O*-lys	Hexylamine	25	Dioxane	**4a**	31	1.06	41	95%
3	β-gluco-*O*-lys	Hexylamine	35	Dioxane	**4b**	35	1.12	46	95%
4	α-manno-*O*-	Hexylamine	25	Dioxane	**5a**	52	1.09	69	95%

	lys								
5	α-manno-*O*-lys	Hexylamine	35	Dioxane	**5b**	67	1.10	89	95%
6	α-manno-*O*-lys	Hexylamine	25	DMF	**5a**	35	1.08	46	95%
7	α-manno-*O*-lys	Hexylamine	35	DMF	**5b**	38	1.12	51	95%
8	β-gluco-*O*-lys	N_3PEGNH_2	25	DMF	**4c**	34	1.11	45	90%
9	α-manno-*O*-lys	N_3PEGNH_2	25	DMF	**5c**	17	1.22	22	80%

Table 2.1: Synthesis of Glycopolypeptides at RT, [a]M/I indicates monomer to initiator ratio, [b]Molecular weight and polydispersity index was estimated from GPC, [c]Degree of polymerization (DP) from GPC, [d]Total isolated yield.

The FT-IR of this reaction mixture after 24 h showed complete disappearance of the NCA anhydride stretch indicating that the polymerization reaction proceeded to completion. However after 6 h, the reaction mixture which was homogeneous during the onset of the polymerization became heterogeneous and white powdery precipitate was observed.

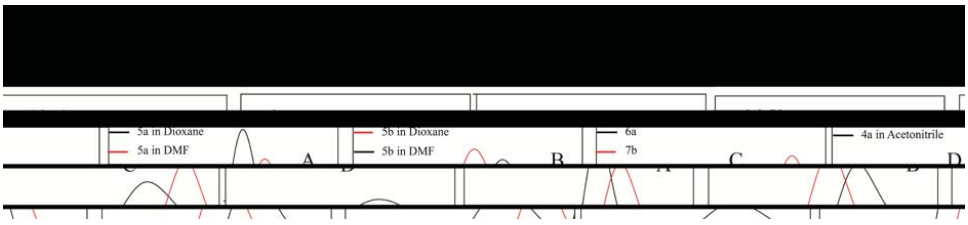

Figure 2.1: Size exclusion chromatogram of (A, B) homopolypeptides **5a** and **5b** synthesized in dioxane and DMF, (C) diblock copolypeptides **6a** and **7b** and (D) **4a** in acetonitrile (DMF/0.1M LiBr, 60 ºC, RI).

The number average molecular weight of the precipitated polymer **4a** was estimated to be 73,000 by GPC and a broad molecular weight distribution with a PDI of 1.5 was observed (Table 2.1, run 1). Control reactions in which **3a** was incubated with only 1,8-bis(dimethylamino)naphthalene (0.25 to 1 eq of **3a**) showed no change in the anhydride IR stretch even after 48 h thereby showing that the primary amine initiator was only responsible for initiation of the polymerization reaction. Since 1,8-

bis(dimethylamino)naphthalene did not initiate polymerization, we used this as an additive in all the subsequent polymerization reactions.

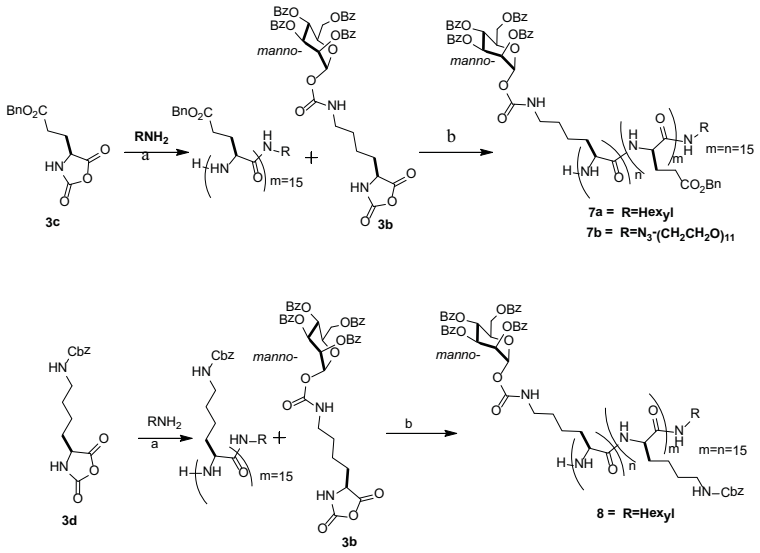

a) DMF, RT; b) DMF, 0.25eq. Proton Sponge, 30h, rt, 95%, c) 10% TFA in DCM, 30 min

Scheme 2.3: Schematic representation of synthesis of diblock copolypeptides.

Since a broad molecular weight distribution of **4a** was observed and the molecular weight obtained was much higher than expected, the polymerization of **3a** was attempted again in dry dioxane using hexylamine as the initiator (M/I = 25, 35) in the presence of 0.25 eq of 1,8-bis(dimethylamino)naphthalene "proton sponge" (Table 2.1, run 2 and 3). Both the polymerization reactions went to completion in 24 hrs as was observed by FT-IR. The resulting polymer **4a** and **4b** was purified by reprecipitation and the structure was identified by ^{1}H and ^{13}C NMR. The molecular weight distribution observed from GPC was monomodal and found to be reasonably narrow (Figure 2.1). The M_n was estimated to be 31,300 and 34,900 while the PDI was calculated to be 1.06 and 1.12 for **4a** and **4b** respectively. The higher molecular weight that is observed is due to incomplete initiation by hexylamine as has been observed before. We then attempted the polymerization of **3b** (α-manno-*O*-lys NCA) with hexyl amine as the initiator (M/I = 25, 35) in dioxane (Scheme 2.2; Table 2.1, run 4 and 5). The molecular weight distribution was again found to be reasonably narrow although

the molecular weights of the resulting polymer **5a** and **5b** was estimated to 52,000 and 67,400 respectively. The polymers were also thoroughly characterized by ^{1}H and ^{13}C NMR. To study the effect of polar solvent on the polymerization reaction, we carried out the same polymerization in dry DMF (Table 2.1, run 6 and 7). The resulting polymers formed in DMF had a molecular weight which was much closer to the expected molecular weights based on the M/I ratio. To prove that the initiator was incorporated into the polymer, we carried out the polymerization of **3a** and **3b** in DMF with azido-PEG-NH_2 (n=11) as the initiator. The resultant polymers **4c** and **5c** were purified by multiple reprecipitation and then characterized by NMR and FT-IR. The FT-IR of **4c** and **5c** show sharp peak at 2110 cm^{-1} that is characteristic for the organo azide stretch.

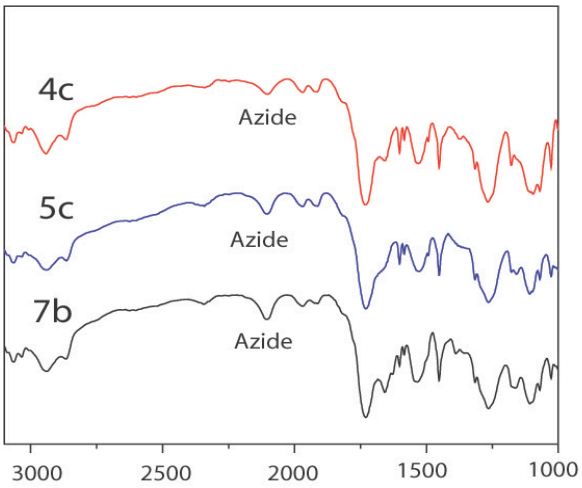

Figure 2.2: FT-IR of end-functionalized polymers **4c**, **5c**, and **7b**.

Usage of this bifunctional azido-PEG-amine initiator allows the synthesis of end functionalized polymer which can be further manipulated using Cu(I) catalyzed azide-alkyne "click chemistry".[27]

Diblock copolymers were prepared by combining **3a** and **3b** with conventional NCA's as shown in Scheme 2.3. For example, the polymerization of p-methoxybenzyl-*l*-glutamate (PMBn-Glu) NCA (**3e**) was first initiated with hexylamine as initiator (M/I=15) in DMF. After completion of the first stage polymerization (3h) as observed by FT-IR, the second monomer **3a** (M_1:M_2 = 15:25) and "proton sponge" was added to the reaction mixture

(Table 2.2, run 1). The polymerization proceeded to completion in high conversion to yield polymer **6a** in predictable monomer composition as observed by ^{1}H NMR. The ratio of PMBn-glu and β-gluco-*O*-lys was estimated to be 1:1.5 (expected 1:1.7) from

			Initiator			Product Polymer		
Run no	First Monomer (M_1)	Second Monomer (M_2)	$[M_1]:[M_2]/I$	Polymer	Expected M_n*10^3	Observed $Mn*10^{3\,b}$	M_w/M_n [b]	Yield[c]
1	PMBn-glu	β-gluco-*O*-lys	15:25	**6a**	22.895	36.0	1.15	90%
2	Bn-*l*-glu	α-manno-*O*-lys	15:15	**7a**	14.695	16.5	1.11	95%
3	Z-lys	α-manno-*O*-lys	15:15	**8**	15.295	16.4	1.14	95%
4[a]	Bn-*l*-glu	α-manno-*O*-lys	15:15	**7b**	15.165	19.0	1.07	95%

Table 2.2: Synthesis of diblock copolypeptides using hexylamine as initiator in DMF at rt, [a]For run 4, azide-PEG-NH_2 (n=11) was used as the initiator, [b]Molecular weight and polydispersity index was estimated from GPC, [c] Total isolated yield.

their characteristic signals in the ^{1}H NMR. The GPC showed narrow molecular weight distribution with a PDI of 1.15. The polymer **6a** was then treated with 10% TFA in dichloromethane at RT for 30 min to deprotect the p-methoxybenzyl group. The polymer **9** thus formed was then characterized by ^{1}H and ^{13}C NMR to confirm the complete deprotection of the *p*-methoxybenzyl group. Thus we were able to make an amphiphilic diblock co-polymer having a hydrophobic benzoate protected glucose and a hydrophilic carboxylic acid on the polypeptide backbone. Similarly, other diblock copolypeptides were synthesized with **3b** and conventional NCA's like γ-benzyl-*l*-glutamate NCA and Z-Lys NCA in high yield with narrow molecular weight distribution (Table 2.2). The presence of the initiator in the block copolymer was again confirmed by synthesizing a block co-polymer of **3b** and γ-benzyl-*l*-glutamate NCA with azido-PEG-NH_2 (n=11) as the initiator (Table 2.2, run 4). The presence of the 2100 cm^{-1} organo azide stretch in FT-IR for the resultant polymer indicated that the initiator was successfully incorporated into the polymer chain. The amount of azido-

PEG-NH_2 incorporated into this block copolymer was estimated by attaching fluorescein alkyne to the aizde functionalized polymer **7b** using Cu(I) catalyzed azide alkyne "click chemistry". The amount of aizde groups incorporated was estimated from UV-VIS spectroscopy to be around 0.75 mol/mol of polymer **7b**. Hence, we were also able to synthesized fluorescently labelled block co-polypeptides using this methodology.

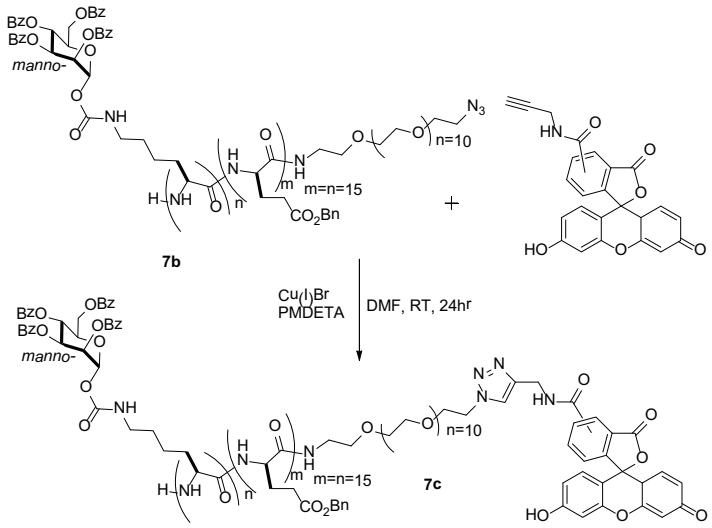

Scheme 2.4: Schematic representation of click reaction of Azido labeled block copolymer **7b** with fluorescein-alkyne.

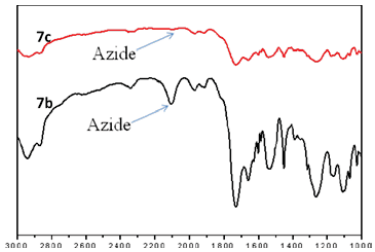

Figure 2.3: FT-IR spectra for azide functionalized polymer **7b** and the crude reaction mixture upon completion of the click reaction (**7c**).

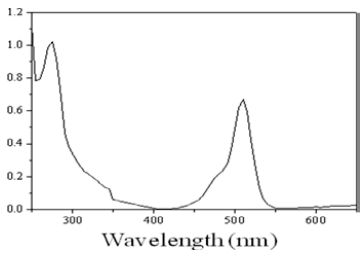

Figure 2.4: UV-VIS spectrum of the fluorescein labelled polymer **7c** solution (10 μM) in DMF/pH7, 100 mM phosphate buffer mixture.

*2.3.1 Method for estimation of azide incorporation into block copolypeptide (7**b**)*

The block copolypeptide **7b** was converted to **7c** using click chemistry. The theoretical concentration of the fluorescein labelled polymer **7c** was calculated using the M_n value of 19,000 kDa that was obtained from GPC. Since only one fluorescein moiety will be conjugated to the polymer if all the polymer chains have one azide group attached to its end, the concentration of fluorescein in solution would be equal to the concentration of the polymer. The concentration of fluorescein in solutions of **7c** was estimated from its absorption spectra (λ_{max}=510 nm, Є=90,000 $M^{-1}cm^{-1}$) in DMF/pH7 phosphate buffer mixtures.[28] The percentage of azide group incorporated was estimated from the ratio of the experimentally calculated concentration from absorption spectra of fluorescein to the theoretical concentration calculated from M_n values of **7b**.

2.4 Conclusion

We have reported a very easy three step synthesis of an *O*-glycosylated lysine-NCA using a stable glycosyl donor and a commercially available protected amino acid. The highlight of the synthesis is that the key glycosylation step and the subsequent deprotection reaction proceeds to completion in near quantitative yield. This ease of synthesis allows us to synthesize these monomers in very high yield and we believe would be useful to several groups interested in synthesis of glycopeptides. The glycosylated NCA's were then polymerized using commercially available simple

amine initiators to yield well defined high molecular weight homopolypeptides and diblock copolypeptides in very high yields. Addition of 1,8-Bis(dimethylamino)naphthalene ("proton sponge") was necessary for the successful completion of the polymerization reaction, although its exact role is not yet fully understood. We were also able to synthesize end-functionalized, amphiphilic and fluorescently labelled polymers using our methodology. As extension the saponification of the esters from the sugar residues of the synthesized glycopolypeptides to get completely water soluble glycopolypeptides and further lectin binding studies on the resulting water soluble glycopolypeptides will be discussed in the next chapter.

The spectral data of the selected compounds are available from **Appendix I**.

2.5 References

1) Hadjichristidis, N.; Iatrou, H.; Pitsikalis, M.; Sakellariou, G. *Chem. Rev.* **2009,** *109* (11), 5528-5578;
2) Deming, T. J. *J. Polym. Sc., Part A: Polym. Chem.* **2000,** *38* (17), 3011-3018.
3) Aoi, K.; Tsutsumiuchi, K.; Okada, M. *Macromolecules* **1994,** *27* (3), 875-877;
4) Aoi, K.; Itoh, K.; Okada, M. *Macromolecules* **1995,** *28* (15), 5391-5393;
5) Aoi, K.; Tsutsumiuchi, K.; Aoki, E.; Okada, M. *Macromolecules* **1996,** *29* (12), 4456-4458;
6) Tsutsumiuchi, K.; Aoi, K.; Okada, M. *Macromolecules* **1997,** *30* (14), 4013-4017.
7) Rüde, E.; Westphal, O.; Hurwitz, E.; Fuchs, S.; Sela, M. *Immunochemistry* **1966,** *3* (2), 137-151.
8) Gibson, M. I.; Hunt, G. J.; Cameron, N. R. *Org. & Biom. Chem.* **2007,** *5* (17), 2756-2757.
9) a) Kramer, J. R.; Deming, T. J. *J. Am. Chem. Soc.* **2010**, 132, 15068-15071. b) Kramer, J. R.; Deming, T. J. *J. Am. Chem. Soc.* **2012**, *134*, 4112−4115.
10) Wang, Y.; Kiick, K. L. *J. Am. Chem. Soc.* **2005,** *127* (47), 16392-16393.
11) Huang, J.; Habraken, G.; Audouin, F.; Heise, A. *Macromolecules* **2010,** *43* (14), 6050-6057.
12) Sun, J.; Schlaad, H. *Macromolecules* **2010,** *43* (10), 4445-4448.
13) Gamblin, D. P.; Scanlan, E. M.; Davis, B. G. *Chem. Rev.* **2008,** *109* (1), 131-163;
14) Albertin, L.; Cameron, N. R. *Macromolecules* **2007,** *40* (17), 6082-6093;
15) Chen, G.; Tao, L.; Mantovani, G.; Geng, J.; Nyström, D.; Haddleton, D. M. *Macromolecules* **2007,** *40* (21), 7513-7520;
16) Ladmiral, V.; Mantovani, G.; Clarkson, G. J.; Cauet, S.; Irwin, J. L.; Haddleton, D. M. *J. Am. Chem. Soc.* **2006,** *128* (14), 4823-4830;
17) Ladmiral, V.; Melia, E.; Haddleton, D. M. *Eur. Polym. J.* **2004,** *40* (3), 431-449;
18) Spain, S. G.; Gibson, M. I.; Cameron, N. R. *Journal of Polymer Science Part A: Polym. Chem.* **2007,** *45* (11), 2059-2072;
19) Ting, S. R. S.; Min, E. H.; Escalé, P.; Save, M.; Billon, L.; Stenzel, M. H. *Macromolecules* **2009,** *42* (24), 9422-9434.
20) Deming, T. J. *Soft Matter* **2005,** *1* (1), 28-35.

21) Hotha, S.; Kashyap, S. *J. Am. Chem. Soc.* **2006,** *128* (30), 9620-9621.

22) Sureshkumar, G.; Hotha, S. *Tet. Lett.* **2007,** *48* (37), 6564-6568.

23) a) Sureshkumar, G.; Hotha, S. *Chem. Comm.* **2008,** (36), 4282-4284. b) Asif Y. Shaikh's thesis.

24) Pati, D.; Shaikh, A. Y; Hotha, S.; Sen Gupta, S. *Polym. Chem*. *2011*, **2**, 805-811.

25) Shaikh, A. Y.; Sureshkumar, G.; Pati, D.; Sen Gupta, S.; Hotha, S. *Org.and Biomol. Chem.2011,* **9**, 5951-5959.

26) Fournier, D.; Hoogenboom, R.; Schubert, U. S. *Chem. Soc. Rev.* **2007,** *36* (8), 1369-1380.

27) Punna, S.; Kaltgrad, E.; Finn, M.G. *Bioconjugate Chem*. **2005**, *16*, 1536.

28) Choi, M.F.; Hawkins, P. *Spect*. *Lett*. **1994**, *27*, 1049-1063.

Chapter 3

Controlled Synthesis of *O*-Glycopolypeptide Polymers and their Molecular Recognition by Lectins

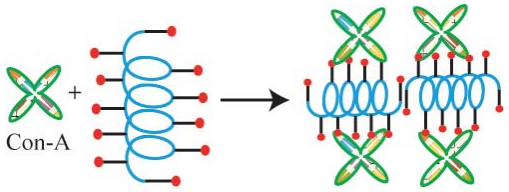

Glycopolypeptides Con-A cluster

ABSTRACT. The facile synthesis of high molecular weight water soluble *O*-glycopolypeptide polymers by the ring opening polymerization of their corresponding *N*-carboxyanhydride (NCA) in very high yield (over all yield >70%) is reported. The *per*-acetylated-*O*-glycosylated lysine-NCA monomers, synthesized using stable glycosyl donors and a commercially available protected amino acid in very high yield, was polymerized using commercially available amine initiators. The synthesized water soluble glycopolypeptides were found to be α-helical in aqueous solution. However, we were able to control the secondary conformation of the glycopolypeptides (α-helix versus non-helical structures) by polymerizing racemic amino acid glyco NCA's. We have also investigated the binding of the glycopolypeptide poly(α-manno-*O*-lys) with the lectin *Con-A* using precipitation and hemagglutination assays as well as by isothermal titration calorimetry (ITC). The ITC results clearly show that the binding process is enthalpy driven for both α-helical and non-helical structures, with negative entropic contribution. Binding stoichiometry for the glycopolypeptide poly(α-manno-*O*-lys) having a non-helical structure was slightly higher as compared to the corresponding polypeptide which adopted an α-helical structure.

This chapter has been adapted from the corresponding paper;

"Controlled Synthesis of *O*-Glycopolypeptide Polymers and their Molecular Recognition by Lectins" **Debasis Pati**, Asif Y. Shaikh, Soumen Das, Pavan Kumar Nareddy, Musty J. Swamy, Srinivas Hotha and Sayam Sen Gupta *Biomacromolecules* **2012**, *13*, 1287-1295.

3.1 Introductions

Glycopolymers, synthetic polymers featuring pendant carbohydrate moieties, have been of particular interest to the field of tissue engineering and drug delivery.[1-12] This interest is derived from the complex roles that carbohydrates play in vivo, particularly in biomolecular recognition events such as extracellular recognition, adhesion, cell growth regulation, cancer cell metastasis, and inflammation.[13-14] The key to the recognition process is their interactions with carbohydrate-binding protein receptors known as lectins.[15-16] The interaction between lectins and carbohydrates is weak; dissociation constants, K_d, are typically 10^{-3}–10^{-6} M, but may be greatly enhanced through polyvalency. Since glycopolymers are typically polyvalent as they have several pendant carbohydrate groups; they present a platform for which multiple copies of a carbohydrate can be presented simultaneously, thus enhancing their affinity and selectivity for lectins many folds. Carbohydrate recognising receptors are found on many cell surfaces. An excellent example is the asialoglycoprotein receptor (ASGP-R) displayed on the hepatocyte cell surface that interacts uniquely with galactose/N-acetyl-β-galactosamine containing carbohydrate ligands.[17-20] Galactose containing synthetic linear glycopolymers can therefore be used to guide hepatocyte adhesion through this unique ASGP-R–carbohydrate interaction. This strategy has been used to design extra cellular matrices using galactose containing synthetic polymers for liver tissue engineering.[21] Similarly, the use of glycopolymers as vehicles for therapeutics has also shown a lot of promise.[8-12]

However, a majority of these synthetic glycopolymers are acrylate/acrylamide based and controlled radical polymerization is used to synthesize polymers with controlled molecular weight, glycosylation density, and position attributes that are necessary for biological recognition processes. However, the lack of biocompatibility of some of these polymers can render it difficult for application in medicine such as drug delivery or tissue engineering. On the other hand glycopolypeptides (glycopolymers with pendant carbohydrates on a polypeptide backbone) not only mimic the molecular composition of proteoglycans but also has the ability to fold into well-defined secondary structures (e.g., helix).[22-23] Therefore it is desirable to develop methodologies that afford easy and well defined synthetic glycopolypeptides. Although well defined polypeptides based on natural and unnatural amino acids have

been very successfully synthesized by the ring opening polymerization of their corresponding *N*-carboxyanhydrides (NCA),[24-29] the synthesis of glycopolypeptide still remains a major challenge.[30-31] Synthesis of glycopolypeptides by post polymerization modification of synthetic polypeptides on the contrary has been more successful and several methods have been reported recently.[32-36]

We have recently reported the synthesis of the *per*-*O*-benzoylated-D-glyco-*l*-lysine carbamate NCA from a stable glycosyl donor and a commercially available protected amino acid in very high yield (overall yield >70%).[37] These monomers underwent ring opening polymerization using simple primary amine initiators to form well defined, high molecular weight homo glycopolypeptides and diblock co-glycopolypeptides. However attempts to synthesize the fully deprotected water soluble glycopolypeptide from these polypeptides failed (Chapter II) as we were unable to efficiently deprotect the bulky benzoate groups. We hereby report a very efficient synthesis fully water soluble glycopolypeptides that were synthesized from the ring opening polymerization of *per*-*O*-acetylated-D-glyco-*l*-lysine carbamate NCA monomers. Although these glycopolypeptides are predominantly α-helical in solution, we demonstrate that our synthetic methodology allows us to alter their secondary structures from α-helical to non-helical structure. We have also investigated the binding of these glycopolypeptides with the lectin *Con-A* with the objective of understanding the role of the secondary structure of these polypeptides on *Con-A* binding.

3.2 Experimental Section

3.2.1 Materials and methods

Propargyl-1, 2 orthoesters of the corresponding carbohydrates were prepared according to literature procedure.[38-40] CbzLys(Boc)OBn was synthesized using standard literature procedure.[41] $HAuCl_4$, triphosgene and azido-PEG-amine (n=11) were obtained from Aldrich and Polypure Inc. All other chemicals used were obtained from Merck, India. Diethyl ether, petroleum ether (60^o-80^oC), ethylacetate, dichloromethane, tetrahydrofuran, dioxane were brought from Merck and dried by conventional methods and stored in the glove box. FT-IR spectra were recorded on Perkin Elmer FT-IR spectrum GX instrument by making KBr pellets. Pellets were

prepared by mixing 3mg of sample with 97mg of KBr. ^{1}H NMR spectra were recorded on Bruker Spectrometers (200 MHz, 400 MHz or 500 MHz). ^{13}C NMR and DEPT spectra were recorded on Bruker Spectrometer (50 MHz, 100MHz or 125MHz) and reported relative signals according to deuterated solvent used. HRMS data was recorded on MALDI-TOF using 2,5-dihydroxybenzoic acid as solid matrix. Size-exclusion chromatography of the glycopolypeptides was performed using an instrument equipped with Waters 590 pump with a Spectra System RI-150 RI detector. Separations were effected by 10^5, 10^3 and 500 Å Phenomenex 5µ columns using 0.1M LiBr in DMF eluent at 60 °C at the samples concentrations of 5mg/ml. A constant flow rate of 1 mL/min was maintained, and the instrument was calibrated using polystyrene standards.

3.2.2 Solvent drying

Ethyl acetate and dichloromethane was dried with P_2O_5 and CaH_2 and stored on activated molecular sieves 4A^o after distillation. Tetrahydrofuran was passed through activated alumina and then dried with sodium wire under reflux and the freshly distilled solvent was used subsequently. Dioxane was first distilled from CaH_2 and then dried with sodium wire under reflux and freshly distilled solvent was transferred into the glove box for subsequent uses. n-Hexane was dried with sodium wire under reflux for several hours and subsequently distilled and stored on activated molecular sieves 4Aº. All other solvent drying procedures were followed using protocols described in Purification of Laboratory Chemicals, Fourth Edition by Perrin D.D. and Armarego W.L.F.

*3.2.3 General procedure for the Synthesis of amino acid glycosyl carbamates (**2a**, **2b**, 2b'and **2c**)*

To a solution of propargyl 1,2-orthoester (0.1 mmol), CbzL\DLys(Boc)OBn and activated 4Å molecular sieves powder (50 mg) in anhydrous CH_2Cl_2 (5 mL) was added $HAuCl_4$ (10 mol%) under argon atmosphere at room temperature. The reaction mixture was stirred at room temperature for the specified time and the reaction mixture was filtered and the filtrate was concentrated in vacuo. The resulting residue was purified by silica gel column chromatography using ethyl acetate-petroleum ether as the mobile phase to afford the compounds **2a**, **2b, 2b'** and **2c**.

Compound **2a**: $[\alpha]_D^{25}$ = +4.4(*c*1.0, $CHCl_3$); ^{1}H NMR (200.13MHz, $CDCl_3$): δ 1.15-1.91(m, 6H), 1.98, 2.03, 2.04, 2.12(4s, 12H), 3.12(td, 2H, *J* = 2.1, 6.5, 13.5Hz), 3.98(t, 1H, *J* = 6.5 Hz), 4.06(dd, 1H, *J* = 7.7, 11.4Hz), 4.11(d, 1H, *J* = 1.0 Hz), 4.15(d, 1H, *J* = 3.1 Hz), 4.39(m, 1H), 5.11(s, 2H), 5.05(dd, 1H, *J* = 3.5, 10.4 Hz), 5.17(d, 1H, *J* = 3.8 Hz), 5.29(dd, 1H, *J* = 8.1, 10.4 Hz), 5.39(d, 2H, *J* = 3.4 Hz), 5.62(d, 1H, *J* = 8.2 Hz), 7.32-7.38(m, 10H); ^{13}C NMR (50.32MHz, $CDCl_3$): δ 20.4(3C), 20.5, 22.0, 28.7, 31.8, 40.4, 53.5, 60.8, 66.7, 66.8, 66.9, 67.7, 70.6, 71.1, 93.0, 127.9-128.5, 135.1, 136.1, 153.7, 155.9, 169.4, 169.7, 170.0, 170.2, 172.0; MALDI-TOF(m/z): Calcd for $C_{36}H_{44}KN_2O_{15}$: 783.2379, Found: 783.2333.

Compound **2b**: $[\alpha]_D^{25}$ = +22.1(*c*1.0, $CHCl_3$); ^{1}H NMR (200.13MHz, $CDCl_3$): δ 1.10-1.92(m, 6H), 1.99, 2.02, 2.08, 2.17(4s, 12H), 3.13(q, 2H, *J* = 6.1, 12.3Hz), 3.98-4.16(m, 2H), 4.30(dd, 1H, *J* = 4.7, 12.5Hz), 4.41(m, 1H), 4.98(t, 1H, *J* = 5.7 Hz), 5.10(d, 2H, *J* = 1.5 Hz), 5.17(d, 2H, *J* = 3.4 Hz), 5.23-5.43(m, 4H)6.01(d, 1H, *J* = 1.4 Hz), 7.32-7.38(m, 10H); ^{13}C NMR (50.32MHz, $CDCl_3$): δ 20.5(3C), 20.6, 22.2, 28.8, 32.0, 40.6, 53.5, 61.9, 65.4, 66.8, 67.0, 68.4, 68.8, 70.0, 91.1, 127.9-128.5, 135.1, 136.1, 153.0, 155.9, 169.4, 169.6, 170.0, 170.1, 172.1; MALDI-TOF(m/z): Calcd for $C_{36}H_{44}KN_2O_{15}$: 783.2379, Found: 783.2373.

Compound **2b'**: $[\alpha]_D^{25}$ = +30.7(*c*1.0, $CHCl_3$); ^{1}H NMR (400.13MHz, $CDCl_3$): δ 1.16-1.92(m, 6H), 1.92, 1.94, 2.08, 2.09(4s, 12H), 3.13(m, 2H), 3.94-4.00(m, 1H), 4.03(dd, 1H, *J* = 2.4, 12.3 Hz), 4.21(dd, 1H, *J* = 4.5, 12.3Hz), 4.33(m, 2H), 4.99(t, 1H, *J* = 5.7 Hz), 5.04(d, 2H, *J* = 3.3 Hz), 5.10(dd, 1H, *J* = 12.3, 23.8Hz), 5.18-5.35(m, 3H), 5.43 (d, 1H, *J* = 8.1 Hz), 6.01(d, 1H, *J* = 1.8 Hz), 7.32-7.38(m, 10H); ^{13}C NMR (100.63MHz, $CDCl_3$): δ 20.5(2C), 20.6, 20.7, 22.2, 28.9, 32.1, 40.7, 53.6, 62.0, 65.5, 66.9, 67.1, 68.4, 68.8, 70.0, 91.2, 128.0-128.5, 135.2, 136.1, 153.0, 155.9, 169.4, 169.7, 170.0, 170.6, 172.1; MALDI-TOF(m/z): Calcd for $C_{36}H_{44}KN_2O_{15}$: 783.2379, Found: 783.2376.

Compound **2c**: $[\alpha]_D^{25}$ = -7.7(*c*1.0, $CHCl_3$); ^{1}H NMR (200.13MHz, $CDCl_3$): δ 1.30-1.89(m, 6H), 1.95, 2.00, 2.03, 2.03, 2.05, 2.08, 2.14(7s, 21H), 3.09(q, 2H, *J* = 5.7, 12.4 Hz), 3.64-3.93(m, 3H), 4.02-4.19(m, 4H), 4.31-4.44(m, 2H), 4.47(s, 1H), 4.93(dd, 2H, *J* = 3.3, 10.3 Hz), 5.07(dd, 1H, *J* = 3.7, 10.3 Hz), 5.09(s, 2H), 5.12-5.28(m, 3H), 5.34(d, 1H, *J* = 3.3 Hz), 5.41(d, 1H, *J* = 8.3 Hz), 5.59(d, 1H, *J* = 8.3 Hz), 7.32-7.39(m,

10H); ^{13}C NMR (50.32MHz, $CDCl_3$): δ 20.4, 20.5(4C), 20.7(2C), 22.1, 28.8, 32.0, 40.4, 53.4, 60.7, 61.7, 66.5, 66.9, 67.1, 68.9, 70.4, 70.6, 70.9, 72.5, 73.1, 75.6, 92.5, 100.8, 127.9-128.6, 135.1, 136.1, 153.6, 155.9, 169.0, 169.5, 169.8, 170.0, 170.1, 170.3(2C), 172.1; MALDI-TOF(m/z): Calcd for $C_{48}H_{60}KN_2O_{23}$: 1071.3224, Found: 1071.3218.

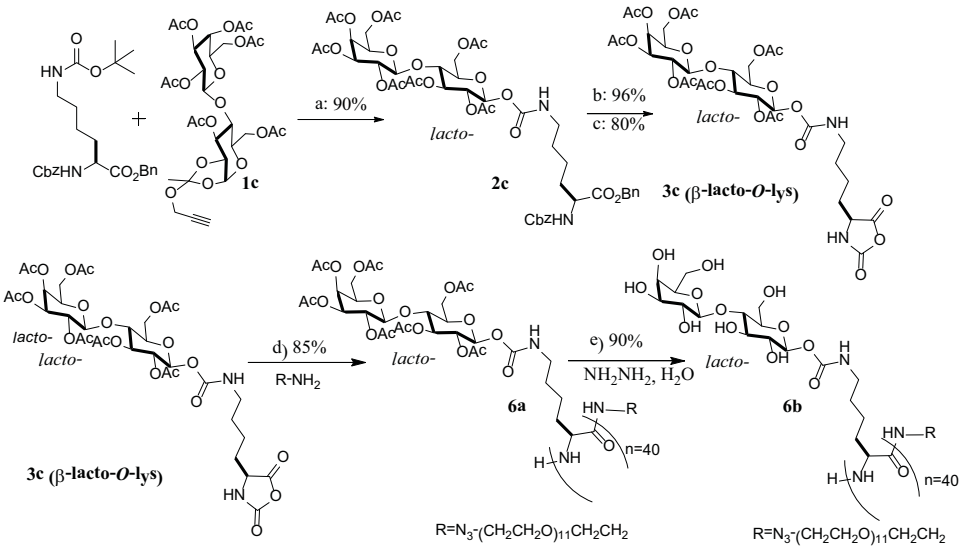

a) $HAuCl_4$, CH_2Cl_2, rt, 0.5h, 4Å MS Powder, Yield (80-95%); b) Pd/C, H_2, 400psi, CH_3OH, 12h, Yield (> 95%); c) Triphosgene, THF, α-pinene, 70°C, Yield (85%), d) Dioxane, Proton Sponge(1.0 equiv), 24 hrs, RT, e) Methanol, Hydrazine hydrate (25 equiv), 6 hrs.

Scheme 3.1: Schematic representation of general Synthesis of Glycopolypeptides by the ring-opening polymerization of their glycosylated amino acid NCA's.

3.2.4 General procedure for the synthesis of glyco N-carboxyanhydrides (glyco-NCA)

Hydrogenolysis of compounds **2a**, **2b, 2b'** and **2c** was carried out using 10% Pd/C in MeOH/EtOAc (9:1) at 400 psi for 12 h. After completion of the reaction, the reaction mixture was filtered and concentrated under reduced pressure to afford *per-O*-acetylated-D-Galactose-*l*-lysine carbamate, *per-O*-acetylated-D-Mannose-*d/l*-lysine carbamate and *per-O*-acetylated-D-Lactose-*l*-lysine carbamate in almost quantitative yield. The resulting compounds were directly used for NCA synthesis without any further purification.

3a, 3b** and **3b': To a solution of *per*-*O*-acetylated-D-Galactose-*l*-lysine carbamate or *per*-*O*-acetylated-D-Mannose-*l/d*-lysine carbamate (500 mg, 0.96 mmol) in freshly distilled out tetrahydrofuran (10 ml) was added accordingly a solution of triphosgene (142 mg, 0.480 mmol) in anhydrous tetrahydrofuran (2ml) under argon and the reaction mixture was heated to 50°-55°C. α-pienene (0.228 ml, 1.44 mmol) was then added and the reaction mixture was allowed to stir for an additional 1 hr. The reaction mixture was then cooled to room temperature and then poured into dry hexane (300 ml) to afford a white precipitate; which was filtered off quickly and crystallized two more times using a mixture of ethyl acetate and petroleum ether. Finally, the white precipitate of glyco *N*-carboxyanhydride **3a**, **3b** and **3b'** obtained was dried under vacuum and transferred into the glove box. Final yield: 425 mg, 80%.

3c: To a solution *per*-*O*-acetylated-D-Lactose-*l*-lysine carbamate (500 mg, 0.618 mmol) in freshly distilled out tetrahydrofuran (10 ml) was added a solution of triphosgene (91.70 mg, 0.309 mmol) in anhydrous tetrahydrofuran (2ml) under argon and the reaction mixture was heated to 50°-55°C. α-pienene (0.147ml, 0.927 mmol) was then added and the reaction mixture was allowed to stir for an additional 1 hrs. The reaction mixture was then cooled to room temperature and then poured into dry hexane (300 ml) to afford a white precipitate; which was filtered off quickly and crystallized two more times using a mixture of ethyl acetate and petroleum ether. Finally, the white precipitate of glyco *N*-carboxyanhydride (**3c**) was dried under vacuum and transferred into the glove box. Final yield: 410 mg, 80%.

Compound **3a**: ^{1}H NMR (400.13MHz, $CDCl_3$): δ 1.35-1.82(m, 6H), 1.98, 2.03, 2.04, 2.14(4s, 12H), 3.12(td, 2H, *J* = 2.1, 6.5, 13.7 Hz), 4.04-4.20(m, 3H), 4.33(bs, 1H), 5.09(dd, 1H, *J* = 3.3, 10.5 Hz), 4.25(dd, 1H, *J* = 8.5, 10.3 Hz), 5.30(m, 1H), 5.42(d, 1H, *J* = 3.1 Hz), 5.62(d, 1H, *J* = 8.3 Hz), 7.14(bs, 1H); ^{13}C NMR (100.61MHz, $CDCl_3$): δ 20.5, 20.6(2C), 20.7, 21.6, 28.8, 31.0, 40.3, 57.4, 60.9, 66.8, 68.0, 70.7, 71.4, 93.3, 152.4, 154.1, 169.8, 170.0(2C), 170.1, 170.5, FT-IR(Dioxane) 1785 and 1858 cm^{-1} νco (unsymmetrical stretching).

Compound **3b**: ^{1}H NMR (500.13MHz, CD_2Cl_2): δ 1.35-1.88(m, 6H), 1.99, 2.03, 2.07, 2.16(4s, 12Hz), 3.23(q, 2H, *J* = 6.7, 12.6 Hz), 3.68(t, 1H, *J* = 6.5 Hz), 4.08(m, 1H), 4.13(dd, 1H, *J* = 2.8, 12.2 Hz), 4.23(dd, 1H, *J* = 4.6, 12.2 Hz), 4.35(dd, 1H, *J* = 4.7, 6.9 Hz), 5.20-5.35(m, 3H), 5.94(d, 1H, *J* = 1.7 Hz), 6.72(bs, 1H); ^{13}C NMR (125.76MHz,

CD_2Cl_2): δ 20.8(2C), 20.9(2C), 22.2, 29.3, 31.6, 40.7, 57.9, 62.7, 66.1, 68.9, 69.3, 70.5, 91.7, 152.3, 153.8, 170.0, 170.3, 170.4, 170.6, 171.2, FT-IR(Dioxane) 1785 and 1858 cm^{-1} $^{\nu}$co (unsymmetrical stretching).

Compound **3b'**: ^{1}H NMR (400.13MHz, CD_2Cl_2): δ 1.35-1.88(m, 6H), 1.99, 2.03, 2.07, 2.16(4s, 12Hz), 3.23(q, 2H, *J* = 6.7, 12.6 Hz), 3.68(t, 1H, *J* = 6.5 Hz), 4.08(m, 1H), 4.13(m 1H), 4.23(dd, 1H, *J* = 4.6, 12.2 Hz), 4.35(dd, 1H, *J* = 4.7, 6.9 Hz), 5.20-5.35(m, 3H), 5.96(m, 1H), 7.2(bs, 1H); ^{13}C NMR (100.61MHz, CD_2Cl_2): δ 20.8(2C), 20.9(2C), 22.2, 29.3, 31.6, 40.7, 57.9, 62.7, 66.1, 68.9, 69.3, 70.5, 91.7, 152.3, 153.8, 170.0, 170.3, 170.4, 170.6, 171.2, FT-IR(Dioxane) 1785 and 1858 cm^{-1} $^{\nu}$co (unsymmetrical stretching).

Compound **3c**: ^{1}H NMR (500.13MHz, CD_2Cl_2): δ 1.15-1.88(m, 6H), 1.94, 2.01, 2.03, 2.04, 2.05, 2.10, 2.12(7s, 21H), 3.18(m, 2H), 3.75(d, 1H, *J* = 7.9 Hz), 3.86(t, 1H, *J* = 9.1 Hz), 3.91(t, 1H, *J* = 5.9 Hz), 4.05-4.17(m, 3H), 4.32(t, 1H, *J* = 5.5 Hz), 4.50(d, 1H, *J* = 8.0 Hz), 4.56(d, 1H, *J* = 12.0 Hz), 4.97(m, 2H), 5.05(m, 1H), 5.14(t, 1H, *J* = 7.4 Hz), 5.22(t, 1H, *J* = 9.0 Hz), 5.35(d, 1H, *J* = 2.7 Hz), 5.60 (d, 1H, *J* = 8.2 Hz), 6.65(s, 1H); ^{13}C NMR (125.76MHz, CD_2Cl_2): δ 20.7(2C), 20.8(3C), 20.9, 21.0, 22.0, 29.3, 31.5, 40.5, 57.9, 61.3, 61.7, 67.1, 69.2, 70.7, 71.2, 71.2, 72.6, 73.7, 75.8, 93.1, 101.2, 152.2, 154.3, 169.4, 170.0, 170.1, 170.3, 170.4, 170.4, 170.6, 170.8, FT-IR(Dioxane) 1785 and 1858 cm^{-1} $^{\nu}$co (unsymmetrical stretching).

3.2.5 General procedure for the synthesis of glycopolypeptides

To a solution of glyco-*L/D*-lysine NCA (100 mg/ml) in dry dioxane was added with "proton sponge" *N*,*N*'-tetramethylnapthalene (1.0 equivalent to monomer; 1 M) as an additive and azido-PEG-amine (0.5 M) as the initiator inside the glove box. The progress of the polymerization were monitored by FT-IR spectroscopy by comparing with the intensity of the initial NCA's anhydride stretching at 1785 cm^{-1} and 1858 cm^{-1}. The reactions generally completed within 36 h. Aliquotes were removed after completion of polymerization for GPC analysis. Finally the solvent was removed under reduced pressure from the reaction mixture. The resulting residue was redissolved in dichloromethane and then the polymer precipitated out by addition of methanol. The precipitated polymer was collected by centrifugation and dried to afford white glycopolypeptides **4a**, **4c**, **5a**, **5c** and **6a** in almost 85-90% yield. For synthesis of polymers **5e** and **5g**, **3b** (α-manno-*O-l*-lys NCA) and **3b'** (α-

manno-*O*-*d*-lys NCA) were mixed in equal proportions (by weight) and then polymerization was carried out as has been described above.[42-44]

Polymer No	Polymer Name	Structure of Polymer	Polymer No	Polymer Name
4a	30-β-galac-*O*-*l*-lys, P=Ac	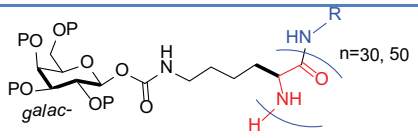	**4b**	30-β-galac-*O*-*l*-lys(OH), P=H
4c	50-β-galac-*O*-*l*-lys, P=Ac		**4d**	50-β-galac-*O*-*l*-lys(OH), P=H
5a	30-α-manno-*O*-*l*-lys, P=Ac	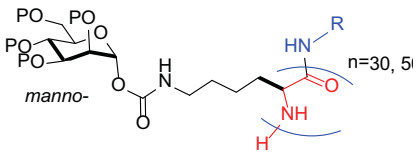	**5b**	30-α-manno-*O*-*l*-lys(OH), P=H
5c	50-α-manno-*O*-*l*-lys, P=Ac		**5d**	50-α-manno-*O*-*l*-lys(OH), P=H
5e	Rac-30-α-manno-*O*-*l*/*d*-lys, P=Ac	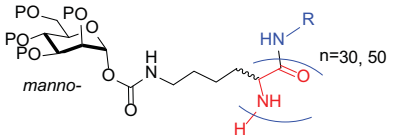	**5f**	Rac-30-α-manno-*O*-*l*/*d*-lys(OH), P=H
5g	Rac-50-α-manno-*O*-*l*/*d*-lys, P=Ac		**5h**	Rac-50-α-manno-*O*-*l*/*d*-lys(OH), P=H
6a	30-β-lacto-*O*-*l*-lys, P=Ac	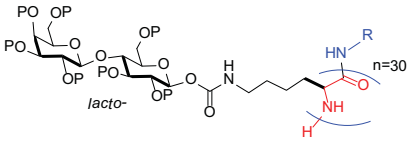	**6b**	30-β-lacto-*O*-*l*-lys(OH), P=H

Table 3.1: Different glycopolypeptides synthesized by our methodology.

Polymer **4a**. ^{1}H NMR (400.13 MHz, $CDCl_3$): δ 1.30-1.97(m, 6H), 1.98-2.14(4s, 12H), 3.07-3.30(m, 2H), 3.62-3.68(m, for CH_2CH_2O unit in initiator), 3.55-3.90 (m, 1H), 4.04-4.40(m, 3H), 5.00-5.55(m, 3H), 5.50-5.76(m, 1H), 5.56-5.95 (amide H's).

Polymer **4c**. ^{1}H NMR (400.13 MHz, $CDCl_3$): δ 1.30-1.97(m, 6H), 1.98-2.14(4s, 12H), 3.07-3.30(m, 2H), 3.62-3.68(m, for CH_2CH_2O unit in initiator), 3.55-3.90 (m, 1H), 4.04-4.40(m, 3H), 5.00-5.55(m, 3H), 5.50-5.76(m, 1H), 5.56-5.95 (amide H's).

Polymer **5a**: ^{1}H NMR (400.13 MHz, $CDCl_3$): δ 1.20-1.98(m, 6H), 1.99-2.16(4s, 12Hz), 3.10-3.40(m, 2H), 3.62-3.68(m, for CH_2CH_2O unit in initiator), 4.0-4.32(m, 4H), 5.10-5.60(m, 3H), 5.80-5.98(m, 1H).

Polymer **5c**: ^{1}H NMR (400.13 MHz, $CDCl_3$): δ 1.20-1.98(m, 6H), 1.99-2.16(4s, 12Hz), 3.10-3.40(m, 2H), 3.62-3.68(m, for CH_2CH_2O unit in initiator), 4.0-4.32(m, 4H), 5.10-5.60(m, 3H), 5.80-5.98(m, 1H).

Polymer **5e**: ^{1}H NMR (400.13 MHz, $CDCl_3$): δ 1.20-1.98(m, 6H), 1.99-2.16(4s, 12Hz), 3.10-3.40(m, 2H), 3.62-3.68(m, for CH_2CH_2O unit in initiator), 4.0-4.32(m, 4H), 5.10-5.60(m, 3H), 5.80-5.98(m, 1H).

Polymer **5g**: ^{1}H NMR (400.13 MHz, $CDCl_3$): δ 1.20-1.98(m, 6H), 1.99-2.16(4s, 12Hz), 3.10-3.40(m, 2H), 3.62-3.68(m, for CH_2CH_2O unit in initiator), 4.0-4.32(m, 4H), 5.10-5.60(m, 3H), 5.80-5.98(m, 1H).

Polymer **6a**: ^{1}H NMR (400.13 MHz, $CDCl_3$): δ 1.15-1.92(m, 6H), 1.94-2.12(br, m, 21Hz), 3.10-3.18(m, 2H), 3.62-3.68(m, for CH_2CH_2O unit in initiator), 3.70-3.90(m, 2H), 4.0-4.20(m, 4H), 4.40-4.58(m, 3H), 4.90-5.09(m, 3H), 5.15-5.35(m, 3H), 5.50-5.60 (m, 1H).

3.2.6 Deprotection procedure for the glycopolypeptides

Hydrazine monohydrate (25 equiv) was added to the solutions of all the acetyl protected glycopolypeptides in methanol (10 mg/mL) and the reactions were stirred for 7-8 h at room temperature. Reactions were quenched by addition of acetone and then solvent was removed almost completely under reduced pressure. The solid residues were dissolved in deionised water and transferred to dialysis tubing (3.5 and 12 KDa molecular weight cut off according to polymer molecular weight). The samples were dialyzed against deionized water for 3 days, with water changes once every two hours for the first day, and then thrice per day. Dialyzed polymers were lyophilized to yield glycopolypeptides (4b, 4d, 5b, 5d, 5f, 5h and 6b) as white fluffy solids (around 90% yield).

Polymer **4b**: ^{1}H NMR (400.13 MHz, D_2O): δ 1.10-2.01(m, 6H), 3.12(m, 2H), 3.65-3.70(m, for CH_2CH_2O unit in initiator), 3.58-3.82 (m, 7H), 3.85-3.95(m, 1H), 3.98-4.32(m, 1H), 5.20-5.45(m, 1H).

Polymer **4d**: ^{1}H NMR (400.13 MHz, D_2O): δ 1.10-2.01(m, 6H), 3.12(m, 2H), 3.65-3.70(m, for CH_2CH_2O unit in initiator), 3.58-3.82 (m, 7H), 3.85-3.95(m, 1H), 3.98-4.32(m, 1H), 5.20-5.45(m, 1H).

Polymer **5b**: ^{1}H NMR (400.13 MHz, D_2O): δ 1.08-2.01(m, 6H), 3.10-3.322 (m, 2H), 3.65-3.70(m, for CH_2CH_2O unit in initiator), 3.70-3.93 (m, 7H), 3.85-3.95(m, 1H), 3.98-4.32(m, 1H), 5.70-5.89(m, 1H).

Polymer **5d**: ^{1}H NMR (400.13 MHz, D_2O): δ 1.08-2.01(m, 6H), 3.10-3.322 (m, 2H), 3.65-3.70(m, for CH_2CH_2O unit in initiator), 3.70-3.93 (m, 7H), 3.85-3.95(m, 1H), 3.98-4.32(m, 1H), 5.70-5.89(m, 1H).

Polymer **5h**: ^{1}H NMR (400.13 MHz, D_2O): δ 1.08-2.01(m, 6H), 3.10-3.322 (m, 2H), 3.65-3.70(m, for CH_2CH_2O unit in initiator), 3.70-3.93 (m, 7H), 3.85s-3.95(m, 1H), 3.98-4.32(m, 1H), 5.70-5.89(m, 1H).

Polymer **6b**: ^{1}H NMR (400.13 MHz, D_2O): δ 1.15-1.88(m, 6H), 3.10-3.18(m, 2H), 3.46-3.54(m, 2H), 3.65-3.70(m, for CH_2CH_2O unit in initiator), 3.55-4.0(m, 11H), 4.35-4.47(m, 1H), 5.35-5.48(m, 1H).

3.2.7 Circular Dichroism Measurements

Aqueous solution of glycopeptides **4b**, **4d**, **5b**, **5d, 5f, 5h** and **6b** were filtered through 0.22 μm syringe filters. CD (190-250 nm) spectra of the glycopolypeptides (0.50 mg/mL in deionized water) were recorded (JASCO CD SPECTROPOLARIMETER, Model Name J-815) in a cuvette with 1 mm path length. All the spectra were recorded for an average of 3 scans and the spectra were reported as a function of molar ellipticity [θ] v_s wavelength. The molar ellipticity was calculated using the standard formula, $[\theta]=(\theta \times 100 \times M_w)/(C \times l)$, where θ = experimental ellipticity in millidegrees, M_w = average molecular weight, C = concentration in mg/mL and l = path length in cm. The % α helicity was calculated by using the formula % α helicity = $(-[\theta]_{222\,nm} + 3000)/ 39000$[45].

3.2.8 Lectin Interactions

3.2.8.1 Turbiditymetry Assay

ConA (0.4 mg/mL) interactions with glycopolypeptides (5b and 5d) were studied in the buffer solution (pH=7.4) containing 0.01M KH_2PO_4, 1 mM $MnCl_2$, 1mM $CaCl_2$

and 1mM NaCl. The turbidity was measured by using UV-Visible spectrometer (Perkin–Elmer Carry 300 Spectrometer) at a wavelength of 360 nm.

3.2.8.2 Quantitative Precipitation Assay

Quantitative precipitations and analysis were carried out by a method modified of Brewer, as adapted by Cloninger and coworkers, was employed, using a *Con-A* solution of 30 μM. A known concentration of lectin was added to the different concentrations of ligand and the precipitation was centrifuged and collected by two more times washing with Tris buffer. *Con-A* and ligand were prepared in precipitation buffer (Tris-HCl pH 7.5, 90 mM NaCl, 1 μM CaCl2, 1μM MnCl2), vortexed briefly to mix for 1 min and then incubated for 5 h at 22^{o}C. The final concentration of *Con-A* was 35μM (assuming *Con-A* as tetramer, Mw= 104000 Da). White precipitates were pelted by centrifugation at 5000 g for 2 min. Supernatants were removed by pipet and pellets were gently washed twice with cold buffer. Pellets were then resuspended in 450 μL 100 mM α-methyl mannopyranoside, and a clear solution was observed after 10-15 min at room temperature. Protein content was determined by measuring the absorbance at 280 nm. The solutions were analyzed for protein content using $A_{280}^{1\%}$ = 13.7 for lectin solutions.

3.2.8.3 Hemagglutination Assay

Rabbit erythrocytes (10%) resuspended in PBS pH 7.4 was purchased from Lampire, Inc. PBS buffer (35 μL) containing Ca^{+2} and Mn^{+2} (0.1mM each) was added to all wells except those of the first column of a standard 96-well polycarbonate microtiter plate. Samples (35 μL) at the highest concentrations were then added to the first and second columns of every lane. The mixtures in column 2 were then taken through serial 2-fold dilutions by mixing and transferring 35 μL into the next column, with the last 35 μL being discarded. *Con-A* (35 μL, 0.00625 mg/mL) was then added to all wells and mixed well. As a control to display the gelation of con-A and rabbit erythrocytes in the absence of an inhibitor, one lane contained only con-A (35 μL, 0.00625 mg/mL) + buffer (35 μL) in every well. As a control to show the settling properties of the rabbit erythrocytes, one lane contained only 70 μL buffer. The mixed solutions were incubated at room temperature for one hour. After this time, 6 μL of 10% rabbit erythrocytes was added to every well and mixed well. The plate was

monitored very few hours, with final settling of the erythrocytes occurring after one day. The polyvalent effect is defined as the ratio of minimum concentration of mannose required to inhibit agglutination vs. the corresponding concentration of mannose provided by the material of interest. Since the experiment involves serial two-fold dilutions, the experimental error is usually assumed to be 50%, although repeated experiments were quiet reproducible in results. The plate was monitored very few hours, with final settling of the erythrocytes occurring after one day.

3.2.8.4 Isothermal titration Calorimetry

Calorimetric titrations were performed on a VP-ITC isothermal titration calorimeter from MicroCal (Northampton, MA), essentially as described earlier.[50,51] Briefly, 5 µL aliquots of a 200-300 µM glycopolymers solution were added at 7 min intervals via a rotating stirrer syringe to a 70 µM solution of *Con-A* (subunits) contained in a 1.445 ml sample cell. Samples were dialyzed extensively against 50 mM Hepes Buffer pH 7.4 (containing 0.9 M NaCl, 1 mM $CaCl_2$, 1 mM $MnCl_2$ and 0.02 % of sodium azide) and degassed prior to loading into the cell. Since the first injection was often found to be inaccurate, a 2 µL injection was added first and the resultant point was deleted before the remaining data were analyzed using the *'one set of sites'* binding model in MicroCal Origin ITC analysis software as described earlier.[50,51] The analysis yielded values of the following parameters: number of binding sites (*n*), binding constant for the interaction (K_b), and enthalpy of binding (ΔH_b). From these values free energy of binding ($\Delta G°_b$) and entropy of binding (ΔS_b) were calculated according to the following basic thermodynamic equations:

$$\Delta G°_b = - RT \ln K_b \quad \text{.....} \quad (1)$$

$$\Delta G°_b = \Delta H_b - T\Delta S_b \quad \text{.....} \quad (2)$$

3.3 Results and Discussion

3.3.1 Synthesis of O-glycopolypeptides

We have recently reported the synthesis of *per-O*-benzoylated-D-glyco-*l*-lysine carbamate by reaction of ε-Boc protected CbzLysOBn and propargyl-1, 2-orthoester of *per-O*-benzoylated-glucose/mannose in presence of $HAuCl_4/CH_2Cl_2$/4Å MS

powder/rt.[38-40] The highlight of this reaction is the near quantitative yield of the glycosidation step (>80%) which allows the synthesis of their corresponding NCA's with overall yield of 70%. The same methodology was used to synthesize *per*-*O*-acetylated-D-glyco-*l*-lysine carbamate from their corresponding propargyl-1, 2-orthoester of *per*-*O*-acetylated carbohydrates. Accordingly, glycosylation reaction between ε-Boc protected CbzLysOBn and propargyl-1, 2-orthoester of galactose, mannose and lactose was conducted in the presence of $HAuCl_4$ and 4 Å Molecular Sieves powder in CH_2Cl_2 at room temperature to afford the carbamates **2a**, **2b, 2b'** (*d*-lysine) and **2c** in around 80-90% yield (Scheme 3.1). Furthermore, we continued our journey towards the glyco-NCA in two steps: first, we subjected the glycoconjugates **2a, 2b, 2b'** and **2c** to hydrogenolysis using 10% Pd/C at 400psi to obtain *per*-*O*-acetylated-D-galactose-*l*-lysine carbamate, *per*-*O*-acetylated-D-mannose-*l*-lysine carbamate and *per*-*O*-acetylated-D-lactose-*l*-lysine carbamate. They were then subsequently converted to their corresponding NCA's **3a** (β-galacto-*O*-*l*-lys), **3b** (α-manno-*O*-*l*-lys), **3b'** (α-manno-*O*-*d*-lys) and **3c** (β-lactose-*O*-*l*-lys) using triphosgene and α-pienene in 80% yield after three crystallizations (Scheme 3.1). The purified NCAs **3a, 3b, 3b'** and **3c** were thoroughly characterized by NMR and FT-IR spectroscopic studies.

Polymerization of **3a**(β-galac-*O*-lys NCA) was carried out in the presence of 1.0 eq of *N*,*N*'-tetramethylnapthalene "proton sponge", using azido-PEG-NH_2 (n=11) as the initiator (M/I = 30, 50) in dry dioxane as has been described before (Scheme 3.1). The progress of the polymerization was followed by monitoring the disappearance of the anhydride stretch of the NCA ring at 1785 and 1858 cm^{-1}as was observed by FT-IR. The resulting polymer **4a** and **4c** were purified by reprecipitation and the structure was identified by ^1H and ^{13}C NMR. The molecular weight distribution observed from GPC was monomodal and found to be reasonably narrow. Its molar mass was estimated from the relative intensity of the peak at 3.62-3.68 ppm due to characteristic protons present in the initiator (O-CH_2-CH_2) with the proton peaks of the acetate group (CH_3CO-) present in the carbohydrate moiety (1.98 – 2.14 ppm). The M_n was estimated to be 21,654 and 32,698 while the PDI was calculated to be 1.12 and 1.14 for **4a** and **4c** respectively. Slightly higher molecular weight that is observed is probably due to incomplete initiation by azido-PEG-NH_2. In the same

way, **3b** (α-manno-*O*-*l*-lys NCA) was polymerized using azido-PEG-NH_2 (n=11) as the initiator (M/I = 30, 50) in dioxane (Table 3.1, run 3 and 4). The molecular weight distribution was again found to be reasonably narrow (PDI 1.08 and 1.10 respectively), and the molecular weights of the resulting polymer **5a** and **5c** was estimated to 19,646 and 30,690 respectively. Polymerization of **3c** (β-lacto-*O*-*l*-lys NCA), using azido-PEG-NH2 (n=11) as the initiator (M/I = 30) in dry dioxane (Scheme 3.1) afforded polymer **6a**. The molecular weight distribution observed from GPC was monomodal while the molecular weight and PDI was calculated to be 28,220 and 1.07 respectively. Although *per*-*O*-acetate-D-Lactose-*O*-*l*-serine NCA has been synthesized before, their polymerization to the corresponding glycopolypeptide has not been reported.[52] It should be noted that all the molecular weights obtained were reasonably close to their expected molecular weights. This is in contrast to transition metal catalyzed polymerization of the *C*-linked glycopolypeptides reported recently, where the molecular weights obtained were nearly 3 times that of the expected molecular weights.[30-31] All the glycopolypeptides obtained were then deprotected by using $NH_2.NH_2$, H_2O in MeOH to remove the acetyl groups present in the carbohydrate moiety. The deprotected polymers were then purified by extensive dialysis against deionized water to afford fully water soluble glycopolypeptides **4b**, **4d**, **5b**, **5d, 5f, 5h** and **6b**. The complete removal of the acetyl groups was confirmed by the absence of the acetyl protons in the ^{1}H NMR of the water soluble glycopolypeptides.

Run No	Monomer (M)	Protected Polymer						Deprotected Polymer	
		M/I[a]	M^b_{exp}	Polymer	M_n[c]	M_w/M_n[d]	DP[e]	Polymer	Conformation[f]
1	β-galac-*O*-*l*-lys	30	15630	4a	21654	1.12	42	4b	α-helix
2	β-galac-*O*-*l*-lys	50	25670	4c	32698	1.14	64	4d	α-helix
3	α-manno-*O*-*l*-lys	30	15630	5a	19646	1.08	38	5b	α-helix
4	α-manno-*O*-*l*-lys	50	25670	5c	30690	1.10	60	5d	α-helix

5	Rac-α-manno-*O*-*l*/*d*-lys	30	15630	5e	18642	1.08	36	5f	Non-helical
6	Rac-α-manno-*O*-*l*/*d*-lys	50	25670	5g	28180	1.10	55	5h	Non-helical
7	β-lacto-*O*-*l*-lys	30	24330	6a	28220	1.07	35	6b	α-helix

Table 3.2: [a]M/I indicates monomer to initiator ratio, [b]Expected molecular weight calculated from monomer: Initiator, [c]Number average molecular weight calculated from NMR, [d]Polydispersity index was estimated from GPC (DMF/0.1M LiBr, 60 ºC, RI) and calibrated with polystyrene standards, [e]Degree of polymerization from 1HNMR (DP), [f]Secondary conformation was determined by CD spectra were measured in water.

All the glycopolypeptides above, were synthesized by the polymerization of enantiomerically pure glyco-*O*-*l*-lysine NCA's to afford glycopeptides having a backbone composed only of *l*-lysine. We were interested in synthesizing glycopolypeptides which would have a backbone composed of racemic *l*/*d*-lysine. This would allow us to study the properties of glycopolypeptides with a racemic peptide backbone.[42-44] To accomplish this, we synthesized α-manno-*O*-*l*-lysine NCA (**3b**) and α-manno-*O*-*d*-lysine NCA (**3b'**) from their corresponding *l*- or *d*-lysine amino acid glyco conjugates. These NCA's (**3b** and **3b'**) were mixed in equal proportions and polymerized to afford polymers **5e** and **5g**. The acetate groups of **5e** and **5g** were then deprotected to afford fully water soluble glycopolypeptide **5f** and **5h**.

To prove that the initiator was incorporated into the polymer, the resultant polymers **4a** and **5a** were purified by multiple reprecipitations and then characterized by NMR and FT-IR. The FT-IR of **4a** and **5a** show sharp peak at 2110 cm^{-1} that is characteristic for the organo azide stretch (Figure 3.1). Usage of this bifunctional azido-PEG-amine initiator allows the synthesis of end functionalized polymer **4a** and **5a** which was further manipulated using Cu(I) catalyzed azide-alkyne "click chemistry" with fluorescein alkyne (Scheme 3.2). [53] After click reactions the azide intensity decreased by >80% (Figure 3.1).

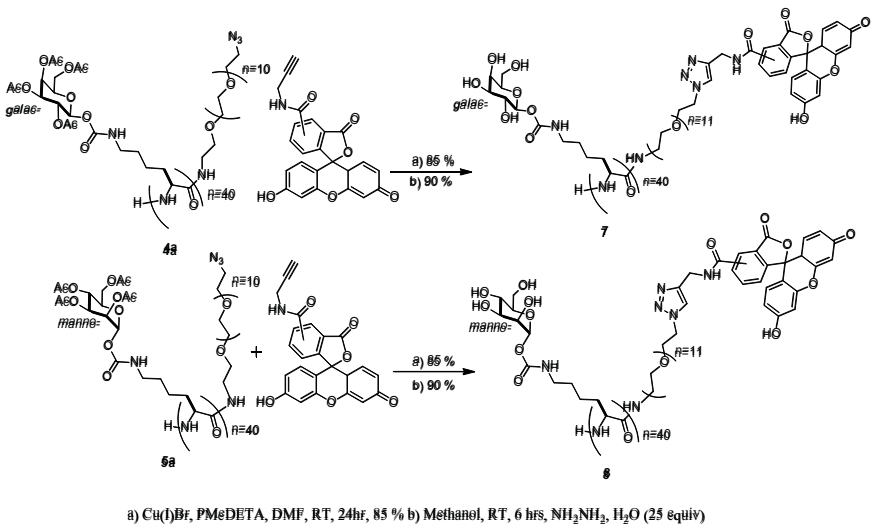

a) Cu(I)Br, PMeDETA, DMF, RT, 24hr, 85 % b) Methanol, RT, 6 hrs, NH_2NH_2, H_2O (25 equiv)

Scheme 3.2: Synthesis of fluorescently labelled Glycopolypeptides **7** and **8.**

The fluorescein labeled glycopolypeptides were deprotected by hydrazine monohydrate in methanol to obtained water soluble fluorecein labeled glycopolypeptides, **7** and **8** respectively (Scheme 3.2), the polymers were characterized by ^{1}H NMR. These fluorescein labeled glycopolypeptides can be used to study their cellular internalization and trafficking as has been shown before.[54, 55]

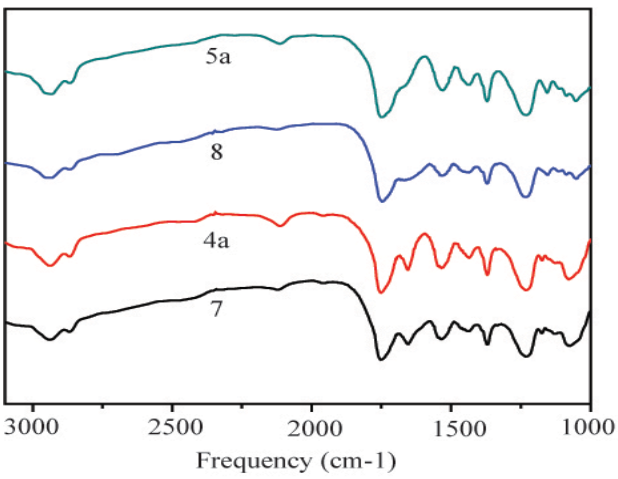

Figure 3.1: FT-IR of azide end functionalized glycopolypeptides before (**4a** and **5a**) and after click reaction with fluorescein-alkyne (**7** and **8**).

3.3.2 Polymerization of racemic amino acids

All the glycopolypeptides described in the previous section were synthesized by the polymerization of enantiomerically pure glyco-*O*-*l*-lysine NCA's to afford glycopeptides having a backbone composed only of *l*-lysine. We were interested in synthesizing glycopolypeptides which would have a backbone composed of racemic *DL*-lysine. This would allow us to study the properties of glycopolypeptides with a racemic peptide backbone.[42-44] To accomplish this, we synthesized α-manno-*O*-*l*-lysine NCA (**3b**) and α-manno-*O*-*d*-lysine NCA (**3b'**) from their corresponding *l*- or *d*-lysine amino acid glyco conjugates. These NCA's (**3b** and **3b'**) were mixed in equal proportions and polymerized to afford polymers **5e** and **5g**. The acetate groups of **5e** and **5g** were then deprotected to afford fully water soluble glycopolypeptide **5f** and **5h**. We were interested to investigate if stereoselection occurred during polymerization of racemic glyco-NCA's to afford stereoblock polymers. The following experiments were performed to investigate that.

Polymerization A: To a solution of α-manno-*O*-*l*-lys NCA **(3b**; 6.6 mg; 12.1μmol**)** in dry 1,4-dioxane was added proton sponge (1 eq, 3 mg) and initiator N_3-PEG-amine (1 eq, 151 μL from a 0.082 M stock solution) in the glove box. The reaction was allowed to proceed for 10 mins after which the FT-IR was recorded. The FT-IR showed complete disappearance of the anhydride stretch at 1785 and 1858 cm^{-1} that is characteristic of the NCA. To the above reaction mixture was then added α-manno-*O*-*l*-lys NCA **(3b**; 69 mg; 126 μmol**)** and α-manno-*O*-*d*-lys NCA **(3b'**; 75 mg; 137 μmol**).** The reaction was allowed to proceed for around 10 h after which the FT-IR showed around 50% disappearance of the anhydride stretch. Therefore, the reaction was around 50% complete. At this time, half of the reaction mixture was removed and the solvent was removed under reduced pressure. The resultant material was dissolved in dichloromethane and then was washed with 2N HCl. The resultant precipitate was recrystallized thrice from dichloromethane-diethylether mixture to remove any unreacted monomer, thus affording polymer **X**.

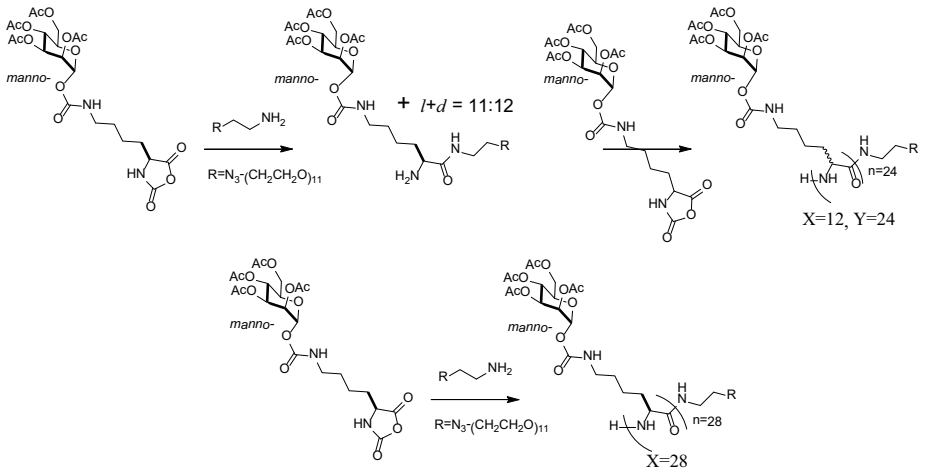

Scheme 3.3: Schematic representation of the synthesis of racemic glycopolypeptides.

The other half of the reaction mixture was allowed to run for an additional 12 h. FT-IR showed complete disappearance of the anhydride stretch. The solvent was then removed under reduced pressure. The resultant material was dissolved in dichloromethane and then was washed with 2N HCl. The resultant precipitate was recrystallized thrice from dichloromethane-diethyl ether mixture to remove any unreacted monomer, thus affording polymer **Y**. The progress of polymerization was monitored by GPC (Figure 3.2A).

Polymerization B: To a solution of α-manno-*O*-*l*-lys NCA **(3b**; 6.6 mg; 12.1µmol**)** in dry 1,4-dioxane was added proton sponge (1 eq, 3 mg) and initiator N_3-PEG-amine (1 eq, 151 µL from a 0.082 M stock solution) in the glove box. The reaction was allowed to proceed for 10 mins after which the FT-IR was recorded. The FT-IR showed complete disappearance of the anhydride stretch at 1785 and 1858 cm^{-1} that is characteristic of the NCA. To the above reaction mixture was then added α-manno-*O*-*l*-lys NCA **(3b**; 138 mg; 252 µmol**).** The reaction was allowed to proceed for around 24 hrs after which the FT-IR showed around complete disappearance of the anhydride stretch, indicating completion of the polymerization reaction. The solvent was then removed under reduced pressure. The resultant material was dissolved in dichloromethane and then was washed with 2N HCl. The resultant precipitate was

recrystallized thrice from dichloromethane-diethylether mixture to remove any unreacted monomer, thus affording polymer **Z**.

The circular dichroism spectra of **X**, **Y** and **Z** is shown below:

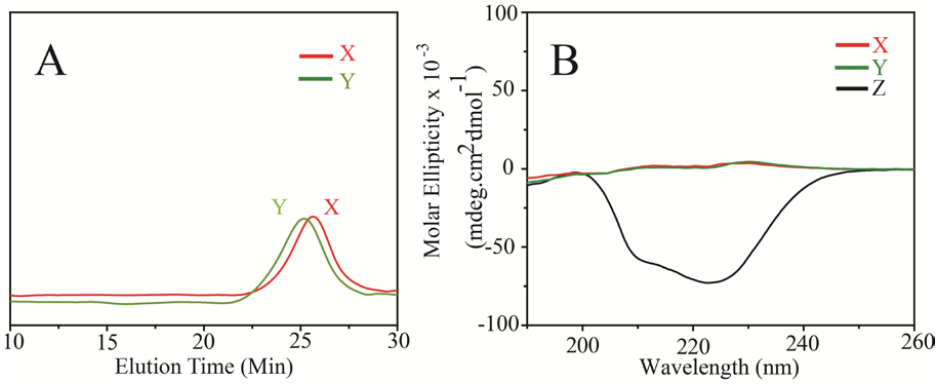

Figure 3.2: A) GPC of Polymer **X** [Rac-α-D-Mannose-*O*-*l*/*d*-lys] (X) and Polymer **Y** [Rac-α-D-Mannose-*O*-*l*/*d*-lys (Y), B) CD Spectra of the glycopolypeptides were measured in acetonitrile, Polymer **X** [Rac-α-D-Mannose-*O*-*l*/*d*-lys], (B) Polymer **Y** [Rac-α-D-Mannose-*O*-*l*/*d*-lys], (C) Polymer **Z** [25-α-D-Mannose-*O*-*l*-lys].

The CD spectra of **Z** displays characteristic peaks at 208 and 222 nm which are characteristic of the α-helix. Polymer **X** and **Y** display no characteristic CD signal (Figure 3.2B). It is to be noted that in both the cases, polymerization was initiated by the reaction product arising of a 1:1 mixture of α-manno-*O*-*l*-lys NCA and N_3-PEG-amine. Hence if stereoselection took place in polymerization A, all the α-manno-*O*-*l*-lys NCA would be first incorporated followed by α-manno-*O*-*d*-lys NCA. This would mean that on completion of 50% reaction, the polymer **X** would have a CD signal indicative of an α-helix which would finally disappear upon completion of the reaction (polymer **Y**). However, the CD was found to be identical at 50% and 100% completion of reaction (polymer **X** and **Y**). This shows that no stereoselection takes place and there is a random incorporation of L and D glyco-NCA's during polymerization.

3.3.3 Conformation of glycopolypeptides in water

The conformation of the glycopolypeptides in solution was investigated by circular dichroism (CD). The fully deprotected polymer poly(glyco-*O*-lys) **4b**, **4d**, **5b**, **5d** and **6b** all of which have a polypeptide backbone compose of enantiomerically pure *L*-lysine, were found to be α-helical in water with a characteristic minima at 208 and

222 nm (Figure 3.3 & 3.4). For example, poly-(β-galacto-*O*-*l*-lys) polypeptide was found to be 70% helical in water at RT. The percentage helicity of **4d** as a function of temperature was also studied using CD (Figure 3.4A). It was found that the α-helical conformation got disrupted as the temperature was increased from 0°C to 70°C. The polymer regained its helicity completely upon cooling it back to 0°C. The percentage of helicity of these glycopolypeptides was found to be dependent of the length of the glycopolypeptide. For example, the percentage helicity of poly-(α-manno-*O*-*l*-lys) **5d** (60 mer) was 62% while the % helicity of its corresponding 38 mer (**5b**) decreased to 30% at rt (Figure 3.3). The conformation of the deprotected polypeptide poly-(β-lacto-*O*-*l*-lys) **6b** was also studied as a function of temperature. This polymer was also observed to be α-helical in water and the helicity content was determined to be 55% at rt. (Figure 3.4B)

Glycopolypeptides **5f** and **5h**, where the polypeptide backbone consisted of racemic *l*/*d*-lysine, showed no helicity (helicity <2% in water at rt, Figure 3.3). This was expected since a backbone having a racemic amino acid is not expected to fold into an α-helix as has been shown before.[42-44] However, it must be noted that if stereo-block polymers containing blocks of *l* and *d* glyco-amino acids would also give no CD signal, although experiments described above shows that stereoselection does not occur during polymerization.

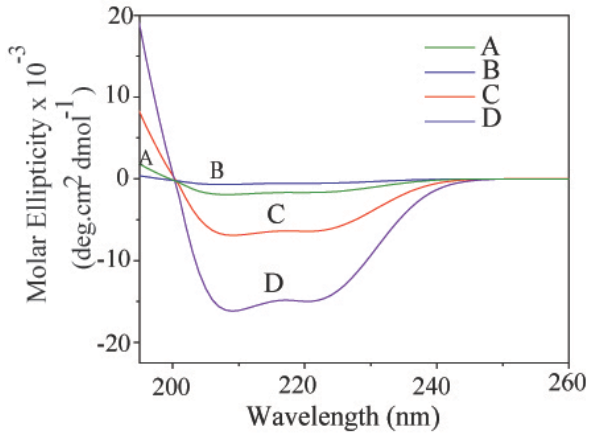

Figure 3.3: CD Spectra of the glycopolypeptides in water. (A) Polymer **5h** [Rac-50-α-D-Mannose-*O*-*l*/*d*-lys], (B) Polymer **5f** [Rac-30-α-D-Mannose-*O*-*l*/*d*-lys], (C) Polymer **5b** [30-α-D-Mannose-*O*-*l*-lys] and (D) Polymer **5d** [50-α-D-Mannose-*O*-*l*-lys].

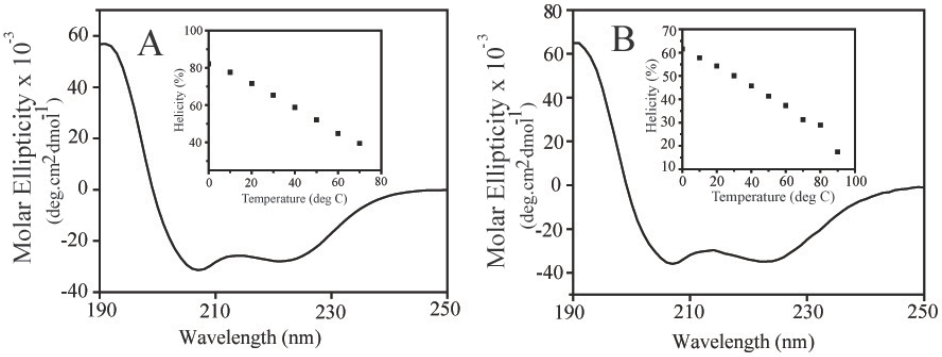

Figure 3.4: Circular dichroism spectra of (A) poly(β-gal-*O-l*-lys) **4d** and (B) poly(β-lacto-*O-l*-lys) **6b** at 20°C (0.5 mg/mL). Inset: Percentage of α-helicity content (% helicity calculated using molar ellipticity at 222 nm) as a function of temperature.

3.3.4 Design of glycopolypeptides for lectin binding study

We chose a set of four glycopolypeptides to probe their binding to the lectin *Con-A* and also probe the difference between helical and non-helical polypeptides. While glycopolypeptide **5h** and **5d** have the same structure and similar molecular weights, their secondary structures are different. CD measurements show **5d** to be α-helical (62% helicity) whereas the **5h** shows no secondary structure (< 2% helicity) at rt (Figure 3.3). Similarly glycopolypeptides **5b** (30% α-helical) and **5f** (non-helical, <2% helicity) have similar molecular weight but differ in their secondary structures. It is expected that a predominantly α-helical polypeptide will be stiff and good binding is likely be observed only if the distance between two sugar units matches exactly to the distance between two binding sites. This is unlikely in most cases as have been observed by Kobayashi *et al.* [56] where a rigid helical poly(glycosyl phenyl isocyanate) was observed to have very little specific interactions with lectins while the equivalent polymer with a flexible phenylacrylamide showed good binding. On the contrary, Kiick *et al.* [57] have showed that a helical backbone in polypeptides can be superior to coiled structures for binding to lectin CT B_5.[57] Hence conformational factors that determine binding are complex. Since our synthetic methodology allows synthesis of polypeptides with the same structure and molecular weight but with different secondary conformation (for example **5h** and **5d**), we can probe the effect of secondary conformation of glycopolypeptides on lectin binding.

3.3.4.1 Interaction of glycopolypeptides with Con-A

3.3.4.1.1 Turbiditymetry Assay

The tetrameric protein *Con-A* is known to specifically bind to mannosyl and glucosyl residues. Hence the multivalent glycopolypeptide poly-(α-manno-*O*-lys) **5b** and 5d is expected to interact with the tetrameric *Con-A* to form large aggregates. The recognition and binding abilities of glycopolypeptides **5b** and **5d** were therefore estimated by turbidity measurements. The turbidity variation due to the interaction of poly-(α-manno-*O*-lys) having two different molecular weights (**5b** and **5d**) with *Con-A* is presented in Figure 3.5. As can be observed for both the polymers, the turbidity first increases with increasing glycopolypeptide concentration and finally reaches a plateau. At this point, the turbidity does not increase with increasing glycopolypeptide concentration and can be considered as an optimum value for the

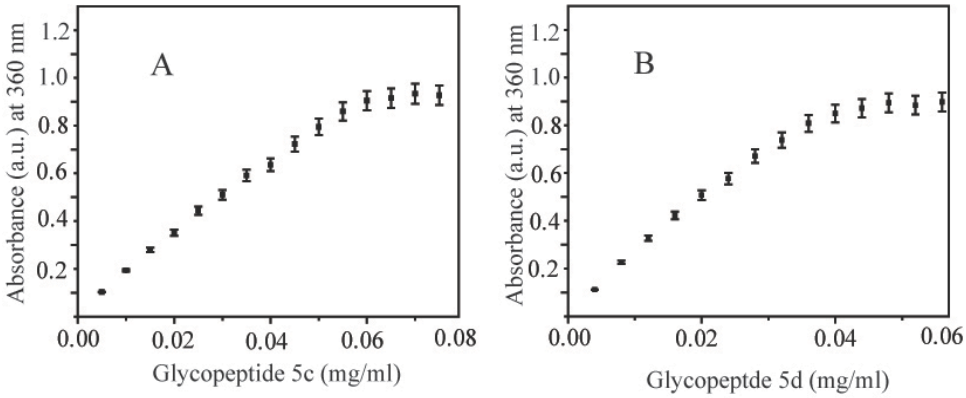

Figure 3.5: *Concanavalin-A* lectin interaction with poly-(α-manno-*O*-lys) **5b** (A) and **5d** (B). Turbidity as a function of poly(α-manno-*O*-lys) glycopolypeptide concentration with *Con-A* in an aqueous buffer solution at room temperature.

binding of the glycopolypeptide to *Con-A*. The optimum value for **5b** and **5d** for [*Con-A*] = 0.4 mg/mL was found to be 0.06 mg/mL and 0.04 mg/mL respectively. This shows that the saturation for **5d** occurs at a lower concentration than **5b**. This is expected since **5d** has a higher molecular weight than **5b** and hence is expected to bind at lower concentrations. Control experiments with glycopolypeptide poly(β-galacto-*O*-lys) **4b** or **4d** showed no turbidity showing that the specificity of poly(α-manno-*O*-lys) towards the lectin *Con-A* .

3.3.4.1.2 Precipitation and Hemagglutination Assay

In all experiments the ratio of the mannose functionalized polypeptide to *Con-A* increased with increasing amount of the glycopolypeptide and then remained fairly constant after a maximum had been reached (Figure 3.5 & 3.6). The stoichiometry of binding (number of *Con-A* tetramer per glycopolypeptide) was determined to be 4, 5, 3.5 and 3.5 for **5d**, **5h**, **5b** and **5f** respectively.

Preliminary studies on the binding of the mannose containing glycopolypeptides (**5b**, **5d**, **5f** and **5h**) with *Con-A* was evaluated by performing precipitation and hemagglutination assays.

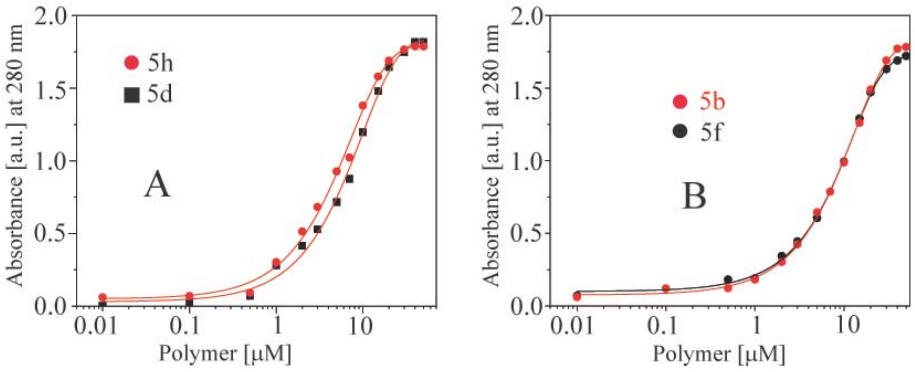

Figure 3.6: Quantitative Precipitation Results, A:[50-α-D-Manno-*O-l*-lys(**5d**) and Rac-50-α-Manno-*O-l/d*-lys(**5h**)], B:[30-α-D-Manno-*O-l*-lys(**5b**) and Rac-30-α-Manno-*O-l/d*-lys (**5f**)]. All series were fit to a sigmoidal curve to determine the half maximal concentration required for precipitation. The stoichiometry was determined as previous reported by Brewer *et al.* [46] The precipitation assay was performed to determine the number of mannose units available in the glycopolypeptides (**5b**, **5d**, **5f** and **5h**) for binding to each *Con-A* lectin.

Polymer	Length (DP)[a]	Conformation[b]	Stoichiometry (ConA: Polypeptide)	$P_{(Mannose:ConA)}$
5d [50-α-manno-*O-l*-lys(OH)]	60	α-helix	4	15
5h [Rac-50-α-manno-*O-l/d*-	55	Non-helical	5	11

lys(OH)]				
5b [30-α-manno-*O-l*-lys(OH)]	38	α-helix	3.5	11
5f [Rac-30-α-manno-*O-l/d*-lys(OH)]	36	Non-helical	3.5	10

Table 3.3: (DP)[a] was estimated from the ^{1}H NMR integration of the polymer, Conformation[b]= Circular Dichroism was done in DI water, Stoichiometry and P was calculated from the average of three experiments reported in Table 3.3.

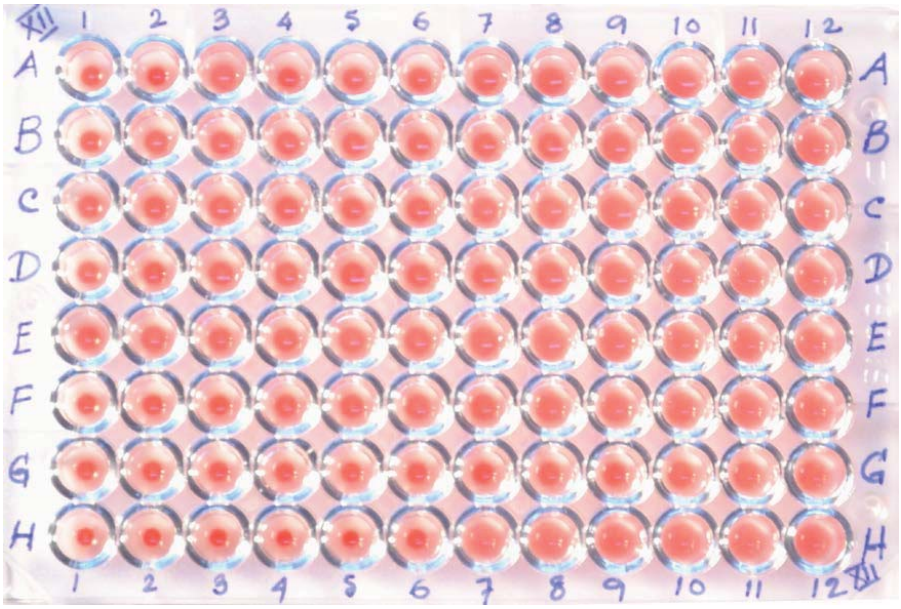

Figure 3.7: A typical HA Assay Plate: Demonstrating the lowest amount of Polymers required to inhibit the Erythrocytes-*Con-A* agglutination with respect to monomeric mannose. The final inhibition doses reported were taken as an average of 3 plates. Column 1 (A) α-Methyl-mannopyranoside (5 mg/ml), (B) Polymer **5d** (1 mg/mL) [50-α-D-Mannose-*O-l*-lys], (C) Polymer **5h** (1 mg/mL) [Rac-50-α-D-Mannose-*O-l/d*-lys], (D) Polymer **5b** (1 mg/mL) [30-α-D-Mannose-*O-l*-lys], (E) Polymer **5f** (1 mg/mL) [Rac-30-α-D-Mannose-*O-l/d*-lys], Column 2-12 contains serial two- fold dilution from these values, Row (H) 1-6 and 7-12 wells contains only buffer and *Con-A* with Erythrocytes.

The data from the experiments suggest (Table 3.3) that the number of mannopyranoside units in the polypeptide bound per *Con-A* tetramer for a

glycopolypeptide having a helical structure is slightly higher than the corresponding glycopolypeptide with no secondary structure (**5d** versus **5h** and **5b** versus **5f**).

Hemagglutination assays (HA) were performed with glycopolypeptides (**5b**, **5d**, **5f** and **5h**) to get preliminary information regarding binding affinity,[49] the use of HA to measure inhibition of protein carbohydrate interactions is well documented (Figure 3.7) and gives us an essential entry-level comparison of the different mannose containing glycopolypeptides synthesized by us. When compared to the control monomer methyl mannose, poly(α-manno-*O*-lys) glycopolypeptides **5b**, **5d**, **5f** and **5h** , showed an increase in binding affinity ranging from 15-36 folds per mannose unit.

Polymer	Length (DP)[a]	Conformation[b]	Stoichiometry (ConA: Polypeptide)	P(Mannose:Con A)[c]
5d [50-α-manno-*O-l*-lys(OH)]	60	α-helix	4	15
5h [Rac-50-α-manno-*O-l/d*-lys(OH)]	55	Non-helical	5	11
5b [30-α-manno-*O-l*-lys(OH)]	38	α-helix	3.5	11
5f [Rac-30-α-manno-*O-l/d*-lys(OH)]	36	Non-helical	3.5	10

Table 3.4: Hemagglutination Assay; (DP)[a] was estimated from the ^{1}H NMR integration of the polymer, Conformation[b]= Circular Dichroism were recorded in DI water, P[c]= From the average of three plates, lowest inhibition polymer concentration was taken for calculation.

This indicates an increase in activity toward *Con-A* of 1 order of magnitude per mannose unit which is suggestive of a glycoside clustering motif of all the synthesized glycopolypeptides. Since the error associated with the dose determination is a factor of 2, as dictated by the 2-fold dilutions of the assay, the polyvalency's of **5b**, **5d**, **5f** and **5h** are the same within experimental error.

3.3.4.1.3 Isothermal Titration Calorimetry

Results of representative calorimetric titrations obtained for the binding of glycopolymers to *Con-A* at 25 °C are shown in Figure 3.8. Figures 3.8C and 3.8D correspond to the titration of *Con-A* with glycopolypeptides **5d** and **5h**, respectively. While the upper panels in these two figures show the exothermic heat released upon binding at each injection, the lower panels show plots of incremental heat released as a function of the *ligand/Con-A* subunit ratio. Nonlinear least squares fits of the data to *one set of sites* model (shown as solid lines) indicate that the experimental data could be described well by this model as judged by the high quality of the fits. Similar high

Polymer	Conformation[a] (Units)[b]	n[c]	K_a (M^{-1}) x 10^{-6}	ΔH (kcal/mol)	ΔS (cal/mol/K)	Polyvalency (sugar)
α-Methyl mannopyranoside		1	0.0051	-10(±0.07)	-17 (±0.25)	1
5b [30-α-manno-*O-l*lys(OH)]	α-Helix (38 units)	7(±0.5)	2.(±0.44)	-81 (±3.3)	-243 (± 1.4)	12
5f [Rac-30-α-manno-*O-l/d* -lys(OH)]	Non-Helical (36 units)	8 (±0.7)	4(±0.29)	-88 (±2.7)	-266 (± 5.7)	22
5d [50-α-manno-*O-l*-lys(OH)]	α-Helix (60 units)	9(±0.1)	10(±3.51)	-95(±2.1)	-288(± 17.7)	33
5h [Rac-50-α-manno-O-*l/d* -lys(OH)]	Non-Helical (55 units)	10(±0.6)	9 (±2.52)	-115 (±1.4)	-354 (± 3.5)	32

Table 3.5: Values shown are average of 2 independent titrations. [a]Determined from CD spectra were recorded in water. [b]Degree of polymerization was determined by ^{1}H NMR. [c]Number of *Con-A* subunit per glycopolypeptides.

quality data were obtained for the titration of *Con-A* with glycopolypeptides **5b** and **5f** (Figure 3.8A & 3.8B). In each case very similar data were obtained in duplicate experiments and the average values of binding constants (K_b), stoichiometry of

binding (n), enthalpy of binding (ΔH_b) and entropy of binding (ΔS_b) obtained from the calorimetric titrations for the interaction of all the glycopolymers with *Con-A* are listed in Table 3.5. A comparison of the binding constants, stoichiometry and thermodynamic parameters obtained from the ITC studies yielded a number of interesting features. Firstly, the stoichiometry of binding is higher for the longer glycopolymers (**5d** and **5h**), but it does not increase in proportion to the increase in chain length, which can be attributed to steric factors. More interestingly, the binding constant increases by 2-4 fold for the longer glycopeptides. Since even the shorter glycopeptides (**5b** and **5f**) already have a large number of covalently attached mannose residues in close proximity, this additional increase in binding affinity may be attributed to the increased statistical probability of the binding event due to the increase in the number of accessible sugar residues for binding. Finally, the racemic glycopolypeptides were found to exhibit a slightly higher binding stoichiometry as compared to the α-helical counterparts, which may be due to their slightly longer lengths.

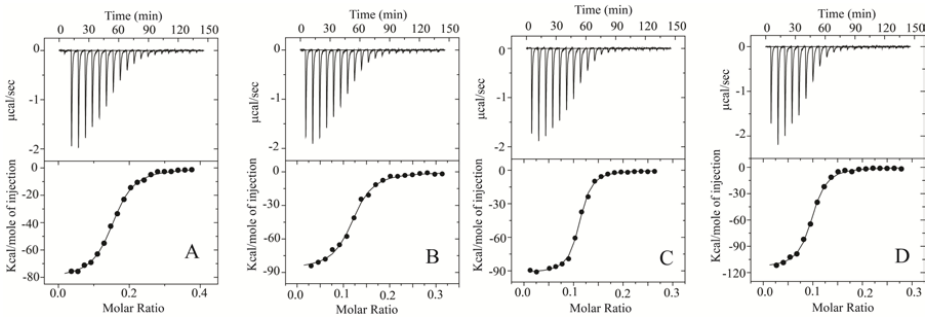

Figure 3.8: Isothermal Titration Calorimetry: Calorimetric titration of *Con-A* with A [30-α-manno-*O*-*l*-lys(OH) **5b**], B [Rac-30-α-manno-*O*-*l*/*d*-lys(OH) **5f**], C [50-α-manno-*O*-*l*-lys(OH)] **5d**] and D [Rac-50-α-manno-*O*-*l*/*d*-lys(OH) **5h**] at 298 K. Upper panels show the ITC raw data obtained from 20 automatic injections of 5 µL aliquots of the glycopeptide (in the syringe) into 1.445 mL *Con-A* in the ITC cell. Lower panels show the integrated heat of binding obtained from the raw data.

ITC studies show that there is very little difference in the number of *Con-A* monomer units bound per polypeptide for glycopolypeptides having an α-helical conformation (**5b**, **5d**) and with no secondary structure (**5f**, **5h**) of similar molecular weight. Similar trend is also observed for the precipitation assay (Figure 3.6), although the stoichiometry determined from the precipitation assay is higher for all the

glycopolypeptides used in this study. Precipitation assays are semi-quantitative, and are known to overestimate stoichiometry of binding, since a macroscopic precipitation event could result from even partially saturated binding events. To understand the stoichiometry for *Con-A* binding with the different glycopolypeptides, a qualitative estimation of the length of the different glycopolypeptides in solution would be useful. The three limiting conditions for the length of the glycopolypeptides can be assumed as (a) purely α-helical (b) coiled structure with the freely jointed chain and (c) coiled structure with extended chain. The length of the glycopolypeptide (n=60) under these limiting cases can be estimated to be 8.6 nm, 7.9 nm and 21.7 nm. This indicates that polypeptides with purely α-helical and the freely jointed conformation can have similar length. Since racemic glycopolypeptide **5f** and **5h** have a slightly higher binding stoichiometry than their helical counterparts, they have a conformation which is probably in between a freely jointed chain and extended chain (more towards a freely jointed chain). However, more structural studies are required to justify this.

3.3.4.1.4 Enthaply entropy compensation during glycopolypeptide binding to Con-A

The polyvalent effect observed for all the polypeptides were low and only 1 order of magnitude higher (per mannose) than their corresponding monomer α-methyl mannopyranoside. Polyvalency arises from mainly two related but distinct terms: (i) multivalent binding (the ability of one glycopolypeptide to bind to multiple lectin binding sites) and (ii) glycoside clustering (a ligand concentration effect). While the former shows mild binding enhancements (typically 1 order of magnitude) the later shows very large enhancements (two orders and higher). Since our synthetic glycopolypeptides only show small binding enhancements, we believe that this effect is due to glycoside clustering and not due to multivalent binding. It must be noted that both the ITC and HA assay shows similar affinity data and polyvalency for all the glycopolypeptides used in this study (Table 3.4, Figure 3.7). A closer look at the ITC data gives us an idea why two glycopolypeptides with differing secondary structure have similar binding constants. It is observed that the ΔH_b values are higher for the non-helical polymers (**5f** and **5h**) as compared to the helical polymers (**5b** and **5d**) for the same (comparable) length, whereas the ΔS_b values are higher for the helical polymers. This can be rationalized in the following way. The non-helical polymers are more flexible than their helical counterparts and hence bind better to the lectin,

which results in a larger enthalpy change. On the other hand, the higher ΔS_b values for the helical polymers are consistent with the entropy penalty being less for binding to a rigid structure. However, it should be noted that the differences in the enthalpy of binding and entropy of binding for the helical versus non-helical polymers are relatively small and also partially compensate each other resulting in nearly comparable values of binding constant.

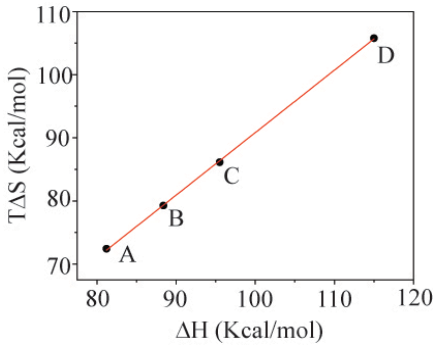

Figure 3.9: Enthalpy-entropy compensation plot for the *Con-A*/*glycopolypeptide* interaction A[30-α-manno-*O*-*l*-lys(OH) **5b**], B[Rac-30-α-manno-*O*-*l*/*d*-lys(OH) **5f**], C[50-α-manno-*O*-*l*-lys(OH) **5d**] and D[Rac-50-α-manno-*O*-*l*/*d*-lys(OH) **5h**].

A careful examination of the ΔH_b and ΔS_b values for the different glycopolypeptides (both helical and non-helical) suggested that the changes in enthalpy and entropy are compensatory in nature. This is clearly seen in a plot of $-\Delta H_b$ versus $-T\Delta S_b$ shown in Fig. 3.9. A linear least squares fit of the data yielded a slope of 0.99 indicating that the enthalpy of binding and entropy of binding are exactly compensated in the binding of the glycopolypeptides to *Con-A*. Such close compensation of enthalpy and entropy of binding has been observed for a large number of protein-ligand interactions including lectin-carbohydrate interactions and this phenomenon has been attributed to the reorganization of water structure around the binding site on the protein and the ligand. A number of studies suggest that water molecules play an important role in lectin-carbohydrate interaction.[50,51,58-60] Indeed, ITC studies provided evidence indicating the involvement of water molecules in the binding of manno-oligosaccharides to *Con-A*. [61] In view of this, the enthalpy-entropy compensation observed here can be explained in terms of changes in water structure during the *Con-A/glycopolypeptide* association.

3.4 Conclusions

We have reported a very easy three step synthesis of *per*-acetylated-*O*-glycosylated lysine-NCA using a stable glycosyl donor and a commercially available protected amino acid. The highlight of the synthesis is that the key glycosylation step and the subsequent deprotection reaction proceeds to completion in near quantitative yield. The glycosylated NCA's were then polymerized using commercially available simple amine initiators to yield well defined high molecular weight glycopolypeptides in very high yields. We have also reported the synthesis of poly-(β-lacto-*O*-lys) glycopolypeptides having a disaccharide lactose as the pendant side group which demonstrates that this methodology can be extended to synthesize glycopolypeptides having complex carbohydrates on its side chains. Poly-(β-galacto-*O*-lys) glycopolypeptide was also synthesized. Since certain cancer cells like HepG2 cells have receptors that bind specifically to β-galactose, we believe these polymers can be used for drug delivery. The fully water soluble glycopolypeptides were found to be α-helical in aqueous solution. However, we were able to control the secondary conformation of the glycopolypeptides by polymerizing racemic amino acid glyco NCA's. The poly(α-manno-*O*-lys) polypeptides synthesized by us also bind specifically to the lectin *Con-A* and the binding affinity was found to be nearly same between polypeptides having enantiomerically pure *l*-lysine and the corresponding *l/d*-lysine backbone.

The selected spectra of the reported compounds are available from the **Appendix III**.

3.5 References

(1) Godula, K.; Rabuka, D.; Nam, K.; Bertozzi, C. *Angew. Chem. Int. Ed.* **2009**, *48*, 4973-4976.

(2) Liu, S.; Maheshwari, R.; Kiick, K. L. *Macromolecules* **2009**, *42*, 3-13.

(3) Manning, D. D.; Hu, X.; Beck, P.; Kiessling, L. L. *J. Am. Chem. Soc.* **1997**, *119*, 3161-3162.

(4) Mortell, K. H.; Gingras, M.; Kiessling, L. L. *J. Am. Chem. Soc.* **1994**, *116*, 12053-12054.

(5) Prescher, J. A.; Bertozzi, C. R. *Nat Chem Biol* **2005**, *1*, 13-21.

(6) Wang, Y.; Kiick, K. L. *J. Am. Chem. Soc.* **2005**, *127*, 16392-16393.

(7) Albertin, L.; Cameron, N. R. *Macromolecules* **2007**, *40*, 6082-6093.

(8) Chen, G.; Tao, L.; Mantovani, G.; Geng, J.; Nyström, D.; Haddleton, D. M. *Macromolecules* **2007**, *40*, 7513-7520.

(9) Ladmiral, V.; Mantovani, G.; Clarkson, G. J.; Cauet, S.; Irwin, J. L.; Haddleton, D. M. *J. Am.Chem.Soc.* **2006***, 128,* 4823-4830.

(10) Ladmiral, V.; Melia, E.; Haddleton, D. M. *Eu. Polym. J.* **2004**, *40*, 431-449.

(11) Spain, S. G.; Gibson, M. I.; Cameron, N. R. *J.Polym. Sci. Part A: Polym. Chem.* **2007**, *45*, 2059-2072.

(12) Ting, S. R. S.; Min, E. H.; Escalé, P.; Save, M.; Billon, L.; Stenzel, M. H. *Macromolecules* **2009**, *42*, 9422-9434.

(13) Gamblin, D. P.; Scanlan, E. M.; Davis, B. G. *Chem. Rev.* **2008**, *109*, 131-163.

(14) Seeberger, P. H.; Werz, D. B. *Nature* **2007**, *446*, 1046-1051.

(15) Ambrosi, M.; Cameron, N. R.; Davis, B. G. *Org. Biomol. Chem.* **2005**, *3*, 1593-1608.

(16) Ting, S. R. S.; Chen, G.; Stenzel, M. H. *Polym. Chem.* **2010**, *1*, 1392-1412.

(17) Mammen, M.; Choi, S.-K.; Whitesides, G. M. *Angew. Chem. Int. Ed.* **1998**, *37*, 2754-2794.

(18) Connolly, D. T.; Townsend, R. R.; Kawaguchi, K.; Bell, W. R.; Lee, Y. C. *J. Biol. Chem.* **1982**, *257*, 939-945.

(19) Weigel, P. H.; Oka, J. A. *J. Biol. Chem.* **1983**, *258*, 5095-5102.

(20) Weigel, P. H.; Yik, J. H. N. *Biochim. Biophys. Acta.* **2002**, *1572*, 341-363.

(21) Cho, C. S.; Seo, S. J.; Park, I. K.; Kim, S. H.; Kim, T. H.; Hoshiba, T.; Harada, I.; Akaike, T. *Biomaterials* **2006**, *27*, 576-585.

(22) Deming, T. J. *Soft Matter* **2005**, *1*, 28-35.

(23) Lu,H.; Wang J.; Bai1,Y.; Lang,J.W.; Liu,S.; Lin,Y.; Cheng, J. *Nature Communications,* **2011***, 2,* 206-214.

(24) Deming, T. J. *J. Polym. Sci. Part A: Polym. Chem.* **2000**, *38*, 3011-3018.

(25) Hadjichristidis, N.; Iatrou, H.; Pitsikalis, M.; Sakellariou, G. *Chem. Rev.* **2009**, *109*, 5528-5578.

(26) Aoi, K.; Tsutsumiuchi, K.; Aoki, E.; Okada, M. *Macromolecules* **1996**, *29*, 4456-4458.

(27) Aoi, K.; Tsutsumiuchi, K.; Okada, M. *Macromolecules* **1994**, *27*, 875-877.

(28) Rüde, E.; Westphal, O.; Hurwitz, E.; Fuchs, S.; Sela, M. *Immunochemistry* **1966**, *3*, 137-151.

(29) Tsutsumiuchi, K.; Aoi, K.; Okada, M. *Macromolecules* **1997**, *30*, 4013-4017.

(30) Kramer, J. R.; Deming, T. J. *J. Am. Chem. Soc.* **2010**, *132*, 15068-15071.

(31) Kramer, J. R.; Deming, T. J. *J.Am Chem.Soc.* **2012**, *134*, 4112-4115.

(32) Huang, J.; Habraken, G.; Audouin, F.; Heise, A. *Macromolecules* **2010**, *43*, 6050-6057.

(33) Sun, J.; Schlaad, H. *Macromolecules* **2010**, *43*, 4445-4448.

(34) Huang, J.; Bonduelle, C.; Thévenot, J.; Lecommandoux, S.; Heise, A. *J. Am. Chem. Soc.* **2012**, 134, 119-122.

(35) Metzke, M.; Connor, N.; Maiti, S.; Nelson, E.; Guan, Z. *Angew. Chem. Int. Ed.* **2005**, *44*, 6529-6533.

(36) Schatz, C.; Louguet, S.; Meins, J-F.; Lecommandoux, S. *Angew. Chem. Int. Ed.* **2009**, *48*, 2572-2575.

(37) Pati, D.; Shaikh, A. Y.; Hotha, S.; Sen Gupta, S. *Polym. Chem.* **2011**, *2*, 805-811.

(38) Shaikh, A. Y.; Sureshkumar, G.; Pati, D.; Sen Gupta, S.; Hotha, S. *Org. Biomol. Chem.* **2011** *9*, 5951-5959.

(39) Hotha, S.; Kashyap, S. *J. Am. Chem. Soc.* **2006**, *128*, 9620-9621.

(40) Sureshkumar, G.; Hotha, S. *Chem. Comm.* **2008**, 4282-4284.

(41) Wiejak, S.; Masiukiewicz, E.; Rzeszotarska, B. *Chem. Pharm. Bull.* **1999,** *47*, 1489-1490.

(42) Hanson, J.A.; Li, Z.; Deming T. J. *Macromolecules* **2010**, *43*, 6268-6269.

(43) Chen, C.; Wang, Z.; Li, Z. *Biomacromolecules* **2011**, *12*, 2859–2863.

(44) Gabrielson, N. P.; Lu, H.; Yin, L.; Li, D.; Wang, F.; Cheng, J. *Angew. Chem. Int. Ed.* **2009**, *48*, 2572-2575.

(45) Morrow, J. A.; Segal, M. L.; Lund-Katz, S.; Philips, M. C.; Knapp, M.; Rupp, B.;Weigraber, K. H. *Biochemistry* **2000**, *39*, 11657-11666.

(46) Bhattacharyya, L.; Brewer C. F.; Brown, R. D.; Koenig, S. H. *Biochemistry* **1985,** *24*, 4974-4980.

(47) Cairo, C. W.; Gestwicki, J. E.; Kanai, M.; Kiessling, L. L. *J. Am. Chem.Soc*. **2002**, *124*, 1615-1619.

(48) Woller E.K.; Cloninger M.J.; *Org. Lett.* **2002**, *4*, 7-10.

(49) Kaltgard, E.; Finn, M. G. Application of Polyvalent Carbhohydrate display on Virus Particles **2009**, ISBN-10: 3639201655, ISBN-13: 978-3639201659.

(50) Sultan, N. A. M.; Swamy, M. J. *Arch. Biochem. Biophys.* **2005**, *437,* 115-125.

(51) Narahari, A.; Singla, H.; Nareddy, P. K.; Bulusu, G.; Surolia, A.; Swamy, M. J. *J. Phys. Chem. B.* **2011**, *115*, 4110-4117.

(52) Gibson, M.I.; Hunt, G.J.; Cameron, N.R.; *Org. Biomol. Chem*. **2007**, *5*, 2756-2757.

(53) Punna, S.; Kaltgrad, E.; Finn, M. G. *Bioconjugate Chem.* **2005**, *16*, 1536-1541.

(54) Mangold, S. L.; Carpenter, R. T.; Kiessling, L. L. *Org. Lett.* **2008**, *10*, 2997-3000.

(55) Owen, R. M.; Gestwicki, J. E.; Young, T.; Kiessling, L. L. *Org. Lett.* **2002**, *4*, 2293-2296.

(56) Hasegawa, T.; Kondoh, S.; Matsuura, M.;Kobayashi K.; *Macromolecules* **1999**, *32*, 6595-6603.

(57) Polizzotti, B.D.; Kiick, K.L.; *Biomacromolecules* **2006**, *7*, 483-490.

(58) Gupta, D.; Cho, M.; Cummings, R. D.; Brewer, C. F. *Biochemistry* **1996**, *35*, 15236-15243.

(59) Swaminathan, C. P.; Gupta, D.; Sharma, V.; Surolia, A. *Biochemistry* **1997**, *36*, 13428-13434.

(60) Surolia, A.; Sharon, N.; Schwarz, F. P. *J. Biol. Chem.* **1996**, *271*, 17697-17703.

(61) Swaminathan, C. P.; Surolia, N.; Surolia, A. *J. Am. Chem. Soc.* **1998**, *120*, 5153-5159.

Chapter 4

Multiple Topologies from Glycopolypeptide-Dendron Conjugate Self-Assembly: Nanorods, Micelles and Organogels

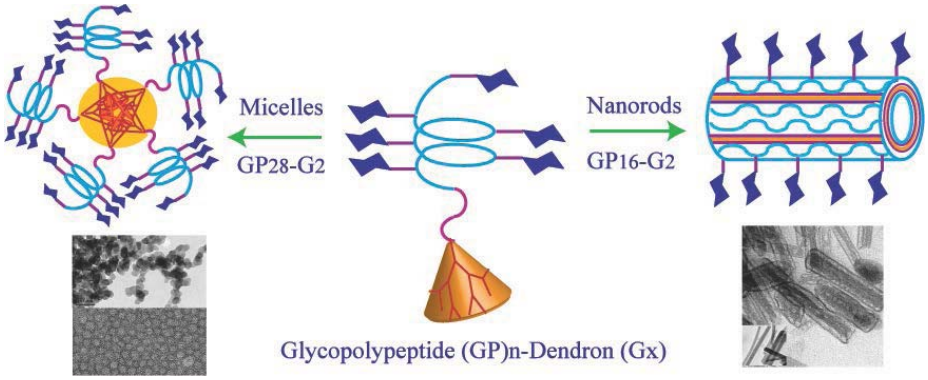

ABSTRACT: Glycopolypeptides were synthesized by ring opening polymerization of glycosylated NCA monomer and attached to hydrophobic dendrons at one chain end by 'click' reaction to obtain amphiphilic anisotropic macromolecules. We show that by varying polypeptide chain length and dendron generation, organogel was obtained in DMSO while nanorods and micellar aggregates were observed in aqueous solutions. Assemblies in water were characterized by electron microscopy and dye encapsulation. Secondary structure of the glycopolypeptide chain was shown to affect the morphology whereas the chain length of poly(ethylene glycol) linker between glycopolypeptide and dendron did not alter rod-like assemblies. Bioactive surface chemistry of these assemblies displaying carbohydrate groups was demonstrated by interaction of mannose-functionalized nanorods with *Con-A*.

This chapter has adapted from the corresponding paper;

Debasis Pati, Nagendra Kalva, Soumen Das, Guruswamy Kumaraswamy, Sayam Sen Gupta and Ashootosh V. Ambade *J. Am. Chem. Soc.* **2012**, *134*, 7796-7802.

4.1 Introduction

Glycopolymers, *viz.* synthetic polymers with carbohydrate moieties in the side chain, have been of immense interest to the field of tissue engineering and drug delivery.[1-3] This interest stems from the fact that carbohydrates play complex roles *in vivo*, particularly in biomolecular recognition events, I have already discussed in details in the Chapter **I** (Sec 1.1 and 1.2). For glycopolymers to be used as delivery vehicles and as biomaterials, it would be advantageous if these could be assembled into supramolecular nanostructures that can be tuned to appropriately display their carbohydrate moieties. Thus, amphiphilic block copolymers containing glycopolymers as one of their blocks represent an interesting motif to build self-assembled nanostructures.[5-10] For example, glucose-grafted polybutadiene-block-polystyrene was shown to self-assemble into vesicles in organic as well as aqueous media.[5] However, synthetic glycopolymers[11-18] typically do not form well-defined secondary structures and, that may render them less effective for biological recognition processes.[19] On the other hand, glycopolypeptides (GP), wherein sugar units are attached to a polypeptide backbone, mimic the molecular composition of proteoglycans and have been demonstrated to fold into well-defined secondary structures (e.g. α-helix), that allows ordered display of the carbohydrate moieties.[20-21] Hence, they represent suitable candidates for biological applications. This has led to a surge in reports on their synthesis as has been discussed in detail in chapter 1.3 & 1.4.[22-30] Here, we combine the advantages of glycopolypeptides with the microstructural tunability conferred by a block copolymer architecture, and demonstrate that such systems assemble into macromolecular assemblies whose geometry is determined by parameters that characterize the block copolymer such as chain length and backbone conformation. Only one report recently appeared on multiple morphologies obtained from poly(γ-benzyl-*l*-glutamate)-*b*-poly(galactosylated propargylglycine) amphiphilic block copolymers by varying the GP content.[31]

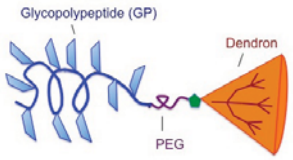

Figure 4.1: Schematic representation of glycopolypeptide-dendron conjugates.

Here we report the synthesis and self-assembly of GP-dendron conjugates for the first time, where dendrons are perfectly branched, wedge-shaped molecules. Our work is inspired by previous reports of dendron-containing macromolecules where the hydrophobicity of the dendron drives phase separation and macromolecular assembly at low polymer concentrations, while non-covalent interactions between the other block and structural asymmetry guide the self-assembly.[32-45] Dendron containing macromolecules is a broad class that includes linear-dendritic copolymer wherein linear polymer chains are attached to either periphery and/or focal point of the dendron, and dendron-rod and dendron-rod-coil type molecules wherein a rigid-rod-like small molecule is attached to focal point of dendron that is further connected to a linear polymer in the latter case. We hypothesized that the highly anisotropic molecular architecture realized from attaching dendron to one chain end of a GP, would provide an interesting motif to investigate self assembly. We prepared an amphiphilic block copolymer comprising a linear hydrophilic GP block with significant helicity, connected through a flexible amphipathic poly(ethylene glycol) (PEG) linker to a perfectly branched hydrophobic dendron (Figure 4.1; Table 4.1). We selected the gallate benzyl ether dendron with long alkyl chains so that the glycopolypeptides will be relatively polar conferring the amphiphilicity necessary for block copolymer assembly. Given the chemical and structural anisotropy in these block copolymers, we anticipate a strong tendency towards microphase segregation between the blocks. Our choice for the block copolymer allows us to independently tune (i) the size of the hydrophobic dendron (by varying the number of generations), as well as (ii) the chain length, and (iii) amphiphilicity of the polar glycopolypeptide (due to the protecting groups on the sugar residues). Finally, we can also independently vary the secondary structure in the polypeptide backbone and length of the PEG linker. We demonstrate that varying the molecular attributes of the glycopolypeptide-dendron block copolymer selectively affords various glycosylated morphologies such as micelles, nanorods, and gels.

Polymer Name RnGP-Gx†	R	Sugar residue	m	Structure of the Polymer
Ac16GP-G1	Ac	β-glucose	11	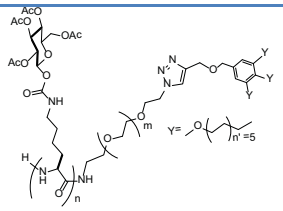
Ac28GP-G1	Ac	β-glucose	11	
16GP-G1	H	β-glucose	11	
28GP-G1	H	β-glucose	11	
Ac16GP-G2	Ac	β-glucose	11	
Ac28GP-G2	Ac	β-glucose	11	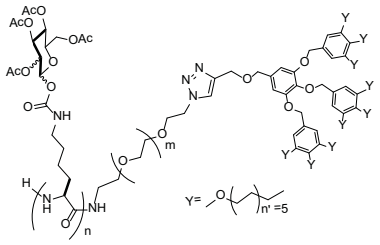
16GP-G2	H	β-glucose	11	
28GP-G2	H	β-glucose	11	
***manno*14GP-G2**	H	α-mannose	11	
***manno*28GP-G2**	H	α-mannose	11	
14HEG-GP-G2	H	β-glucose	5	

***rac*14GP-G2**	H	β-glucose	11	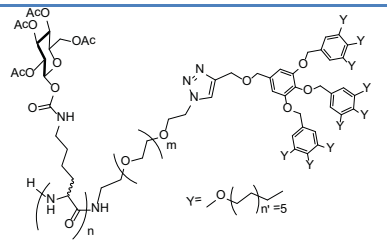
16GP-TEG-G2	H	β-glucose	2	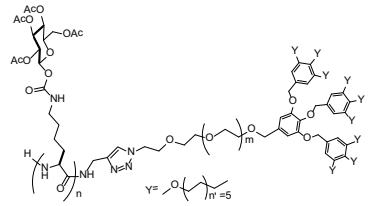

Table 4.1: Structural Parameters of GP-dendron Copolymers, n = GP chain length, R = Ac or H

4.2 Experimental Section

4.2.1 General

Propargyl 1,2 orthoesters of the corresponding carbohydrates were prepared according to literature procedure.[46-49] CbzLys(Boc)OH was obtained from Aldrich and converted to CbzLys(Boc)OBn using standard literature procedure.[50] $HAuCl_4$, triphosgene and azido-PEG-amine (n=11) were obtained from Aldrich and Polypure Inc. All other chemicals used were obtained from Merck, India. Diethyl ether, petroleum ether (b.p. 60˚-80˚C), ethylacetate, dichloromethane, tetrahydrofuran, dioxane were bought from Merck and dried by conventional methods and stored in the glove box. Ethyl acetate and dichloromethane were dried with P_2O_5 and CaH_2 and stored on activated molecular sieves 4Å after distillation. Tetrahydrofuran was passed through activated alumina and then dried on sodium wire and freshly distilled before use. Dioxane was distilled from CaH_2 and then refluxed with sodium wire and freshly distilled solvent was used. n-Hexane was dried with sodium wire, distilled and stored on activated molecular sieves 4Å for use. All the other solvent drying procedures were

followed from Purification of Laboratory Chemicals, 4th Edition by D.D. Perrin and W.L.F.Armarego.

FT-IR spectra were recorded on Perkin Elmer FT-IR spectrum GX instrument by making KBr pellets. Pellets were prepared by mixing 3mg of sample with 97mg of KBr.^{1}H NMR spectra were recorded on Bruker Spectrometers (200 MHz, 400 MHz or 500 MHz).^{13}C NMR and DEPT spectra were recorded on Bruker Spectrometer (50 MHz, 100MHz or 125MHz) and signals relative to deuterated solvent are reported. Size-exclusion chromatography of the glycopolypeptides was performed using an instrument equipped with Waters 590 pump with a Spectra System RI-150 RI detector. Separations were effected by 10^5, 10^3 and 500 Å Phenomenex 5μ columns using 0.1M LiBr in DMF eluent at 60 °C at the sample concentration of 5mg/ml. A constant flow rate of 1 mL/min was maintained, and the instrument was calibrated using polystyrene standards.Samples were imaged using a Quanta 200 3D scanning electron microscope (SEM). Prior to SEM imaging, the sample was sputter coated using a Polaron SC 7630 sputter coater giving Au thickness of 5 nm on the sample. An LSM 710 Carl Zeiss laser scanning confocal microscope (LSCM) was used to image the fluorescent samples. He-Ne laser (543 nm) and an Argon-ion laser (488 and 514 nm) were used for the experiments.TEM measurements were done at 200 kV on an FEI Technai F20 instrument. Gelation of Ac16GP-G2 in acetonitrile (concentration = 0.9 wt%) was monitored using dynamic oscillatory rheology.

4.2.2 Circular Dichroism Measurements

Aqueous solutions of all the glycopolypeptides and the glycopolypeptide-conjugated dendrons were filtered through 0.22 μm syringe filters. CD (190-260 nm) spectra of the glycopolypeptides (0.25-1.0 mg/mL in acetonitrile or deionized water) were recorded (JASCO CD SPECTROPOLARIMETER, Model J-815) in a cuvette with 1 mm path length. All the spectra were recorded for an average of 3 scans and the spectra were reported as a function of molar ellipticity [θ] vs wavelength.[51]

4.2.3 Sample preparation for Scanning Electron Microscopy

Glycopolypeptide-dendron conjugates (**Ac16GP-G2, Ac28GP-G2**) were dissolved in acetonitrile at about 0.7 wt% and left for 1 h at room temperature and deprotected samples (**16GP-G2**, **28GP-G2**) were dissolved in dimethyl sulfoxide at1

wt% and left for 5 h at room temperature. Finally, the solvent was removed by lyophilization. The freeze-dried samples were analyzed by scanning electron microscopy.

4.2.4 Sample preparation for Transmission Electron Microscopy

The 0.1 wt% solution of the polymer was spotted on carbon coated 400 mesh copper grid about 10 μL, kept for 15-20 min, the excess solvent was removed by touching the edge of the grid with Whatman filter paper, then grid was negatively stained by 0.2 wt% uranyl-acetate for 20 sec, and excess solvent was removed. Grid was washed twice with deionized water to remove excess unbound uranyl-acetate from the grid. Grids were dried in desiccator for 20h and analyzed by transmission electron microscopy.

4.2.5 SAXS

SAXS measurements were performed on a Bruker Nanostar equipped with a rotating anode generator (18 kW) operated at a voltage of 45 kV and current of 100 mA (λ= 1.54 Å). The X-rays are collimated through a three-pinhole system, and data is acquired using a 2D gas filled Hi-Star detector over a q-range of 0.011-0.2 $Å^{-1}$. The detector was calibrated using a silver behenate sample. Samples were sealed in quartz capillaries having an outer diameter of 2 mm and wall thickness of ≈10μm. The capillary was filled with gel sample and after proper sealing, the polymer sample (1 wt% of Ac16GP-G2 in Acetonitrile) was heated to 50^{o}C and cooled back to room temperature before data collection. Data was corrected for background scattering (including solvent scattering from acetonitrile and air scattering). The 2D data were reduced to 1D by circularly averaging, using the software provided with the instrument.

Rheology was performed in a Couette geometry using the MCR 301 rheometer. For the gelation experiments reported in this work, the 0.9 wt% of Ac16GP-G2 in acetonitrile was first heated to 45^{o}C, above the gel point, and was then cooled to 25^{o}C. The initial time in the gelation experiment was when the sample was cooled to 25^{o}C. Isothermal time sweep experiments at 25^{o}C were performed at a frequency of 1 rad/s and at small oscillation amplitude of 0.5%, ensuring that the sample response is in the linear visco-elastic regime.

4.3 Synthetic Procedures

*4.3.1 General procedure for the synthesis of amino acid glycosyl carbamates(**2a, 2a'** and **2b**)*

To a solution of propargyl 1,2-orthoester (0.1 mmol) of D-Glucose or D-Mannose, Cbz-*l**d*-Lys(Boc)OBn (0.11 mmol) and activated 4Å molecular sieves powder (50 mg) in anhydrous CH_2Cl_2 (5 mL) was added $HAuCl_4$ (10 mol%) under argon atmosphere at room temperature. The reaction mixture was stirred at room temperature for the specified time and filtered. The filtrate was concentrated in vacuo. The resulting residue was purified by silica gel column chromatography using ethyl acetate-petroleum ether as the mobile phase to afford the compounds *per-O*-tetra-acetate-β-gluco-Cbz-*l*-lys-OBn(**2a**), *per-O*-tetra-acetate-β-gluco-Cbz-*d*-lys-OBn(**2a'**) and *per-O*-tetra-acetate-α-manno-Cbz-*l*-lys-OBn(**2b**) respectively.

Compound **2a**: $[\alpha]_D^{25}$= +4.4(*c*1.0, $CHCl_3$); ^{1}H NMR (400.13MHz, $CDCl_3$): δ 1.20-1.57(m, 4H), 1.60-1.75 (m, 1H), 1.76-1.92 (m, 1H), 2.01(s, 3H), 2.03 (m, 6H), 2.06 (s, 3H), 2.96-3.20 (m, 2H), 3.71-3.90 (m, 1H), 4.05-4.15 (m, 1H), 4.29 (dd, 1H, *J* = 4.25, 12.50 Hz), 4.40 (dd, 1H, *J* =7.3, 12.50 Hz), 5.0 (t, *J* = 5.2 Hz, 1H), 5.05-5.14 (m, 4H), 5.15-5.30 (m, 3H), 5.41(d, 1H, *J* = 8.01 Hz), 5.65 (d, 1H, *J* = 8.2 Hz), 7.27-7.43 (m, 10H); ^{13}C NMR (50.32MHz, $CDCl_3$): δ 20.55(2C), 20.6, 20.7, 22.1, 28.87, 32.16, 40.87, 53.57, 61.41, 67.06, 67.18, 67.78, 70.17, 72.35, 72.78, 92.72, 128.12-128.64, 135.2, 136.1, 153.73, 155.97, 169.44, 169.45, 170.05, 170.63, 172.12; MALDI-TOF(m/z): Calcd for $C_{36}H_{44}KN_2O_{15}$: 783.2379, Found: 783.2333.

Compound **2b**: $[\alpha]_D^{25}$= +22.1(*c*1.0, $CHCl_3$); ^{1}H NMR (200.13MHz, $CDCl_3$): δ 1.10-1.92(m, 6H), 1.99, 2.02, 2.08, 2.17(4s, 12H), 3.13(q, 2H, *J* = 6.1, 12.3Hz), 3.98-4.16(m, 2H), 4.30(dd, 1H, *J* = 4.7, 12.5Hz), 4.41(m, 1H), 4.98(t, 1H, *J* = 5.7 Hz), 5.10(d, 2H, *J* = 1.5 Hz), 5.17(d, 2H, *J* = 3.4 Hz), 5.23-5.43(m, 4H), 6.01(d, 1H, *J* = 1.4 Hz), 7.32-7.38(m, 10H); ^{13}C NMR (50.32MHz, $CDCl_3$): δ 20.5(3C), 20.6, 22.2, 28.8, 32.0, 40.6, 53.5, 61.9, 65.4, 66.8, 67.0, 68.4, 68.8, 70.0, 91.1, 127.9-128.5, 135.1, 136.1, 153.0, 155.9, 169.4, 169.6, 170.0, 170.1, 172.1; MALDI-TOF(m/z): Calcd for $C_{36}H_{44}KN_2O_{15}$: 783.2379, Found: 783.2373.

*4.3.2 General procedure for the glycoN-carboxyanhydrides **3a, 3a'** and **3b'***

Hydrogenolysis of compounds *per*-*O*-tetra-acetate-β-gluco-*l*-lys(**2a**), or *d*-lys(**2a'**) and *per*-*O*-tetra-acetate-β-manno-*l*-lys(**2b**)were carried out using 10% Pd/C in MeOH/EtOAc (9:1) at 400 psi for 12 hrs. After completion of the reaction, the reaction mixture was filtered and concentrated under reduced pressure to afford *per*-*O*-acetylated-D-Glucose-*l**d*-lysine carbamate and *per*-*O*-acetylated-D-Mannose-*l*-lysine carbamate in almost quantitative yield. The resulting compounds were directly used for NCA synthesis without any further purification.

***3a, 3a'and 3b'*:**To a solution of *per*-*O*-acetylated-D-Glucose-*l**d*-lysine carbamate or *per*-*O*-acetylated-D-Mannose-*l*-lysine carbamate (0.96 mmol) in freshly distilled tetrahydrofuran (5 mL) was added accordingly a solution of triphosgene (142 mg, 0.484 mmol) in anhydrous tetrahydrofuran (2mL) under argon and the reaction mixture was heated to 50°-55°C. α-pienene (0.222 ml, 1.44 mmol) was then added and the reaction mixture was allowed to stir for an additional 2 h. The reaction mixture was then cooled to room temperature and poured into dry hexane (300 ml) to afford a white precipitate, which was filtered off quickly and crystallized two more times using a mixture of ethyl acetate and petroleum ether. Finally, the white precipitate of glyco-*N*-carboxyanhydride *per*-*O*-acetylated-D-Glucose-*l*-lysine carbamate NCA(**3a**), or *per*-*O*-acetylated-D-Glucose-*d*-lysine carbamate NCA(**3a'**) or *per*-*O*-acetylated-D-Mannose-*l*-lysine carbamate NCA(**3b**) obtained was dried under vacuum and transferred into the glove box. Final yield 80%.

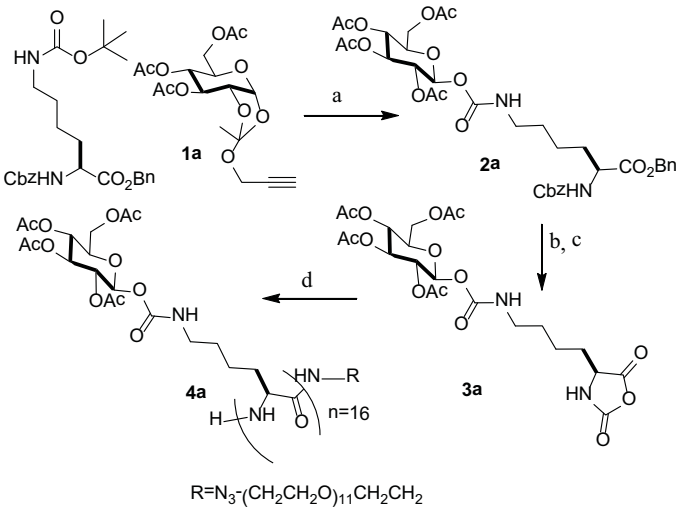

a) $HAuCl_4$, CH_2Cl_2, rt, 0.5h, 4A° MS Powder, Yield (80%); b) Pd/C, H_2, 400 psi, CH_3OH, 12h, Yield (> 95%); c) Triphosgene, THF, α-pienene, 70°C, Yield (80%); d) Dioxane, Proton Sponge(1.0 equiv), 24 hrs, RT.

Scheme 4.1: Synthesis of protected-glycopolypeptides by ring opening polymerization.

Compound **3a**: ^{1}H NMR (400.13MHz, CD_3CN): δ 1.2-1.6(m, 4H), 1.65-1.92 (m, 2H), 1.95, 1.99, 2.00, 2.02 (4s, 12H), 3.10(dd, 2H, *J* = 6.26, 12.52 Hz), 3.88-4.0(m, 1H), 4.06(dd, *J* = 2.14, 12.52 Hz,1H), 4.21 (dd, 1H, *J* = 4.6, 12.52 Hz), 4.28-4.40 (m, 1H), 5.02(dd,*J*= 8.63, 9.88 Hz 1H), 5.08(d, 1H, *J* = 9.77 Hz), 5.34(t, 1H, *J* = 9.5 Hz),5.73(d, 1H, *J* = 8.59 Hz), 6.84(bs, 1H); ^{13}C NMR (100.61MHz, CD_3CN): δ19.81, 19.86(2C), 19.88, 21.6, 28.56, 30.72, 40.13, 57.34, 61.57, 67.89, 70.09, 72.03, 72.14, 92.24, 151.91, 153.90, 169.33, 169.52, 169.83, 170.29, 171.07.

Compound **3b**:^{1}H NMR (500.13MHz, CD_2Cl_2): δ 1.35-1.88(m, 6H), 1.99, 2.03, 2.07, 2.16(4s, 12Hz), 3.23(q, 2H, *J* = 6.7, 12.6 Hz), 3.68(t, 1H, *J* = 6.5 Hz), 4.08(m, 1H), 4.13(dd, 1H, *J* = 2.8, 12.2 Hz), 4.23(dd, 1H, *J* = 4.6, 12.2 Hz), 4.35(dd, 1H, *J* = 4.7, 6.9 Hz), 5.20-5.35(m, 3H), 5.94(d, 1H, *J* = 1.7 Hz), 6.72(bs, 1H);^{13}C NMR (125.76MHz, CD_2Cl_2): δ 20.8(2C), 20.9(2C), 22.2, 29.3, 31.6, 40.7, 57.9, 62.7, 66.1, 68.9, 69.3, 70.5, 91.7, 152.3, 153.8, 170.0, 170.3, 170.4, 170.6, 171.2.

4.3.3 General procedure for the synthesis of glycopolypeptides

To a solution of glyco or manno-*l**d*-lysine NCA (100 mg/mL) in dry dioxane was added "proton sponge" *N*,*N*'-tetramethylnapthalene (1.0 equivalent to monomer; 1 M) as an additive and azido-PEG-amine (0.5 M) as the initiator inside the glove box. The progress of the polymerization was monitored by FT-IR spectroscopy by comparing with the intensity of the initial NCA anhydride stretching at 1789 cm^{-1} and 1852 cm^{-1}. The reactions were generally complete within 36 hrs. Aliquots were removed after completion of polymerization for GPC analysis. Finally the solvent was removed under reduced pressure. The resulting residue was dissolved in dichloromethane and then the polymer was precipitated out by addition of methanol. The precipitated polymer was collected by centrifugation and dried to afford white glycopolypeptides**Ac16GP**, **Ac28GP**, **Ac8GP** and **Ac*manno*14GP** in ~ 85-90% yield.

For synthesis of **Ac*rac*14GP,** 3a(β-gluco-*O*-*l*-lys NCA) and 3a'(β-gluco-*O*-*d*-lys NCA) were mixed in equimolar quantities and then polymerization was carried out as above.

For synthesis of polymer **Ac16GP-alkyne**, 3a(β-gluco-*O*-*l*-lys NCA) NCA (100 mg/mL) in dry dioxane was added "proton sponge" N,N'-tetramethylnapthalene (1.0 equivalent to monomer; 1 M) as an additive and propargyl-amine (0.3 M) as the initiator inside the glove box and then polymerization was carried out as has been described above.

For synthesis of polymer **Ac14GP-HEG-N_3**, 3a(β-gluco-*O*-*l*-lys NCA) NCA (100 mg/mL) in dry dioxane was added "proton sponge" N,N'-tetramethylnapthalene (1.0 equivalent to monomer; 1 M) as an additive and azido-HEG-amine (0.5 M) as the initiator inside the glove box and then polymerization was carried out as has been described above.

For synthesis of polymer **Ac*gluco-manno*(3:1)-14GP, 3a**(β-gluco-*O*-*l*-lys NCA) and **3b** (α-manno-*O*-*l*-lys NCA) were mixed in 3:1 proportions (by weight) and then polymerization was carried out as has been described above.

Polymer **Ac16GP**. ^{1}H NMR (400.13 MHz, $CDCl_3$): δ 1.25-1.86(m, 6H), 1.98-2.10(m, 12H), 2.90-3.24(m, 3H), 3.62-3.68(m, for CH_2CH_2O unit in initiator 44H), 3.70-4.0 (m, 1H), 4.0-4.15(m, 1H), 4.17-4.35 (m, 1H), 4.9-5.15 (m, 2H), 5.2-5.5 (m, 1H), 5.56-5.80 (m, 1H).

Polymer **Ac28GP**: ^{1}H NMR (400.13 MHz, $CDCl_3$): δ 1.25-1.86(m, 6H), 1.98-2.10(m, 12H), 2.90-3.24 (m, 3H), 3.62-3.68(m, for CH_2CH_2O unit in initiator44H), 3.70-4.0 (m, 1H), 4.0-4.15(m, 1H), 4.17-4.35 (m, 1H), 4.9-5.15 (m, 2H), 5.2-5.5 (m, 1H), 5.56-5.80 (m, 1H).

Polymer **Ac8GP**: ^{1}H NMR (400.13 MHz, $CDCl_3$): δ 1.25-1.88(m, 6H), 1.99-2.1(4s, 12Hz), 3.3-3.4 (m, 1H), 3.45-3.57 (m, 1H), 3.7-3.95 (m, 1H), 3.62-3.68(m, for CH_2CH_2O unit in initiator44H), 4.0-4.15(m, 1H), 4.17-4.4 (m, 1H), 4.9-5.17(m, 2H), 5.20-5.35(m, 1H), 5.5-5.75 (m, 1H).

Polymer **Ac*rac*14GP**:^{1}H NMR (400.13 MHz, $CDCl_3$): δ 1.25-1.86(m, 6H), 1.98-2.10(m, 12H), 2.75-3.40(m, 2H), 3.45-3.57 (m, 1H), 3.62-3.68(m, for CH_2CH_2O unit in initiator44H), 3.70-4.0(m, 1H), 4.05-4.24(m, 1H), 4.9-5.15(m, 2H), 5.25-5.5(m, 1H), 5.55-5.80(m, 1H).

Polymer **Ac*manno*14GP**: ^{1}H NMR (400.13 MHz, $CDCl_3$): δ 1.25-1.88(m, 6H), 1.95-2.15(4s, 12Hz), 3.0-3.45 (m, 4H), 3.75-4.4(m, 1H), 3.62-3.68(m, for CH_2CH_2O unit in initiator 44H), 5.0-5.5(m, 2H), 5.7-5.85(m, 1H).

Polymer **Ac*manno*28GP**: ^{1}H NMR (400.13 MHz, $CDCl_3$): δ 1.25-1.88(m, 6H), 1.95-2.15(4s, 12Hz), 3.0-3.45 (m, 4H), 3.75-4.4(m, 1H), 3.62-3.68(m, for CH_2CH_2O unit in initiator 44H), 5.0-5.5(m, 2H), 5.7-5.85(m, 1H).

Polymer **Ac[*gluco*+*manno*](3:1)14GP**: ^{1}H NMR (400.13 MHz, $CDCl_3$): δ 1.25-1.86(m, 6H), 1.98-2.10(m, 12H), 2.90-3.24(m, 3H), 3.62-3.68(m, for CH_2CH_2O unit in initiator 44H), 3.70-4.0 (m, 1H), 4.0-4.15(m, 1H), 4.17-4.35 (m, 1H), 4.9-5.15 (m, 2H), 5.2-5.5 (m, 1H), 5.56-5.80 (m, 1H).

Polymer **Ac16GP-alkyne**: ^{1}H NMR (400.13 MHz, $CDCl_3$): δ 1.25-1.86(m, 6H), 1.98-2.10(m, 12H), 2.90-3.24(m, 3H), 2.76(s, for alkyne proton in initiator 1H), 3.70-4.0 (m, 1H), 4.0-4.15(m, 1H), 4.17-4.35 (m, 1H), 4.9-5.15 (m, 2H), 5.2-5.5 (m, 1H), 5.56-5.80 (m, 1H).

Polymer **Ac14GP-HEG-N_3**: ^{1}H NMR (400.13 MHz, $CDCl_3$): δ 1.25-1.88(m, 6H), 1.95-2.15(4s, 12Hz), 3.0-3.45 (m, 4H), 3.75-4.4(m, 1H), 3.62-3.68(m, for CH_2CH_2O unit in initiator 24H), 5.0-5.5(m, 2H), 5.7-5.85(m, 1H).

4.3.4 General procedure for synthesis of alkyne-containing dendrons

Dendrons with benzylic alcohol at the focal point (G1-CH_2OH or G2-CH_2OH) were synthesized by following reported procedure.[52,53] Then propargylation was carried out as follows.

In a dry three-neck round bottom flask NaH (1.2 mol, 60% suspension in mineral oil) was taken and washed with hexanes under argon. Dry THF and dendron with benzyl alcohol at the focal point (G1-CH_2OH or G2-CH_2OH, 1 mol) were added and stirred for 10 min followed by addition of propargyl bromide (1.1 mol). The reaction mixture was stirred for 10 h and poured in water. It was extracted with dichloromethane, organic layer was washed with water, brine and dried over anhydrous sodium sulfate before concentrating on rotary evaporator. The crude product was purified by silica gel flash column chromatography eluting with a mixture of ethyl acetate and hexanes (Dendrons were synthesized by Dr. Ashootosh V. Ambade's student Nagendra Kalva in NCL).

G1-alkynyl: Yield (75 %); ^{1}H NMR (200.13MHz, $CDCl_3$) δ: 0.88(t, 9H,J=6.7Hz), 1.26-1.45(overlapped peaks,54H),1.76(m,6H),2.47(t,1H,J=2.4Hz),3.97(m,6H),4.16(d,2H,J=2.3Hz),4.51(s,2H), 6.54(s,2H).

G2-alkynyl: Yield (70 %); ^{1}H NMR (200.13MHz, $CDCl_3$) δ:0.88(t,27H,J=7Hz),1.26-1.45(overlapped peaks,162H),1.70(m,18H),2.47(s,1H),3.76(t,4H,J=6.2Hz),3.87(t,8H,J=6.4), 3.92(t,6H,J=6.5Hz),4.13(d, 2H),4.96(s, 2H),5.00(s, 4H),6.62(s,6H),6.66(2H, s).

4.3.5 Synthesis of TEG azide-containing G2 dendron

Dendron with carboxylic acid at the focal point (G2-COOH) was synthesized by following reported procedure.[54] G2-COOH (1 mol) was dissolved in dry dichloromethane in a dry three-neck round bottom flask and 1-ethyl-3-(3-dimethylaminopropyl)carbodiimide (EDC, 1.2 mol) and 4-dimethylamino pyridine (DMAP, cat.) were added, and stirred for 20 min followed by addition of azidoethoxy-ethoxy-ethanol(1.1 mol). The reaction mixture was stirred at rt for 24 h and poured in water. It was extracted with dichloromethane, organic layer was washed with water,

brine and dried over anhydrous sodium sulfate before concentrating on rotary evaporator. The crude product was purified by silica gel flash column chromatography eluting with a mixture of ethyl acetate and hexanes (Dendron were synthesized by Dr. Ashootosh V. Ambade's student Nagendra Kalva in NCL).

G2-TEG-azide: Yield (30 %); ^{1}H NMR (200.13MHz, $CDCl_3$) δ:0.87(t, 27H, J=7Hz),1.26-1.41(overlapped peaks,162H),1.71(m,18H), 3.33 (m, 2H), 3.66 (m, 4H), 3.73 (m,4H), 3.87(m, 18H), 4.45(m, 2H), 5.02 (s, 6H), 6.58(2H, s), 6.62(s,4H), 7.40 (S, 2H)

4.3.6 Synthesis of glycopolypeptide-dendron conjugates by "click reaction"

To a solution of azide-PEG end-functionalized acetyl protected glycopolypeptide (**Ac16GP** and**Ac28GP**) in THF/methanol/water (2:1:0.2) was added alkynyl-dendron (**G1** and **G2**) (1.5 eq) and resultant reaction mixture was degassed by three freeze-pump-thaw cycles. $CuSO_4$ (0.2 eq) and sodium ascorbate (0.4 eq) were then added and the reaction was allowed to proceed for 24 h under argon atmosphere (Scheme 2). The progress of the reaction was monitored by the disappearance of the azide stretch at 2115 cm^{-1} in FT-IR (Figure 4.3). When > 95% of the azide peak had disappeared, the solvent was removed under reduced pressure. The reaction mixture was dissolved in ethyl acetate and washed multiple times with aqueous ammonia solution to remove the copper salt. Then the solvent was evaporated completely under reduced pressure. Excess dendron alkyne (**G1** and **G2**) was removed by multiple washings with mixed solvent (Ethylacetate : Hexane = 0.1:0.9). The off-white compounds were dried under vacuum overnight at 45˚C to afford polymers **Ac16GP-G1**, **Ac28GP-G1**, **Ac16GP-G2** and **Ac28GP-G2**.

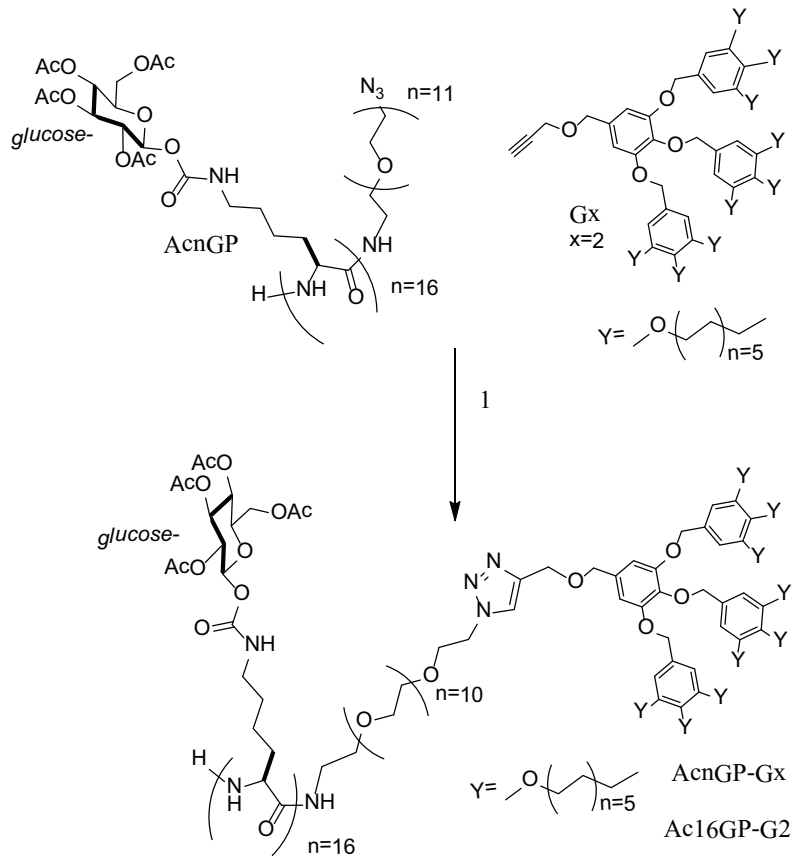

1) $CuSO_4$/Sodium ascorbate (0.2 mol%), THF: MeOH:H_2O = 1:1:0.2

Scheme 4.2: Synthesis of glycopolypeptide-dendron conjugates.

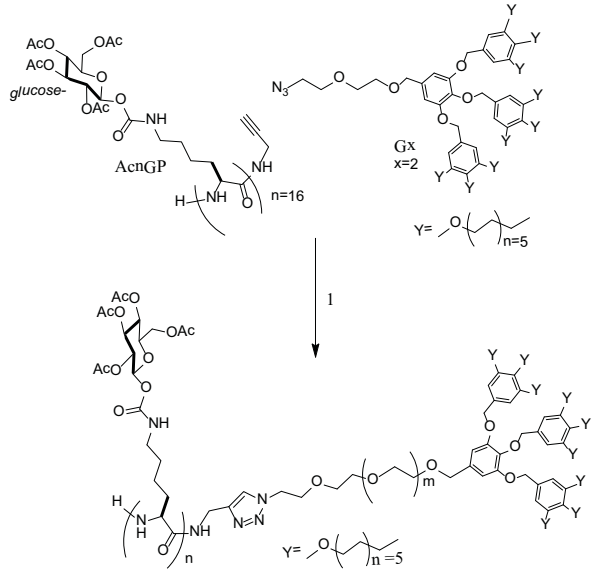

1) THF,MeOH, H_2O, $CuSO_4$, Na-ascorbate

Scheme 4.3: Synthesis of Ac16TEGGP-G2.

In the synthesis of the polymer **Ac*rac*14GP-G2**, **Ac*manno*14GP-G2** and **Ac8GP-G2**, polymer **Ac*rac*14GP, Ac*manno*14GP** and **Ac8GP** were clicked with only second generation dendron (**G2**). Polymers were thoroughly characterized by ^{1}H NMR, IR and CD spectroscopy.

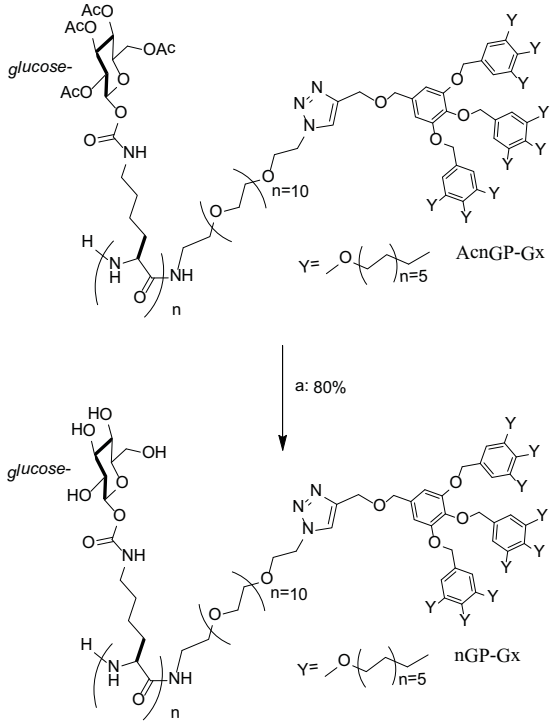

Scheme 4.4: Synthesis of fully deprotected glycopolypeptide-dendron conjugates.

Polymer **Ac16GP-G1**:^{1}H NMR (400.13 MHz, $CDCl_3$): δ0.7-0.9(m, 9H), 1.1-1.2(m, 66H), 1.25-1.86(m, 6H), 1.98-2.10(m, 12H), 2.90-3.24 (m, 3H), 3.62-3.68(m, for CH_2CH_2O unit in initiator 44H), 3.70-4.0 (m, 1H), 4.0-4.15(m, 1H), 4.17-4.35 (m, 1H), 4.9-5.15 (m, 2H), 5.2-5.5 (m, 1H), 5.56-5.80 (m, 1H), 6.46-6.55(m, 2H), 7.65-7.8(m, 1H).

Polymer**Ac28GP-G1**: ^{1}H NMR (400.13 MHz, $CDCl_3$): δ0.7-0.9(m, 9H), 1.1-1.2(m, 66H),1.25-1.86(m, 6H), 1.98-2.10(m, 12H), 2.90-3.24 (m, 3H), 3.62-3.68(m, for CH_2CH_2O unit in initiator 44H), 3.70-4.0 (m, 1H), 4.0-4.15(m, 1H), 4.17-4.35 (m, 1H), 4.9-5.15 (m, 2H), 5.2-5.5 (m, 1H), 5.56-5.80 (m, 1H), 6.5-6.7(m, 2H), 7.65-7.8(m, 1H).

Polymer **Ac16GP-G2**: ^{1}H NMR (400.13 MHz, $CDCl_3$): δ0.7-0.9(m, 27H), 1.1-1.2(m, 198H), 1.25-1.86(m, 6H), 1.98-2.10(m, 12H), 2.90-3.24 (m, 3H), 3.62-3.68(m, for

CH_2CH_2O unit in initiator 44H), 3.70-4.0 (m, 1H), 4.0-4.15(m, 1H), 4.17-4.35 (m, 1H), 4.9-5.15 (m, 2H), 5.2-5.5 (m, 1H), 5.56-5.80 (m, 1H), 6.46-6.55(m, 8H), 7.65-7.8(m, 1H).

Polymer **Ac28GP-G2**: ^{1}H NMR (400.13 MHz, $CDCl_3$): δ0.7-0.9(m, 27H), 1.1-1.2(m, 198H), 1.25-1.86(m, 6H), 1.98-2.10(m, 12H), 2.90-3.24 (m, 3H), 3.62-3.68(m, for CH_2CH_2O unit in initiator 44H), 3.70-4.0 (m, 1H), 4.0-4.15(m, 1H), 4.17-4.35 (m, 1H), 4.9-5.15 (m, 2H), 5.2-5.5 (m, 1H), 5.56-5.80 (m, 1H), 6.5-6.7(m, 8H), 7.65-7.8(m, 1H).

Polymer**Ac*rac*14GP-G2**: ^{1}H NMR (400.13 MHz, $CDCl_3$): δ0.7-0.9(m, 27H), 1.1-1.2(m, 198H),1.25-1.86(m, 6H), 1.98-2.10(m, 12H), 2.75-3.40(m, 2H), 3.45-3.57 (m, 1H), 3.62-3.68(m, for CH_2CH_2O unit in initiator 44H), 3.70-4.0(m, 1H), 4.05-4.24(m, 1H), 4.9-5.15(m, 2H), 5.25-5.5(m, 1H), 5.55-5.80(m, 1H), 6.5-6.7(m, 8H), 7.65-7.8(m, 1H).

Polymer **Ac*manno*14GP-G2**: ^{1}H NMR (400.13 MHz, $CDCl_3$): δ0.7-0.9(m, 27H), 1.1-1.2(m, 198H),1.25-1.88(m, 6H), 1.95-2.15(4s, 12Hz), 3.0-3.45 (m, 4H), 3.75-4.4(m, 1H), 3.62-3.68(m, for CH_2CH_2O unit in initiator 44H), 5.0-5.5(m, 2H), 5.7-5.85(m, 1H), 6.5-6.7(m, 8H), 7.65-7.8(m, 1H).

Polymer **Ac8GP-G2**: ^{1}H NMR (400.13 MHz, $CDCl_3$): δ0.7-0.9(m, 27H), 1.1-1.2(m, 198H),1.25-1.88(m, 6H), 1.99-2.1(4s, 12Hz), 3.3-3.4 (m, 1H), 3.45-3.57 (m, 1H), 3.7-3.95 (m, 1H), 3.62-3.68(m, for CH_2CH_2O unit in initiator 44H), 4.0-4.15(m, 1H), 4.17-4.4 (m, 1H), 4.9-5.17(m, 2H), 5.20-5.35(m, 1H), 5.5-5.75 (m, 1H), 6.5-6.7(m, 8H), 7.65-7.8(m, 1H).

Polymer **Ac*manno*28GP-G2**: ^{1}H NMR (400.13 MHz, $CDCl_3$): δ0.7-0.9(m, 27H), 1.1-1.2(m, 198H),1.25-1.88(m, 6H), 1.95-2.15(4s, 12Hz), 3.0-3.45 (m, 4H), 3.75-4.4(m, 1H), 3.62-3.68(m, for CH2CH2O unit in initiator 44H), 5.0-5.5(m, 2H), 5.7-5.85(m, 1H), 6.5-6.7(m, 8H), 7.65-7.8(m, 1H).

Polymer **Ac*gluco-manno*(3:1)-14GP-G2**: ^{1}H NMR (400.13 MHz, $CDCl_3$): δ0.7-0.9(m, 27H), 1.12-1.25(m, 198H), 1.25-1.86(m, 6H), 1.98-2.20(m, 12H), 2.75-3.4 (m, 3H), 3.62-3.68(m, for CH_2CH_2O unit in initiator 44H), 3.70-4.0 (m, 1H), 4.0-4.17(m,

1H), 4.17-4.35 (m, 1H), 4.9-5.15 (m, 2H), 5.2-5.5 (m, 1H), 5.56-6.2 (m, 1H), 6.46-6.55(m, 8H), 7.65-7.8(m, 1H).

Polymer **Ac14GP-HEG-G2**: ^{1}H NMR (400.13 MHz, $CDCl_3$): δ0.7-0.9(m, 27H), 1.12-1.25(m, 198H), 1.25-1.86(m, 6H), 1.98-2.20(m, 12H), 2.75-3.4 (m, 3H), 3.62-3.68(m, for CH_2CH_2O unit in initiator 24H), 3.70-4.0 (m, 1H), 4.0-4.17(m, 1H), 4.17-4.35 (m, 1H), 4.9-5.15 (m, 2H), 5.2-5.5 (m, 1H), 5.56-6.2 (m, 1H), 6.46-6.55(m, 8H), 7.65-7.8(m, 1H).

Polymer **Ac16GP-TEG-G2**: ^{1}H NMR (400.13 MHz, $CDCl_3$): δ0.7-0.9(m, 27H), 1.12-1.25(m, 198H), 1.25-1.86(m, 6H), 1.98-2.20(m, 12H), 2.75-3.4 (m, 3H), 3.62-3.68(m, for CH_2CH_2O unit in initiator 12H), 3.70-4.0 (m, 1H), 4.0-4.17(m, 1H), 4.17-4.35 (m, 1H), 4.9-5.15 (m, 2H), 5.2-5.5 (m, 1H), 5.56-6.2 (m, 1H), 6.46-6.55(m, 8H), 7.65-7.8(m, 1H).

4.3.7 Deprotection procedure for the glycopolypeptide-dendron conjugates

Hydrazine monohydrate (25 eq) was added to the solutions of all the acetyl protected glycopolypeptides in tetrahydrofuran (10 mg/mL) and the reactions were stirred for 7-8 h at room temperature. Reactions were quenched by addition of acetone and then solvent was removed almost completely under reduced pressure. The solid residues were dissolved in a mixture of dimethylsulfoxide and deionized water (1:1) and transferred to dialysis tubing (3.5 and 12 KDa molecular weight cut-off according to polymer molecular weight). The samples were dialyzed against deionized water for 3 days, with water changes once every two hours for the first day, and then thrice per day. Dialyzed polymers were lyophilized to yield glycopolypeptide-dendrons as white fluffy solids (~70% yield).

Polymer **16GP-G1**. ^{1}H NMR (400.13 MHz, DMSO-d_6): δ0.65-1.85(m, 81H), 2.75-3.3(m, 4H), 3.3-3.60(m, for CH_2CH_2O unit in initiator, 44H), 3.61-4.0 (m, 2H), 4.1-4.75(m, 1H), 4.80-5.42(m, 2H), 6.40-6.6(m, 2H), 7.0-7.4(m, 1H).

Polymer **28GP-G1**: ^{1}H NMR (400.13 MHz, DMSO-d_6): δ 0.65-1.85(m, 81H), 2.75-3.3(m, 4H), 3.3-3.60(m, for CH_2CH_2O unit in initiator, 44H), 3.61-4.0 (m, 2H), 4.1-4.75(m, 1H), 4.80-5.42(m, 2H), 6.40-6.6(m, 2H), 7.0-7.4(m, 1H).

Polymer **16GP-G2**: ^{1}H NMR (400.13 MHz, DMSO-d_6): δ0.65-1.85(m, 231H), 2.75-3.3(m, 4H), 3.3-3.60(m, for CH_2CH_2O unit in initiator, 44H), 3.61-4.0 (m, 2H), 4.1-4.75(m, 1H), 4.80-5.42(m, 2H), 6.40-6.6(m, 8H), 7.0-7.4(m, 1H).

Polymer **28GP-G2**:^{1}H NMR (400.13 MHz, DMSO-d_6): δ 0.65-1.85(m, 231H), 2.75-3.3(m, 4H), 3.3-3.60(m, for CH_2CH_2O unit in initiator, 44H), 3.61-4.0 (m, 2H), 4.1-4.75(m, 1H), 4.80-5.42(m, 2H), 6.40-6.6(m, 8H), 7.0-7.4(m, 1H).

*4.3.8 Synthesis of Fluorescein attached **Ac16GP-G2***

10 mg (0.9 μM) of **Ac16GP-G2** was dissolved in 1 mL freshly distilled tetrahydrofuran. Then fluorescein N-hydroxysuccinimide ester 0.8 mg (1.8 μM) was added to the reaction mixture and allowed to stir for 12 h (Scheme 4.5). The solvent was removed under reduced pressure, residue dissolved in ethyl acetate, organic layer was washed with water to remove excess fluorescein. Finally, polymer was precipitated from dichloromethane into methanol and dried to afford fluorescein labeled glycopolypeptide-dendron conjugate, **FrAc16GP-G2**.

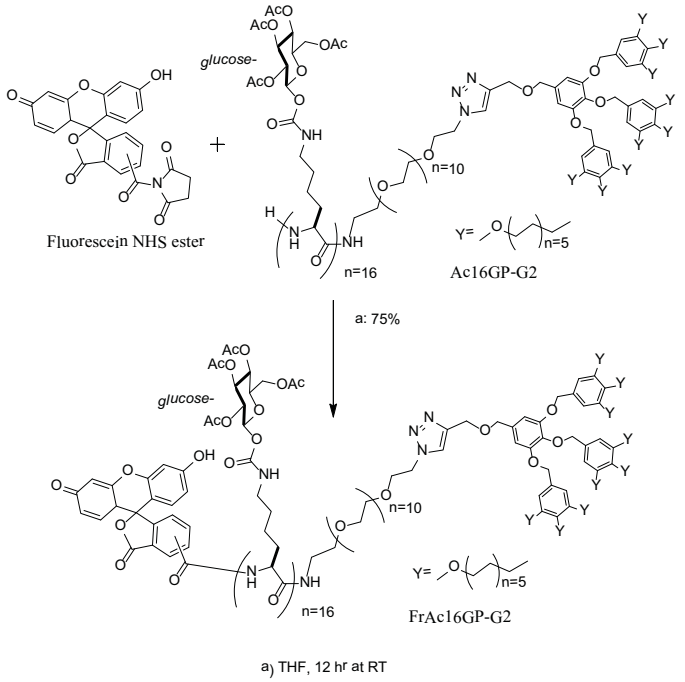

Scheme 4.5: Synthesis of fluorescein labeled glycopolypeptide-dendron conjugates.

4.3.9 Sample preparation for confocal microscopy

Polymer **FrAc16GP-G2** was dissolved in acetonitrile at 0.7 wt% and 50μL solution was placed on glass slide and covered by cover slip. After 30 min the imaging was done by confocal microscope.

4.3.10 Synthesis of 8GP-G2

To a solution of glyco-*l*-lysine NCA (25 mg/ml) in dry dioxane was added "proton sponge" *N*,*N*'-tetramethylnapthalene (1.0 eq w.r.t. monomer; 1 M) as an additive and azido-PEG-amine (0.1 M) as the initiator in the monomer to initiator ratio of 7, inside the glove box. The progress of the polymerization was monitored by FT-IR spectroscopy by comparing with the intensity of the initial NCA anhydride stretching at 1789 cm^{-1} and 1852 cm^{-1}. Polymer **Ac8GP** was isolated in the way described above. It was clicked with G2-dendron to afford **Ac8GP-G2** as described above, and characterized by IR spectroscopy. Polymer **Ac8GP-G2** was deprotected using the same procedure to obtain polymer **8GP-G2**. Sample was prepared for transmission electron microscopy in the same way described before at 0.1 wt% polymer concentration in water.

4.3.11 Quantitative Precipitation Assay

Quantitative precipitations and analysis were carried out by modification of Brewer'smethod,[55, 56] as adapted by Cloninger and coworkers,[57] using a *Con-A* solution of 35 μM. A known concentration of lectin (35 μM for *manno*-14GP-G2 and *manno*-28GP-G2 and 17.5 μM for *gluco-manno*(3:1)-14GP-G2) was added to different concentrations of polymer ***manno*-14GP-G2, *gluco-manno*(3:1)-14GP-G2** and ***manno*-28GP-G2** and the precipitate was centrifuged and collected washing with Tris buffer. *Con-A* and ligand were prepared in precipitation buffer (Tris-HCl pH 7.5, 90 mM NaCl, 1 μM $CaCl_2$, 1μM $MnCl_2$), vortexed briefly to mix for 1 min and then incubated for 5 h at 22 ˚C. The final concentration of *Con-A* was 35μM (assuming *Con-A* as tetramer, Mw= 104,000 Da). White precipitates were pelted by centrifugation at 5000 rpm for 2 min. Supernatants were removed by pipet and pellets were gently washed twice with cold buffer. Pellets were then resuspended in 400 μL 100 mM α-methyl mannopyranoside, and completely dissolved with in 10-15 mins incubation at room temperature. Protein content was determined by measuring the

absorbance at 280 nm. The solutions were analyzed for protein content using $A_{280}^{1\%}$ = 13.7 for lectin solutions.

4.3.12 Fluorescence Emission Spectroscopy

1.7 mg of polymer **28GP-G2** was mixed in 2 mL of dimethylsulfoxide:water = 1:1 mixture and dialyzed against water. The final stock solution 40 μM was serially diluted to 18, 12, 3.4, 0.9, 0.3 and 0.1 μM of 2000 μL stock solutions of each. 15 μL Nile Red (stock solution 0.8 mg/mL in DMSO, 2.52 mM) was added to each of the different concentration of the polymer (**28GP-G2**). Then the emission spectra were recorded by exciting at 530 (Figure 4.12).

For ***manno*28GP-G2** 40, 20, 10, 5, 2.5, 1.25, 0.625, 0.312 and 0.156 μM of 2000 μL stock solutions of each were prepared. 15 μL Nile Red (stock solution 1 mg/mL in DMSO, 3.15mM) was added to each of the different concentration of the polymer (*manno*28GP-G2). Then the emission spectra were recorded by exciting at 530 nm (Figure 4.9). For **16GP-G2** and **16GP-G1** 40 μM solution in pure water was prepared and 18 μL of Nile Red (2.52 mM in DMSO) was added. Then the emission spectra were recorded by exciting at 530 nm.

4.4 Results and Discussion

4.4.1 Synthesis of Glycopolypeptides

We recently reported a simple and versatile methodology for synthesis of GPs via ring-opening polymerization of a carbohydrate appended N-carboxyanhydride (NCA).[47-49] This method assures incorporation of sugar residues on every repeat unit. Using our procedure, azide-PEG terminated glycopolypeptides of two different chain lengths (DP = 16, 28; calculated from 1H NMR) based on poly-*l*-lysine with pendant acetyl protected D-glucose were synthesized. The ratio of weight fractions of hydrophobic and hydrophilic blocks is an important parameter used to control block copolymer morphology.[58-61] Hence, the chain lengths were targeted based on considerations of the hydrophilic-lipophilic balance (HLB) so that the weight fraction of hydrophobic (dendron) part in our polymers does not exceed 26%.

Run No	Monomer (NCA)	Polymer (code) AcnGP	M/I[a]	M_w/M_n [b]	DP (NMR)[c]	Yield[d]	Helicity (CD)[e]
1	β-gluco-*O*-*l*-lys	Ac16GP	14	1.05	16	90%	α-helix
2	β-gluco-*O*- *l*-lys	Ac28GP	26	1.12	28	90%	α-helix
3	β-gluco-*O*- *l*-lys	Ac8GP	7	1.07	8	85%	α-helix
4	β-gluco-*O*- *l**d*-lys	Ac*rac*14GP	12	1.09	14	90%	Coil structure
5	α-manno-*O*- *l*-lys	Ac*manno*14GP	12	1.17	14	90%	α-helix
6	α-manno-*O*- *l*-lys	Ac*manno*28GP	26	1.18	28	90%	α-helix
7	β-gluco-*O*- *l*-lys/ α-manno-*O*-*l*-lys	Ac*gluco*-*manno*(3:1)-14GP	12	1.17	14	85%	α-helix
8	β-gluco-*O*- *l*-lys	Ac16GP-alkyne	12	1.18	16	90%	α-helix
9	β-gluco-*O*- *l*-lys	Ac14GP-HEG-N_3	12	1.11	14	85%	α-helix

Table 4.2: [a]M/I indicates monomer to initiator ratio [For polymer (1-7) initiator (I) is N3PEG11NH2, for Ac16GP-alkyne initiator is propargyl amine and for Ac14GP-HEG-N3initiator is N3HEGNH2], [b]polydispersity index was estimated from GPC (0.1M LiBr in DMF solvent running system elution rate 1mL/min at 60˚C, [c]Degree of polymerization (DP) from NMR (molar mass of the glycopolypeptides were calculated by taking as standard the initiator peak at 3.62-3.68 ppm for 44 protons for PEG_{11}, 24 protons for HEG and 12 protons for TEG linker with respect to that glycosyl part was integrated by using the acetate peaks at 1.97-2.14 ppm), [d]Total isolated yield, [e]Circular dichroism were recorded in acetonitrile.

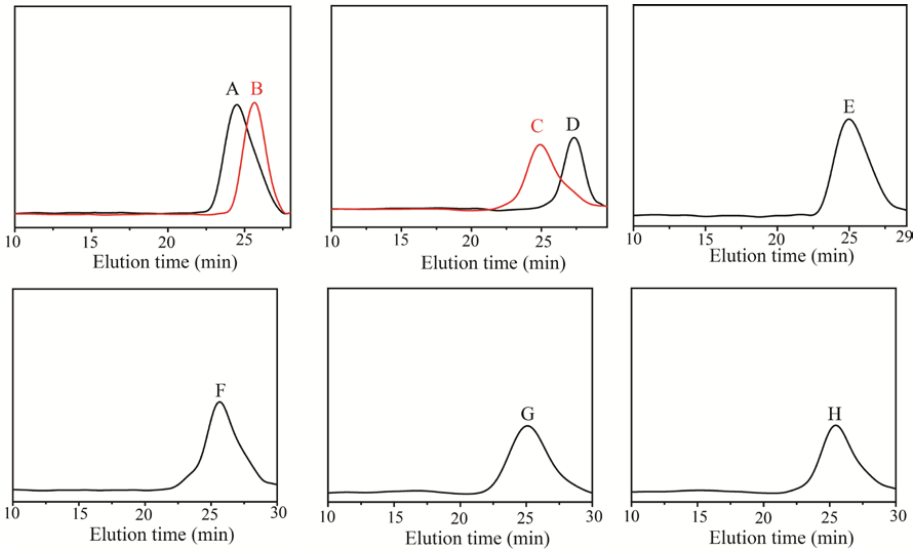

Figure 4.2: Size exclusion chromatogram of *per-O*-acetylated-glycopolypeptides A) Ac28GP, B) AC16GP, C) *manno*28GP, D) Ac8GP, E) Ac14GP-HEG-N_3, F) Ac-*gluco-manno*(3:1)-14GP G) Ac16GP-alkyne and H) Ac14GP-HEG-N_3 in eluent at 1mL/min elution rate (DMF/0.1M LiBr, 60 ºC, RI).

4.4.2 Synthesis and characterization of GP-dendron copolymers

The azide-functionalized GPs (Ac16GP-N_3 and Ac28GP-N_3) and dendrons up to second generation (G1 and G2) with alkyne at the focal point were clicked together using the [3+2] copper catalyzed azide-alkyne cycloaddition (CuAAC) reaction. This reaction, often called 'click reaction', has emerged as an important tool for preparation of novel polymeric architectures.[62-69] Four different acetyl (Ac) protected GP-dendron conjugates described hence forth as Ac16GP-G1, Ac28GP-G1, Ac16GP-G2, and Ac28GP-G2 were obtained. Structures of these polymers are shown in Table 4.1. The obtained GP-dendron copolymers were characterized by NMR, IR and GPC techniques to ascertain the structural integrity and purity was checked by measuring the intensity before and after "click reaction" at 2115 cm^{-1} stretching specific for azide functionality (Figures 4.3).

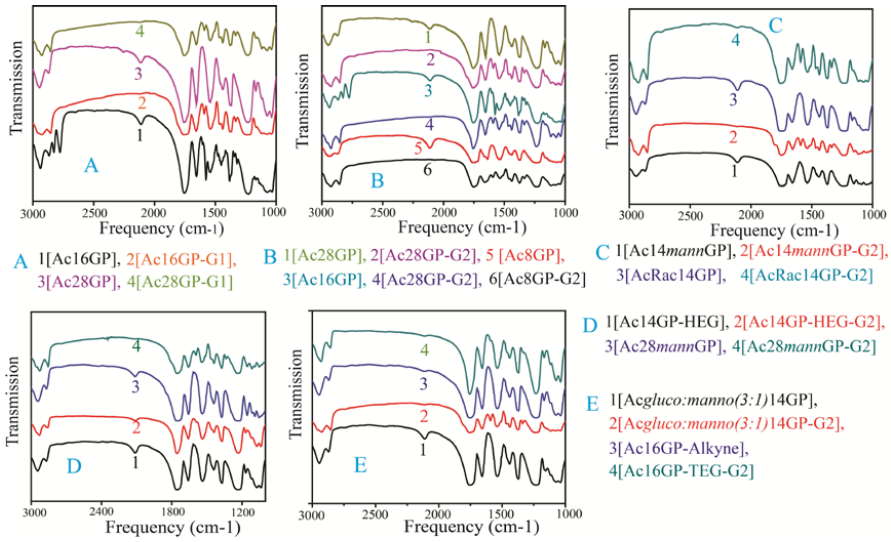

Figure 4.3: FT-IR spectra of azide end functionalized glycopolypeptides before and after click reaction in the Figure 4.2.A-4.2.E.

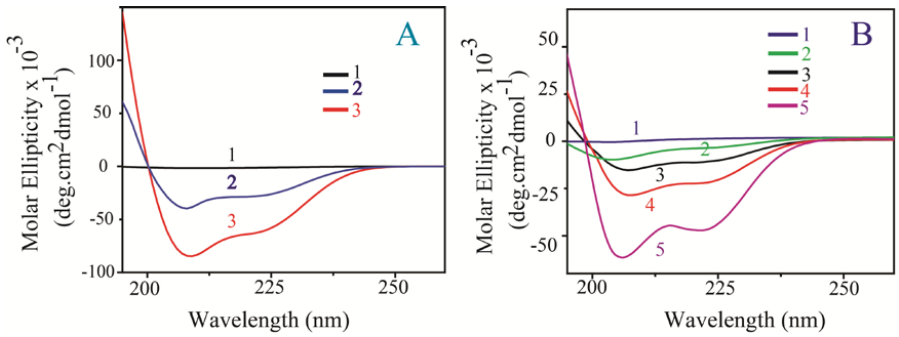

Figure 4.4: CD spectra were recorded of the glycopolypeptides in acetonitrile, A) Ac*rac*14GP (1), Ac16GP (2), Ac28GP (3) and the glycopolypeptide-dendron conjugates in water, B) *rac*14GP-G2 (1), 16GP-G2 (2), 16GP-G1 (3), 28GP-G2 (4), 28GP-G1 (5).

4.4.3 Assembly of protected GP-dendron copolymers in Organic Solvent

All acetylated polymers were soluble in common organic solvents. Interestingly, when a 0.7 wt% clear solution of Ac16GP-G2 in acetonitrile was left for a few minutes at room temperature, it turned into a gel that did not flow on inverting a tube of 1 cm diameter (*viz.* the yield stress exceeded ≈ 20 Pa). Gelation was observed only for Ac16GP-G2 that had the highest weight fraction of the hydrophobic part (19.4%). On the other hand, 0.7 wt% solution of Ac28GP-G2 and both the G1-attached GPs

(Ac16GP-G1 and Ac28GP-G1) did not gel indicating that increased hydrophilicity in the amphiphilic glycopolypeptide does not lead to gelation.

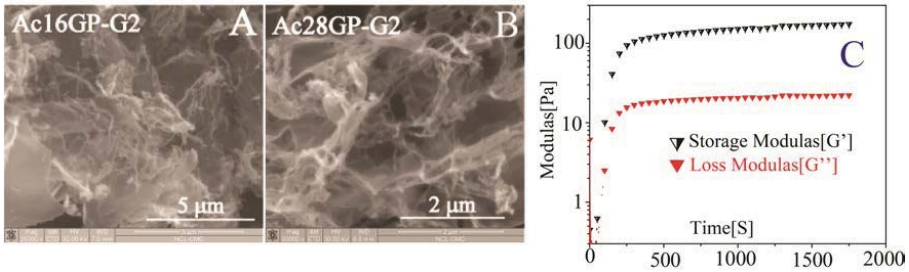

Figure 4.5: SEM Images of the freeze dried solutions of (A) Ac16GP-G2, (B) Ac28GP-G2 at 0.7 wt% in acetonitrile, (C) Rheology of Ac16GP-G2 gel at 0.9 wt% in acetonitrile.

Packing of α-helical chains by noncovalent interactions has been suggested as a driving force for polypeptide self-assembly into polymersomes and sheet-like structures.[54, 70, 71] We hypothesized that, in polar aprotic solvent such as acetonitrile, gelation could be driven by hydrophobicity of dendrons that is further aided by packing of helical GP chains. Since both the components take part in intermolecular interactions a physically cross linked network is obtained rather than isolated self-assembled structures that results in a gel.

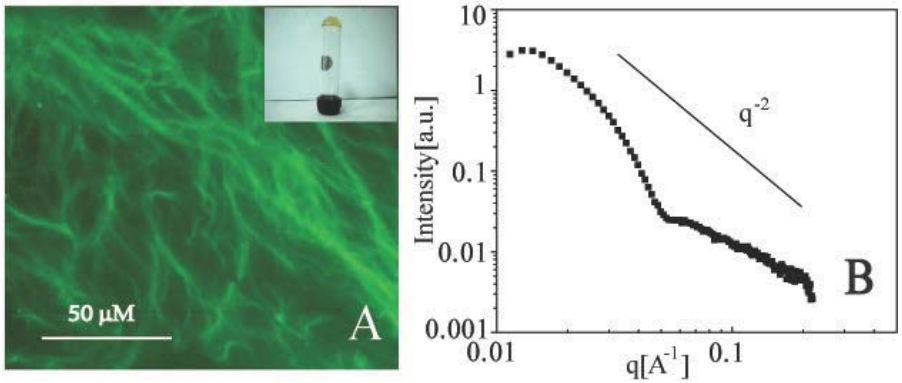

Figure 4.6: A) Confocal microscopy image of the gel from a fluorescently labeled Ac16GP-G2 Inset: picture of the gel in inverted tube; (B) SAXS data for 1 wt% Ac16GP-G2 in acetonitrile.

The microstructure of the gel was further investigated by confocal scanning microscopy of a gel formed by fluorescently labeled Ac16GP-G2, which shows a network of fibers typical of gels (Figure 4.6A). Small-angle X-ray scattering (SAXS) analysis provides further insight into the local structure of the gel fibers (Figure 4.6B).

The envelope of scattering curve decays with a power law of q^{-2} suggesting that the GP-dendron block copolymers might organize into locally flat sheet-like structures. While this structural interpretation is not unambiguous,[72] it is consistent with scanning electron micrographs (SEM) of freeze dried assemblies of the block copolymers (Figure 4.5A & B).

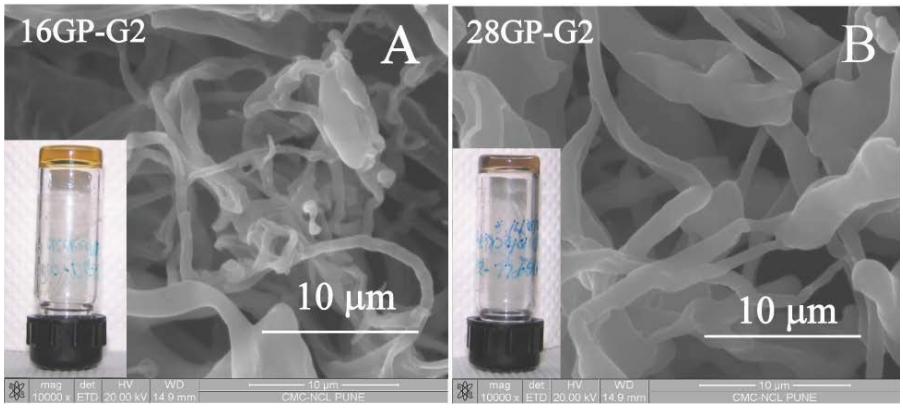

Figure 4.7: SEM image of A) 16GP-G2 and (B) 28GP-G2 in DMSO at 1 wt%; inset shows corresponding picture of the gel.

4.4.4 Assembly of deprotected GP-dendron copolymers in aqueous solution

The promise of glycopolymers is fully realized when the carbohydrate moieties are in the deprotected form so they can bind biological targets. Towards this goal, all the polymers were de-acetylated using hydrazine hydrate to obtain nGP-Gx that are now truly amphiphilic with carbohydrate moieties carrying OH groups. Evidence for presence of secondary structure in the GP component was obtained from CD spectra that show a peak at 222 nm, typical of helical polypeptides (Figure 4.4A). Interestingly, gelation was observed after deprotection also in a more polar and aprotic solvent *viz.* DMSO. There are several examples of organogels in DMSO and intermolecular hydrogen bonding has been suggested as the mechanism for gelation[73-77] while polysaccharide chains are also known to aggregate in DMSO.[78] Both 16GP-G2 and 28GP-G2 formed organogel in DMSO at room temperature at 1 wt% that do not flow (Figure 4.7A & B). Both the gels were also analyzed by SEM using freeze-dried assemblies that show a network of fiber-like structures (Figure 4.7A & B).

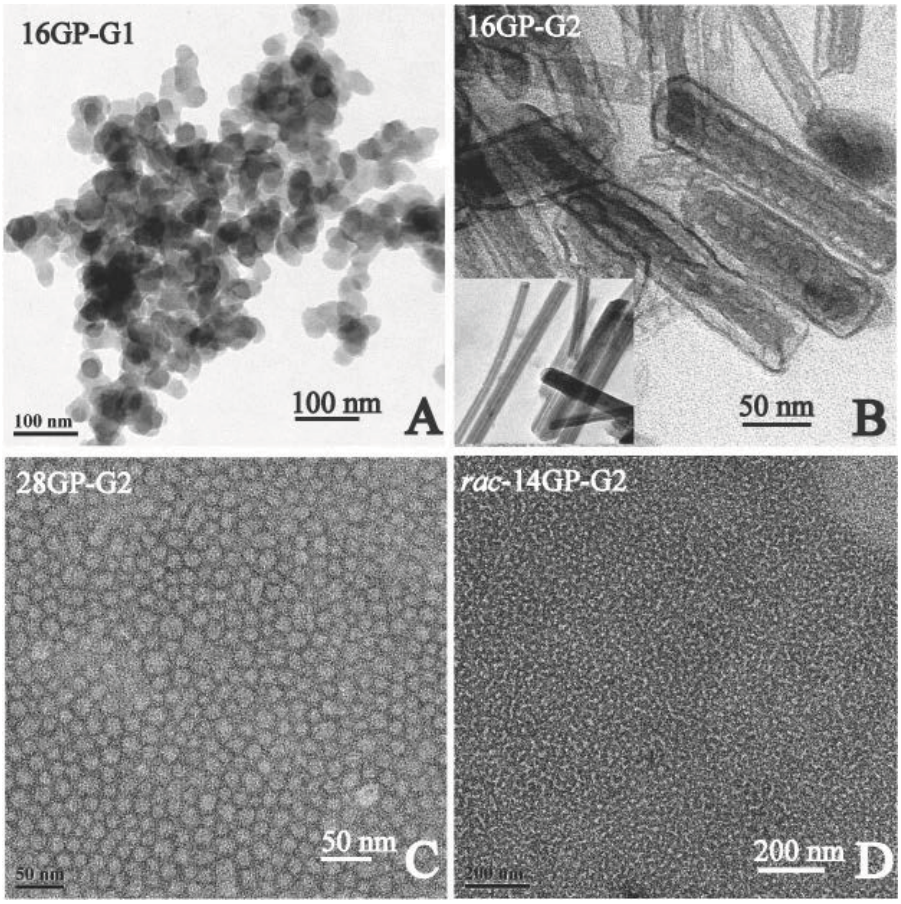

Figure 4.8: TEM images of A) 16GP-G1, (B) 16GP-G2, (C) 28GP-G2, (D) rac14GP-G2 in water (0.1 wt%) with uranyl acetate as negative stain.

Clear solutions in water, selective solvent for the GP block, could be prepared by dialysis of 0.1 wt% solutions of the polymer in DMSO: H2O (1:1) against deionized water. Initially, water was added drop wise to the solution of polymer in DMSO to induce aggregation of hydrophobic dendron block and formation of the morphology. This was followed by extensive dialysis for complete removal of organic solvent. To visualize the aggregates formed, a drop of the solution was deposited on a carbon-coated grid and analyzed by transmission electron microscopy (TEM) using uranyl acetate as negative staining agent. 16GP-G1 and 28GP-G2 exhibited aggregated micellar structures (Figures 4.8) while 28GP-G1 understandably did not show a well-defined morphology due to a higher weight fraction of hydrophilic part (93.7%) (Figure 4.9 C).

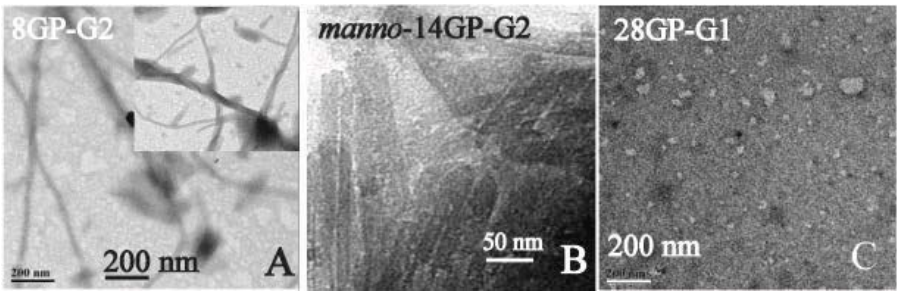

Figure 4.9: TEM images of A) 8GP-G2 , B) manno-14GP-G2 and C) 28GP-G1 at 0.1 wt% in water with uranyl acetate as negative stain.

The most interesting structures however were exhibited by 16GP-G2, which forms rod-like assemblies that are hundreds of nm in length with a uniform width of about 50 nm. For molecules with anisotropic shapes, that includes dendron-rod-coil and dendron-coil type molecules[79-82] formation of nanostructures with high aspect ratio is known, however our assemblies were found to contain a compartmentalized interior as well, when observed under high magnification (Figure 4.8). These assemblies are stable in solution, at least up to several weeks. We propose that each self-assembly is primarily directed by relative hydrophobic content with the glycopolypeptide block forming hydrophilic exterior and dendrons forming the hydrophobic interior. We estimate that the volume ratio of the hydrophilic rod-coil to the hydrophobic dendron is in accord with the packing parameter arguments for the formation of rod-like structures (Figure 4.10).[83]

4.4.5 The Mechanistic Explanation Of the self-assemblies

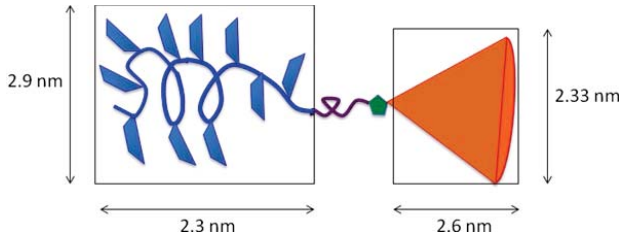

Figure 4.10: Graphical representation of the 16GP-G2 conjugated system.

The dimensions for glycopolypeptide (GP, n = 16) were estimated from an energy minimized structure.8 Based on these values (shown above) volume of each part is first calculated separately.

Taking the GP helical rod to be a cylinder, its volume will be

$V_{GP} = \pi R2h = 3.142 \times (1.45)2 \times 2.3 = 15.2\ nm^3$

For simplicity, we assume that the PEG linker exists as a random coil. Therefore, an estimate of its size is given by V_{PEG} = (4π/3)(C∞nl2/6)3/2 where C∞ = 4 is the characteristic ratio of PEG in water, n =33 is the number of bonds and l = 0.154 nm is the bond length. This results in a size of the PEG linker of ≈ 1.6 nm3.

The approximate dimensions for G2-dendron were estimated from literature 52-54 as follows. The height of the conical region is 2.6 nm, taken from Table 4.3 in ref 52. The diameter of the cone can be estimated either from the volume or the surface area of the spherical supramolecular dendrimer.[54] These result in estimates of 2.22 nm and 2.44 nm, respectively. Therefore, we assume an average size of 2.33 nm.

The volume of the conical dendron is given by:

$V_{d\text{-}cone}$= 1/3 x πR2h = 1/3 x 3.142 x (1.165)2x 2.6 = 3.7 nm^3

However, when the rigid dendron moieties pack within the hydrophobic core of the assembled structure, steric constraints will prevent them from packing as densely as, for example, alkane chains in a surfactant tail. Therefore, the volume of the hydrophobic region is likely to exceed that of just the conical dendron. An extreme estimate for the size of the dendron is obtained by considering a cylindrical volume with the radius and height of the dendron. This estimate is given by:

$V_{d\text{-}cyl}$= πR2h = 3.142 x (1.165)2x 2.6 = 11.1 nm^3

Thus, we estimate that the ratio of volumes of hydrophobic (dendron) and hydrophilic (GP and PEG) parts is between $V_{d\text{-}cone}/(V_{PEG}+ V_{GP})$ = 0.22 and $V_{d\text{-}cyl}/(V_{PEG}+ V_{GP})$ = 0.66. In the surfactant literature, Israelachvili has defined a packing parameter = v_o/al, where v_o is the hydrophobic tail volume, a is the head group area and l is the length of the hydrophobic tail. This packing parameter can be considered a geometric ratio of the area of the hydrophobic part = v_o/a, of the surfactant to the hydrophilic part, a. For the rigid block copolymer solution structures in our work, we define a modified packing parameter, p = $V_{hydrophobic}/V_{hydrophilic}$, in analogy to the Israelachvili packing parameter. Thus, the packing parameter, p = $V_{hydrophobic}/V_{hydrophilic}$ is between 0.22 and 0.66, and is consistent with that for a cylindrical structure (p = 0.5).

However, such simple geometric arguments are inadequate to rationalize the formation of compartmentalized structures. The structural rigidity in these systems, and the possibility of π-π interactions in the wedge segments are likely to contribute to the formation of complex structures such as compartmentalized rods. For 16GP-G2,

the weight fraction of dendron is significant (25.7%), whereas for 28GP-G2 it decreases to 17%. Thus, for shorter hydrophilic chain the molecules are arranged presumably in a curled-up bilayer structure, which may account for the formation of nanorods, whereas for the longer hydrophilic chain, a transition to micelles is favoured. To test whether polymers with even shorter hydrophilic chains would form rod-like morphology, a homologue of 16GP-G2 with 8 glycopeptide units was synthesized. It was found to assemble into longer nanofibers although the polymer sample itself is polydisperse. Thus, it may be possible to obtain nanorods and nanofibers of predictable dimensions by using dendron-appended monodisperse oligo-glycopeptides of certain chain length. Toward this goal, synthesis of short glycopeptide oligomers with exact number of repeat units using solid phase synthesis is currently underway in our laboratory.

It is important to note that volume fraction of the hydrophilic chains, which influences the self-assembly of these polymers is in turn influenced by the secondary structure. Helicity in the polypeptide segments will result in a more compact conformation relative to a random coil chain. Further, inter chain interactions are also likely to be affected by the polypeptide chain helicity. Thus, a polymer with no secondary structure should exhibit a morphology that is different from the one shown by a polymer with considerable helicity.[84-87] To test this hypothesis in the case of GP-dendron copolymers, we synthesized a glycopolypeptide of 14 repeat units, by using racemic mixture of monomers. CD spectrum of this polymer shows complete absence of helicity (Figure 4.4B). Aqueous solution of the dendron conjugate from this polymer rac14GP-G2, where the carbohydrate units are in deprotected form, was then analyzed by transmission electron microscopy. Figure 4.12C&D shows that it does not form rod-like morphology, suggesting a strong correlation between secondary structure of the polymer and the resultant self-assembly.

The amphipathic poly(ethylene glycol) linker between the glycopolypeptide and dendron is made up of 11 repeat units. To investigate whether it plays a part in the self-assembly of these polymers, we prepared two more polymers based on 16GP polypeptide chain and G2 dendron – one with triethylene glycol linker (16GP-TEG-G2) and the other with hexaethylene glycol linker (14GP-HEG-G2). Self-assembly of the two deprotected polymers was studied in aqueous solutions at 0.1 wt%. TEM images showed that both 16GP-TEG-G2 and 14GP-HEG-G2 (Figures 4.11A and

4.11B) form rod-like morphology. This clearly illustrates that the length of PEG linker does not influence self-assembly of these macromolecules into rod-like structures.

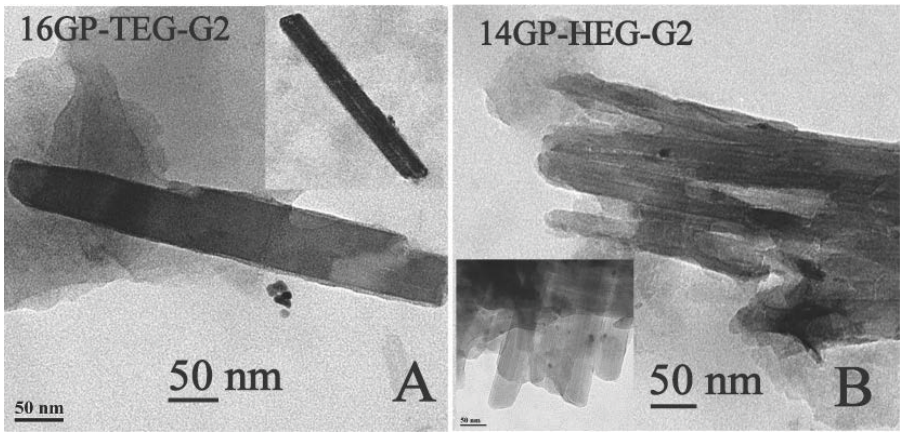

Figure 4.11: TEM images of A) 16GP-TEG-G2, (B) 16GP-HEG-G2 in water (0.1 wt%) with uranyl acetate as negative stain.

As an additional proof of presence of the micellar assemblies we carried out dye encapsulation experiments. Nile Red, a hydrophobic dye was sequestered in the interior of micellar assemblies from 28GP-G2 and the rod-like assemblies from 16GP-G2 in aqueous solutions, as evidenced by visual change in color of the solution and also from fluorescence emission spectrum, which shows a broad peak with λ_{max} at 630 nm when excited at 530 nm (Figure 4.13). This suggests that hydrophobic guest molecules can be loaded into these bioactive micellar assemblies. Similarly, dye encapsulation was also observed with 16GP-G1 (Figure 4.13).

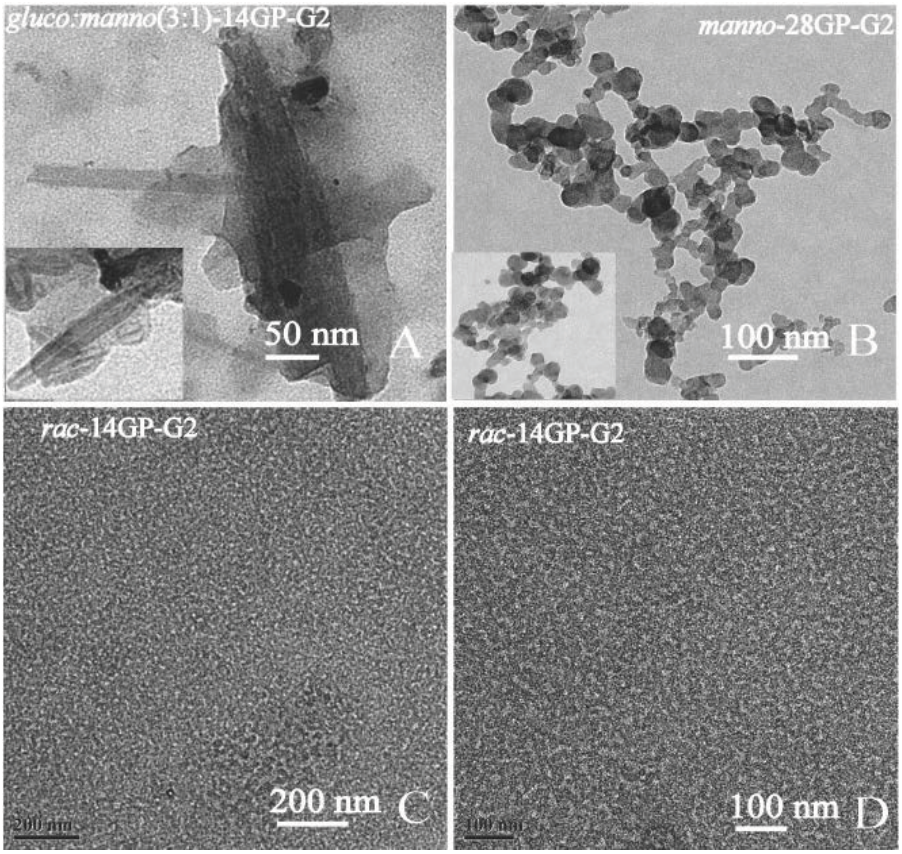

Figure 4.12: TEM images of A) gluco:manno(3:1)-14GP-G2, B) manno-28GP-G2 and C) and D) rac-14GP-G2 at 0.1 wt% in water with uranyl acetate as negative stain.

To determine critical micelle concentration (cmc) value for assemblies from 28GP-G2, fluorescence emission spectra of the encapsulated dye at different concentrations of the polymer were recorded by exciting at 530 nm. Around 1μM concentration, a red shift in the λ_{max}, typical for emission spectrum of Nile Red in aqueous environment, was observed (Figure 4.13) and the plot of λem of Nile Red vs. concentration of polymer has the shape typical for a cmc curve.

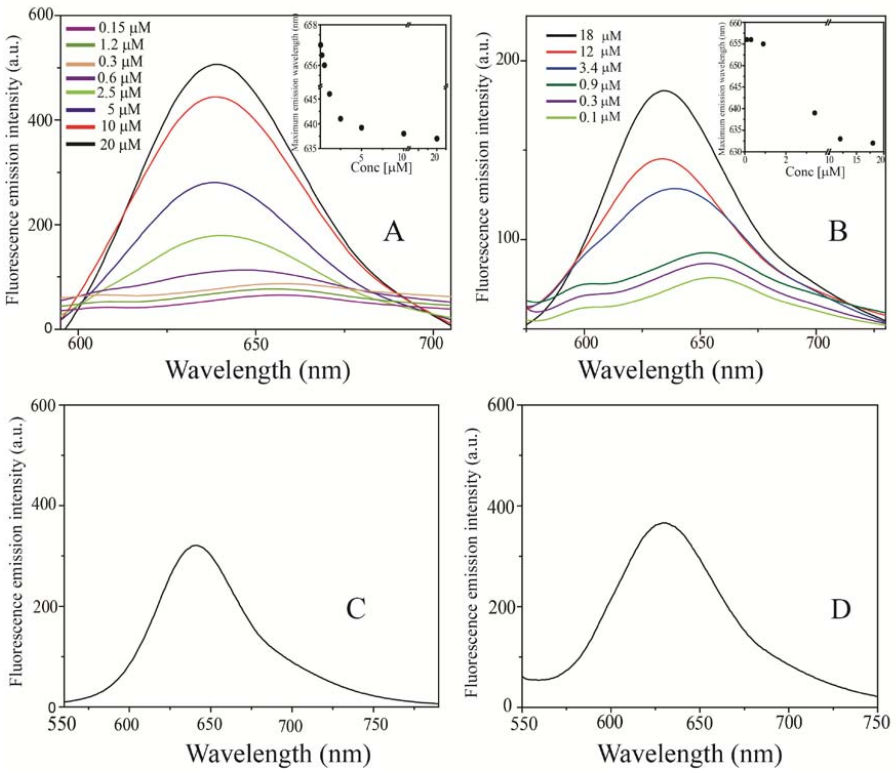

Figure 4.13: Fluorescence emission spectra of Nile Red in aqueous solution of A) 28GP-G2, B) manno28GP-G2 at different concentrations of polymer and C) 16GP-G2 and D) 16GP-G1 at one concentration of polymer. Inset: Plot of λ_{em} of Nile Red vs. concentration of amphiphiles at 530 nm excitation wavelength.

4.4.6 Interaction with Lectins

Multivalent interactions such as protein-carbohydrate interactions are involved in many biological processes and are known to depend on ligand density and stoichiometry among other factors.[88] Lectins are oligomeric proteins that are involved in cellular signalling via such interactions.[88] Artificial glycoconjugates assemblies that present sugar moieties on the surface in an organized fashion could be used to interrupt undesired protein-carbohydrate interactions. To demonstrate the functional nature of our nanostructures towards this goal, we synthesized D-mannose containing GP and clicked it to the G2-dendron. This polymer, manno14GP-G2 was also found to assemble into rod-like structures in water as seen in TEM micrographs (Figure 4.12B). To test the possibility that the rod-like morphology does not necessarily depend on isomerism in sugar residue we prepared a random copolymer of D-glucose and D-

mannose with 3:1 ratio of glucose and mannose, containing PEG(11)-azide at one end and clicked with G2 dendron-alkyne to afford *gluco-manno(3:1)*-14GP-G2. This polymer was found to assemble into nanorods as observed in TEM analysis (Figure 4.12A).

To study the response of these mannose-containing nanorods to lectins we used *Con-A* as a model lectin. The recognition and binding abilities of the mannose-containing nanorods with *Con-A* were estimated by turbidimetric assay where the increase in turbidity by the addition of nanorods to *Con-A* was observed indicative of formation of large aggregates. Further, precipitation assay was performed using a series of dilutions of manno14GP-G2 solution at neutral pH. As the concentration of polymer increased the amount of *Con-A* precipitated also increased as evidenced by absorbance at 280 nm characteristic of *Con-A* (Figure 4.14, plot A). This strongly suggests that carbohydrates on the surface of nanorods are available for interaction with lectins and that these self-assembled structures are functional.

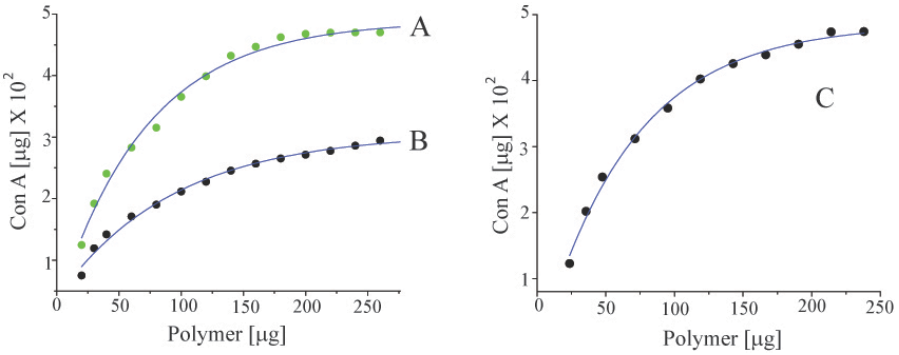

Figure 4.14: Amount of ConA precipitated using various concentrations of A) manno-14GP-G2, B) gluco-manno(3:1)-14GP-G2 rod-like assemblies and C) manno-28GP-G2 spherical assemblies as determined by precipitation assay.

Binding of *Con-A* to glycopolymers with varying number of mannose residues has been used as a tool to study the effect of epitope density in a multivalent ligand on receptor clustering.[89,90] The random copolymer of glucose and mannose containing repeat units [*gluco-manno(3:1)*-14GP-G2] provides an opportunity to vary the density of functionalities on a self-assembled nanostructure. To study the effect of mannose content on *Con-A* binding, precipitation assays were performed with the nanorods assembled from this polymer (Figure 4.14, plot B). Figure 4.14 (plots A and B) shows that amount of precipitated *Con-A* increases with the mannose content in the

copolymer with the amount of precipitated *Con-A* being higher for nanorods displaying only mannose. Thus, lectin binding can be controlled using the amount of receptor sugar residue on the surface of the assembly. Micellar assemblies from *manno*-28GP-G2 (Figure 4.14C) were also found to bind to *Con-A* showing that these miceller assemblies are also functional (Figure 4.14, plot C).

4.5 Conclusion

In summary, we have shown that self-assembled supramolecular structures with a range of one-dimensional to three-dimensional topology are afforded by amphiphilic glycopolypeptide-dendron conjugates based on a single structural motif, that is the wedge-like dendron attached to stiff glyco-polypeptide chains by a coil-like oligo(ethylene glycol). The self-assembly was found to depend upon generation of the dendron, the length of the glycopolypeptide segment, the protected or unprotected form of sugar residue and the extent of helicity of polypeptide backbone but was not affected by the length of PEG linker. Availability of carbohydrate groups on these nanostructures was also demonstrated by lectin binding interaction with *Con-A*. The amount of *Con-A* binding could be varied with mannose content in the self-assembly. Thus, we have clearly illustrated that in principle it is possible to design glyco-conjugate nanostructures of different shapes for specific inter-action with lectins. Further investigations on underlying mechanism of self-assembly of these polymers and incorporation of biocompatible dendrons are the focus of our future work in this direction.

The spectral data of the selected compounds are available from the **Appendix IV**.

4.6 References

1) Spain S. G.; Gibson, M. I.; Cameron N. R. *J. Polym. Sci., Part A: Polym. Chem.* **2007**, *45*, 2059-2072.
2) Schatz, C.; Lecommandoux, S. *Macromol. Rapid Commun.* **2010***, 31,* 1664–1684.
3) Ting, S. R. S.; Chen, G.; Stenzel, M. H. *Polym. Chem.* **2010**, *1*, 1392–1412.
4) Boltje T. J.; Buskas T.; Boons G.-J. *Nature Chem.* **2009**, *1*, 611-622.
5) You, L.; Schlaad, H. *J. Am. Chem. Soc.*, **2006**, *128*, 13336–13337.
6) Schatz, C.; Louguet, S.; Le Meins, J.-F.; Lecommandoux, S. *Angew. Chem. Int. Ed.* **2009**, *48*, 2572 –2575.
7) Schlaad, H.; You, L.; Sigel, R.; Smarsly, B.; Heydenreich, M.; Mantion, A.; Mašić, A. *Chem. Commun.* **2009**, 1478-1480.
8) Li, Z.-C.; Liang, Y.-Z.; Li, F.-M. *Chem. Commun.* **1999**, 1557-1558.
9) Gress, A.; Smarsly, B.; Schlaad, H. *Macromol. Rapid Commun.* **2008**, *29*, 304-308.
10) Chen, G.; Amajjahe, S.; Stenzel, M. H. *Chem. Commun.* **2009**, 1198-1200.
11) Miura, Y. *J. Polym. Sci., Part A: Polym. Chem.* **2007**, *45*, 5031-5036.
12) Dong, C. M.; Sun, X. L.; Faucher, K. M.; Apkarian, R. P.; Chaikof, E. L. *Biomacromolecules*, **2004**, *5*, 224-231.
13) Rabuka, D.; Forstner, M. B.; Groves, J. T.; Bertozzi, C. R. *J. Am. Chem. Soc.* **2008**, *130*, 5947-5953.
14) Ruff, Y.; Buhler, E.; Candau, S. J.; Kesselman, E.; Talmon, Y.; Lehn, J.-M. *J. Am. Chem. Soc.* **2010**, *132,* 2573-2584.
15) Suriano, F.; Pratt, R.; Tan, J. P. K.; Wiradharma, N.; Nelson, A.; Yang, Y.-Y.; Dubois, P.; Hedrick, J. L. *Biomaterials* **2010**, *31*, 2637-2645.
16) Vazquez-Dorbatt, V.; Maynard, H. D. *Biomacromolecules* **2006**, *7*, 2297-2302.
17) Spain, S. G.; Albertin, L.; Cameron, N. R. *Chem. Commun.* **2006**, 4198-4200.
18) Kumar, J.; McDowall, L.; Chen, G.; Stenzel, M. H. *Polym. Chem.* **2011**, *2*, 1879-1886.
19) Polizzotti, B. D.; Kiick, K. L. *Biomacromolecules* **2006**, *7*, 483-490.
20) Kramer, J. R.; Deming, T. J. *J. Am. Chem. Soc.* **2012**, *134*, 4112-4115.

21) Lu, H.; Wang, J.; Bai,Y.; Lang, J. W.; Liu, S.; Lin,Y.; Cheng, J.; *Nature Commun.* **2011***, 2,* 206-214.

22) Aoi, K.; Tsutsumiuchi, K.; Aoki, E.; Okada, M. *Macromolecules* **1996**, *29*, 4456–4458.

23) Shuang, L.; Kiick, K. L. *Polym. Chem.* **2011**, *2*, 1513-1522.

24) Kramer, J. R.; Deming, T. J. *J. Am. Chem. Soc.* **2010**, *132*, 15068-15071.

25) Xiao, C.; Zhao, C.; He, P.; Tang, Z.; Chen, X.; Jing, X. *Macromol. Rapid Commun.* **2010**, *31*, 991-997.

26) Tang, H.; Zhang, D. *Polym. Chem.* **2011**, *2*, 1542-1551.

27) Huang, Y.; Zeng, Y.; Yang, J.; Zeng, Z.; Zhu, F.; Chen, X. *Chem. Commun.* **2011**, *47*, 7509-7511.

28) Huang, J.; Habraken, G.; Audouin, F.; Heise, A. *Macromolecules* **2010**, *43*, 6050-6057.

29) Sun, J.; Schlaad, H. *Macromolecules* **2010**, *43*, 4445-4448.

30) Kempe, K.; Neuwirth, T.; Czaplewska, J.; Gottschaldt, M.; Hoogenboom, R.; Schubert, U. S. *Polym. Chem.* **2011**, *2*, 1737–1743.

31) Huang, J.; Bonduelle, C.; Thévenot, J.; Lecommandoux, S.; Heise, A. *J. Am. Chem. Soc.* **2012**, *134,* 119-122.

32) Wurm, F.; Frey, H. *Prog. Polym. Sci.* **2011**, *36*, 1–52.

33) Rosen, B. M.; Wilson, C. J.; Wilson, D. A.; Peterca, M.; Imam, M. R.; Percec, V. *Chem. Rev.* **2009**, *109*, 6275–6540.

34) Palmer, L. C.; Stupp, S. I. *Acc. Chem. Res.* **2008**, *41*, 1674–1684.

35) Lim, Y.; Lee, E.; Lee, M. *Angew. Chem. Int. Ed.* **2007**, *46*, 9011-9014.

36) Shao, H.; Parquette, J. R. *Angew. Chem. Int. Ed.* **2009**, *48*, 2525-2528.

37) Kim, K. T.; Winnik, M. A.; Manners, I. *Soft Matter* **2006**, *2*, 957-965.

38) Spaenig, F.; Ruppert, M.; Dannhaeuser, J.; Hirsch, A.; Guldi, D. M. *J. Am. Chem. Soc.* **2009**, *131*, 9378-9388.

39) Peterca, M.; Percec V.; Dulcey, A. E.; Nummelin, S.; Korey, S.; Ilies, M.; Heiney, P. A. *J. Am. Chem. Soc.* **2006**, *128*, 6713-6720.

40) Lee, H. I.; Lee, J. A.; Poon, Z. Y.; Hammond, P. T. *Chem. Commun.* **2008**, 3726-3728.

41) Tian, L.; Nguyen, P.; Hammond, P. T. *Chem. Commun.* **2006**, 3489-3491.

42) Lim, Y.; Moon, K.-S.; Lee, M. *J. Mater. Chem.* **2008**, *18*, 2909–2918.

43) Yan, J.-J.; Tang, R.-P.; Zhang, B.; Zhu, X.-Q.; Xi, F.; Li, Z.-C.; Chen, E.-Q. *Macromolecules* **2009**, *42*, 8451-8459.

44) Mackay, M. E.; Hong, Y.; Jeong, M.; Tande, B. M.; Wagner, N. J.; Hong, S.; Gido, S. P.; Vestberg, R.; Hawker, C. J. *Macromolecules* **2002**, *35*, 8391-8399.

45) Gitsov, I. *J. Polym. Sci. Part A: Polym. Chem.* **2008**, *46*, 5295-5314.

46) Sureshkumar, G.; Hotha, S. *Chem. Comm.* **2008**, 4282-4284.

47) Pati, D.; Shaikh, A. Y.; Hotha, S.; Sen Gupta, S. *Polym. Chem.* **2011**, *2*, 805-811.

48) Pati, D.; Shaikh, A.; Das. S.; Nareddy, P. K.; Swamy, M. J.; Hotha, S.; Sen Gupta, S. *Biomacromolecules* **2012** DOI:10.1021/bm201813s.

49) Shaikh, A. Y.; Sureshkumar, G.; Pati, D.; Sen Gupta, S.; Hotha, S. *Org. Biomol. Chem.***2011** *9*, 5951-5959.

50) Wiejak, S.; Masiukiewicz, E.; Rzeszotarska, B.; *Chem. Pharm. Bull.* **1999,** *47*, 1489-1490.

51) Morrow, J. A.; Segal, M. L.; Lund-Katz, S.; Philips, M. C.; Knapp, M.; Rupp, B.;Weigraber, K. H.; *Biochemistry* **2000**, *39*, 11657-11666.

52) Balagurusamy,V. S. K.; Ungar, G.;Percec, V.; Johansson, G. *J. Am. Chem.Soc.***1997**, *119*, 1539.

53) Percec, V.; Cho, W.-D.; Ungar, G.; Yeardley, D. J. P. *J. Am. Chem.Soc.***2001**, *123*, 1302-1315.

54) Percec, V.; Cho, W.-D.; Ungar, G. *J. Am. Chem. Soc.* **2000,** *122,* 10273-10281.

55) Bhattacharyya, L.; Brewer C. F.; Brown, R. D.; Koenig, S. H. *Biochemistry* **1985,** *24*, 4974-4980.

56) Cairo, C. W.; Gestwicki, J. E.; Kanai, M.; Kiessling, L. L. *J. Am. Chem. Soc*. **2002**, *124*, 1615-1619.

57) Woller E.K.; Cloninger M.J.; *Org. Lett.* **2002**, *4*, 7-10.

58) Zhang, L.; Eisenberg, A. *Science* **1995**, *268*, 1728- 1731.

59) Holder S. J.; Sommerdijk, N. A. J. M. *Polym. Chem.* **2011**, *2*, 1018-1028.

60) Discher, D. E.; Eisenberg, A. *Science* **2002**, *297*, 967- 973.

61) Blanazs, A.; Armes, S. P.; Ryan, A. J. *Macromol. Rapid Commun.* **2009**, *30*, 267–277.

62) Tornøe, C. W.; Christensen, C.; Meldal, M. *J. Org. Chem*. **2002**, *67*, 3057-3064.

63) Meldal, M.; Wenzel, C.; Tornøe, C. W. *Chem. Rev.* **2008**, *108*, 2952–3015.

64) Kolb, H. C.; Finn, M. G.; Sharpless, K. B. *Angew. Chem. Int. Ed.* **2001,** *40*, 2004–2021.

65) Iha, R. K.; Wooley, K. L.; Nystrom, A. M.; Burke, D. J.; Kade, M. J.; Hawker, C. J. *Chem. Rev.* **2009** *109*, 5620-5686.

66) Binder, W. H.; Sachsenhofer, R. *Macromol*. *Rapid Commun*. **2007**, *28*, 15–54.

67) Kempe, K.; Krieg, A.; Becer, C. R.; Schubert, U. S. *Chem. Soc. Rev.* **2012**, *41*, 176–191.

68) Hua, C.; Peng, S.-M.; Dong, C.-M. *Macromolecules* **2008***, 41,* 6686-6695.

69) Laurent, B. A.; Grayson, S. M. *J. Am. Chem. Soc.* **2006**, *128*, 4238-4239.

70) Hanson, J. A.; Li, Z.; Deming, T. J. *Macromolecules*, **2010**, *43*, 6268–6269.

71) Bellomo, E. G.; Wyrsta, M. D.; Pakstis, L.; Pochan, D. J.; Deming, T. J. *Nature Mater.* **2004**, 3, 244–248.

72) Foster, T.; Safran, S. A.; T. Sottmann, T.; Strey, R. *J. Chem. Phys.* **2007**, *127*, 204711/1-204711/16.

73) Duan, P.; Zhu, X.; Liu, M. *Chem*. *Commun*. **2011**, *47*, 5569–5571.

74) Deng, W.; Thompson, D. H. *Soft Matter* **2010**, *6*, 1884–1887.

75) George, M.; Snyder, S. L.; Terech, P.; Glinka, C. J.; Weiss, R. G. *J. Am. Chem. Soc.* **2003**, *125*, 10275-10283.

76) Jung, J. H.; Kobayashi, H.; Masuda, M.; Shimizu, T.; Shinkai, S. *J. Am. Chem. Soc.* **2001**, *123*, 8785-8789.

77) Seo, S.-H.; Park, J.-H.; Chang, J.-Y. *Langmuir* **2009**, *25*, 8439–8441.

78) Östlund, A.; Lundberg, D.; Nordstierna, L.; Holmberg, K.; Nydén, Ḿ. *Biomacromolecules* **2009,** *10,* 2401–2407.

79) Kim, J.-K.; Lee, E.; Lee, M. *Angew. Chem. Int. Ed.* **2006**, *45*, 7195 –7198.

80) Zubarev, E. R.; Pralle, M. U.; Sone, E. D.; Stupp, S. I. *J. Am. Chem. Soc.* **2001**, *123*, 4105-4106.

81) Park, C.; Lee, I. H.; Lee, S.; Song, Y.; Rhue, M.; Kim, C. *Proc. Natl. Acad. Sci. USA* **2006**, *103*, 1199–1203.

82) Cornelissen, J. J. L. M.; van Heerbeek, R.; Kamer, P. C. J.; Reek, J. N. H.; Sommerdijk, N. A. J. M.; Nolte, R. J. M. *Adv. Mater.* **2002***, 14,* 489-492.

83) Israelachvili, J. N. *Intermolecular and Surface Forces*, 2nd ed; Academic Press: San Diego, 1991.

84) Chécot, F.; Lecommandoux, S., Gnanou, Y., Klok, H.-A. *Angew. Chem. Int. Ed.* **2002**, *41*, 1339-1343.

85) Klok, H.-A.; Langenwalter, J. F.; Lecommandoux, S. *Macromolecules* **2000**, *33*, 7819-7826.

86) Schneider, J. P; Pochan, D. J; Bulent; O.; Karthikan, R.; Pakstis L.; Kretsinger J. *J. Am. Chem. Soc.* **2002**, *124*, 15030-15037.

87) Ghosh, A.; Haverick, M.; Stump, K.; Yang, X.; Tweedle, M. F.; Goldberger, J. E. *J. Am. Chem. Soc*. **2012**, *134*, 3647–3650.

88) Liu, S.; Kiick, K. *Macromolecules* **2008**, *41*, 764-772.

89) Ladmiral, V.; Mantovani, G.; Clarkson, G. J.; Cauet, S.; Irwin, J. L.; Haddleton, D. M. *J. Am. Chem. Soc*. **2006**, *128*, 4823–4830.

90) Griffith, B. R.; Allen, B. L.; Rapraeger, A. C.; and Kiessling, L. L. *J. Am. Chem. Soc.* **2004**, *126*, 1608-1609.

Chapter 5

Bioactive Polymersomes 'assemblies' derived from Glycopolypeptide-*b*-Polycaprolactone conjugate and the study of their preferential cellular uptake.

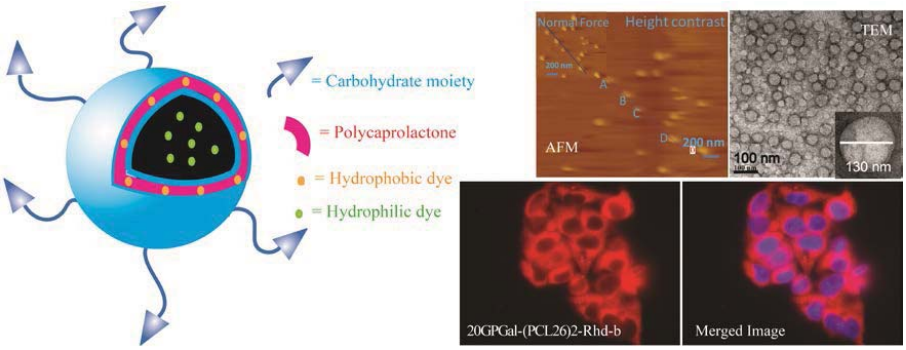

ABSTRACT: Glycopolypeptides were synthesized by ring opening polymerization of glycosylated NCA monomer and attached to hydrophobic polycaprolactone at one chain end by 'click' reaction to obtain amphiphilic anisotropic macromolecules. We show that by varying polypeptide chain length and polycaprolactone chain length nanorods, micellar and vesicular aggregates were observed in aqueous solutions. Assemblies in water were characterized by electron microscopy and dye encapsulation. As both the glycopolypeptides and the polycaprolactones are biocompatible and biodegradable, so might be promising *in vivo* delivery vehicles. To observe the molecular recognition, ASGPR over expressed HepG2 cellular uptake is demonstrated of galactosylated vesicles.

This chapter has been adopted from the corresponding paper, mentioned below;

Pati, D. *et al.* manuscript is under preparation **2013.**

5.1 Introduction

Liposomes have been used for a long time as drug delivery vehicles. The building blocks of liposomes are low molecular weight (<1 KDa) phospholipids. This leads to a low wall thickness of 3-4 nm and thus contributes to many limitations of liposomes for *in vivo* applications such as low stability, permeability, and drug loading capacity. Target specific ligand modification on their surface is not useful since it changes the structure of the "stealth liposomes" to spherical micelles due to change in the hydrophilic/lipophilic balance (HLB). These shortcomings of liposome-based delivery vehicles have given rise to revolutionary development in nanoscience with the fabrication of amphiphilic block co-polypeptide derived core-shell nanostructures such as micelles, vesicles, cylindrical micelles and nanorods among others. Particularly vesicles built up of polymers (also called polymersomes) have several advantages over liposomes.[1-5] Due to high molecular weight of the polymer chains they afford more stable morphology at very dilute concentrations and also possess high loading capacity. Polymersomes also allow the generation of target oriented ligand modifications on their surface since modification of the building blocks keeps the HLB almost constant thereby not affecting the morphology of the polymersome. They are important as cargo delivery vehicles in biomedical field for their biocompatibility, biodegradability and responsiveness to physiological stimuli like pH, temperature, and ionic strength.[6-10]

As has been discussed in Chapter **I** (sections 1.1 and 1.2), the cell membrane is characterized by presence of glycosylated proteins (glycoproteins) that play a key role in molecular recognition. They bind to specific proteins or molecules to regulate cellular processes. There are specific receptors on cell membranes which bind to specific glycoproteins or glycans. For example, the ASGP-receptor in the liver cells binds only to galactosyl moiety. Though their individual binding constant is low (K_a = 10^4-10^6 M^{-1}), by employing poly-valency the overall binding constant is enhanced by hundred to thousand times (K_a = 10^6-10^8 M^{-1}). The effect of polyvalency can also be exploited in drug delivery for efficient targeting. Therefore, synthetic mimics of glycoproteins have the potential to be developed as targeted delivery vehicles. This is the motivation behind synthesis of glycopolypeptide-based amphiphilic copolymers. In the previous chapter, I discussed the diverse topologies obtained from

glycopolypeptide-conjugated dendron self-assemblies. However, those nanostructures were not studied as possible candidates for *in vivo* delivery vehicles due to unknown biocompatibility of the conjugated dendrons. Many biocompatible polymers have been used in development of drug delivery vehicles such as poly(ε-caprolactone) (PCL), poly(L-lactide), poly(ethylene glycol). Some of these have also been incorporated into amphiphilic block copolymers for generation of assemblies intended for use in drug delivery. For example, bovine serum albumin conjugated and galactose-poly(ethylene glycol)-*b*-poly(ε-caprolactone) (Gal-PEG-PCL), PEG-b-PCL-b-poly(2-(diethylamino)ethyl methacrylate) (PEG-PCL-PDEAEMA, asymmetric) as drug carriers and PEG-S-S-PCL for facile loading and triggered intracellular delivery of proteins.[11-13] Among the biocompatible polymers PCL is of particular interest since biomaterials comprising this polymer have been approved by Food and Drug Administration (FDA). Discher and coworkers have shown that poly(ε-caprolactone) conjugated with poly(ethylene glycol) in proper hydrophobic/hydrophilic ratio can be assembled into well defined nano-assemblies that can be used as delivery vehicles *in vivo*.[14] Discher *et al*. have further demonstrated in another example[14] that certain morphologies show preferential cellular uptake, wherein spherical vesicles were taken up by cells more preferably than filomicelles (long cylindrical micelles) under fluid flow conditions because the latter are extended under flow. The circulation time of filomicelles is an order of magnitude higher than that of spherical vesicle, and also they deliver anticancer drug to the tumor cells in mice.

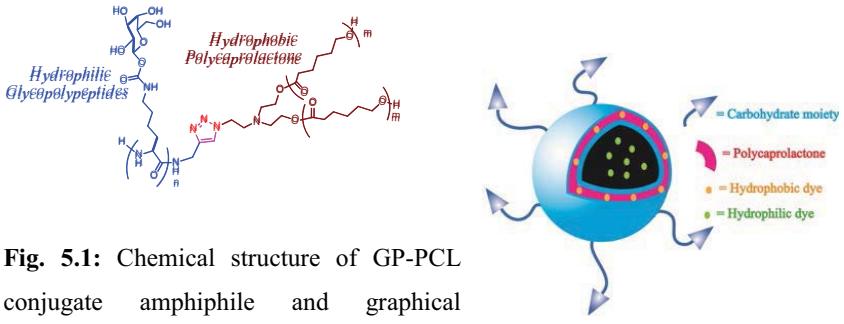

Fig. 5.1: Chemical structure of GP-PCL conjugate amphiphile and graphical representation of vesicle generated from it.

Based on these prior reports, we hypothesized that amphiphilic block copolymers made up of chemically and conformationally different hydrophilic glycopolypeptides (GPs) conjugated to hydrophobic PCL chains should have high tendency for microphase segregation and at proper hydrophobic/hydrophilic ratio would afford well-defined self-assemblies in aqueous solution. Furthermore, if assemblies with different topologies are obtained then preferential cellular uptake could be studied. In this chapter, I will discuss the synthesis of narrow-disperse glycopolypeptide-*block*-poly(ε-caprolactone) copolymers, their assembly into well-defined nanostructures and studies on effect of nanostructure topology on cellular uptake.

Here, we have synthesized GPs containing galactosyl moiety and prepared linear and branched copolymers by conjugating these with PCL using "click chemistry" (CuAAC). Polymers with varying hydrophilic weight fraction were obtained by tuning chain lengths of GP with respect to that of PCL. These polymers were found to assemble into nanorods, vesicles and micelles in dilute aqueous solution. We used the first two morphologies *viz*. nanorods and spherical vesicles for preferential cellular uptake studies. As the GP_{gal} contains galactosyl moiety, it was expected to specifically show the receptor-mediated endocytosis to liver HepG2 cell line; mannosylated GP_{mann}-*b*-PCL copolymers assembled into same morphology were used as control.

5.2 Experimental Section

5.2.1 General

Propargyl 1,2 orthoesters of the corresponding carbohydrates were prepared according to literature procedure.[15-19] Cbz*Lys*(Boc)OH was obtained from Aldrich Chemical Co. and converted to Cbz*Lys*(Boc)OBn using standard literature procedure.[18] $HAuCl_4$, triphosgene and propargyl amine were obtained from Aldrich. All other chemicals used were obtained from Merck, India. Diethyl ether, petroleum ether (b.p. 60˚-80˚C), ethyl acetate, dichloromethane, tetrahydrofuran, dioxane were purchased from Merck, dried by conventional methods and stored in the glove box. Ethyl acetate and dichloromethane were dried with P_2O_5 and CaH_2 and stored on activated molecular sieves (4Å) after distillation. Tetrahydrofuran was passed through

activated alumina and then dried over sodium wire and freshly distilled before use. Dioxane was distilled from CaH_2, refluxed with sodium wire and freshly distilled before use. n-Hexane was dried with sodium wire, distilled and stored on activated molecular sieves (4Å) for use. All the other solvent drying procedures were followed from 'Purification of Laboratory Chemicals' 4th Edition by D.D. Perrin and W. L. F. Armarego.

FT-IR spectra were recorded on Perkin Elmer FT-IR spectrum GX instrument by making KBr pellets. Pellets were prepared by mixing 3mg of sample with 97mg of KBr.^{1}H NMR

spectra were recorded on Bruker Spectrometers (200 MHz, 400 MHz or 500 MHz).^{13}C NMR and DEPT spectra were recorded on Bruker Spectrometer (50 MHz, 100MHz or 125MHz) and signals relative to deuterated solvent are reported. Gel permeation chromatography/light scattering (GPC/LS) was performed on a VISKOTEK TDA 305-040 TRIPLE DETECTOR ARRAY refractive index (RI), viscometer (VISC), low angle light scattering (LALS), right angle light scattering (RALS) GPC/SEC MODULE. Separations were achieved by three columns (T6000M, GENERAL MIXED ORG 300X7.8 MM) and one guard column (TGUARD, ORG GUARD COL 10X4.6 MM), 0.05 M LiBr in DMF as the eluent at 50 °C. GPC/LS samples were prepared at concentrations of 5 mg/mL. A constant flow rate of 1 mL/min was maintained. An LSM 710 Carl Zeiss laser scanning confocal microscope (LSCM) was used to image the fluorescent samples. He-Ne laser (543 nm) and an Argon-ion laser (488 and 514 nm) were used for the experiments.TEM measurements were done at 200 kV on an FEI Technai F20 and F30 instrument.

5.2.2 Circular Dichroism Measurements

Aqueous solutions of all the glycopolypeptide-conjugated polycaprolactones were filtered through 0.45 μm syringe filters. CD (190-260 nm) spectra of the glycopolypeptides (0.25-0.5 mg/mL in deionized water) were recorded (JASCO CD SPECTROPOLARIMETER, Model J-815) in a cuvette with 2 mm path length. All the spectra were recorded for an average of 3 scans and the spectra were reported as a function of molar ellipticity [θ] vs wavelength.[18]

5.2.3 Sample preparation for Transmission Electron Microscopy

Fully deprotected polymers (nGP-PCLm) were dissolved in dimethylsulfoxide and diluted to dimethylsulfoxide : water = 1:1 at 0.05 wt%, filtered with 0.45 μm filter paper and dialyzed thoroughly by deionized water for 2 days. The solution of the polymer (~10 μL) was spotted on carbon coated 400 mesh copper grid, left for 15-20 min, excess solvent was removed by touching the edge of the grid with Whatman filter paper, and negatively stained by 0.2 wt% uranyl-acetate for 20 sec. Grid was washed twice with deionized water to remove excess unbound uranyl-acetate from the grid and dried in desiccator for 20h and analyzed by transmission electron microscopy.

5.2.4 Synthetic procedures

5.2.4.1 General procedure for the synthesis of glycopolypeptides

All the monomers were synthesized by following the previously reported procedure by our group.[15-19] To a solution of galacto- or manno-*l*-lysine NCA (100 mg/mL) in dry dioxane was added "proton sponge" *N,N'*-tetramethylnaphthalene (1.0 equivalent to monomer; 1M) as an additive and propargyl-amine (0.4M) as the initiator inside the glove box. The progress of polymerization was monitored by FT-IR spectroscopy by comparing the intensity of the initial NCA anhydride stretching at 1789 cm^{-1} and 1852 cm^{-1} with that of the sample. The reactions were generally complete within 36 h. Finally solvent was removed under reduced pressure. The resulting residue was dissolved in dichloromethane, washed with 1N HCL to remove "proton sponge" and then polymer was precipitated out by addition of methanol. The precipitated polymer was collected by centrifugation and dried to afford white glycopolypeptides in 85-90% yield.

Run No	Monomer (NCA)	Polymer Name AcnGP	M/I[a]	M_w/M_n[b]	M_w[c]	Yield[d]	Helicity (CD)[e]
1	β-galacto-*O*-*l*-lys	Ac10GP$_{gal}$	10	1.07	16	90%	α-helix
2	β-galacto-*O*-*l*-lys	Ac20GP$_{gal}$	20	1.10	28	90%	α-helix
3	β-galacto-*O*-*l*-lys	Ac25GP$_{gal}$	25	1.07	8	85%	α-helix
4	β-galacto-*O*-*l*-lys	Ac40GP$_{gal}$	40	1.09	14	90%	α-helix
5	α-manno-*O*-*l*-lys	Ac10GP$_{mann}$	10	1.17	14	90%	α-helix
6	α-manno-*O*-*l*-lys	Ac20GP$_{mann}$	20	1.18	28	90%	α-helix

Table 5.1: [a]M/I = monomer to initiator ratio [Initiator (I) is propargyl amine], [b]polydispersity index, [c]Degree of polymerization (DP) were calculated from Gel permeation chromatography equipped with light scattering (GPC/LS) that was performed on a VISKOTEK TDA 305-040 TRIPLE DETECTOR ARRAY refractive index (RI), viscometer (VISC), low angle light scattering (LALS), right angle light scattering (RALS) GPC/SEC MODULE. Separations were achieved by three columns (T6000M, GENERAL MIXED ORG 300X7.8 MM) and one guard column (TGAURD, ORG GUARD COL 10X4.6 MM), 0.05 M LiBr in DMF as the eluent at 50 °C at elution rate 1mL/min. GPC/LS samples were prepared at concentrations of 5 mg/mL. System was calibrated by PMMA standards. [d]Total isolated yield, [e]Circular dichroism spectra measured in acetonitrile.

5.2.4.2 General procedure for synthesis of azide-containing polycaprolactone

Azide-teminated branched and linear poly(ε-caprolactone)s were synthesized by ring-opening polymerization (ROP) of ε-caprolactone using azide-functionalized mono- and diol initiators with Sn(oct)$_2$ as catalyst by Mr. Naganath Patil, a student in Dr. Ambade's group at NCL.

5.2.4.3 Synthesis of glycopolypeptide-polycaprolactone conjugates by "click reaction"

To a solution of alkyne end-functionalized acetyl protected glycopolypeptide (Ac10GP, Ac20GP, Ac25GP and Ac40GP) in THF/methanol/water/DMSO (2:1:0.2:1) was added azide-end functionalized polycaprolactone [(PCL$_{26}$)2, (PCL$_{50}$)2 and

($LPCL_{50}$)] (0.9 eq) and resultant reaction mixture was degassed by three freeze-pump-thaw cycles. Premixed $CuSO_4$ (0.2 eq) and ligand THPTA (0.2 eq) solution and sodium ascorbate (0.4 eq) were added and the reaction was allowed to proceed for 24 h under argon atmosphere (Scheme 5.1 and 5.2). The progress of the reaction was monitored by the disappearance of the azide stretch at 2115 cm^{-1} in FT-IR. When >95% of the azide peak had disappeared, solvent was removed under reduced pressure. The reaction mixture was dissolved in ethyl acetate and washed multiple times with 1N HCL followed by 5wt% disodium salt of ethylenediamino tetraacetate solution to remove the copper salt. Then the solvent was evaporated completely under reduced pressure. The off-white compounds were dried under vacuum overnight at 45 ˚C to afford polymers Ac10GP_{gal}-(PCL_{26})2, Ac20GP_{gal}-(PCL_{26})2, Ac10GP_{mann}-(PCL_{26})2, Ac20GP_{mann}-(PCL_{26})2, Ac20GP_{gal}-(PCL_{50})2, Ac25GP_{gal}-(PCL_{50})2 and Ac40GP_{gal}-(PCL_{50})2 (Scheme 1) and Ac10GP_{gal}-(PCL_{50}) and Ac20GP_{gal}-(PCL_{50}) (Scheme 5.2).

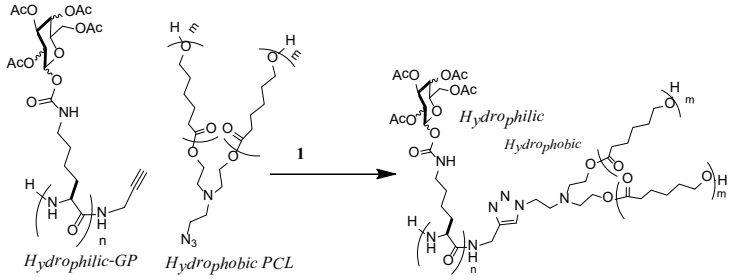

1) CuSO4, Na-ascorbate (0.2 mol%), THF/Methanol/H_2O/DMSO

Scheme 5.1: Synthesis of glycopolypeptide-polycaprolactone conjugates [Ac10GP_{gal}-(PCL_{26})2, Ac20GP_{gal}-(PCL_{26})2, Ac10GP_{mann}-(PCL_{26})2, Ac20GP_{mann}-(PCL_{26})2, Ac20GP_{gal}-(PCL_{50})2, Ac25GP_{gal}-(PCL_{50})2] by "*Click Reaction*".

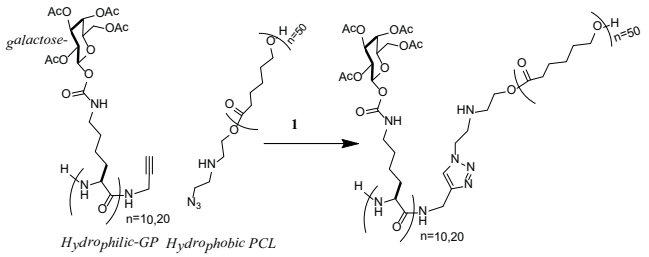

1) CuSO4, Na-ascorbate (0.2 mol%), THF/Methanol/H_2O/DMSO

Scheme 5.2: Synthesis of glycopolypeptides-polycaprolactone conjugates [Ac10GP_{gal}-($LPCL_{50}$) and Ac20GP_{gal}-($LPCL_{50}$)] by "*Click Reaction*".

5.2.4.4 Deprotection procedure for the glycopolypeptide-polycaprolactone conjugates

Hydrazine monohydrate (25 eq) was added to the solutions of all the acetyl protected glycopolypeptides in tetrahydrofuran (10 mg/mL) and the reactions were stirred for 12 h at room temperature. Reactions were quenched by addition of acetone and then solvent was removed completely under reduced pressure. The solid residues were dissolved in a mixture of dimethylsulfoxide and deionized water (1:1), filtered through 0.45μm filter paper and transferred to dialysis tubing (12 KDa MWCO). The samples were dialyzed against deionized water for 3 days, with water changes once every two hours for the first day, and then thrice per day. Dialyzed polymer solutions were lyophilized to yield glycopolypeptide-polycaprolactone conjugates (Scheme 3 and 4) as white fluffy solids (~80% yield).

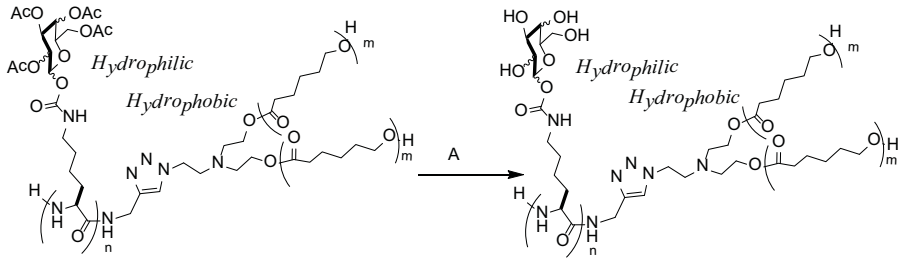

A) THF, Hydrazine hydrate (25 equiv) at RT, 12 h.

Scheme 5.3: Synthesis of deprotected glycopolypeptides-polycaprolactone conjugates [10GP$_{gal}$(OH)-(PCL$_{26}$)2, 20GP$_{gal}$(OH)-(PCL$_{26}$)2, 20GP$_{mann}$(OH)-(PCL$_{26}$)2, 20GP$_{gal}$(OH)-(PCL$_{50}$)2, 25GP$_{gal}$(OH)-(PCL$_{50}$)2].

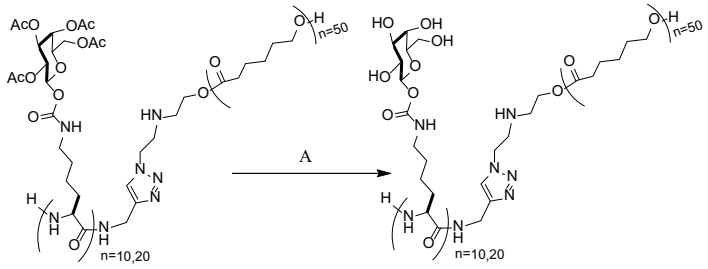

A) THF, Hydrazine hydrate (25 equiv) at RT, 12 h.

Scheme 5.4: Synthesis of deprotected glycopolypeptide-polycaprolactone conjugates [10GP$_{gal}$(OH)-(LPCL$_{50}$) and 20GP$_{gal}$(OH)-(LPCL$_{50}$)].

Polymer Name	Sugar Residue	Repeating units GP	Repeating units of PCL	Chemical Structure
10-GP$_{gal}$(OH)-(PCL$_{26}$)2	β-galactose	10	Branched 52	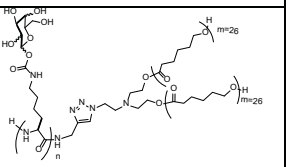
20-GP$_{gal}$(OH)-(PCL$_{26}$)2	β-galactose	20	Branched 52	
10-GP$_{man}$(OH)-(PCL$_{26}$)2	α-mannose	10	Branched 52	
20-GP$_{man}$(OH)-(PCL$_{26}$)2	α-mannose	20	Branched 52	
10-GP$_{gal}$(OH)-(LPCL$_{50}$)	β-galactose	10	Linear 50	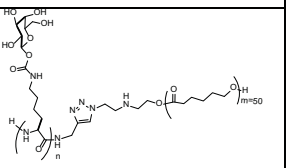
20-GP$_{gal}$(OH)-(LPCL$_{50}$)	β-galactose	20	Linear 50	
20-GP$_{gal}$(OH)-(PCL$_{50}$)2	β-galactose	50	Branched 100	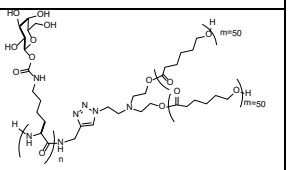
25-GP$_{gal}$(OH)-(PCL$_{50}$)2	β-galactose	50	Branched 100	
40-GP$_{gal}$(OH)-(PCL$_{50}$)2	β-galactose	50	Branched 100	

Table 5.2: Synthesized Amphiphilic polymers.

5.2.4.5 Encapsulation of the hydrophilic dye (Calcein)

Solution of amphiphiles (10-GP$_{gal}$(OH)-(PCL$_{26}$)2, 20-GP$_{gal}$(OH)-(PCL$_{26}$)2 and 20-GP$_{mann}$(OH)-(PCL$_{26}$)2) DMSO (0.5 mg/mL) was added to 100 µL 8 mM of calcein aqueous solution and diluted to 1 mL by gradual addition of DMSO and water mixture

(1:1) to get the amphiphile concentration of 40 and 50 μM respectively. The solution was kept for 3-4 h under continuous stirring. Then, the total mixture was transferred to the dialysis tube (12 KDa MWCO) and kept for dialysis for 30 h to remove DMSO while changing deionized water at 3h interval. After the complete removal of DMSO, the dialysed solution was exchanged three times by dialysis against PBS buffer (100 mM) for 6h. Calcein encapsulated by the assemblies was thoroughly characterized by absorption as well as fluorescence spectroscopy.

5.2.4.6 Encapsulation of the hydrophobic dye (Nile Red)

Solution of amphiphiles (10-GP_{gal}(OH)-(PCL_{26})2, 20-GP_{gal}(OH)-(PCL_{26})2 and 20-GP_{mann}(OH)-(PCL_{26})2) DMSO (0.5 mg/mL) was diluted to 1 mL by gradual addition of DMSO and water mixture (1:1) to get the amphiphile concentration of 40 and 50 μM, respectively. The solution was kept for 3-4 h continuous stirring. Then, the total mixture was transferred to the dialysis tube (12 KDa MWCO) and kept for dialysis to remove DMSO for 30 h while changing deionized water at 3h interval. Then, 10 μL of the dye Nile Red (3 mM in DMSO) was added to the assemblies and kept for 1h for encapsulation in the hydrophobic zone of the assemblies, then thoroughly characterized by absorption as well as fluorescence spectra.

5.2.4.7 End labelled amphiphiles by Rhodamine-B-isothiocyanate

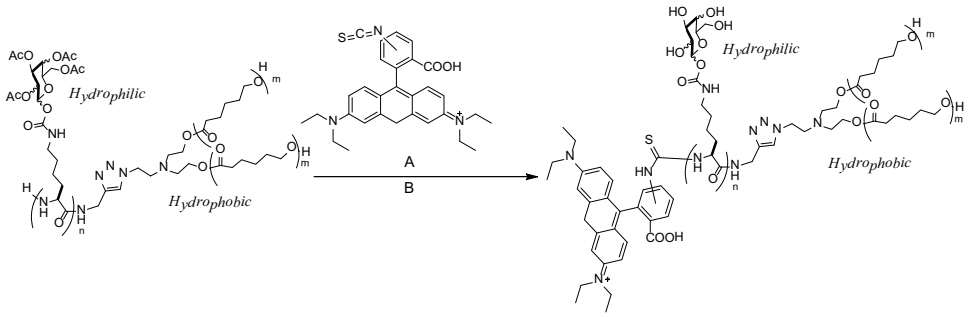

A) THF & B) THF, Hydrazine hydrate (25 equiv) at RT, 12 h.

Scheme 5.5: Represents the end-labelling of the GP-PCL by Rhodamine-B isothiocyanate.

To a solution of Ac10GPgal-(PCL_{26})2 (20 mg/mL solution in THF) was added Rhodamine-B isothiocyanate (0.15 equivalent with respect to the polymer concentration) and the reaction mixture was incubated overnight under inert atmosphere. Solvent was removed from the crude reaction mixture followed by addition of hydrazine hydrate for removal of the acetate groups from carbohydrate moiety. The resultant amphiphilic polypeptide was dried and then redissolved in the mixture of DMSO and water (1:1) at a concentration of 1mg/mL. Finally, the resultant amphiphile solution was dialysed against deionised water for long time for complete removal of the unreacted rhodamine dye. Finally, the Rhodamine-B labelled end functionalized amphiphile was isolated as a solid by freeze-drying and was characterized thoroughly by absorption and emission spectra. Rhodamine labelled Ac20GPgal-(PCL_{26})2 and Ac20GPmann-(PCL_{26})2 was synthesized by the same methodology as discussed above. These Rhodamine labelled amphiphiles were used further for cellular uptake studies.

5.2.4.8 Dynamic light scattering

The amphiphilic glycopolypeptide $20GP_{gal}$(OH)-(PCL_{26})2 was self-assembled in aqueous solution at 0.5 mg/mL concentration by following previously described procedure. Freshly dialysed solution was filtered through a 0.5 μM filter paper and analyzed by dynamic light scattering. Then, the same solution was dialysed against PBS buffer (100 mM) for 6 h and analysed using dynamic light scattering.

5.2.4.9 In vitro cytotoxicity assay

HepG2 cells were seeded in a 96-well plate at a density of 1 $x10^4$ cells/well and incubated for 18 h at 37 °C in MEM containing 10% FBS. The medium was replaced with serum-free MEM. Polymersomes were prepared in serum free MEM and then added to make a final concentration of 40, 35, 30, 25, 20, 15, 10, 8, 6, 4 and 2 μg /well, respectively. Cells were further incubated for 4 h, and then the medium was replaced with MEM containing 10% FBS. After another 40-h incubation at 37 °C, the media was removed and 100 μL solution of MEM containing 10 % FBS with filter sterilized MTT (3-(4,5-Dimethylthiazol-2-yl)-2,5-diphenyltetrazolium bromide) solution (0.45 mg/mL) was added into each well. After incubation at 37 °C for 4 h with MTT, the media was aspirated from the wells and 100 μL DMSO was added to dissolve

insoluble Formosan crystals formed. The absorbance was measured at 550 nm using a microtitre plate reader (Veroscan, Thermo Scientific) and the cell viability was calculated as a percentage relative to untreated control cells.

5.2.4.10 Cellular uptake experiment

HepG2 cells were seeded on glass cover slips at a density of 50,000 per well in MEM containing 10%FBS and incubated for 18 h. The media was replaced with serum-free MEM. Rhodamine-B labeled polymersomes were prepared in serum free MEM and then added to make a final concentration of 60 and 30 µg/well and further incubated for 2 h. The cells were then washed thrice with cold PBS and fixed with 3.5% paraformaldehyde-PBS (pH 7.4) solution for 15 min. The fixative was removed and cells were washed again thrice with cold PBS solution and mounted on glass slides using mounting media containing DAPI to stain the nuclei. Images were acquired using CLSM.

5.3 Results and Discussion

Well-characterized glycopolypeptides with narrow molecular weight distributions were synthesized by propargyl amine initiated ring opening polymerization of galactosylated-lysine *N*-carboxyanhydride (gal-lys-NCA). Polycaprolactones were synthesized by terminal azide modified hydroxyl group initiated ring opening polymerization of ε-caprolactone. The terminal alkyne glycopolypeptides were conjugated to azide functionalized polycaprolactones by using "Click Chemistry" (CuAAC). Finally, the amphiphiles containing hydrophilic GP conjugated hydrophobic PCL, were obtained following very mild deprotection procedure using hydrazine hydrate. The amphiphilic bock copolymers were designed on the basis of the three tunable factors, 1) size of the hydrophilic glycopolypeptides (chain length), 2) size of the hydrophobic polycaprolactone (chain length) and 3) the branching of the hydrophobic polycaprolactone (linear and branched). The appropriate energy contributions of those factors reflect in size, shape and interfacial curvature of the self-assembly.

The GP-PCL amphiphilic block copolymers generate different morphologies, when the hydrophobicity changes from 65% to 46%, well dispersed nanorods and spherical vesicular self-assemblies were obtained from [10-GP_{gal}(OH)-(PCL_{26})2] and

[20-GP$_{gal}$(OH)-(PCL$_{26}$)2] amphiphiles in aqueous solution, respectively. On the other hand at the same molecular weight of the amphiphiles [hydrophobic/hydrophilic ratio constant] 10-GP$_{gal}$(OH)-LPCL$_{50}$ and 20-GP$_{gal}$(OH)-LPCL$_{50}$ containing linear hydrophobic polycaprolactone LPCL$_{50}$ generate nanorods and micelles, respectively. The effect of longer chain length on morphology when the hydrophobic/hydrophilic ratio is in between 46-65%, in amphiphiles [20-GP$_{gal}$(OH)-(PCL$_{50}$)2, 25-GP$_{gal}$(OH)-(PCL$_{50}$)2 and 40-GP$_{gal}$(OH)-(PCL$_{50}$)2].

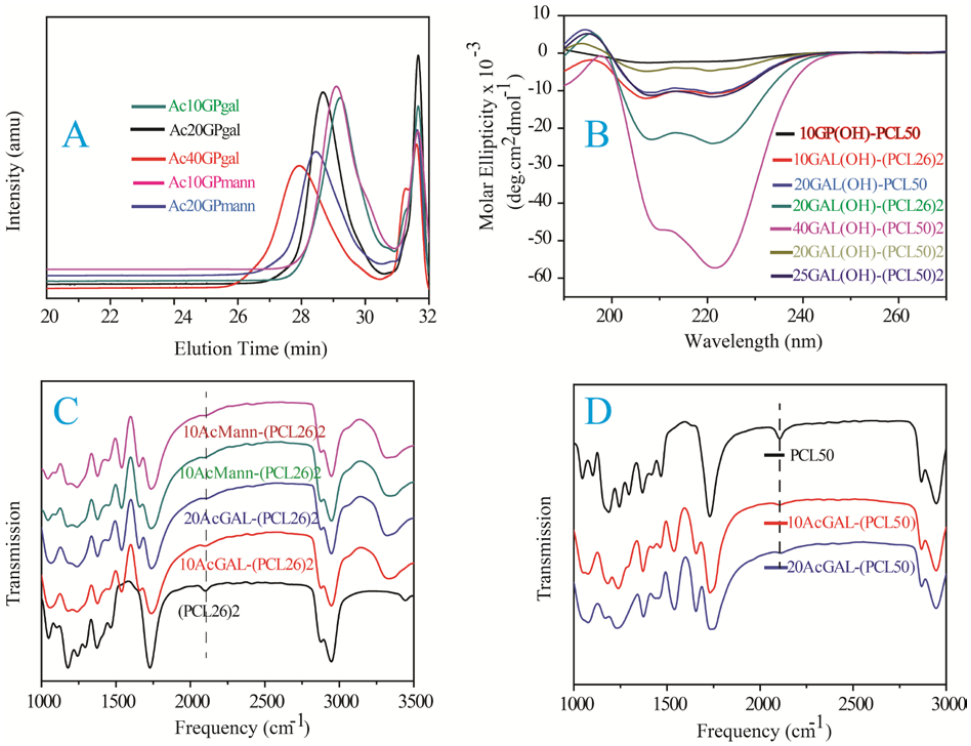

Fig. 5.2: Represents A) GPC curves, B) Circular Dichroism, C) and D) IR-spectra of the synthesized polymers.

5.3.1 Design of Glycopolypeptides conjugated Polycaprolactone copolymers

Azide end functionalized branched polycaprolactone, ([PCL$_{26}$]2) was synthesized following literature reported procedure for controlled ring opening polymerization of ε-caprolactone; its molecular weight is (X). To get proper HLB of amphiphiles, different chain length glycopolypeptides were synthesized by following

the previously developed methodology from our group. Glyco-*lys*-NCA monomer was initiated with propargyl amine (150 mM) with the ratio of 10 and 20 to get alkyne terminated 10-GP_{gal}-*lys* and 20-GP_{gal}-*lys*. They were conjugated with branched polycaprolactone ([PCL_{26}]2) to get 10-GP_{gal}-*lys*-(PCL_{26})2 and 20-GP_{gal}-*lys*-(PCL_{26})2) by using very facile copper-catalyzed azide alkyne cycloaddition (CuAAC), also known as "Click Reaction". Then, the acetyl groups of these GP-PCL conjugates were deprotected to get free hydroxyl groups of carbohydrates by hydrazine hydrate under very mild conditions without affecting the polycaprolactone chains. We designed the amphiphiles 10-GP_{gal}(OH)-*lys*-(PCL_{26})2 and 20-GP_{gal}(OH)-*lys*-(PCL_{26})2 so as to have 65% and 46% hydrophobicity, respectively. Similarly, to observe the effect of chain length at almost same molecular weight linear polycaprolactone [$LPCL_{50}$] was conjugated with 10-GP_{gal}-*lys* and 20-GP_{gal}-*lys* glycopolypeptides to obtain 10-GP_{gal}(OH)-*lys*-($LPCL_{50}$) and 20-GP_{gal}(OH)-*lys*-($LPCL_{50}$) with same hydrophobic weight% as compared to the previous. Furthermore, to observe the influence of longer chain length, higher molecular weight branched polycaprolactone ([PCL_{50}]2) was conjugated with 20-GP_{gal}-*lys*, 25-$_{gal}$-*lys* and 40-GP_{gal}-*lys* glycopolypeptides to obtain 20-GP_{gal}(OH)-*lys*-(PCL_{50})2, 25-GP_{gal}(OH)-*lys*-(PCL_{50})2 and 40-GP_{gal}(OH)-*lys*-(PCL_{26})2 by keeping the hydrophobicity in between 65-46%. All the amphiphiles were designed on the basis of the three major contributing factors to energetics of the assembly, 1) hydrophobic interaction of the polycaprolactones, 2) hydrophilic, helical and hydrogen bonding interactions among the glycopolypeptides and 3) the crystalline packing of polycaprolactone.

5.3.2 Assembly in the aqueous solution

Amphiphilic GP-*b*-PCL copolymers (GP-PCL conjugates) were obtained by deprotection of acetyl groups under mild conditions. Then the polymeric amphiphiles were subjected to dialysis to remove free glycopolypeptide chains (nonconjugated to polycaprolactone) by using large pore size dialysis tube (MWCO 12 KD). The dialyzed solution was washed with methylene chloride. Finally, purified aqueous solution of the amphiphiles was concentrated under vacuum to afford off-white solid. Amphiphiles 10-GP_{gal}(OH)-*lys*-(PCL_{26})2 were redissolved in DMSO and water mixture (1:1) at the concentration of 0.05 wt% and dialyzed thoroughly against deionized water to obtain a solution in pure water. A drop of this solution was placed

on the carbon coated copper grid, negatively stained with uranyl acetate (0.2 wt%) solution. When it was imaged using transmission electron microscopy (TEM) well dispersed nanorods (diameter 10-12 nm) were observed. These nanorods are more than 100 nm in length and are quite stable in aqueous solution for couple of weeks. When the other amphiphile 20-GP_{gal}(OH)-*lys*-(PCL_{26})2 was assembled by following the same way and analyzed under TEM well dispersed vesicles of diameter 50-80 nm and a thickness of 10-12 nm were observed.

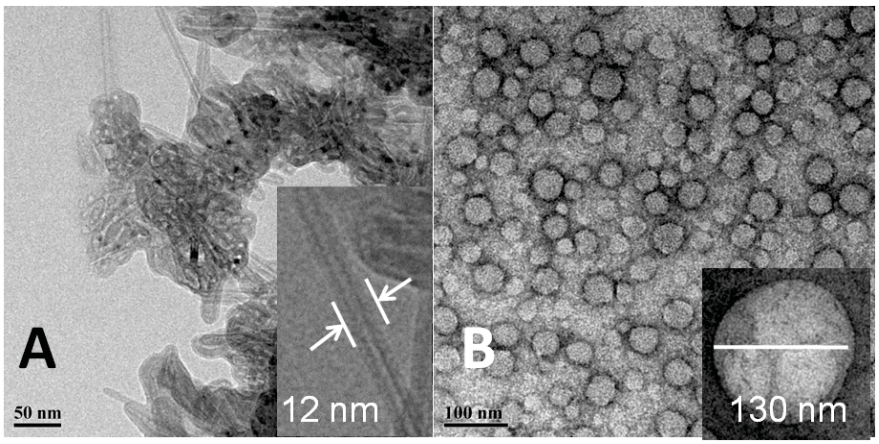

Fig. 5.3: Represents TEM images, A) Nanorods of 10GP_{gal}(OH)-(PCL_{26})2 and B) Vesicles of 20GP_{gal}(OH)-(PCL_{26})2 at 0.05wt% in aqueous solution, negatively stained with 0.2wt% uranyl acetate.

The structure of the same dialyzed compound analyzed under atomic forced microscopy (AFM) on silicon vapor gives the height/diameter ratio (~0.08) close to that observed for a hollow structure (~0.1). This provides a good evidence for vesicular morphology. Circular dichroism (CD) measurements of both the solutions show the peak minima at 208 nm and 222 nm for α-helical secondary structure, which suggests that helix-helix (rod-rod) interaction may exist among the hydrophilic GP block of the amphiphilic copolymers.[19, 20] PEG conjugated PCL copolymers assemble to form lamellar structures with PCL inner core and PEG corona.[21-23] Crystallization of PCL block has been shown to contribute to the rod-like morphology.[21-23]

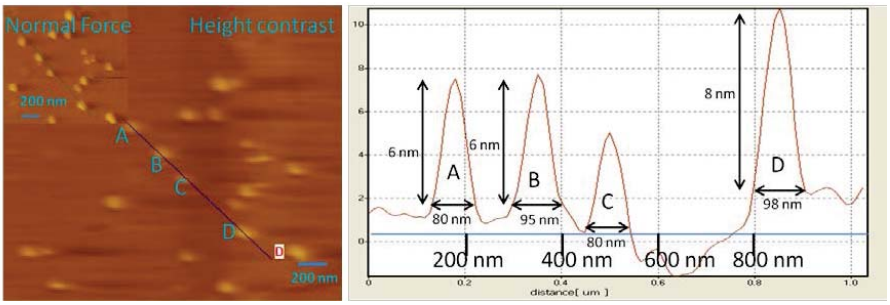

Fig. 5.4: AFM image of the vesicles formed by [20GP$_{gal}$(OH)-(PCL$_{26}$)2] at 0.05wt% in aqueous solution.

In our case also it is possible that the formation of nanorod structure is directed by crystallization of PCL blocks that pack into the hydrophobic core. This crystallization would initially lead to formation of sheet like bilayer structure and then decrease in the surface energy due to longer GP chains (hydrophobic/hydrophilic ratio = 46%) would generate curvature of the bilayer so as to form vesicles. On the other hand, at higher hydrophobic /hydrophilic ratio (65%) closing of the bilayer into a spherical structure (3D) is unfavourable and only unidirectional elongation takes place that affords rod-like morphology.

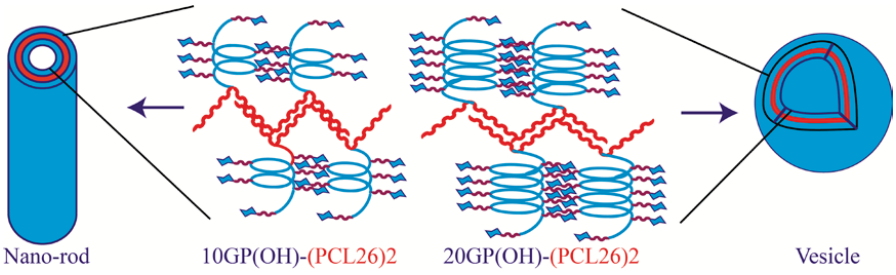

Fig. 5.5: Proposed graphical representation of the nano-rod and vesicle.

To observe the effect of branched vs. linear hydrophobic chain, a linear polycaprolactone [LPCL$_{50}$] was synthesized with almost the same molecular weight as that of branched polycaprolactone [(PCL$_{26}$)2] so that hydrophobic/hydrophilic ratio is kept constant. By following the previously described procedure, alkyne end-functionalized 10-GP$_{gal}$-*lys* and 20-GP$_{gal}$-*lys* were conjugated to LPCL$_{50}$ to get 10-GP$_{gal}$(OH)-*lys*-[LPCL$_{50}$] and 20-GP$_{gal}$(OH)-*lys*-[LPCL$_{50}$]. After deprotection and

purification of the amphiphiles, TEM images were taken. The polymer 10-GP_{gal}(OH)-*lys*-[$LPCL_{50}$] formed nanorods with diameter of 17-18 nm that is 6-8 nm thicker than previous nanorods probably because chain length of the linear hydrophobic PCL in the amphiphilic polymer is almost double of that in the branched polycaprolactone. On the other hand, when 20-GP_{gal}(OH)-*lys*-[$LPCL_{50}$] amphiphile assemblies were imaged under TEM, it showed micelle-like aggregation in the aqueous solution whereas the amphiphiles 20-GP_{gal}(-*lys*-(PCL_{26})2 containing branched polycaprolactone of same 46% hydrophobic weight fraction (same molecular weight) formed vesicles. The linear polycaprolactone in the amphiphiles probably occupies conical shaped volume in the hydrophobic core due to longer length that results in aggregation into miceller morphology with hydrophobic PCL core and hydrophilic GP corona.

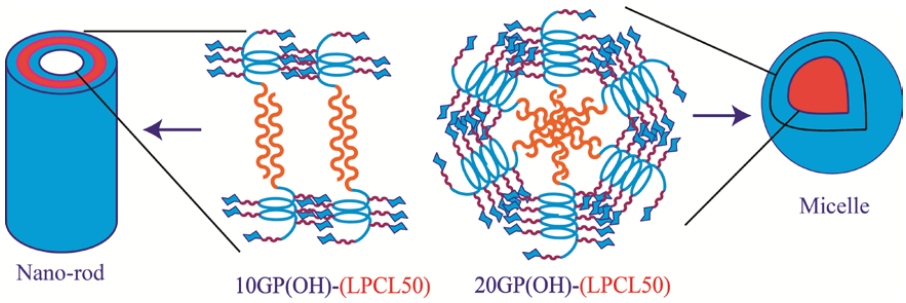

Fig. 5.6: Proposed graphical representation of the nano-rod and micelle.

Name of Polymer	10-GP_{gal}(OH)-(PCL_{26})2	20-GP_{gal}(OH)-(PCL_{26})2	10-GP_{gal}(OH)-($LPCL_{50}$)	20-GP_{gal}(OH)-($LPCL_{50}$)	20-GP_{gal}(OH)-(PCL_{50})2	25-GP_{gal}(OH)-(PCL_{50})2	40-GP_{gal}(OH)-(PCL_{50})2
nGP	10	20	10	20	20	25	40
PCLm	52 (B)	52 (B)	50 (L)	50 (L)	100 (B)	100 (B)	100 (B)
wt % of PCL	64%	47%	63%	46%	63%	58%	46%
Structure Obtained	Nanorod	Vesicle	Nanorod	Micelle, Compound vesicles	Sheet, nanorod	Nanorod	Micelle

Table 5.2: Represents attributes of synthesized nGP-PCLm block copolymers and nanostructure observed in TEM of the self-assembled polymers at 0.05 wt% in DI water. n = Average chain length of glycopolypeptide, m = Average chain length of polycaprolactone, B = branched, L = linear.

Furthermore, to investigate the effect of longer chain length of both hydrophilic GP and hydrophobic PCL, branched PCL with total repeating units of 100 [$(PCL_{50})2$] was synthesized. To keep hydrophobic/hydrophilic ratio constant, 20-GP_{gal}-*lys* and 40-GP_{gal}-*lys* were conjugated to the branched PCL [$(PCL_{50})2$] to obtain 20-GP_{gal}-*lys*-[$(PCL_{50})2$] and 40-GP_{gal}-*lys*-[$(PCL_{50})2$]. From the amphiphile 40-GP_{gal}(OH)-*lys*-[$(PCL_{50})2$], well dispersed micelles of diameter 60-100 nm were observed under TEM.

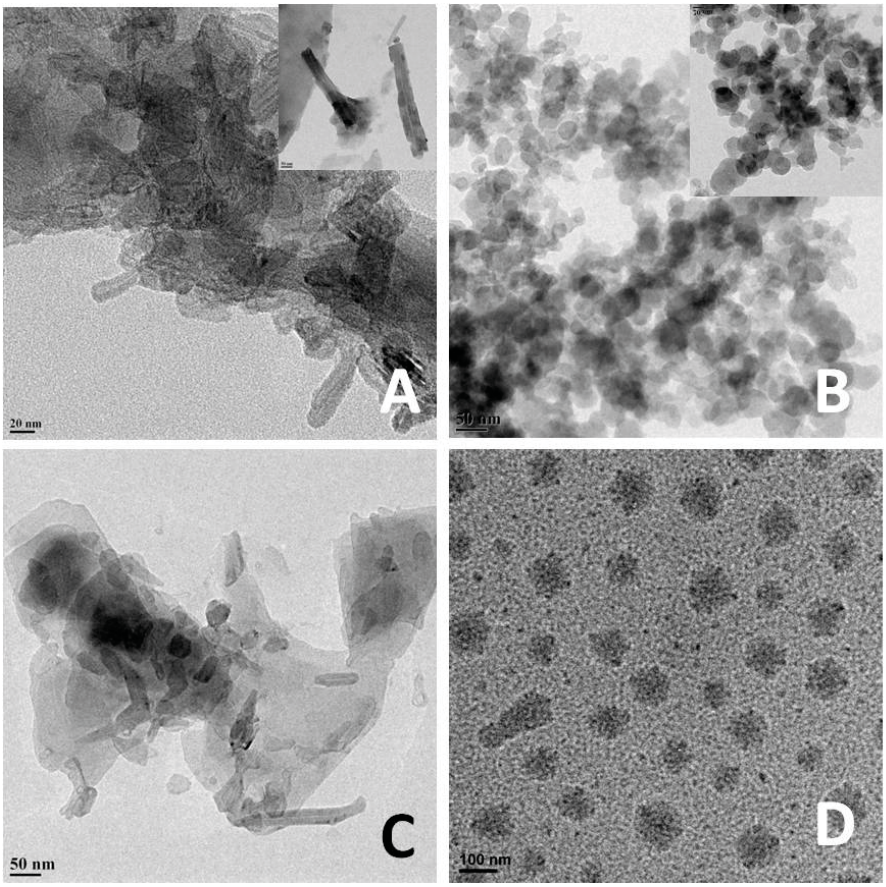

Fig. 5.7: Represents the self-assembly at 0.05wt% in aqueous solution, A) Nanorods of 10GP_{gal}(OH)-(PCL_{26})2, B) Micelle of 20GP_{gal}(OH)-($LPCL_{50}$), C) Sheet and Rods of 25GP_{gal}(OH)-(PCL_{50})2 and D)

Micelle of 40GP$_{gal}$(OH)-(PCL$_{50}$)2 as observed under TEM using negative staining with 0. 05 wt% uranyl acetate.

In this case, long hydrophilic glycopolypeptides dominate the thermodynamics of formation of assembly so that shorter PCL chains are forced to occupy conical shape volume, which is known to form well disperse micelle structure in aqueous solution. On the other hand, 20-GP$_{gal}$(OH)-*lys*-[(PCL$_{50}$)2] amphiphile did not form any well defined structures; a mixture of sheet and rod like structures was observed under TEM. Probably, chain length of GP is not sufficient to decrease the surface energy by reducing interfacial curvature and hydrophobic interaction between longer PCL chains dominates. This is supported by the fact that when longer hydrophilic polymer 25-GP$_{gal}$-*lys* was conjugated to branched PCL - [(PCL$_{50}$)2], the obtained 25-GP$_{gal}$(OH)-*lys*-[(PCL$_{50}$)2] forms rod-like structures.

5.3.3 Hydrophilic and hydrophobic dye encapsulation and dynamic light scattering experiments

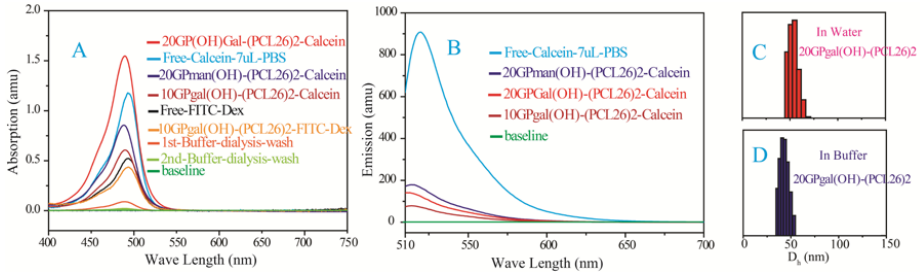

Fig. 5.8: Represents A) Absorption spectra, B) Emission spectra and C) and D) Dynamic light scattering profile for the corresponding amphiphiles.

Among all the glycopolypeptide-PCL conjugates studied, 10-GP$_{gal}$(OH)-(PCL$_{26}$)2, 20-GP$_{gal}$(OH)-(PCL$_{26}$)2 and 20-GP$_{mann}$(OH)-(PCL$_{26}$)2 generate interesting morphologies in the form of elongated rods and vesicles and hence we were interested to probe if these nanostructures were able to encapsulate both hydrophilic (calcein) as well as hydrophobic (Nile Red) dye. Such studies are important for understanding the utility of these materials for drug delivery applications. Calcein was encapsulated during the self-assembly process and hence was expected to be encapsulated inside the vesicles and nanorods. The calcein encapsulated vesicles and nanorods were dialyzed

extensively in water until the water outside the dialysis tube showed no fluorescence that may result from free calcein (Figure 5.8 A; see trace baseline). The vesicle and nanorods solution inside the dialysis tubing still showed colour, which implied that calcein remained encapsulated inside the nanostructures. Furthermore, the emission spectra (Fig. 5.7B) showed significant amount of quenching of the encapsulated dye in comparison to the same concentration of free dye in solution (free calcein solution absorption spectrum shows almost same absorption values with respect to the encapsulated calcein in Fig. 5.7A). The assemblies obtained from the amphiphiles 10-GP_{gal}(OH)-(PCL_{26})2 are also capable to encapsulate the larger dye (FITC-Dextran in Fig 5.7A), which clearly indicates that the rod-like morphology generated by those amphiphiles are hollow. On addition of the hydrophobic dye nile red to those assemblies, they are able to encapsulate it. Fluorescence emission spectra of encapsulated nile red shows peak maxima at 620 nm due to its presence in hydrophobic core of those assemblies.

5.3.4 Cytotoxicity and cellular uptake

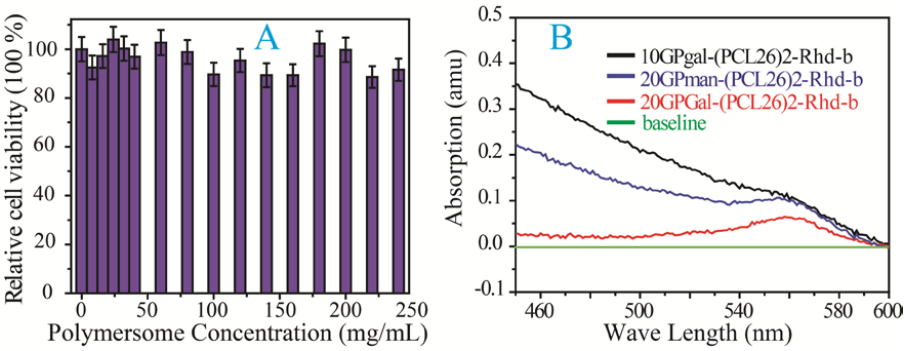

Fig. 5.9: Represents A) Cell viability by MTT assay of rod like morphology generated from amphiphiles 10-GP_{gal}(OH)-(PCL_{26})2 and B) Absorption spectra of the Rhodamine-b end functionalized amphiphiles in aqueous solution.

The cytotoxicity experiment (MTT assay of 10-GP_{gal}(OH)-(PCL_{26})2) shows that these assemblies are not toxic up to 250 µg/mL upon addition to the HepG2 cells after 24 h incubation and more than 90% of cells are viable (Fig. 5.9A). As galactosyl recognition receptors are over-expressed on cellular surface of HepG2 cells, galactosylated vesicles were expected to enter the cells through active targeting.

Confocal imaging was used to monitor the cellular uptake. Rapid cellular endocytosis was observed within 2h for galactosylated Rhodamine-B labeled vesicles at 30μg/mL, whereas mannosylated vesicles, tested as a control, did not show significant cellular uptake at this concentration. At higher concentration (60 μg/mL) however, these vesicles also enter into the cells in significant amount possibly through cellular apoptosis (passive targeting, Fig. 5.10).

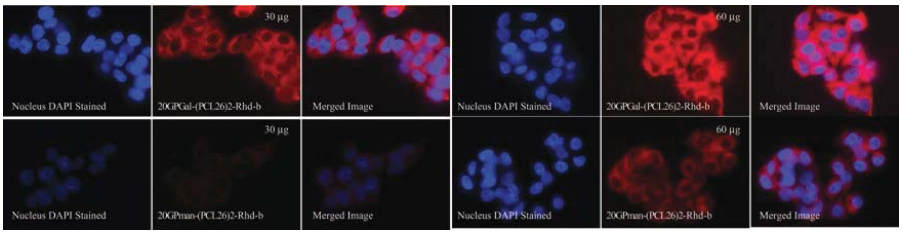

Fig. 5.10: Represents the cellular uptake of HepG2 cells by confocal imaging.

5.4 Conclusion

We demonstrated the successful synthesis of multiple morphologies generated from glycopolypeptide conjugated polycaprolactone and controlled tunabilities by keeping the hydrophilic/lipophilic balance. These assemblies were thoroughly characterized by multiple microscopic as well as spectroscopic techniques. They are capable of encapsulation of hydrophilic as well as hydrophobic dye. They also show the target specificity towards the HepG2 cells. Their promising biocompatibility, stability as well as targetability might be useful for their potential use as delivery vehicles towards liver cancer *in vivo* applications.

5.5 References

1) Discher, D. E.; Eisenberg, A. *Science* **2002**, *297*, 967- 973.
2) Zhang, L.; Eisenberg, A. *Science* **1995**, *268*, 1728- 1731.
3) Allena,C.; Hana,J.; Yua,Y.; Maysingerb,D.; Eisenberg, A. *Journal of Controlled Release* **2000**, 63, 275-286.
4) Ghoroghchian, P. P.; Frail, P. R.; Susumu, K.; Blessington, D.; Brannan, A.K.; Bates,F.S.; Chance, B.; Hammer, D.A.; Therien, M.J. *PNAS* **2005**, 102, 1922-1927.
5) Suriano, F.; Pratt, R.; Tan, J. P. K.; Wiradharma, N.; Nelson, A.; Yang, Y.-Y.; Dubois, P.; Hedrick, J. L. *Biomaterials* **2010**, *31*, 2637-2645.
6) Bermudez, H.; Brannan, A.K.; Hammer, D.A.; Bates, F.S.; Discher, D.E. *Macromlecules* **2002**, *35*, 8203-8208.
7) Ahmed, F.; Discher, D.E. *Journal of Controlled Release* **2004**, *96*, 37-53.
8) Photos, P.J.; Bacakova, L.; Discher, B.; Bates, F.S.; Dischera, D.E. *Journal of Controlled Release* **2003**, *90*, 223-237.
9) Otsukaa , H.; Nagasakib, Y.; Kataoka, K. *Advanced Drug Delivery Review* **2003**, *55*, 403-419.
10) Bellomo, E. G.; Wyrsta, M. D.; Pakstis, L.; Pochan, D. J.; Deming, T. J. *Nature Mater.* **2004**, 3, 244–248.
11) Meng, F.; Hiemstra, C.; Engbers, G.H.M.; Feijen J. *Macromolecules* **2006**, *36*, 3004-3006.
12) Klok, H.-A.; Lecommandoux, S. *Advanced Materials* **2001**, *13*, 1217-1229.
13) Wang, X.; Sun, H.; Meng, F.; Cheng, R.; Deng, C.; Zhong, Z. *Biomacromolecules* **2013** (DOI: dx.doi.org/10.1021/bm4007248).
14) Geng, Y.; Dalhaimer, P.; Cai, S.; Tsai, R.; Tewari, M.; Minko, T.; and Discher, D. *Nature Nanotech.* **2007**, *2*, 249-255.
15) Pati, D.; Kalva, N.; Das, S.; Kumaraswamy, G.; Sen Gupta, S.; Ambade, A. V. *J. Am. Chem. Soc.* **2012**, *134*, 7796−7802.
16) Sureshkumar, G.; Hotha, S. *Chem. Comm.* **2008**, 4282-4284.

17) Pati, D.; Shaikh, A. Y.; Hotha, S.; Sen Gupta, S. *Polym. Chem.* **2011**, *2*, 805-811.

18) Pati, D.; Shaikh, A.; Das. S.; Nareddy, P. K.; Swamy, M. J.; Hotha, S.; Sen Gupta, S. *Biomacromolecules* **2012**, *13*, 1287-1295.

19) Shaikh, A. Y.; Sureshkumar, G.; Pati, D.; Sen Gupta, S.; Hotha, S. *Org. Biomol. Chem.***2011** *9*, 5951-5959.

20) Ghoroghchian, P. P. et al. *Macromolecules* **2006**, *39*, 1673-1675.

21) Ahmed, F.; Discher, D. E. *J. Controlled Release* **2004**, *96*, 37– 53.

22) Loverde, S. M.; Klein, M. L.; Discher, D. E. **2012**, DOI: 10.1002/adma.201103192.

23) Hanson, J. A.; Li, Z.; Deming, T. J. *Macromolecules*, **2010**, *43*, 6268–6269.

24) Bellomo, E. G.; Wyrsta, M. D.; Pakstis, L.; Pochan, D. J.; Deming, T. J. *Nature Mater.* **2004**, 3, 244–248.

Chapter 6

Future aspects of the thesis work

6. A) Inhibition of Cholera Toxins

One of the most infectious disease that can spread in epidemic form is caused by Shiga and cholera toxins and accounts for millions of lives each year throughout the world. These toxins are of the AB_5 bacterial family. Bacterial AB_5 toxins consist of an enzymatically active A subunit that gains entry to susceptible mammalian cells after oligosaccharide (ganglio-side GM1) recognition by the B_5 homopentamer. For prevention, diagnosis and treatment of such diseases, study of receptor-ligand interaction has recently received lot of interest. Many biological processes are initiated by molecules interacting at cell surfaces. If multiple copies of a receptor are arrayed on one surface, and multiple copies of its ligand are displayed on another, then the two surfaces can interact through many individual binding events. These multivalent interactions have long been recognized for their potential to achieve effective adhesion between binding partners, even when individual, monovalent binding interactions are weak. If multivalency is essential for a biological process to occur, then it can also provide an effective strategy for the design of inhibitors, for example, to prevent bacterial toxins from entering cells. In an ideal case, the structure based design of multivalent ligands would also lead to ligands whose backbone or linker portion also interacts favourably with the target, thereby further enhancing affinity to the target beyond gains due to multivalency on generic backbones. In recent years, the structure-based design of multivalent ligands has attracted increasing attention with some of the most successful examples developed for targeting AB_5 toxins. Though several groups are working on the inhibition of the cholera/ Shiga toxins, only three groups have worked on the architectural based ligands design for toxins inhibition[1].

Kitov *et al*. were first to design a structure based inhibitor for Shiga-like toxins contains decavalency[2]. They reported that the decavalent ligand sufficiently inhibits 10 out of 15 binding sites of the five B subunits, each containing three binding sites. The five bivalent ligands are connected to five arms of the glucose moiety. The resulting decavalent ligand was shown to have several million-fold gain in affinity over the monovalent trisaccharide.

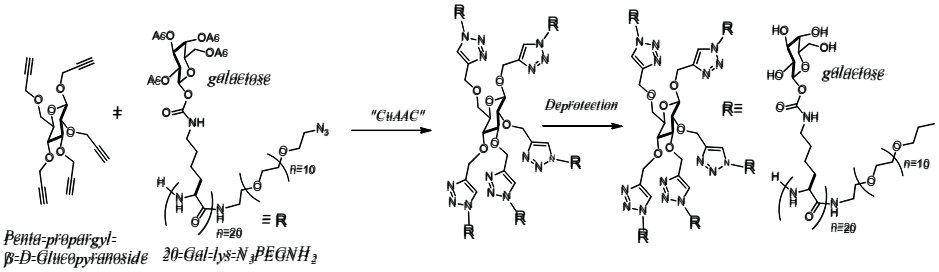

Scheme 6.1: Proposed glycopolypeptide-based pentavalent ligands to inhibit Cholera Toxins.

By utilizing the same concept Zhang *et al*. reported decavalent ligand architecture comprising pentavalent cluster of five bivalent ligands connected through five arms of the pentacyclen[3]. They also reported that specific length of the linker should be about 30 Å to inhibit the toxin binding sites. Polizzotti *et al*. also showed that functionalization of poly(glutamic acid) polymers of two different secondary structures makes them sufficiently active to inhibit cholera toxins[4].

Here, we are proposing the strategy to synthesise a cholera toxin inhibiting ligand from well defined, biocompatible and biodegradable glycopolypeptides using our recently developed, easy and controlled ring opening polymerization of β-galactose-*l*-lysine NCA's by end-functionalized primary amine as initiators. To achieve pentavalent cluster ligand, the end azide functionalized glycopolypeptides will be conjugated to the penta-propargyl β-D-glucopyranoside by "click" reaction.

6. B) Tissue engineering from noodle gels

A principal goal of regenerative medicine is the use of synthetic scaffolds to replace or repair damaged tissues. These scaffolds are modelled on the natural extracellular matrix, which is a porous hydrogel consisting of protein and

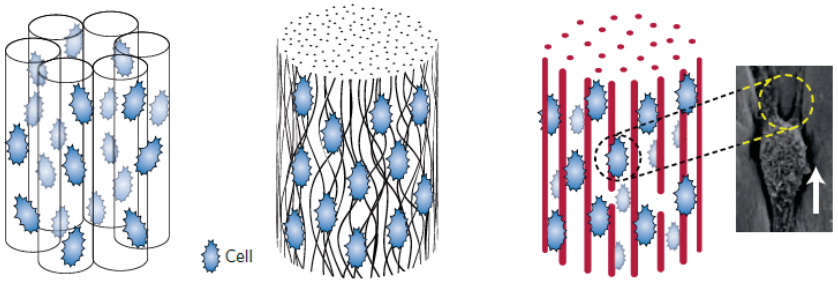

Fig. 6.1: Representation of the nano-fibers for tissue engineering[5].

polysaccharide nanofibers that provide both mechanical support and biochemical signals to cells. In synthetic tissue-engineering scaffolds, nanoscale features must be included that replicate some of the functions of the extracellular matrix. In many cases, such as in tendons, nerves and corneal stroma, control of cell alignment and growth direction is essential to obtain functional tissues[6]. Although many significant advances have been made in the preparation of nanoscale scaffolds capable of supporting cell functions, directed cell growth within these scaffolds has been more challenging.

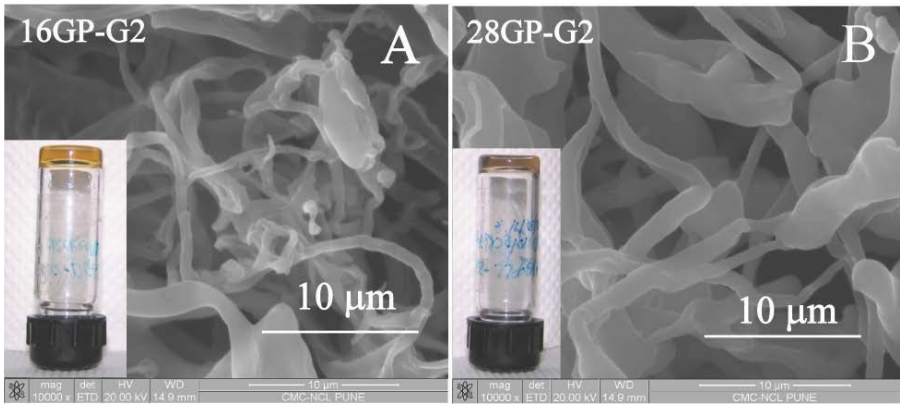

Fig. 6.2: Representation of the nano-fibers in DMSO derived from glycopolypeptides-dendron conjugates[7].

For three-dimensional directional cell growth, hydrogels with oriented channels have been used with some success. However, the microscopic pores usually have no nanoscale orientation to guide cell growth, and the scaffolds are most often preformed, and thus require invasive implantation surgery. Electro-spinning is another approach to prepare scaffolds composed of aligned nanofibres that can direct cell growth. This technique gives nanoscale orientation, but requires high shear and high electric fields that are not compatible with cells. The alignment of liquid crystals at low shear rates has also been used to create scaffolds with nanoscale orientation. Lyotropic liquid crystals of nanoscale phage particles can be mixed with cells and injected into a matrix to yield microscale fibres displaying long-range (greater than 1 cm) ordering of aligned phage[8]. These materials are injectable, allowing minimal invasive surgery, and support growth of neural progenitor cells along the fibre axis. This procedure is promising but will probably require a mechanism to gel the mixture *in vivo* to prevent dilution and loss of orientation. Stupp and co-workers have now found a way to obtain similar

long-range ordering through a liquid-crystalline phase and have combined this with cross linking under cell-compatible conditions to obtain self-supporting, highly oriented noodles for directed cell growth. Cell-containing aligned noodles are prepared by simple pipetting of an aligned bundle solution into salty media. Their discovery stems from the knowledge that peptide amphiphiles assemble in water to form long, cylindrical 'worm like' nanofibres that crosslink in the presence of salts to give hydrogels capable of supporting cell growth[9]. The addition of salts screens repulsions between like-charged nano fibres, allowing them to interact and also grow in length. An ionic media is also used to trigger gelation in polysaccharide and many other beta-sheet forming peptide-based gels[10]. However, similar to other hydrogels used for tissue engineering, the nano fibers in these gels are randomly oriented and do not guide directional cell growth. Recently, by heating the nanofibre suspension of peptide amphiphiles, Stupp and co-workers showed that large plaque-like sheets form that when cooled break apart into highly aligned bundles of nanofibres[11].

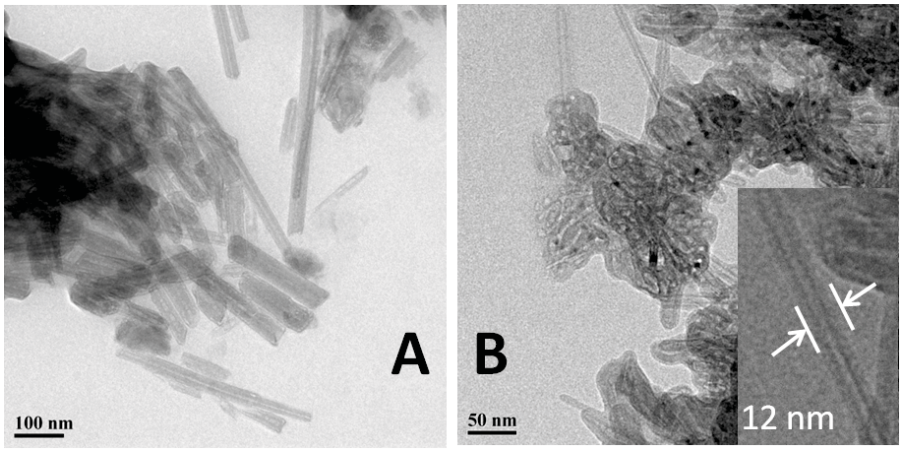

Fig. 6.3: TEM images of the nanofibers for cellular alignments generated from glycopolypeptide-dendron (A) and polycaprolactone (B) conjugates[7, 12].

Human mesenchymal stem cells and cardiomyocytes have shown promising viability in these noodles, and elongate along the nanofibre bundle axes[13]. Key questions at this stage relate to the effectiveness of forming such highly aligned structures within living tissues, as well as how cells and tissues will remodel and degrade the scaffolds over time *in vivo*. Although there are many studies to be carried

out before these gels are proved to be useful in humans, they offer many advantages for directed cell growth *in vitro* and for the formation of nanostructured filaments. We propose here that nanofibres generated from glycopolypeptides conjugated to dendron or polycaprolactones can be promising biomaterials due to combination of benign crosslinking and formation of highly aligned gels in the presence of cells or molecules.

6. C) Development of drug/imaging agent delivery vehicles (nano medicine)

The development of nanomedicine for disease theranostics is progressing at a fast pace and is driven by principles from diverse fields of science in the postgenomic age. Nano-based theranostics are made possible by integrating the application of molecular biomarkers across the range of tests and interventions reaching from disease susceptibility testing and monitoring of clinical outcomes resulting from interventions. However, the terms "nanotheranostics" or "theranostics using nanomedicine" usually reflect the ability of nanocarriers to report on a specific pathological site or cell and to deliver drugs simultaneously directly into these cells[14]. One such strategy that might be relevant for Inflammatory Bowl Disease (IBD) or cancer treatment, is to use multistage, polymeric nanoparticles (NPs) that can entrap therapeutic payloads with gadolinium-based contrast agents that enhance T1 contrast for MRI use [15]. Other potential options include a turn-on, near-infrared, cyanine-based probe for noninvasive intravital optical imaging of hydrogen peroxide . This strategy can report on inflammed areas using intravital optical imaging, and at the same time, H_2O_2 can be used as a therapeutic strategy for gut inflammation if small amounts are delivered to the appropriate site in the gut. Although the number of nanomedicines that are reaching the clinic is dramatically increasing, most of them thus far are cancer treatments [16]. We propose that novel theranostic nanomedicines will be developed for IBD as well as cancer therapy, combining novel therapeutic and molecular imaging modalities such as combinations of targeted NPs that incorporate therapeutic payloads (drug molecules as well as imaging agent) can be coupled to a cell-surface-specific targeting moiety (Figure 6.4). This combined nanotheranostic approach, which will include new therapeutic payloads, possibly coupled with and incorporated into existing "conventional" treatment strategies, combined with novel molecular imaging approaches may revolutionize the management of IBD and cancer therapy[17].

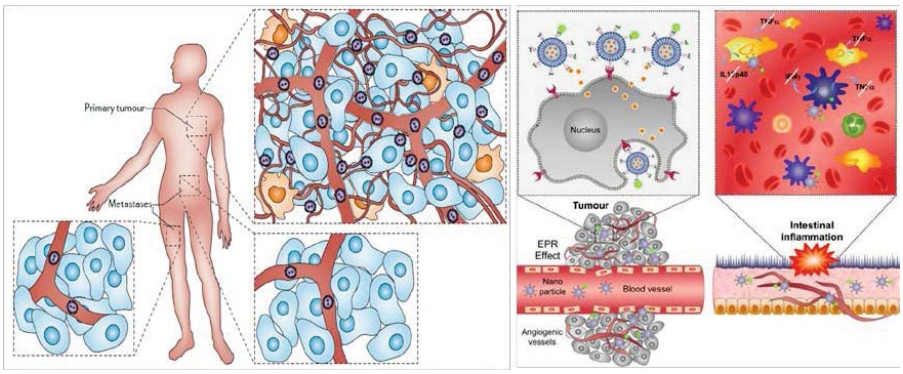

Fig. 6.4: Schematic representation of different mechanisms by which nanoparticles (NPs) can deliver drugs and report on mucosal disease. Lipid-based NPs (as representative nanocarriers) can be employed in a variety of inflammatory and neoplastic mucosal disorders such as in the lungs, skin, and gut. Adapted from papers [16, 17].

Here, our proposal is to develop a nanomedicine derived from glycopolypeptide-polycaprolactone conjugate that is biocompatible, biodegradable and scalable in synthesis. Keeping three major points in mind, 1) Target specificity (As for organ specificity like; liver surface displays over-expressed asilo-glycoprotein receptor; ASGPR specific for galactose), 2) Pay load capacity (Drug; cisplatin, doxorubisin etc., or imaging agent like Galadonium or platinum etc.), 3) Controlled release (Physiological condition) and 4) Immune genie response.

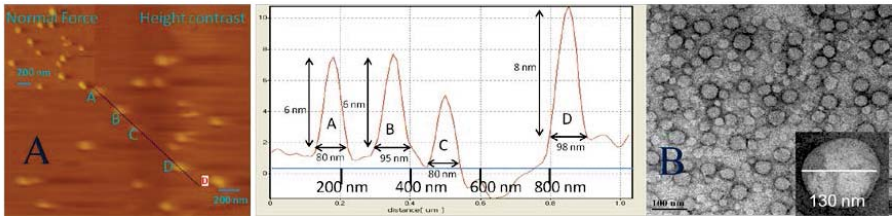

Fig. 6.5: Represented the AFM and the TEM image of the nano-particle derived from glycopolypeptide-polycaprolactone conjugates in aqueous solution [12].

These nanoparticles are well characterized by microscopic technique (AFM, TEM etc) and stability was checked by dynamic light scattering (DLS); dye loading capacity was thoroughly investigated by spectroscopic technique.

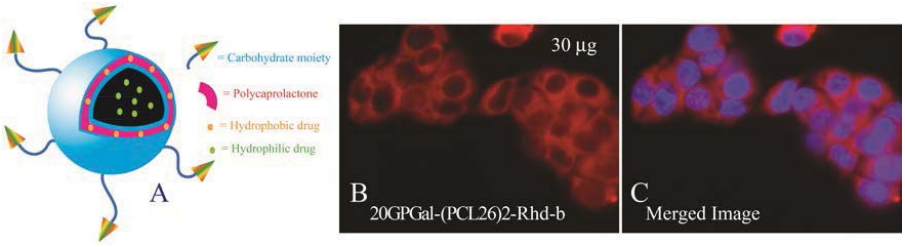

Fig. 6.6: A) Schematic representation of the nano-particle derived from the glycopolypeptides-polycaprolactone conjugated block copolymer, B) the cellular uptake of the rhodamine labeled nano-particle into the HepG2 cells and C) merged image of the DAPI stained nucleus and cytoplasm [12].

These assemblies show promising cellular specificity towards HepG2 cells in *in vitro* study and cell viability is more than 95%. We believe these nanomedicines will be potentially useful in *in vivo* application for the treatment of liver cancer therapy.

6.D) References

1) Merritt, E. A.; Hol, W. G. J. *Curr. Opin. Struct. Biol.* **1995**, *5*, 165-171.

2) Kitov, P. I.; Sadowska, J. M.; Mulvey, G.; Armstrong, G. D.; Ling, H.; Pannu, N. S.; Read, R. J.; Bundle, D. R. *Nature* **2000**, *403*, 669-672.

3) Fan, E.; Zhang, Z.; Minke, W. E.; Hou, Z.; Verlinde, C. L. M. J.; Hol, W. G. J. *J. Am. Chem. Soc.* **2000**, *122*, 2663-2664.

4) Polizzotti, B. D.; Kiick, K. L. *Biomacromolecules* **2006**, *7*, 483-490.

5) Deming, T. J. *Nature Mater.* **2010**, *9*, 535-536.

6) Zhang, S. *et al. Nature Mater.* **2010**, *9*, 594–601.

7) a) Pati D. *et al. Biomacromolecules* **2012**, *13*, 1287-1295. b) Pati, D. *et al. J. Am. Chem. Soc.* **2012**, *134*, 7796-7802.

8) Engel, E. *et al. Trends Biotechnol.* **2007**, *26*, 39–47.

9) Merzlyak, A.; Indrakanti, S.; Lee, S. W. *Nano Lett.* **2009**, *9*, 846–852.

10) Lutolf, M. P.; Hubbell, J. A. *Nature Biotechnol.* **2005**, *23*, 47–55.

11) Hartgerink, J. D.; Beniash, E.; Stupp, S. I. *Proc. Natl Acad. Sci. USA* **2002**, *99*, 5133–5138.

12) Pati, D. **2013** *et al. Manuscript under preparation*.

13) Kirui, D. K.; Khalidov, I.; Wang, Y.; Batt, C. A. **2012**, 10.1016/j.nano. 2012.11.009.

14) Ananta, J. S.; Godin, B.; Sethi, R.; Moriggi, L.; Liu, X.; Serda, E.; Krishnamurthy, R.; Muthupillai, R.; Bolskar, R. D.; Helm, L. *Nat. Nanotechnol.* **2010**, *5*, 815–821.

15) Karton-Lifshin, N.; Segal, E.; Omer, L.; Portnoy, M.; Satchi-Fainaro, R.; Shabat, D. A. *J. Am. Chem. Soc.* **2011**, *133*, 10960–10965.

16) Schroeder, A.; Heller, D. A.; Winslow, M. M.; Dahlman, J. E.; Pratt, G. W.; Langer, R.; Jacks, T.; Anderson, D. G. *Nat. Rev. Cancer.* **2012**, *12*, 39–50.

17) Elinav, E.; Peer, D. ACS Nano **2013**, *Harnessing Nanomedicine for Mucosal Theranostics—A Silver Bullet at Last ?*

Appendix I:

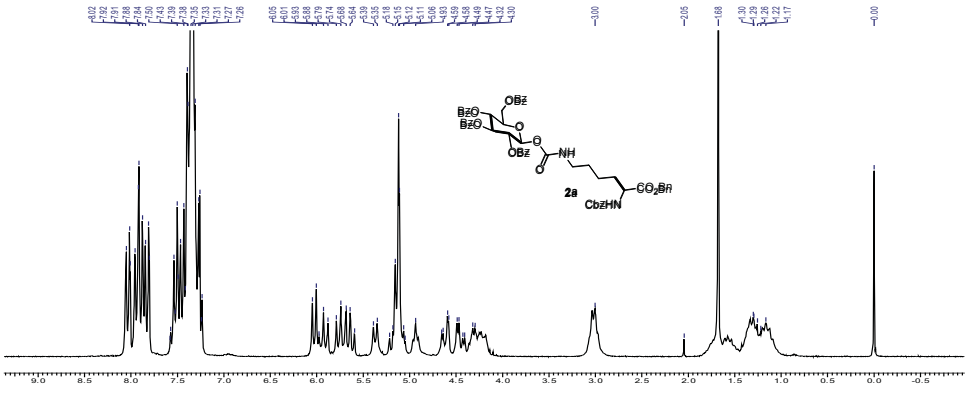

Fig. I.1: ^{1}H spectrum of *per-O-benzoylated-D-Glucose-ϵ-z-l-lysine benzyl ester carbamate* (***2a***).

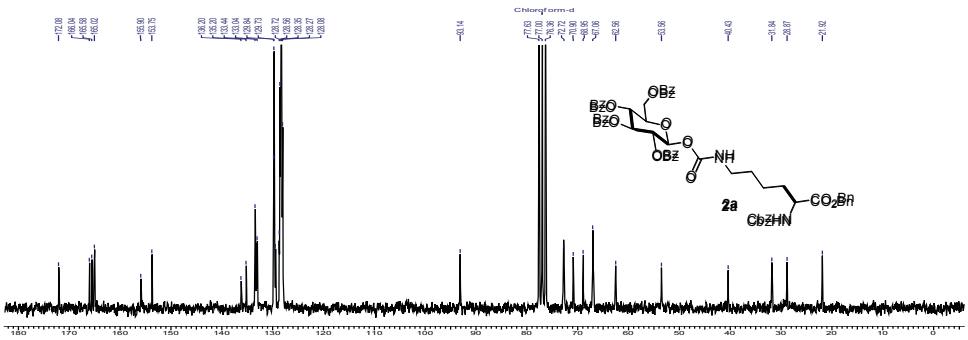

Fig. I.2: ^{13}C spectrum of *per-O-benzoylated-D-Glucose-ϵ-z-l-lysine benzyl ester carbamate* (***2a***).

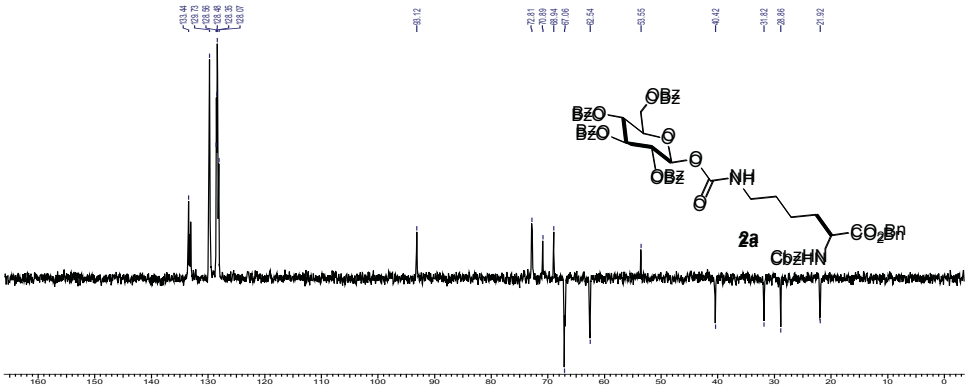

Fig. I.3: Dept of *per-O-benzoylated-D-Glucose-ϵ-z-l-lysine benzyl ester carbamate* (***2a***).

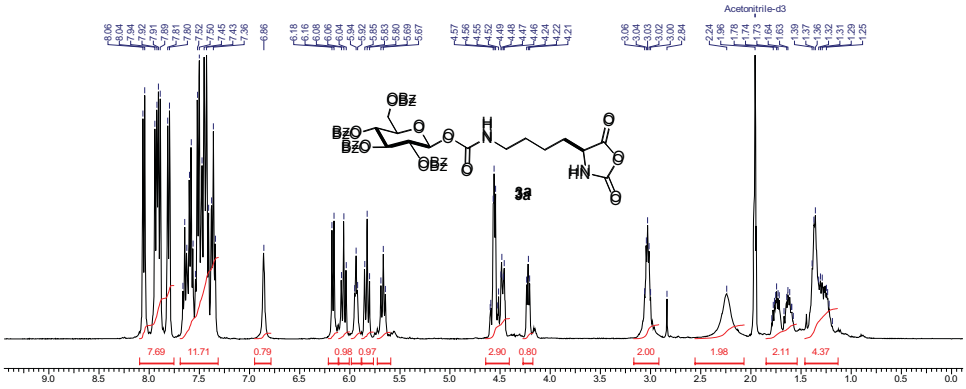

Fig. I.4: ^{1}H spectrum of *per-O-benzoylated-D-Glucose-l-lysine carbamate NCA* (***3a***).

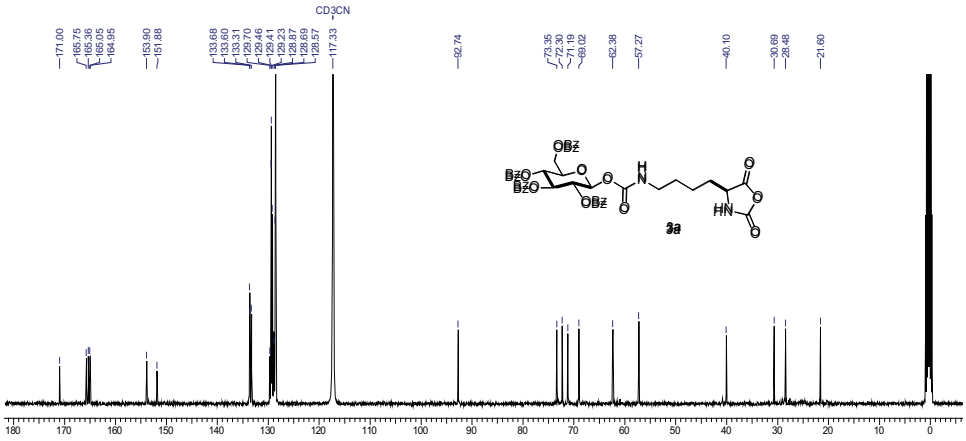

Fig. I.5: ^{13}C spectrum of *per-O-benzoylated-D-Glucose-l-lysine carbamate NCA* (***3a***).

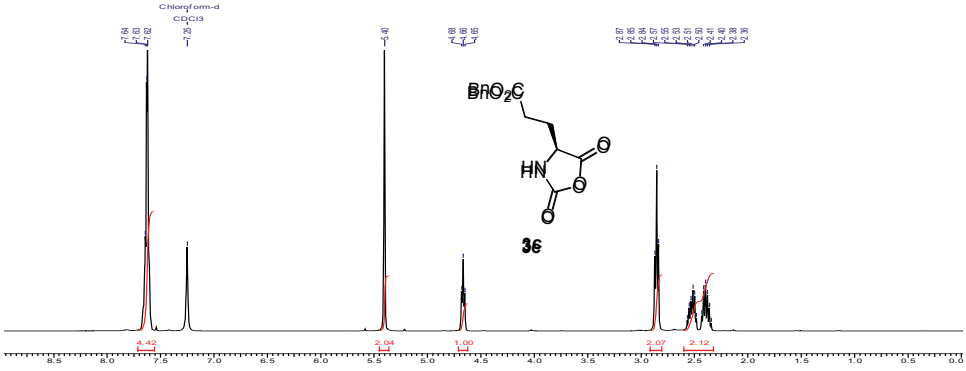

Fig. I.6: ^{1}H spectrum of *γ-Benzyl-l-glutamate- N-carboxyanhydride* (***3c***).

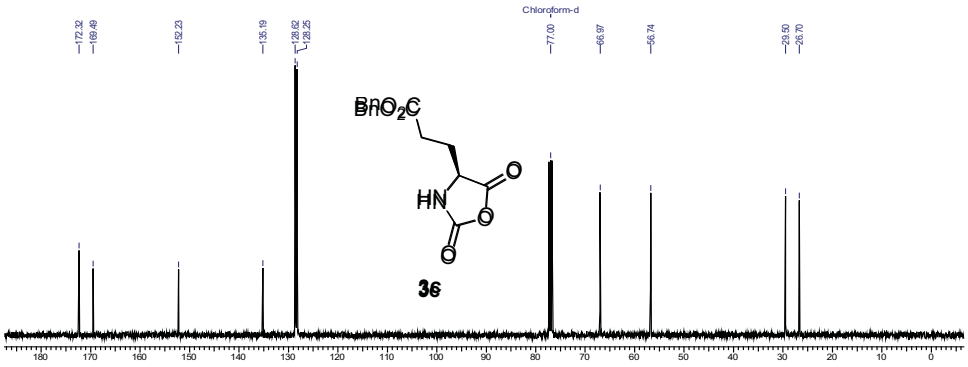

Fig. I.7: ^{13}C spectrum of *γ-Benzyl-l-glutamate- N-carboxyanhydride* ***(3c)***.

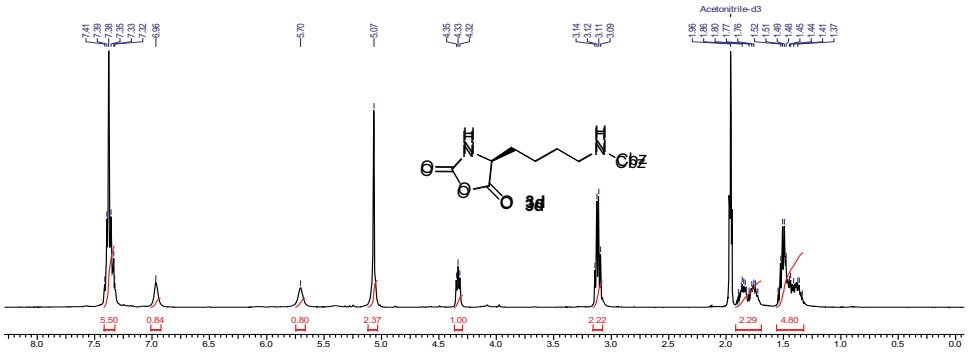

Fig. I.8: ^{1}H spectrum of *ε-N-carbobenzoxy-l-lysine-N-carboxyanhydride* ***(3d)***.

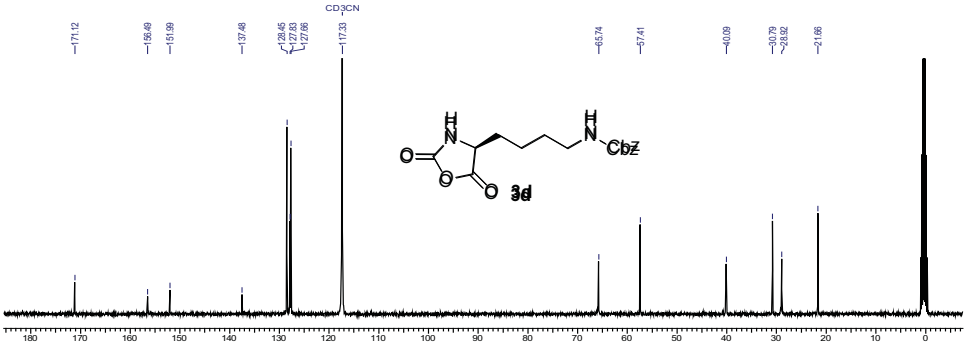

Fig. I.9: ^{13}C spectrum of *ε-N-carbobenzoxy-l-lysine-N-carboxyanhydride* ***(3d)***.

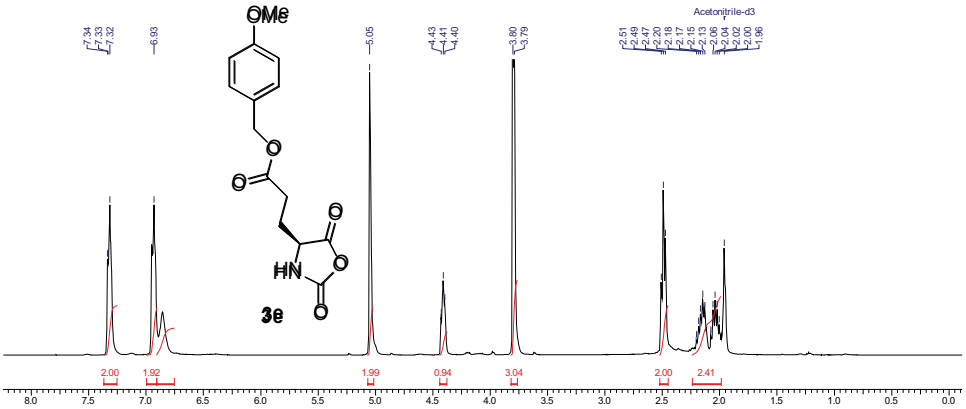

Fig. I.10: ^{1}H spectrum of *γ-p-OMe-benzyl-l-glutamate-N-carboxyanhydride* ***(3e)***.

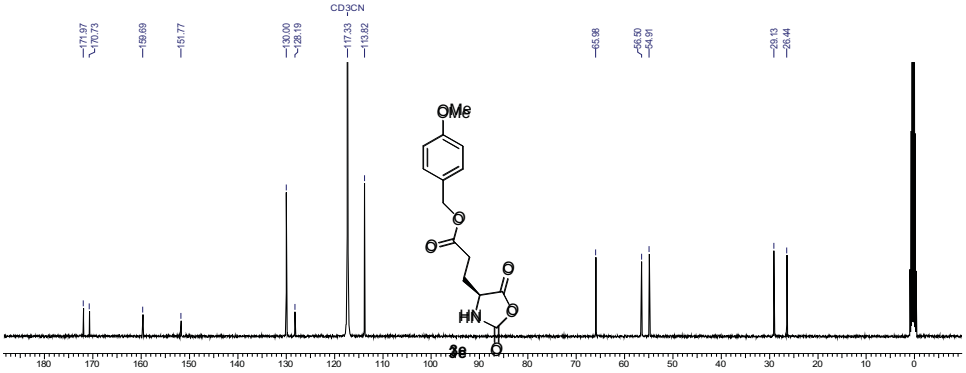

Fig. I.11: ^{13}C spectrum of *γ-p-OMe-benzyl-l-glutamate-N-carboxyanhydride* ***(3e)***.

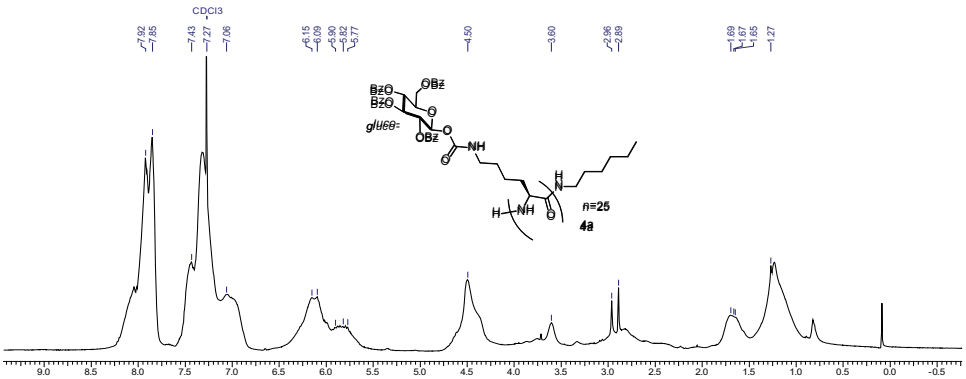

Fig. I.12: ^{1}H spectrum of 25-β-gluco-*O*-lys ***(4a)***.

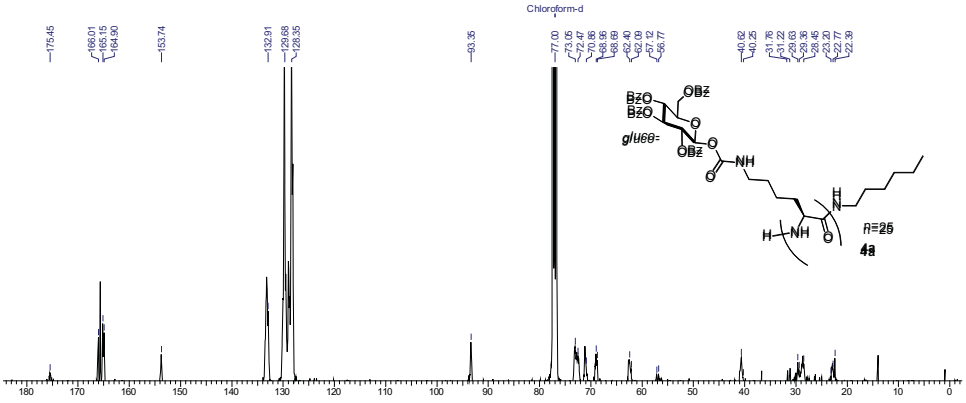

Fig. I.13: ^{13}C spectrum of 25-β-gluco-*O*-lys ***(4a)***.

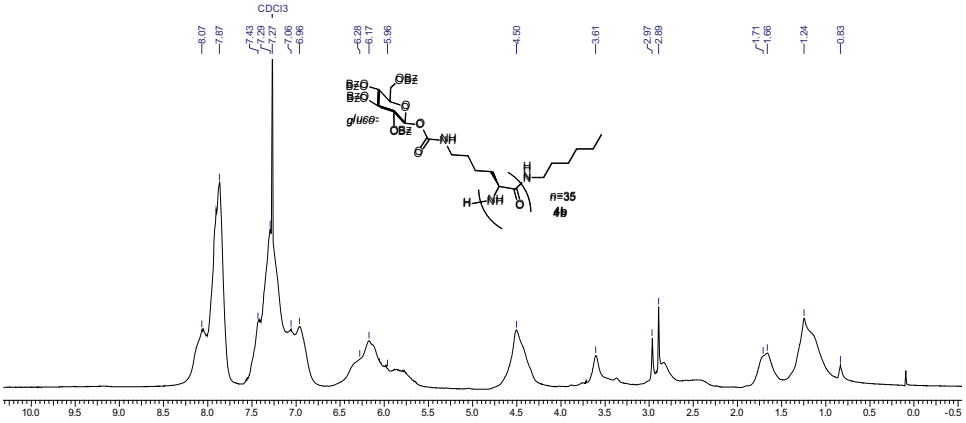

Fig. I.14: ^{1}H spectrum of 35-β-gluco-*O*-lys ***(4b)***.

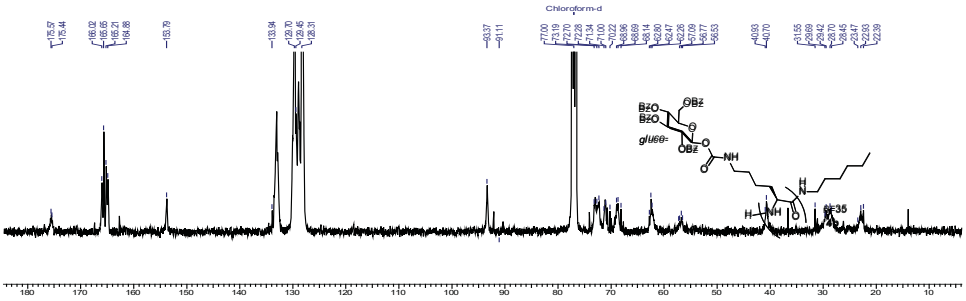

Fig. I.15: ^{13}C spectrum of 35-β-gluco-*O*-lys ***(4b)***.

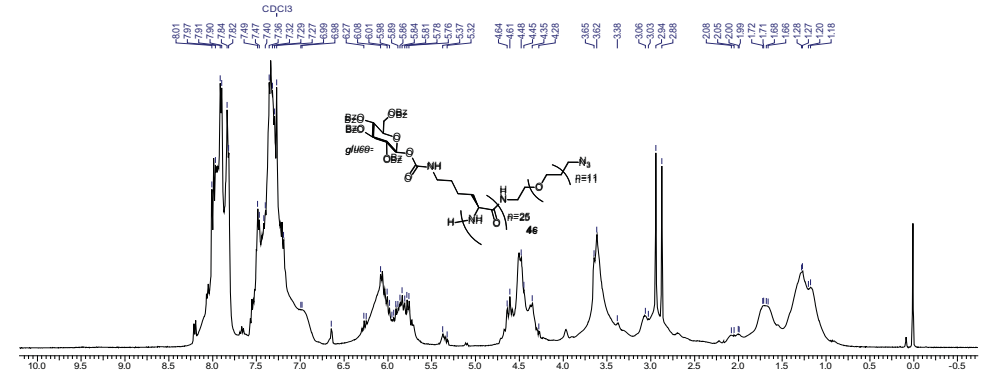

Fig. I.16: [1]H spectrum of 25-β-gluco-*O*-lys ***(4c)***.

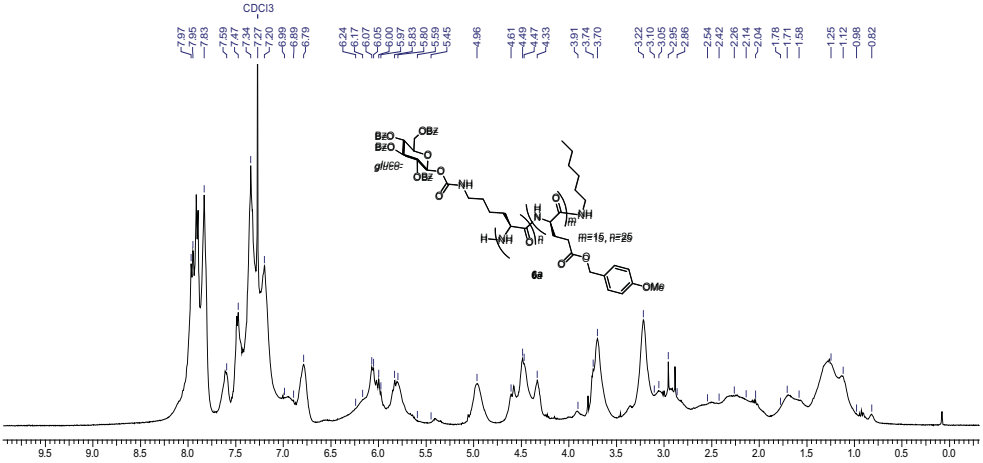

Fig. I.17: [1]H spectrum of *PMBn-b- β-gluco-O-lys* (*6a*).

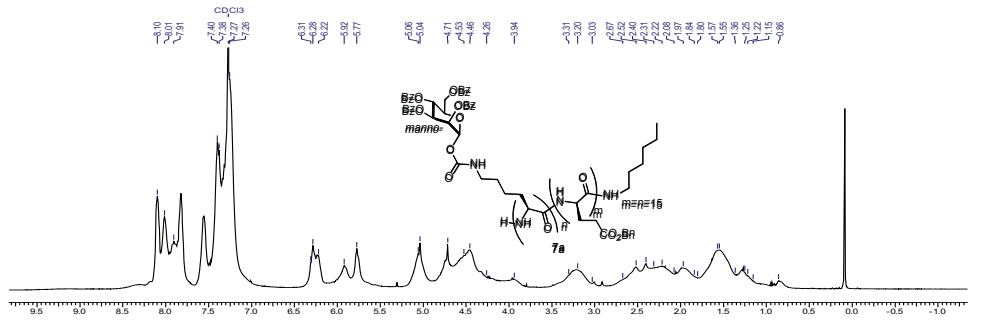

Fig. I.18: [1]H spectrum of *PMBn-b- β-gluco-O-lys* (*6a*).

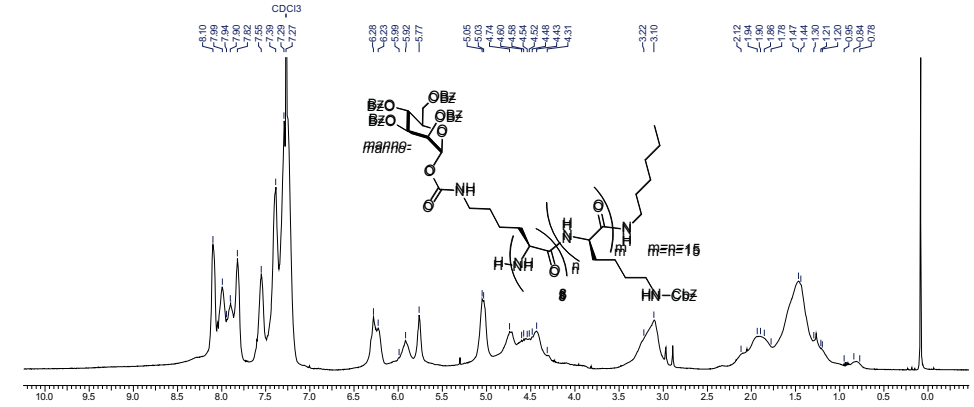

Fig. I.19: ^{1}H spectrum of *ϵ-z-l-lysine-b- β-gluco-O-lys* (***8***).

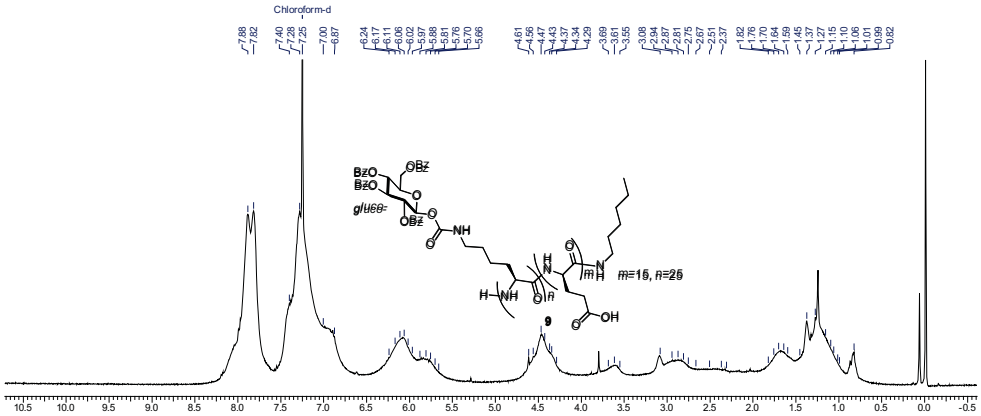

Fig. I.20: ^{1}H spectrum of *ϵ-z-l-lysine-b- β-gluco-O-lys* (***9***).

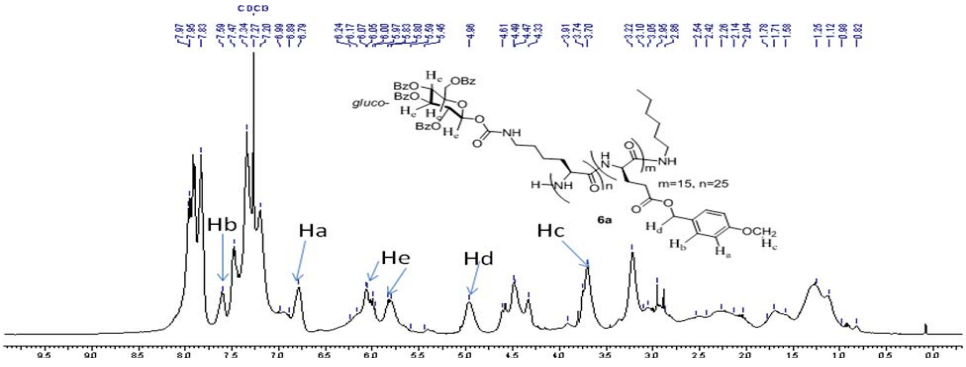

Fig. I.21: ^{1}H spectrum of *ϵ-z-l-lysine-b- β-gluco-O-lys* (***6a***).

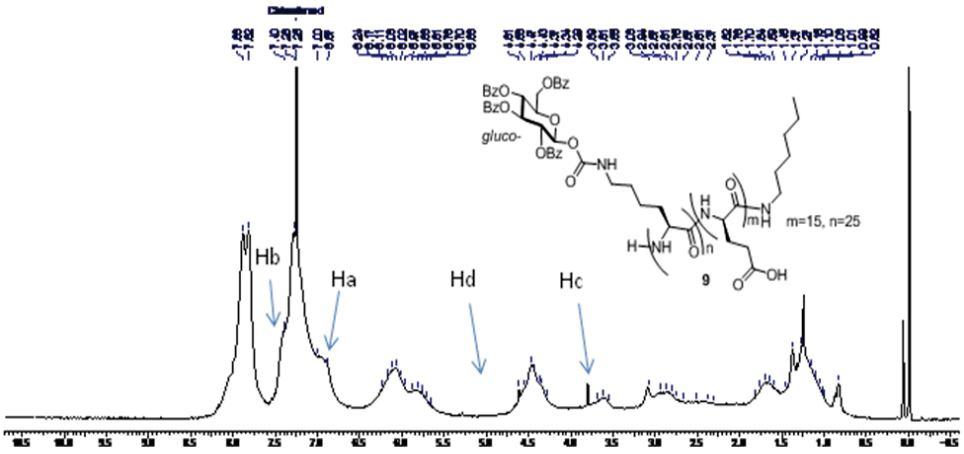

Fig. I.22: ^{1}H spectrum of *ϵ-z-l-lysine-b- β-gluco-O-lys* (***9***).

Appendix II

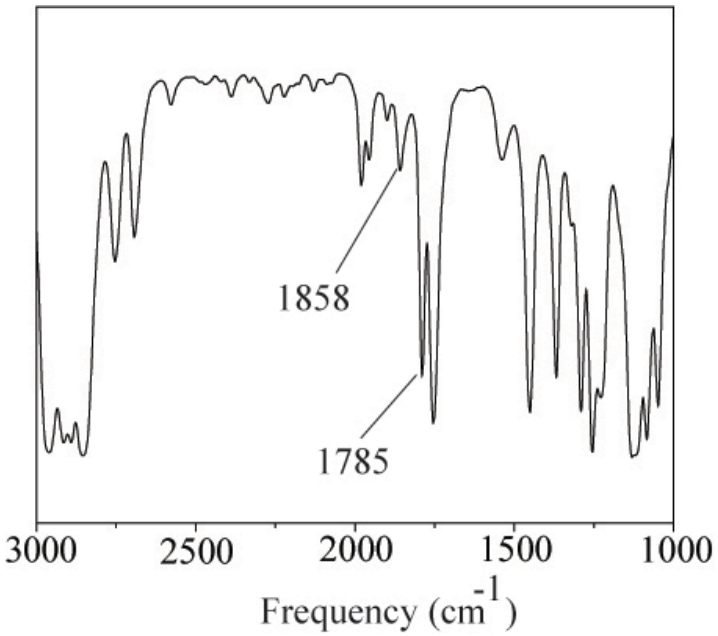

Fig. II.1: FT-IR Spectra of per-*O*-acetylated-D-Lactose-L-lysine NCA shows two unsymmetrical infrared stretching at 1858 and 1785 cm^{-1}.

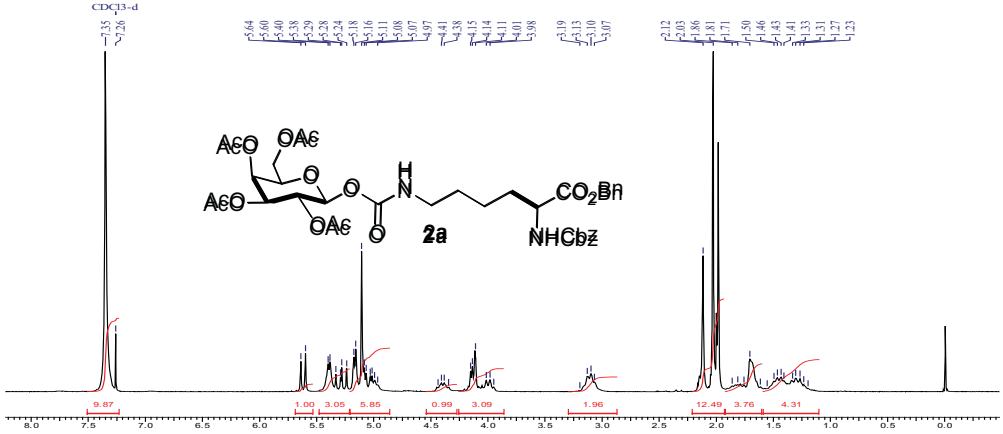

Fig. II.2: ^{1}H NMR of *per-O-acetylated-D-Galactose-l-Є-z-lysine-benzyl ester carbamate (**2a**)*.

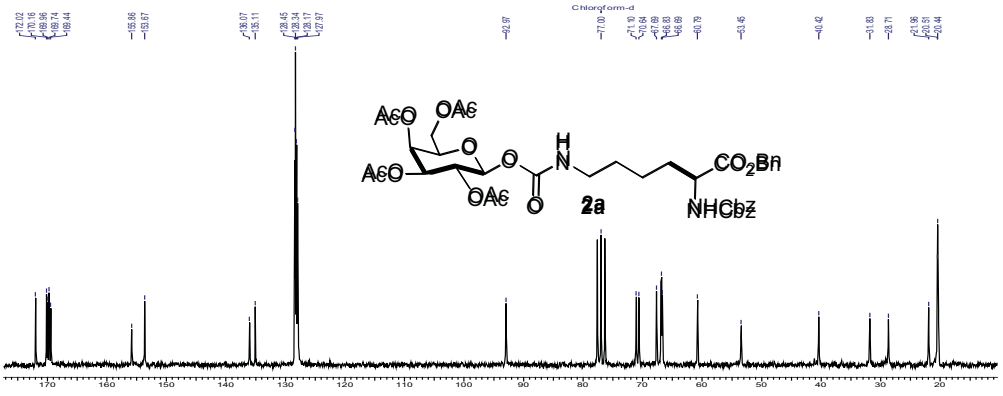

Fig. II.3: ^{13}C NMR of *per-O-acetylated-D-Galactose-l-Є-z-lysine-benzyl ester carbamate (**2a**)*.

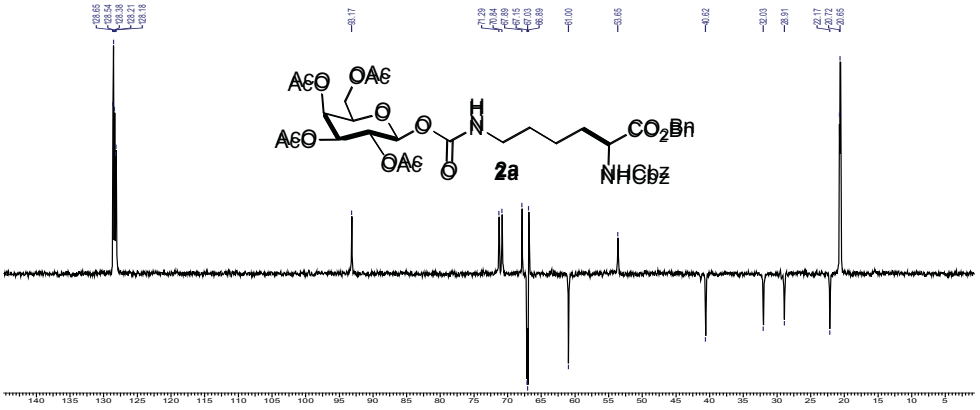

Fig. II.4: Dept of *per-O-acetylated-D-Galactose-l-Є-z-lysine-benzyl ester carbamate (**2a**)*.

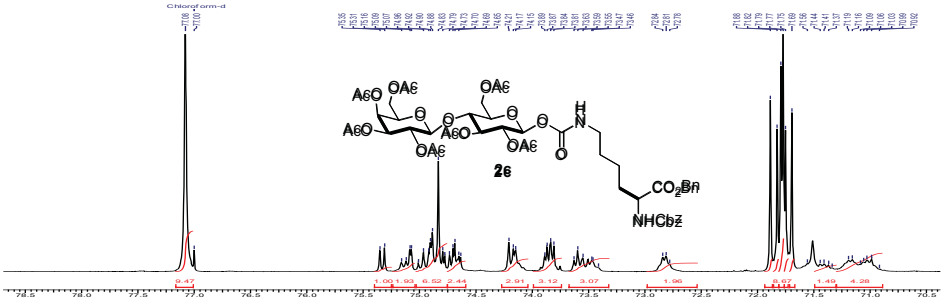

Fig. II.5: ^{1}H NMR of *per-O-acetylated-D-Lactose-l-Є-z-lysine-benzyl ester carbamate (**2c**)*.

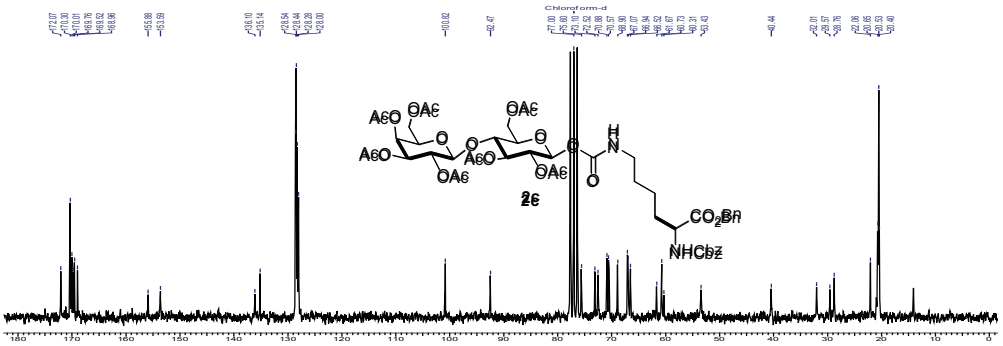

Fig. II.6: ^{13}C spectrum of *per-O-acetylated-D-Lactose-l-Ϲ-z-lysine-benzyl ester carbamate (**2c**)*.

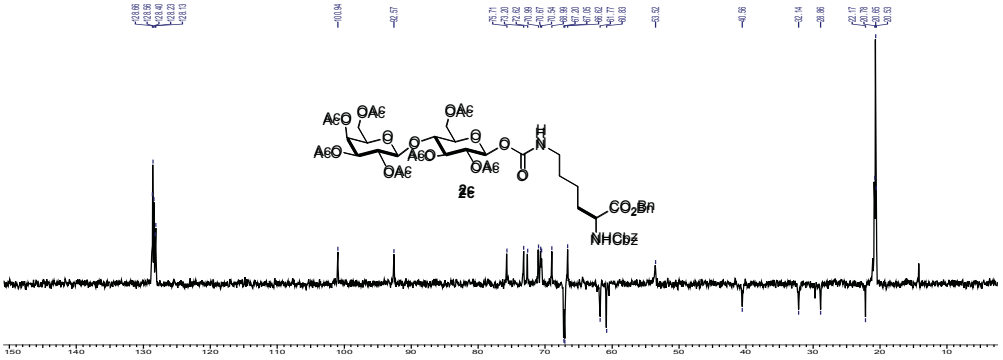

Fig. II.7: Dept spectra of *per-O-acetylated-D-Lactose-l-Ϲ-z-lysine-benzyl ester carbamate (**2c**)*.

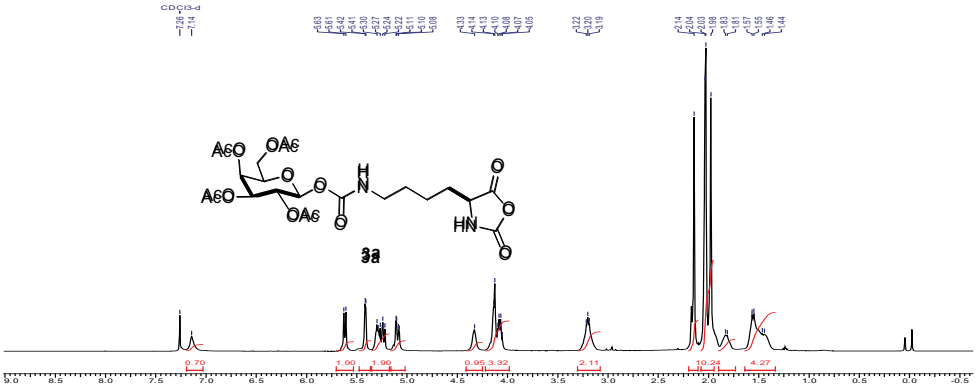

Fig. II.8: ^{1}H NMR of *per-O-acetylated-D-Galactose-l-lysine-carbamate NCA (**3a**)*.

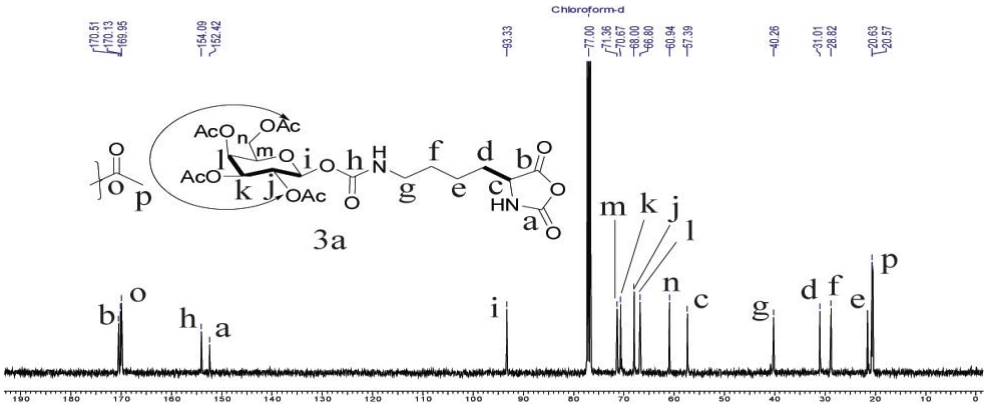

Fig. II.9: ^{13}C spectrum of *per-O-acetylated-D-Galactose-l-lysine-carbamate NCA (**3a**)*.

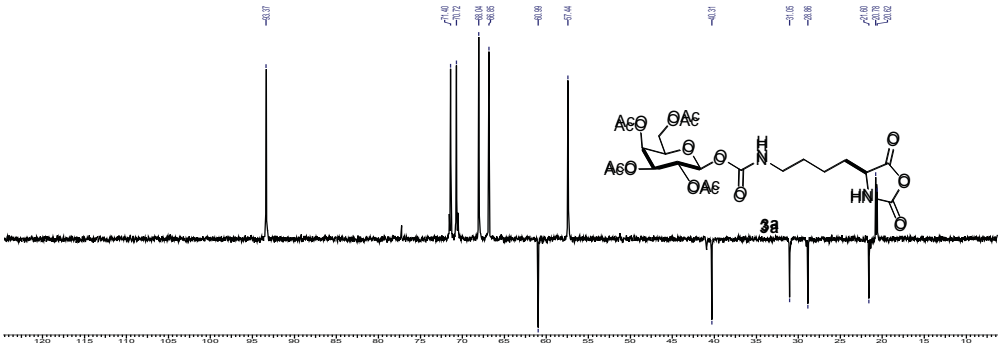

Fig. II.10: Dept spectrum of *per-O-acetylated-D-Galactose-l-lysine-carbamate NCA (**3a**)*.

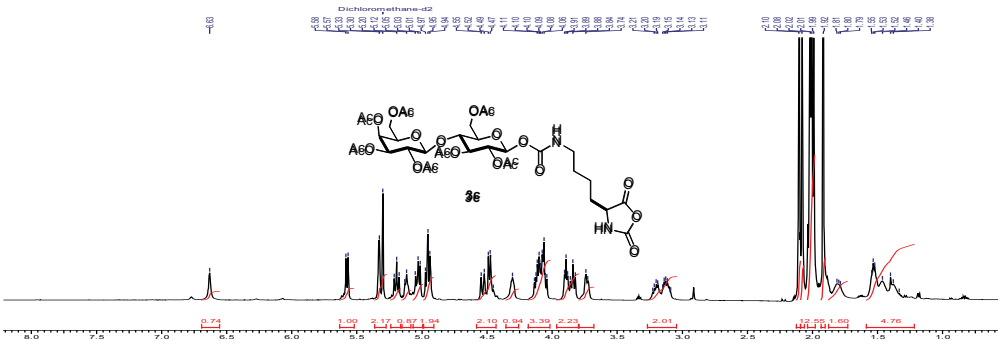

Fig. II.11: ^{1}H NMR of *per-O-acetylated-D-Lactose-l-lysine-carbamate NCA (**3c**)*.

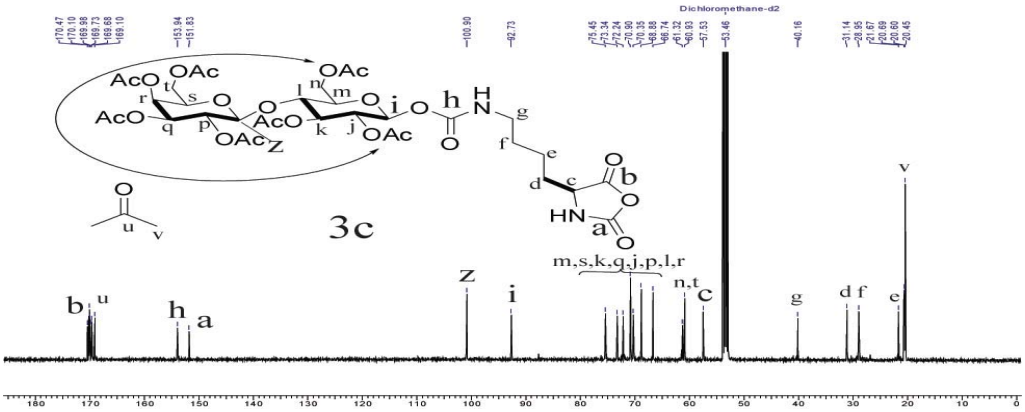

Fig. II.12: ^{13}C spectrum of *per-O-acetylated-D-Lactose-l-lysine-carbamate NCA (**3c**)*.

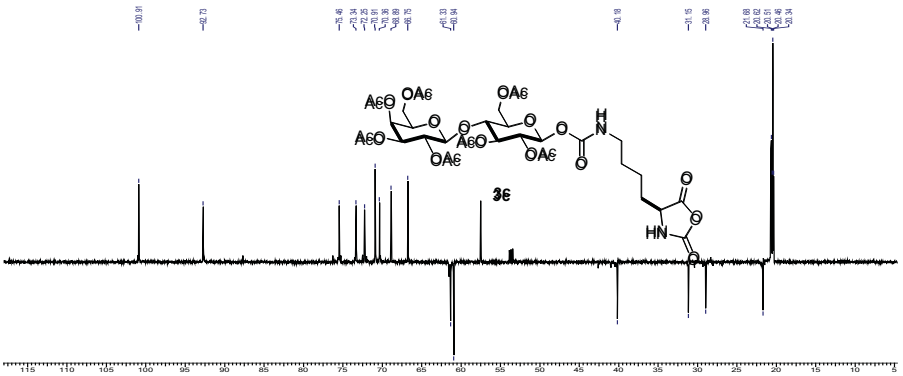

Fig. II.13: Dept spectrum of *per-O-acetylated-D-Lactose-l-lysine-carbamate NCA (**3c**)*.

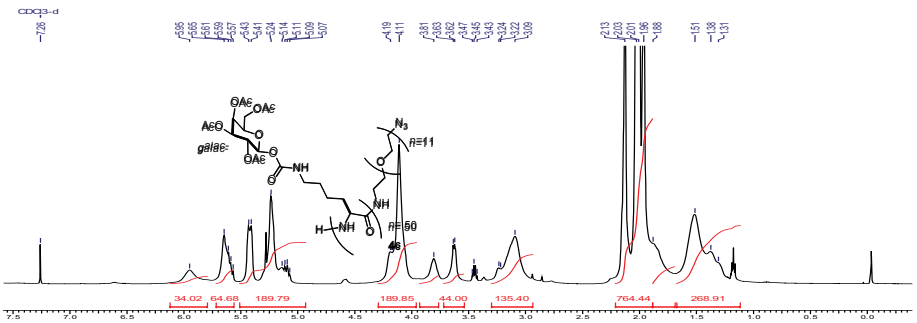

Fig. II.14: ^{1}H spectrum of *50-β-galac-O-l-lys (**4c**)*.

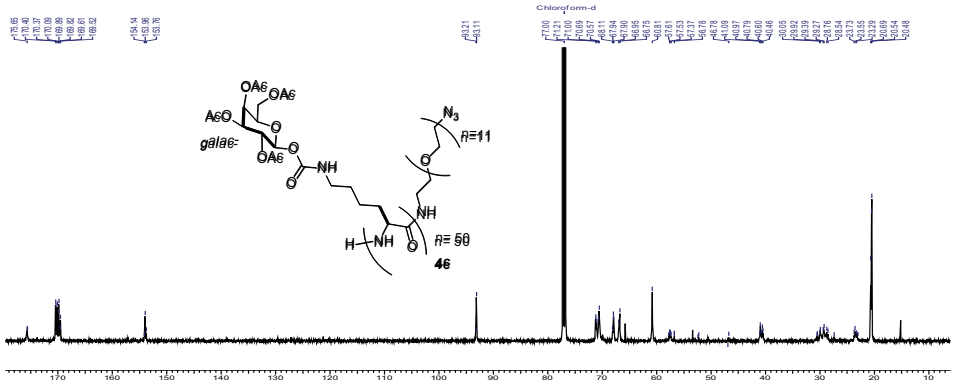

Fig. II.15: ^{13}C spectrum of *50-β-galac-O-l-lys (**4c**)*.

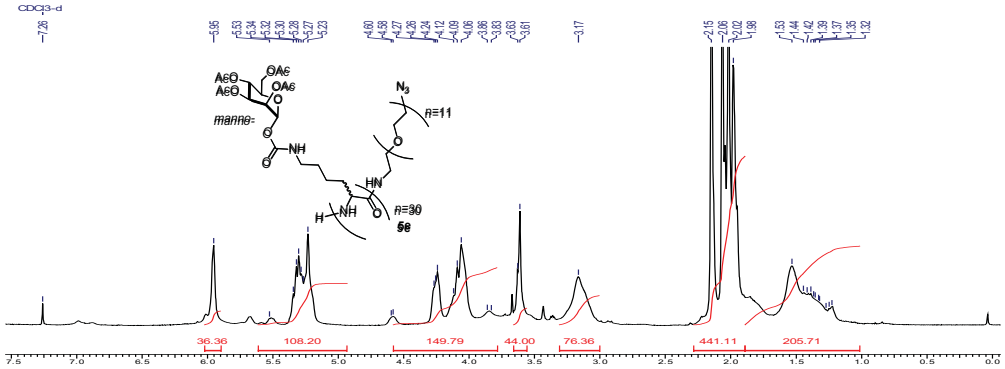

Fig. II.16: ^{1}H spectrum of Rac-30-α-manno-*O-l/d*-lys (***5e***).

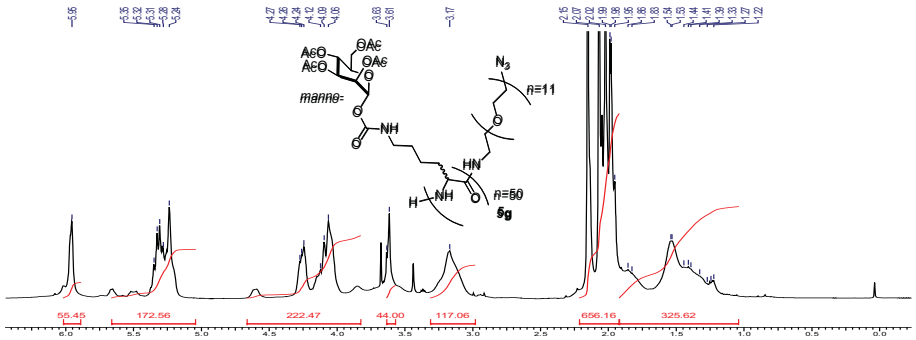

Fig. II.17: ^{1}H spectrum of Rac-50-α-manno-*O-l/d*-lys (***5g***).

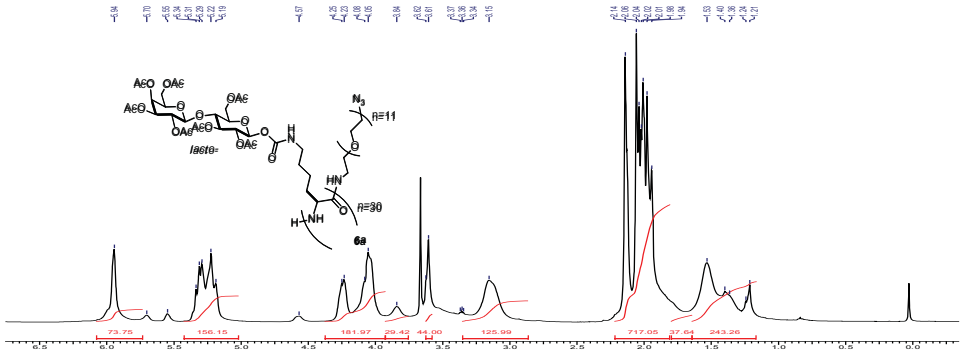

Fig. II.18: ^{1}H spectrum of 30-β-lacto-*O*-*l*-lys (***6a***).

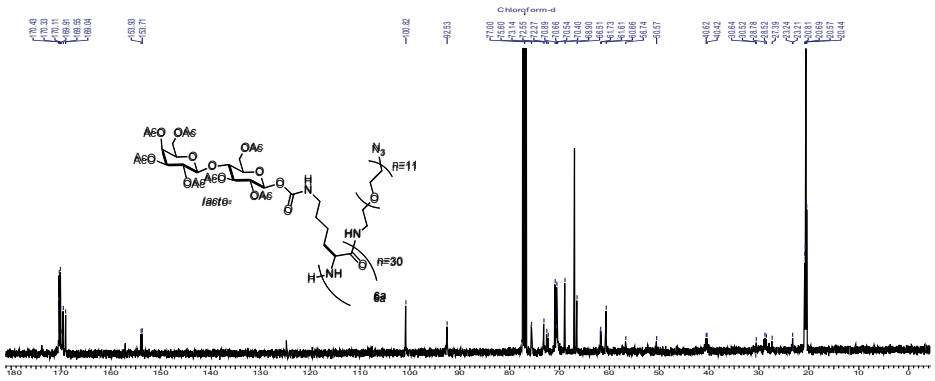

Fig. II.19: ^{13}C spectrum of 30-β-lacto-*O*-*l*-lys (***6a***).

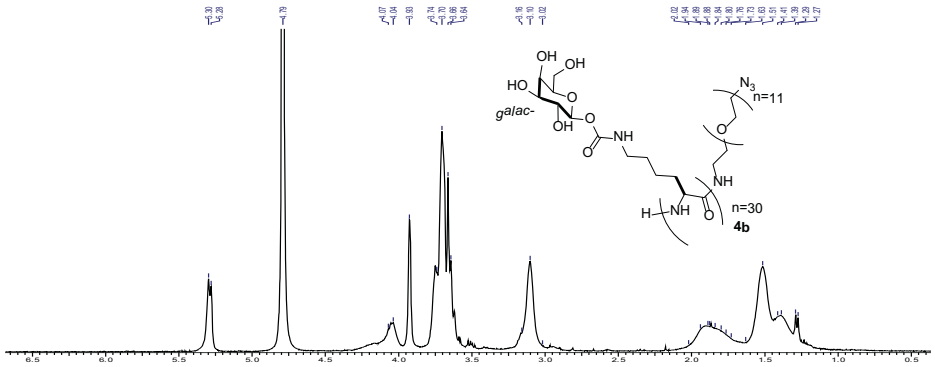

Fig. II.20: ^{1}H spectrum of 30-β-galac-*O*-*l*-lys(OH) (***4b***).

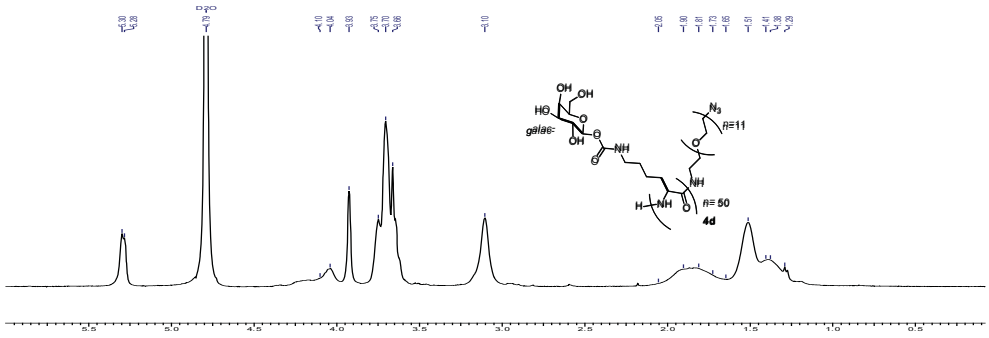

Fig. II.21: ^{1}H spectrum of 50-β-galac-*O*-*l*-lys(OH) (***4d***).

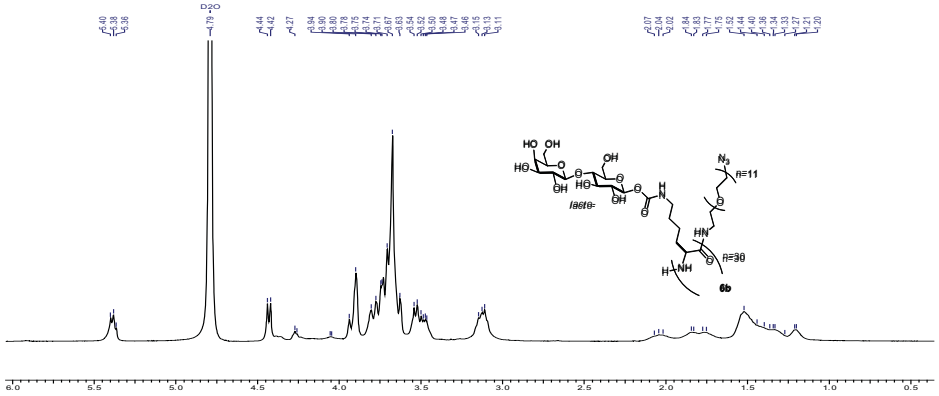

Fig. II.22: ^{1}H spectrum of 30-β-*Lacto*-*O*-*l*-lys(OH) (***6b***).

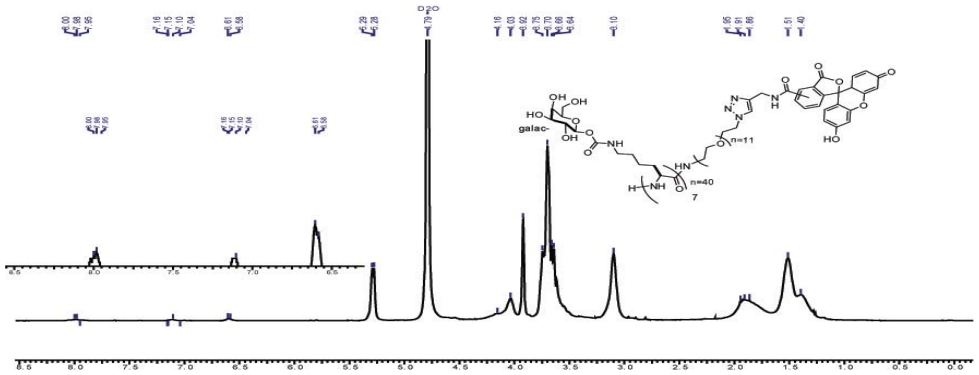

Fig. II.23: ^{1}H spectrum of Fluorescein-40-β-*Galactose*-*O*-*l*-lys(OH) (*7*).

Appendix III:

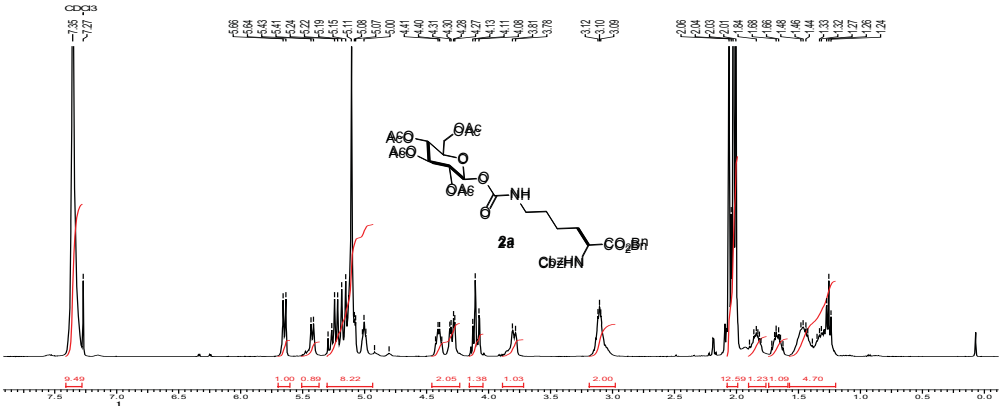

Fig. III.1: ^{1}H NMR of *per-O-tetra-acetate-β-gluco-Cbz-l-lys-OBn* (***2a***).

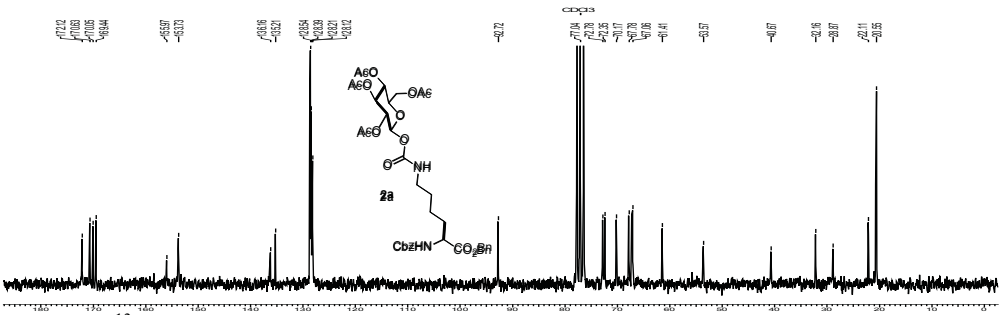

Fig. III.2: ^{13}C spectrum of *per-O-tetra-acetate-β-gluco-Cbz-l-lys OBn*(***2a***).

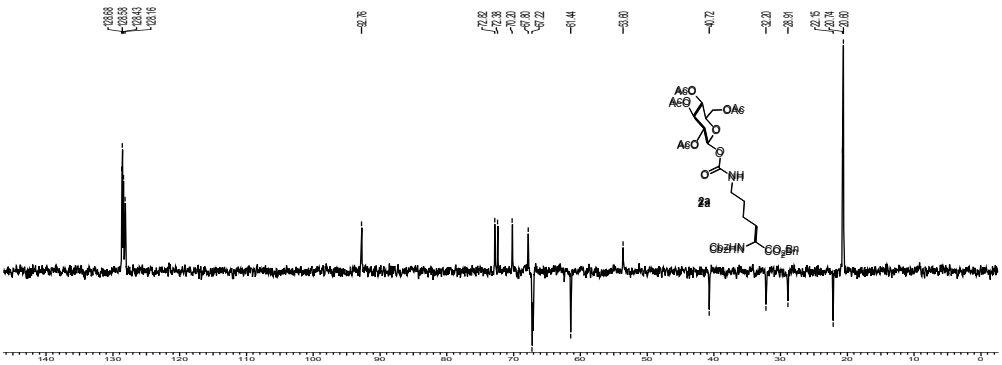

Fig. III.3: Dept of *per-O-tetra-acetate-β-gluco-Cbz-l-lys OBn*(***2a***).

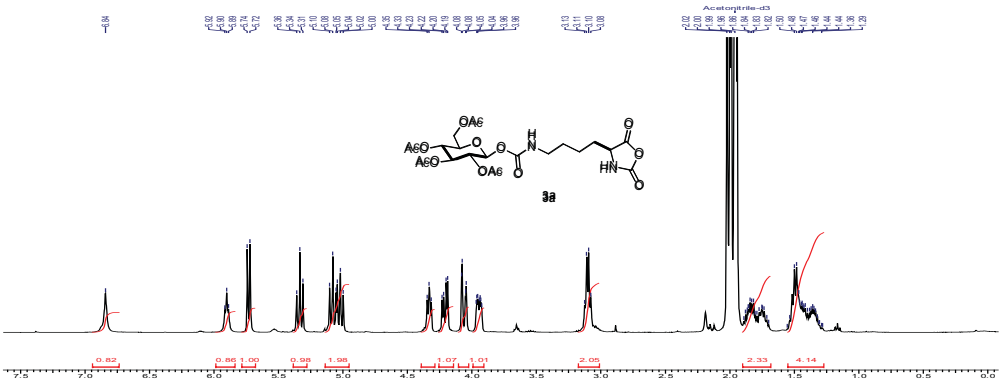

Fig. III.4: ^{1}H NMR of *per-O-acetylated-D-Glucose-l-lysine carbamate NCA(**3a**)*.

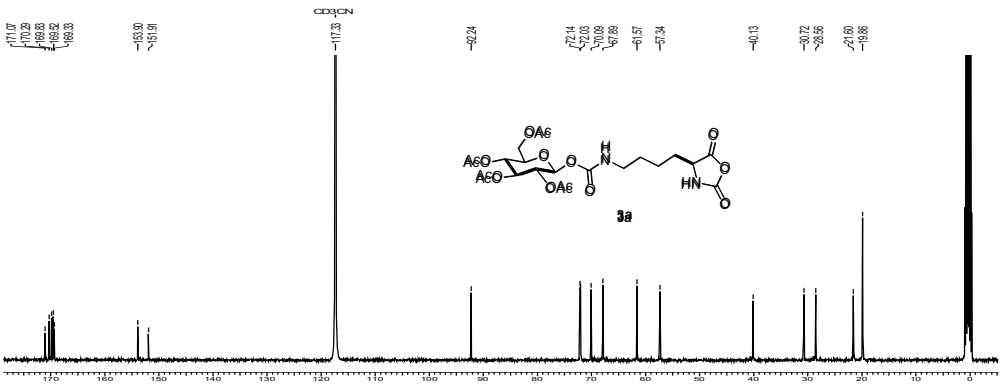

Fig. III.5: ^{13}C NMR of *per-O-acetylated-D-Glucose-l-lysine carbamate NCA(3a)*.

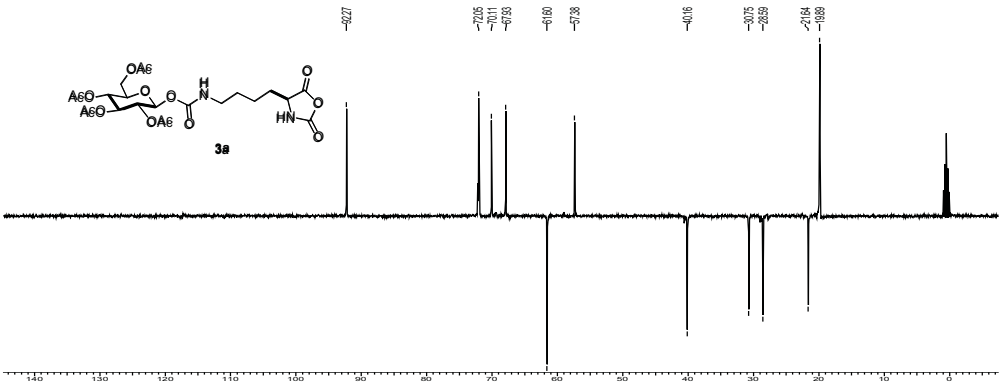

Fig. III.6: Dept of *per-O-acetylated-D-Glucose-l-lysine carbamate NCA(3a)*.

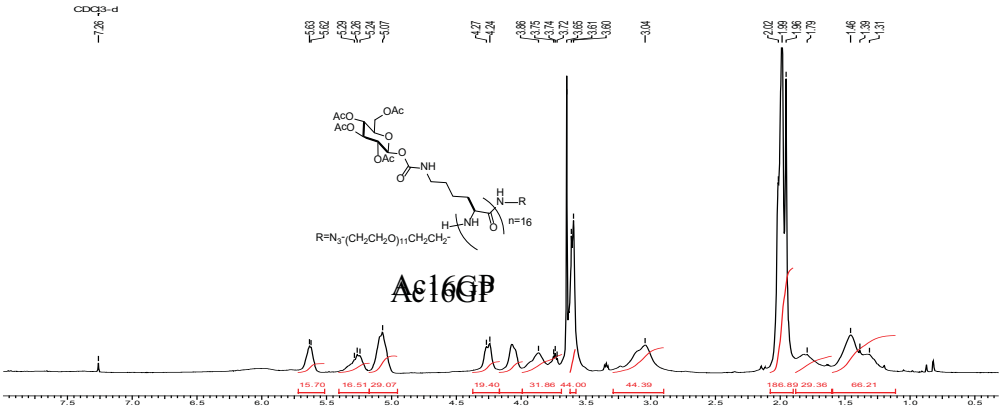

Fig. III.7: ^{1}H NMR of *Ac16GP*.

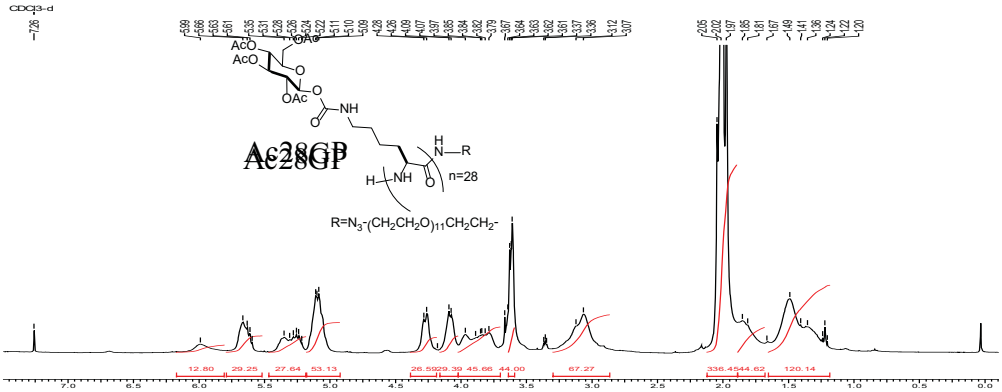

Fig. III.8: ^{1}H NMR of *Ac28GP*.

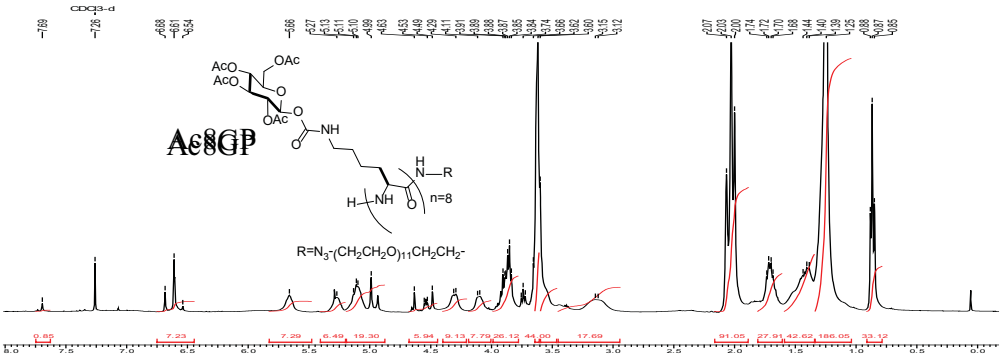

Fig. III.9: ^{1}H NMR of *Ac8GP*.

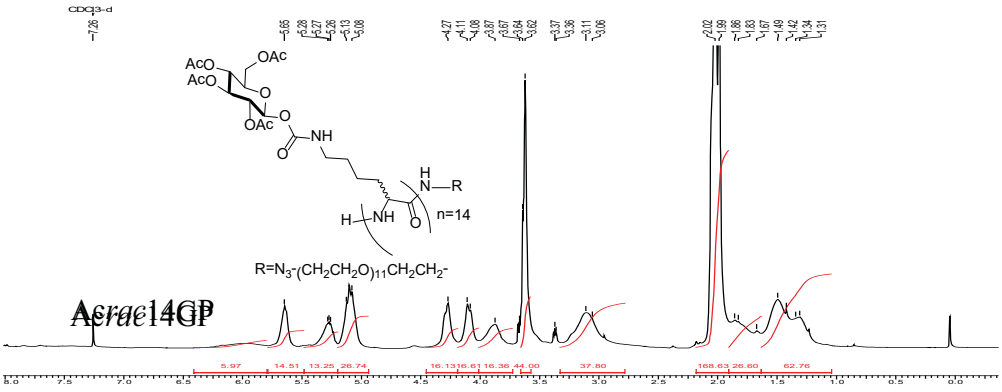

Fig. III.10: ^{1}H NMR of *Acrac14GP*.

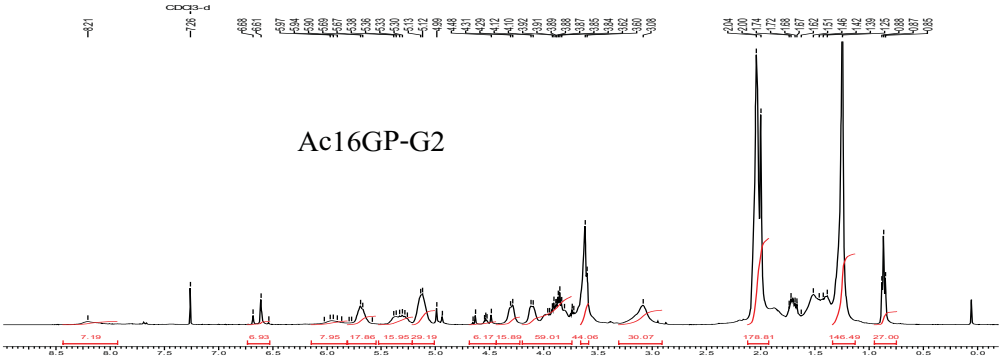

Fig. III.11: ^{1}H NMR of *Ac16GP-G2*.

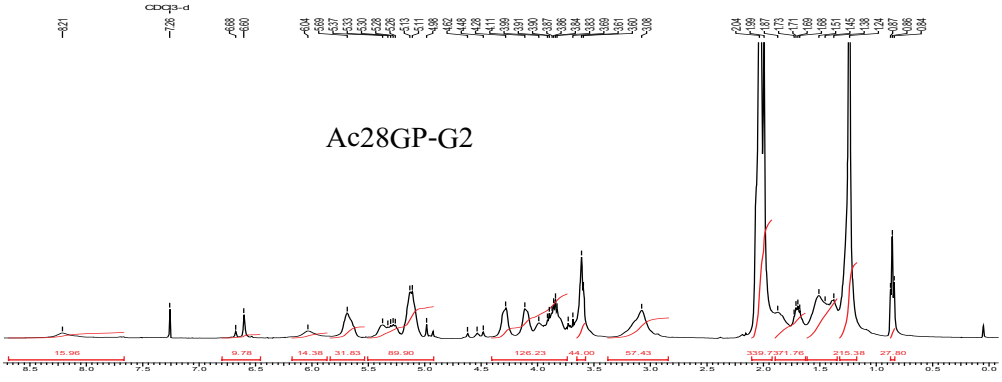

Fig. III.12: ^{1}H NMR of *Ac28GP-G2*.

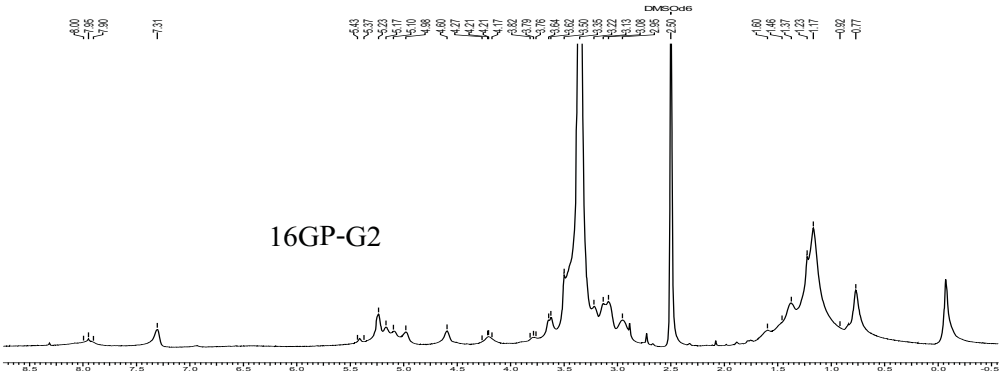

Fig. III.13: ^{1}H NMR of *16GP-G2*.

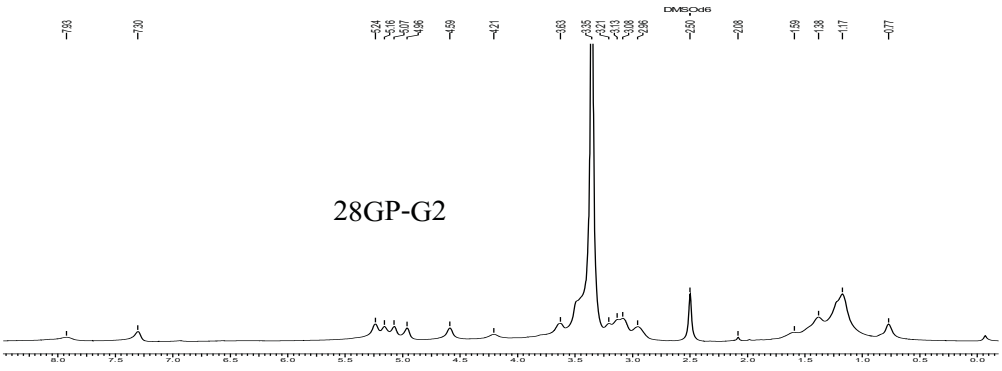

Fig. III.14: ^{1}H NMR of *28GP-G2*.

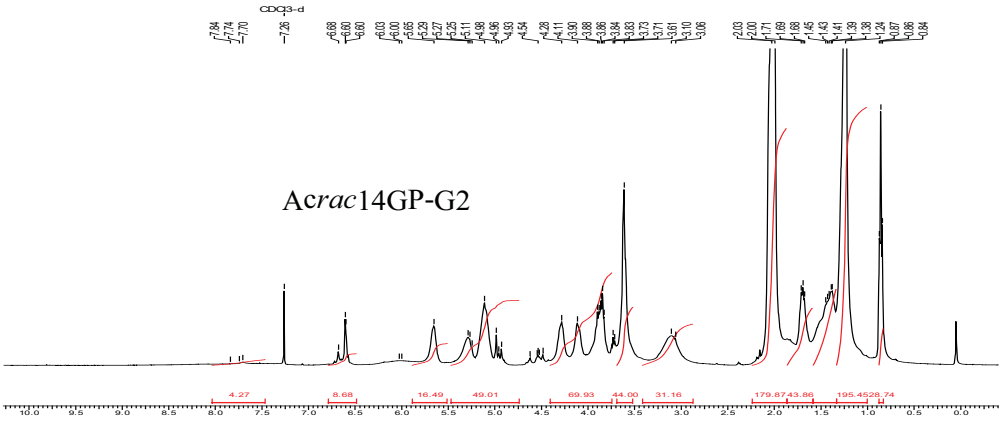

Fig. III.15: ^{1}H NMR of *Acrac14GP-G2*.

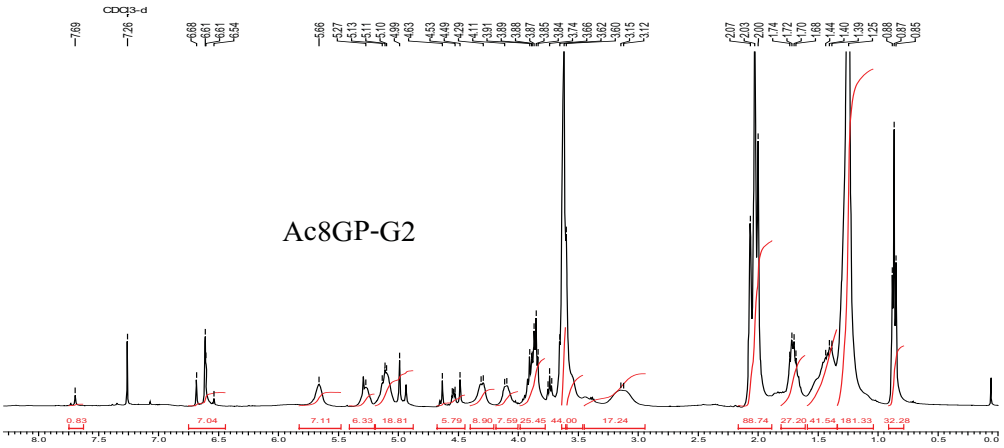

Fig. III.16: ^{1}H NMR of *Ac8GP-G2*.

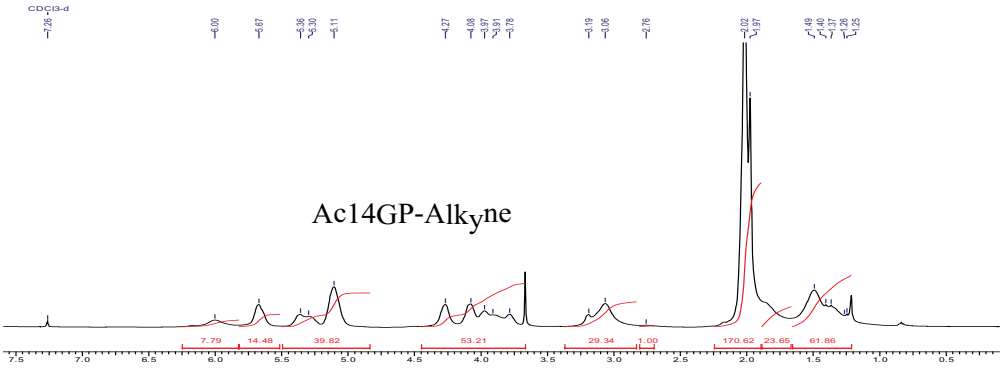

Fig. III.17: ^{1}H NMR of *Ac14GP-Alkyne*.

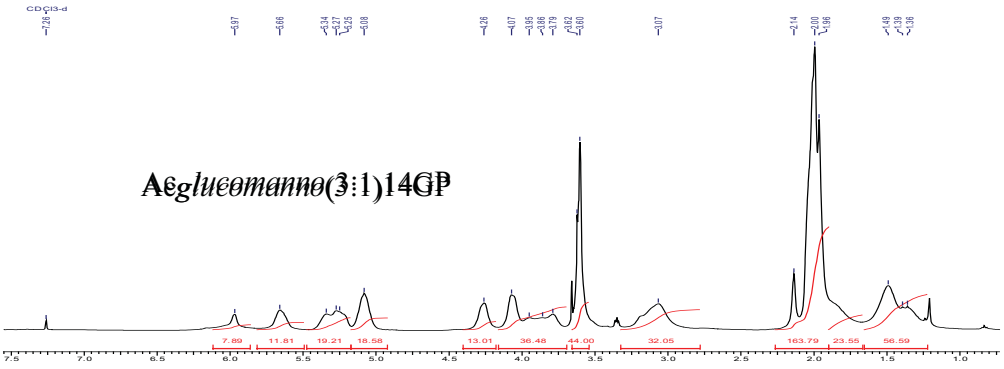

Fig. III.18: ^{1}H NMR of *Acgluco:manno(3:1)14GP*.

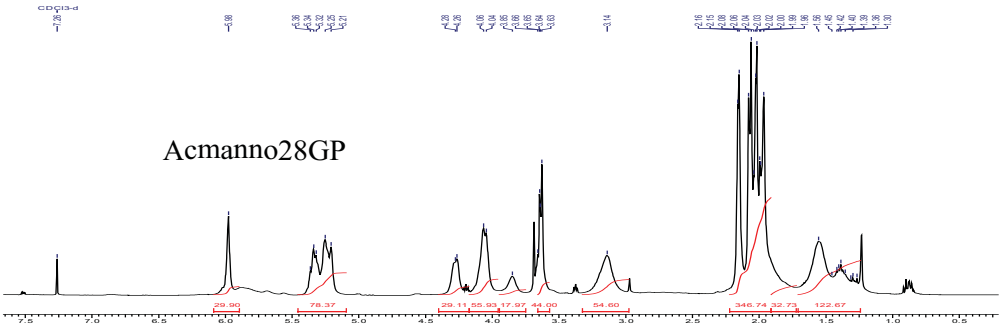

Fig. III.19: ^{1}H NMR of *Acmanno28GP*.

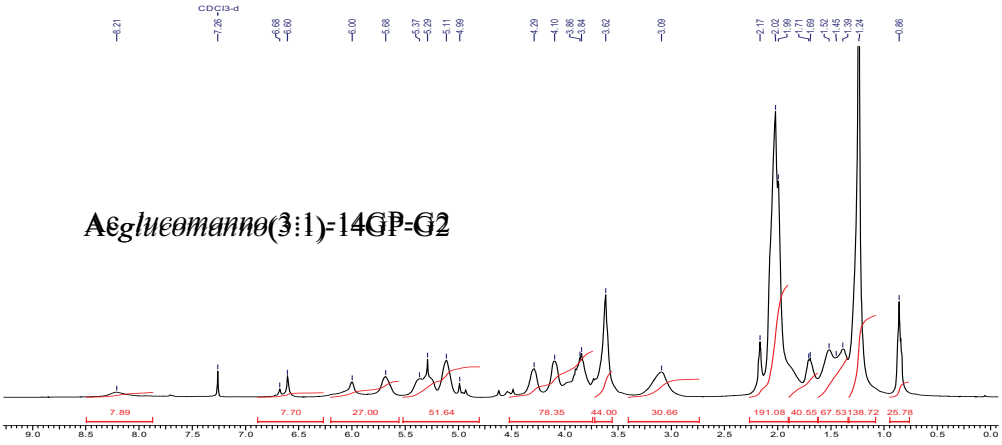

Fig. III.20: ^{1}H NMR of *Acgluco:manno(3:1)14GP-G2*.

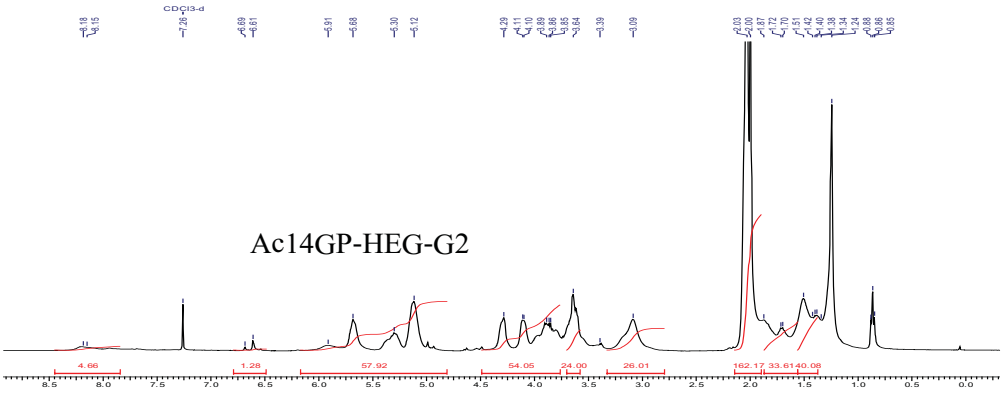

Fig. III.21: ^{1}H NMR of *Ac14GP-HEG-G2*.

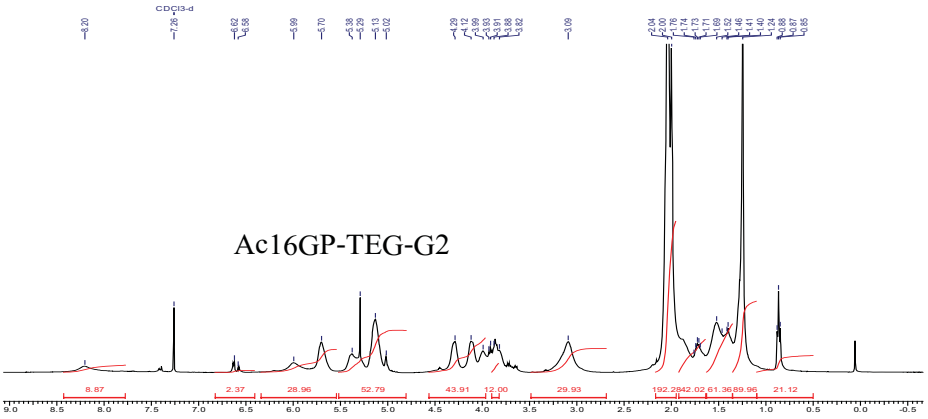

Fig. III.22: ^{1}H NMR of *Ac16GP-TEG-G2*.

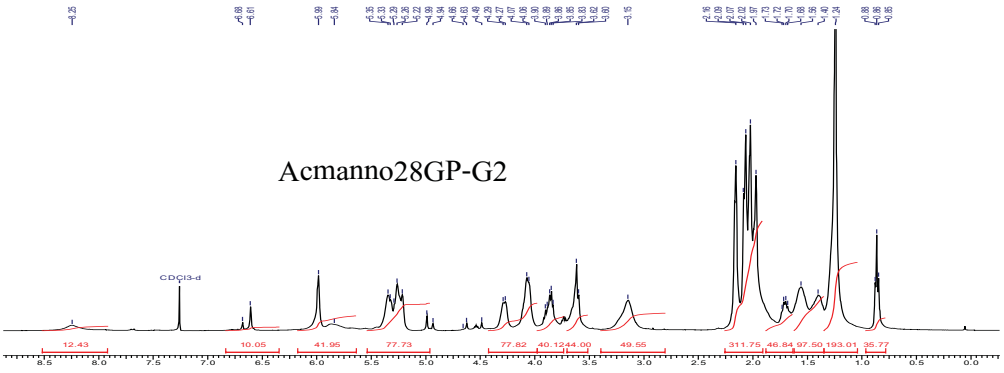

Fig. III.23: ^{1}H NMR of *Acmanno28GP-G2*.

Appendix IV:

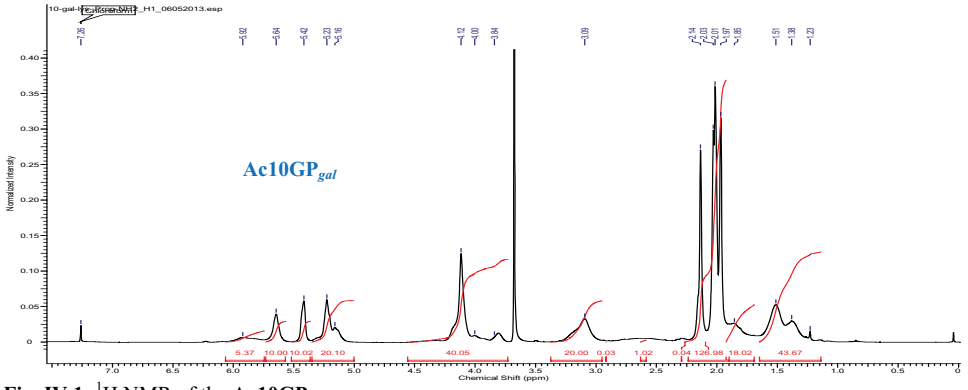

Fig. IV.1: ^{1}H NMR of the **Ac10GP$_{gal}$**.

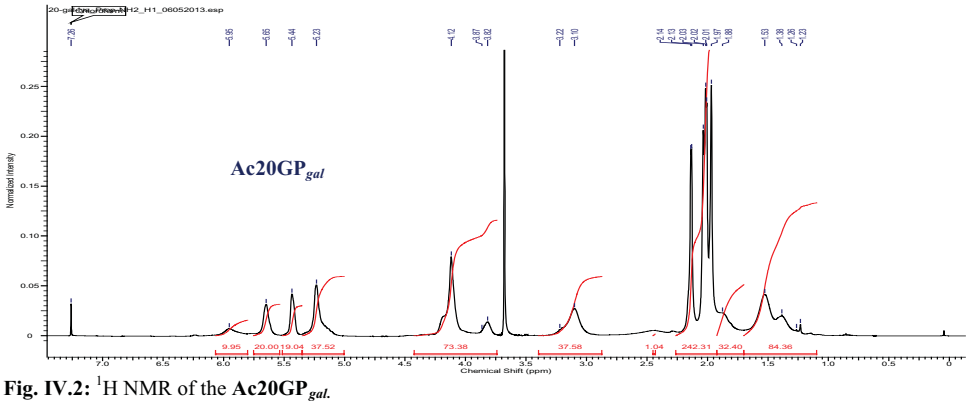

Fig. IV.2: ^{1}H NMR of the **Ac20GP$_{gal}$**.

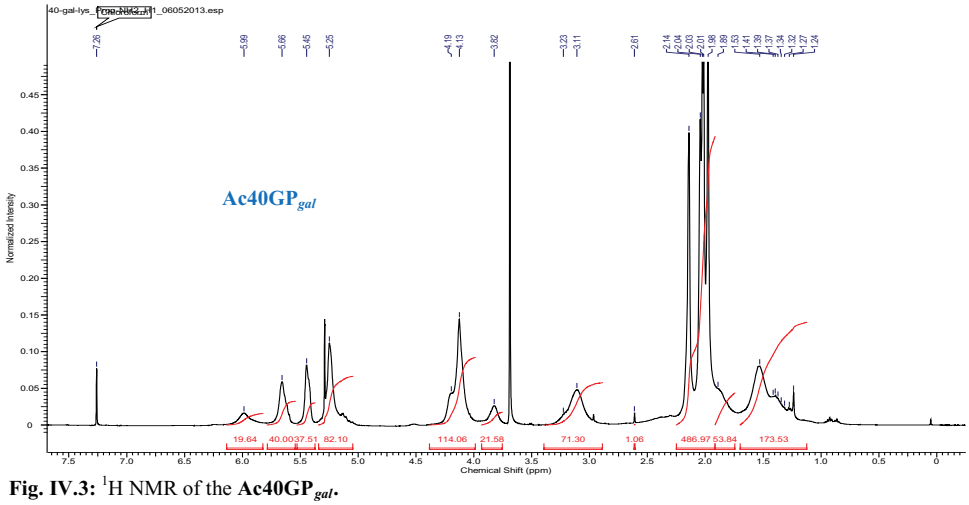

Fig. IV.3: ^{1}H NMR of the **Ac40GP$_{gal}$**.

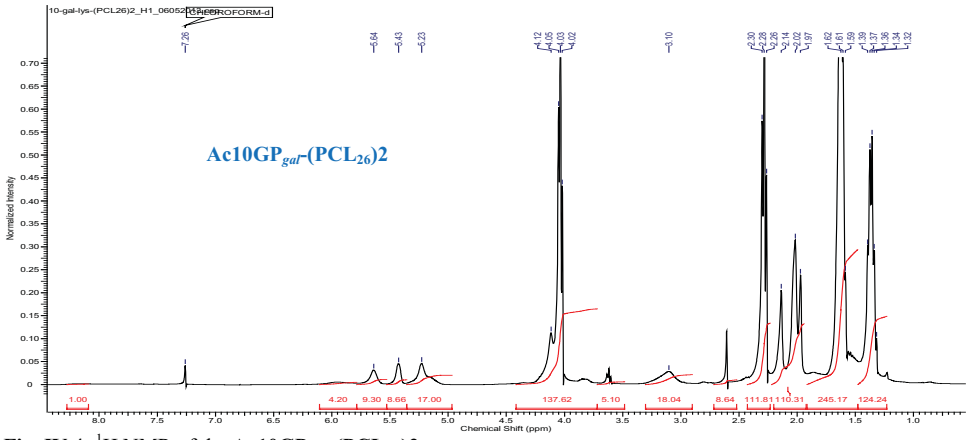

Fig. IV.4: ^{1}H NMR of the **Ac10GP$_{gal}$-(PCL$_{26}$)2.**

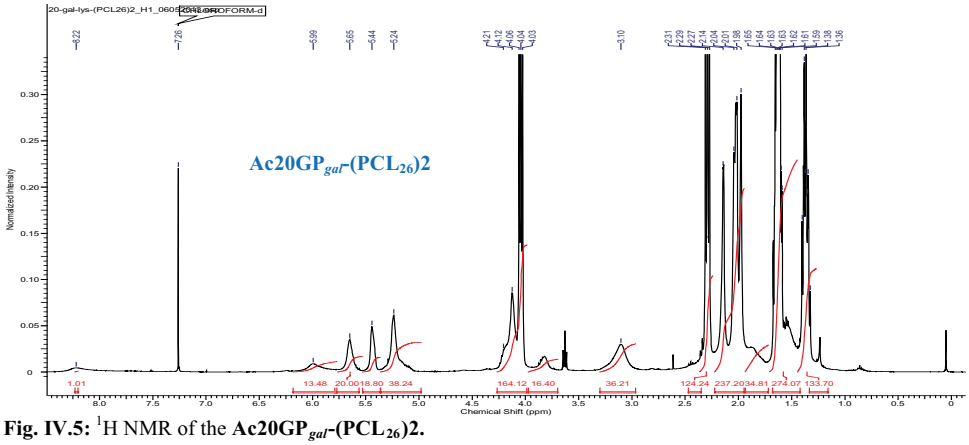

Fig. IV.5: ^{1}H NMR of the **Ac20GP$_{gal}$-(PCL$_{26}$)2.**

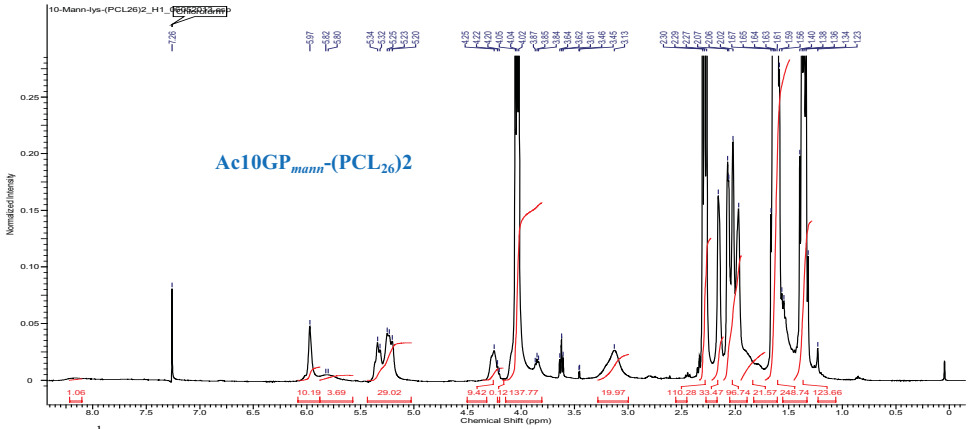

Fig. IV.6: ^{1}H NMR of the **Ac10GP$_{mann}$-(PCL$_{26}$)2.**

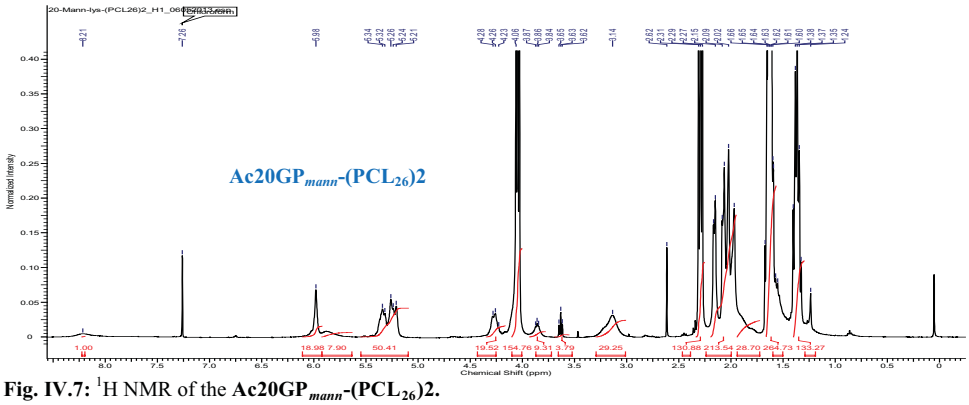

Fig. IV.7: ^{1}H NMR of the **Ac20GP$_{mann}$-(PCL$_{26}$)2.**

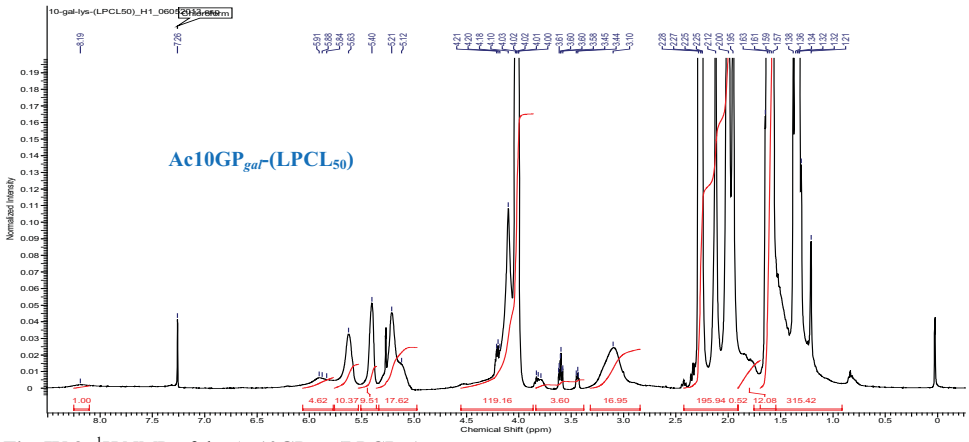

Fig. IV.8: ^{1}H NMR of the **Ac10GP$_{gal}$-(LPCL$_{50}$).**

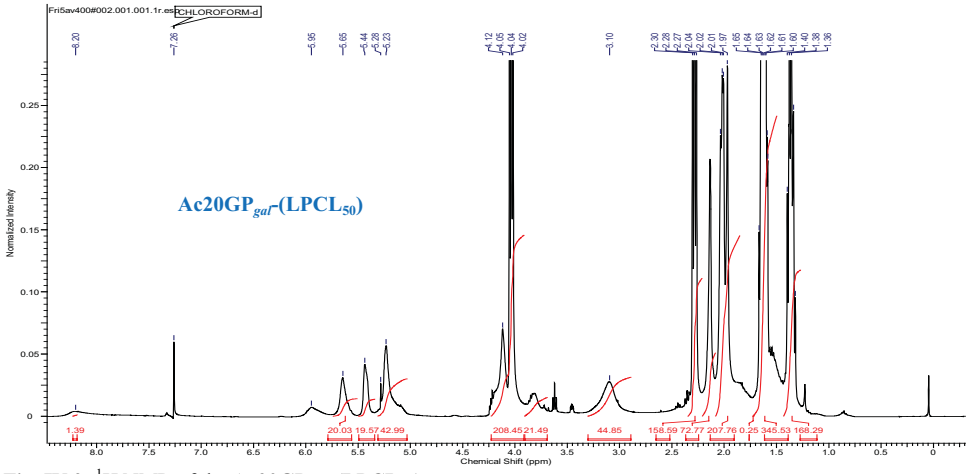

Fig. IV.9: ^{1}H NMR of the **Ac20GP$_{gal}$-(LPCL$_{50}$).**

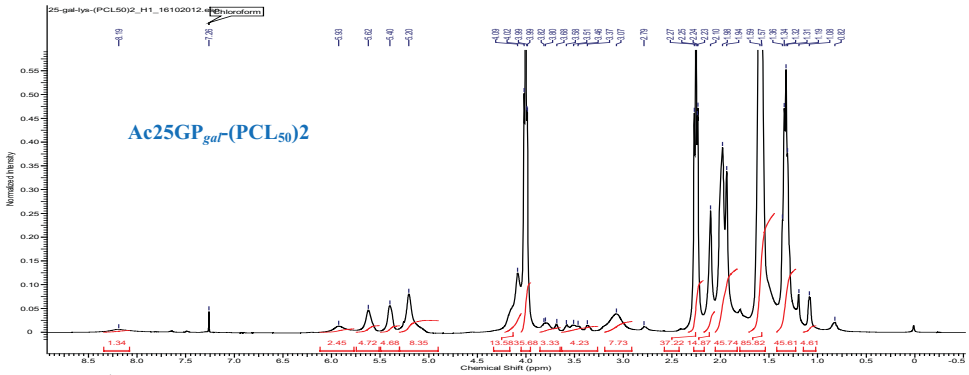

Fig. IV.10: ^{1}H NMR of the **Ac25GP$_{gal}$-(PCL$_{50}$)2.**

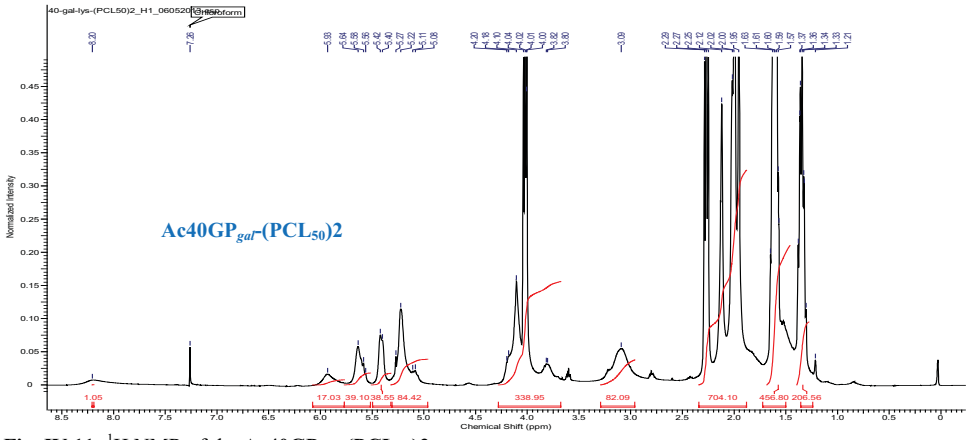

Fig. IV.11: ^{1}H NMR of the **Ac40GP$_{gal}$-(PCL$_{50}$)2.**

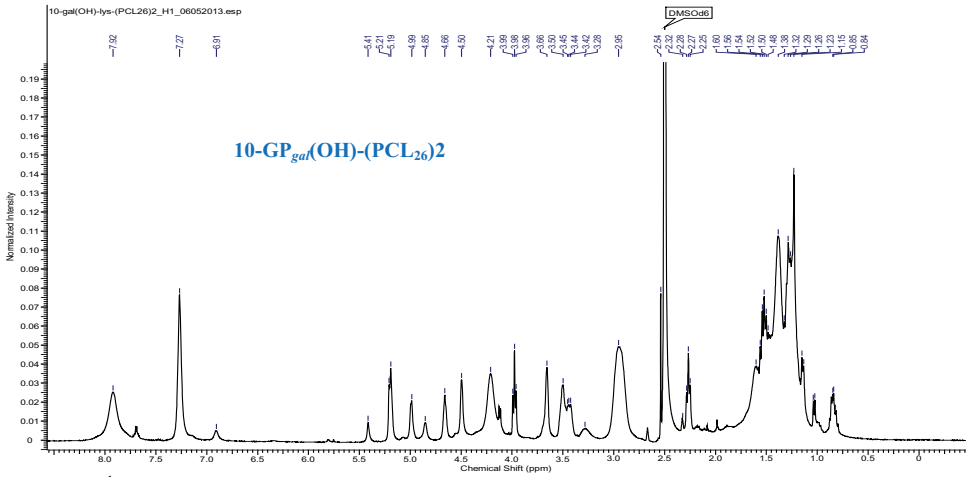

Fig. IV.12: ^{1}H NMR of the **10-GP$_{gal}$(OH)-(PCL$_{26}$)2.**

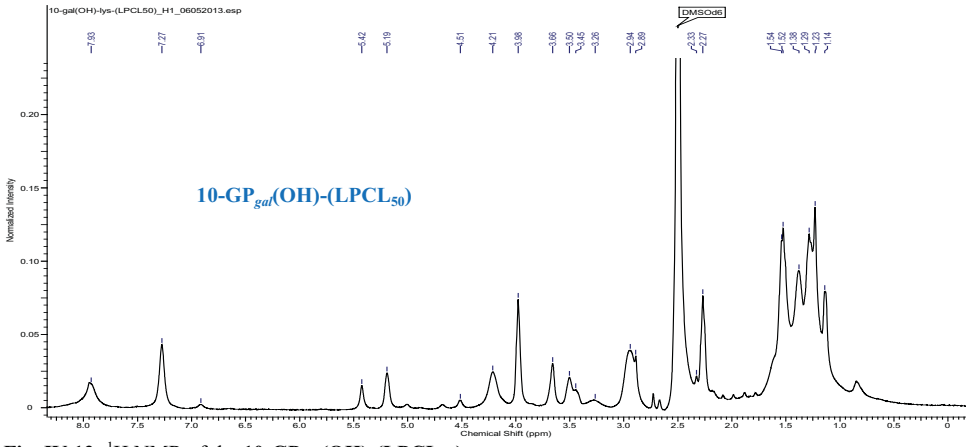

Fig. IV.13: ^{1}H NMR of the **10-GP$_{gal}$(OH)-(LPCL$_{50}$).**

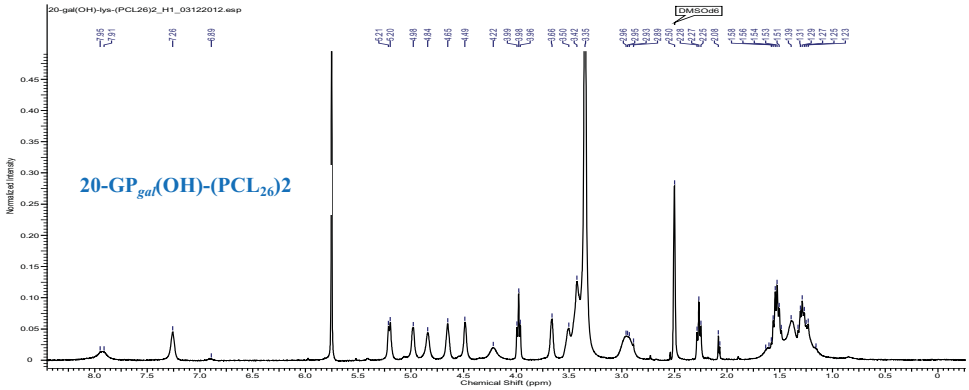

Fig. IV.14: ^{1}H NMR of the **20-GP$_{gal}$(OH)-(PCL$_{26}$)2**.

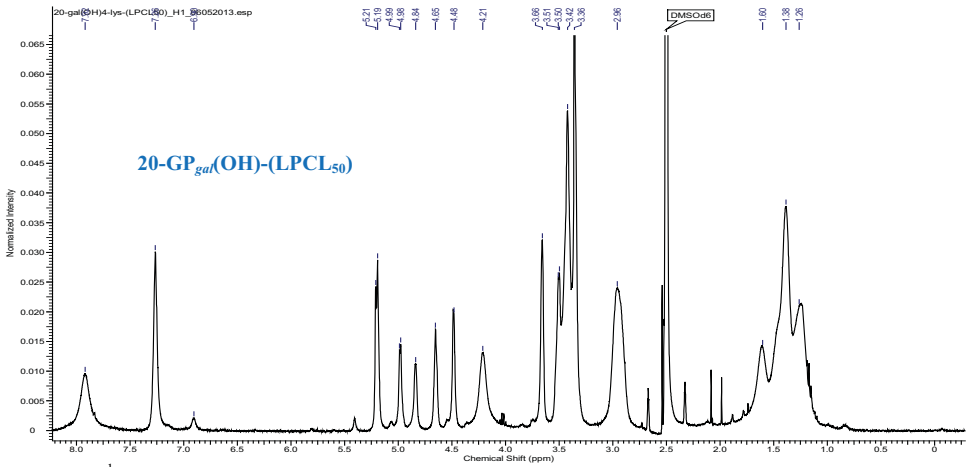

Fig. IV.15: ^{1}H NMR of the **20-GP$_{gal}$(OH)-(LPCL$_{50}$).**

.

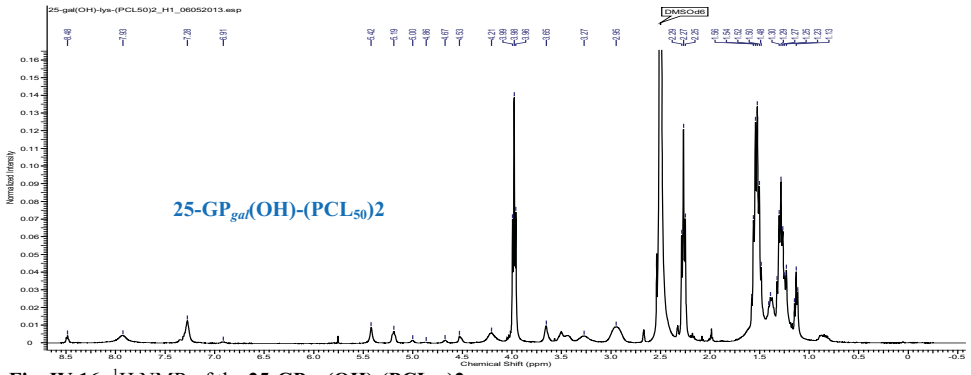

Fig. IV.16: ^{1}H NMR of the **25-GP$_{gal}$(OH)-(PCL$_{50}$)2.**

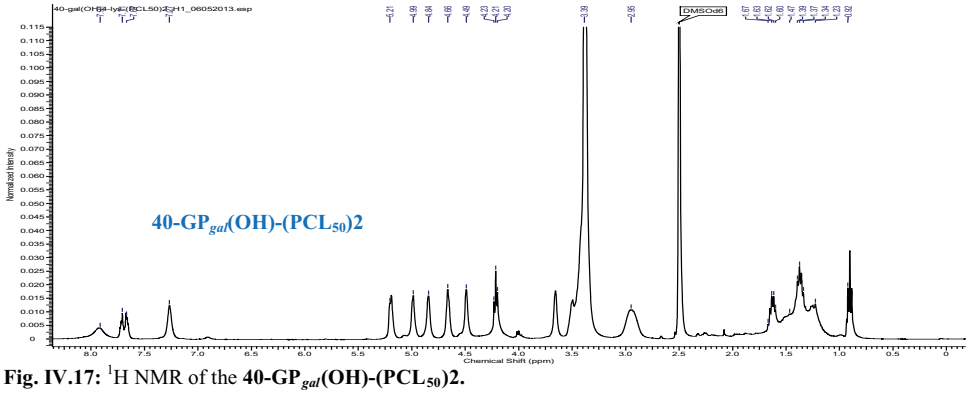

Fig. IV.17: ^{1}H NMR of the **40-GP$_{gal}$(OH)-(PCL$_{50}$)2.**

Publications

- "Multiple Topologies from Glycopolypeptide-Dendron Conjugate Self-Assembly: Nanorods, Micelles, and Organogels" Debasis Pati, Nagendra Kalva, Soumen Das, Guruswamy Kumaraswamy, Sayam Sen Gupta and Ashootosh V. Ambade *Journal of American Chemical Society* **2012**, *134*, 7796-7802.

- "Controlled Synthesis of O-Glycopolypeptide Polymers and their Molecular Recognition by Lectins" Debasis Pati, Asif Y. Shaikh, Soumen Das, Pavan Kumar Nareddy, Musty J. Swamy, Srinivas Hotha and Sayam Sen Gupta *Biomacromolecules* **2012**, *13*, 1287-1295.

- "Synthesis of Silk Fibroin-Glycopolypeptide Conjugates and their Recognition with Lectin" Soumen Das, Debasis Pati, Neha Tewari, Anuya Nisal and Sayam Sen Gupta *Biomacromolecules* **2012**, *13*, 3695−3702.

- "Synthesis and self-assembly of glycopolypeptides" Debasis Pati, Soumen Das, Nagendra Kalva, Guruswamy Kumaraswamy, Ashootosh V. Ambade and Sayam Sen Gupta. *Polymer Preprints (American Chemical Society, Division of Polymer Chemistry)* **2012**, *53*, 221-222.

- "Synthesis of glycopolypeptides by ring opening polymerization of α-amino acid N-carboxyanhydrides (NCA)" Debasis Pati, Asif Y. Shaikh, Srinivas Hotha, Sayam Sen Gupta, *Polym. Chem*. **2011**, *2*, 805-811.

- "Facile synthesis of unusual glycosyl carbamates and amino acid glycosides from propargyl 1,2-orthoesters as glycosyl donors" Shaikh, A. Y.; Sureshkumar, G.; Pati, D.; Sen Gupta, S.; Hotha, S. *Org. Biomol. Chem*.**2011**, *9*, 5951-5959.

- "Clickable" SBA-15 mesoporous materials: synthesis, characterization and their reaction with alkynes. Bharmana Malvi, Bibhas R. Sarkar, Debasis Pati, Renny Mathew, T. G. Ajitkumar and Sayam Sen Gupta. *J. Mater. Chem*., **2009**, *19*, 1409. (Article work highlighted on inside cover page of the journal issue).

- "Glycopolypeptide containing Biocompatible Star Copolymer Assemblies for Receptor-Mediated Drug Delivery" Debasis Pati et al *(Manuscript under preparation* **2013**).

- "Controlled synthesis of glycopolypeptides conjugated star polymer and their potential inhibition ability of Cholera Toxins" Debasis Pati et al (*Manuscript under preparation* **2013**).